UNIVERSITY OF HAWAII LIBRARY JAN 6 '60

Geochimica et Cosmochimica Acta

JOURNAL OF THE GEOCHEMICAL SOCIETY

Executive Editors

C. W. CORRENS, *Göttingen.* E. INGERSON, *Austin, Texas.* L. R. WAGER, *Oxford.*

Editors

L. H. AHRENS, *Capetown.* S. R. NOCKOLDS, *Cambridge.* H. C. UREY, *La Jolla, Calif.*
JOHN VERHOOGEN, *Berkeley, Calif.* A. P. VINOGRADOV, *Moscow.*
W. A. WAHL, *Helsingfors.*

CONTENTS VOLUME 17, NOS. 3/4 NOVEMBER 1959

D. FLINN: An application of statistical analysis to petrochemical data . . . 161
R. D. CHERRY and S. R. TAYLOR: Origin of Be^{10} and Al^{26} in tektites . . . 176
P. A. MOHR: A geochemical study of the shales of the Lower Cambrian Manganese Shale Group of the Harlech Dome, North Wales 186
M. TATSUMOTO and E. D. GOLDBERG: Some aspects of the marine geochemistry of uranium 201
H. PETTERSSON: Manganese and nickel on the ocean floor 209
P. K. WEYL: The change in solubility of calcium carbonate with temperature and carbon dioxide content 214
J. D. GRACE and T. F. BATES: Determination of uranium equilibrium in rocks using α and fission fragment radiography 226
F. E. SENFTLE and A. THORPE: Magnetic susceptibility of tektites and some other glasses 234
J. M. WHITFIELD, J. J. W. ROGERS and J. A. S. ADAMS: The relationship between the petrology and the thorium and uranium contents of some granitic rocks . . 248
J. M. WHITFIELD, J. J. W. ROGERS and M. C. MCEWEN: Relationships among textural properties and modal compositions of some granitic rocks 272
K. S. HEIER and S. R. TAYLOR: Distribution of Ca, Sr and Ba in southern Norwegian pre-Cambrian alkali feldspars 286
M. ICHIKUNI: Teneurs en cuivre et en zinc des eaux thermales au Japon . . . 305
F. A. PANETH: Der meteorit von Breitscheid—I. Einleitung 315
E. VILCSEK: Der Meteorit von Breitscheid—II. Chemische Analyse 320
H. HENTSCHEL: Der Meteorit von Breitscheid—III. Petrographische Untersuchung 323
Der Meteorit von Breitscheid—IV. Radiochemische Untersuchungen:
H. KÖNIG, H. WÄNKE und K. I. MAYNE: Helium und Neon 339
K. GOEBEL und P. SCHMIDLIN: Tritium 342
K. H. EBERT, F. HERNEGGER, H. KÖNIG und H. WÄNKE: Uran 349
H. KÖNIG und H. WÄNKE: Kalium-Argon 350
Papers to be published in future issues 352

QE 351
.A25

PERGAMON PRESS NEW YORK • LONDON • PARIS • LOS ANGELES

GEOCHIMICA ET COSMOCHIMICA ACTA

EXECUTIVE EDITORS

PROF. C. W. CORRENS (1959) *Sedimentpetrographisches Institut der Universität, Lotzestr.* 13, *Göttingen, Germany*
PROF. E. INGERSON (1959–1960) *Department of Geology, University of Texas, Austin* 12, *Texas, U.S.A.*
PROF. L. R. WAGER, F.R.S. (1959–1961) *Department of Geology and Mineralogy, The University Museum, Oxford, England*

EDITORS

PROF. L. H. AHRENS (1959–1960) *Department of Chemistry, University of Capetown, Rondebosch, Cape Province, South Africa*
Dr. S. R. NOCKOLDS (1959) *Department of Mineralogy and Petrology, The University, Cambridge, England*
PROF. H. C. UREY, For. Mem. R. S. (1959) *University of California, La Jolla, California, U.S.A.*
Dr. JOHN VERHOOGEN (1959–1961) *Department of Geology, University of California, Berkeley, California, U.S.A.*
PROF. A. P. VINOGRADOV (1959–1961) *Vernadsky Institute, Moscow, U.S.S.R.*
PROF. W. A. WAHL (1959–1961) *Observatoriegaten* 8, *Helisgfors, Finland*

EDITORIAL ADVISORY BOARD

AMERICAN CONTINENT

A. F. BUDDINGTON, *Princeton*
D. GUIMÃRAES, *Belo Horizonte*
G. E. HUTCHINSON, *New Haven*
B. H. MASON, *New York*
F. WHIPPLE, *Cambridge*
R. WILDT, *New Haven*
H. S. YODER, *Washington*

EUROPE

T. F. W. BARTH, *Oslo*
L. CAPDECOMME, *Toulouse*
E. J. CONWAY, *Dublin*
P. ESKOLA, *Helsinki*
P. GALLITELLI, *Modena*
A. HADDING, *Lund*
O. HAHN, *Göttingen*
H. W. HARVEY, *Plymouth*
F. HEIDE, *Jena*
A. HOLMES, *Edinburgh*
W. Q. KENNEDY, *Leeds*
PH. H. KUENEN, *Gröningen*
S. LANDERGREN, *Stockholm*
F. MASHATSCHKI, *Vienna*
A. MUIR, *Harpenden*
J. ORCEL, *Paris*
E. RAGUIN, *Paris*
E. REINHARD, *Basle*
TH. G. SAHAMA, *Helsinki*
C. E. TILLEY, *Cambridge*
T. VOGT, *Trondheim*

FAR EAST

T. WATANABE, *Tokyo*

Publishing Office: Pergamon Press, Inc., 122 East 55th Street, New York 22, N.Y. (Plaza 3-9651)

Four issues per volume, three volumes per year

Subscription *per annum* (including postage) (A) $51.00; (B) For individual subscribers who write directly to the publisher certifying that the Journal is for their private use, $21.50. Members of the Geochemical Society, or non-members who occasionally publish papers in the Journal, $10.00 *per annum*.

Back numbers, $28.00 per volume

Single issues, $7.00 each

Copyright © 1959 Pergamon Press Ltd.

PERGAMON PRESS, INC.

122 EAST 55TH STREET, NEW YORK 22, N.Y. 4 & 5 FITZROY SQUARE, LONDON W.1

PRINTED IN NORTHERN IRELAND AT THE UNIVERSITIES PRESS, BELFAST.

PERGAMON PRESS

specialized journals for *specialized advertising!*

Advertise in GEOCHIMICA ET COSMOCHIMICA ACTA—

Space is available to all manufacturers of suitable products—the range which will appeal to readers of this journal is extensive and includes spectrometers, seismographs, seismic amplifiers and detectors, hydrometers, humidity instruments, monometers, galvanometers, radiation detectors and pyrometers, colorimeters, fluorometers, petrographic and other microscopes, flame photometers, surveying instruments, voltmeters, lenses and optical elements, mine ventilation instruments, X-ray microanalysers, pumps, pipe-lines, gas detection and measurement apparatus, microphotometers, X-ray films, plates and equipment, samplers of airborne dust and bacteria, telecommunications equipment, gyroscopic instruments, petroleum testing equipment, thermometers of all types, chemicals, oil boring equipment, electronic equipment . . . this list could easily be trebled!

We shall be happy to provide impartial advice as to the suitability of products not listed.

THIS IS ONE OF MORE THAN 50 INTERNATIONAL SCIENTIFIC JOURNALS. SPECIAL REDUCED "COMBINED RATES" ARE OFFERED TO MANUFACTURERS ADVERTISING IN MORE THAN ONE JOURNAL.

For details WRITE OR PHONE to

R. D. MILLER
Advertisement Manager
PERGAMON PRESS LIMITED
Pergamon House,
4 Fitzroy Square,
London W.1
Phone: EUSton 4455 (Ext. 121)

H. L. WOUDHUYSEN
Advertisement Manager
PERGAMON PRESS INC.
122 East 55th Street,
New York 22, N.Y.,
U.S.A.
Phone: Plaza 3-9651

A selection of new titles from our 1959-60 catalogue

CUMULUS DYNAMICS

Edited by **Charles E. Anderson**

Proceedings of the first conference on Cumulus Convection held in May 1959 under the auspices of the Geophysics Research Directorate, U.S. Air Force Cambridge Research Center, Bedford, Mass.

In preparation

DYNAMICS OF CLIMATE

Edited by **Richard L. Pfeffer**

Proceedings of a conference on the application of numerical integration techniques to the problem of the general circulation, sponsored jointly by the Institute for Advanced Study and the U.S. Air Force Geophysics Research Directorate.

35s. net ($6.50)

ORGANIC GEOCHEMISTRY

Edited by **Irving A. Breger**

This treatise will be the first undertaken in the field, and will assure a complete synthesis between the application of the principles of organic chemistry and geology.

In preparation

PRINCIPLES OF METEORITICS

By **E. L. Krinov,** *Academy of Sciences of the U.S.S.R.*

In preparation

A SHORT OUTLINE OF THE GEOLOGY OF THE U.S.S.R.

By **D. V. Nalivkin**

Translated from the Russian by **S. I. Tomkeieff**

An outstanding Russian monograph of great topical interest.

Approx. 50s. net ($7.50)

PERGAMON PRESS

London New York Paris Los Angeles

4 & 5 Fitzroy Square, London, W.1 122 East 55th Street, New York 22, N.Y.

24 Rue des Écoles, Paris V^e^.

Geochimica et Cosmochimica Acta, 1959, Vol. 17, pp. 161 to 175. Pergamon Press Ltd. Printed in Northern Ireland

An application of statistical analysis to petrochemical data

Derek Flinn
Jane Herdman Laboratories of Geology, The University, Liverpool 3.

(*Received* 4 *March* 1959)

Abstract—The development of rapid methods of silicate analysis has made possible the study of chemical variation in rock masses by means of large numbers of analyses. To obtain the maximum benefit from the data in the form of conclusions of stated probability of correctness and numerical estimates of variation and of differences, statistical methods have to be employed. In a recent paper Pitcher and Sinha (1957) publish about fifty rock analyses from the neighbourhood of the Ardara Pluton, Donegal, Eire. In the present paper these data are statistically analysed. Several statistical methods are employed, i.e. *t*-test, one-way and two-way analysis of variance. Each is related to the sampling scheme that it requires and the questions it can answer. Pitcher and Sinha's conclusions are reproduced statistically and given, together with numerical estimates of the probability of their correctness and of the compositional differences they discovered. Further conclusions are also drawn. Consideration of the problem tackled by Pitcher and Sinha and of their data shows that possibly a three-way partially nested analysis of variance is the experimental design best suited to their purpose, but their sampling scheme is not amenable to this form of analysis.

Chemical composition even within an apparently uniform rock mass varies. This variation may be due to a number of independent factors, such as original composition and later metasomatism. The variation in composition may depend on direction in the rock, and on the scale considered. An exposure may show considerable variation in a direction normal to the bedding and none at all parallel to the bedding, and yet there may be little difference in composition between different exposures. Statistical analysis is normally necessary to interpret data collected from such a system.

Pitcher and Sinha (1957) employed an intuitive examination of about fifty rock analyses to show that the contact metamorphism associated with the Ardara Pluton was isochemical. Although statistical methods were not used in planning the experiment, the data were collected in such a way that numerical analysis can be applied to some extent.

Their data have been numerically analysed and their method of collection of data has been examined. Many of the conclusions which Pitcher and Sinha drew from their examination of the data have been verified. Had the data been collected in a manner better suited to numerical analysis further information might have been obtained. Alternative sampling schemes suited to this process are considered.

The Problem and the Data

The Cleengort Pelitic Schists skirt the northern edge of the Ardara Pluton and continue for about $1\frac{1}{2}$ miles beyond the limit of the aureole which surrounds the pluton (Pitcher and Sinha, 1957, Fig. 2, p. 395). These authors show (pp. 394–397) that the schists are a single stratigraphic unit of nearly constant thickness which is largely complete throughout the area under consideration. They dip steeply southwards within the aureole and less steeply outside it. The schists are not of uniform composition across the strike but "often show a weak banding which

marks slight differences in lithology." Samples from the schists were collected both within and without the aureole and were analysed. Comparison of the two groups of analyses showed that the metamorphism was largely isochemical.

The sampling was based on a series of dip-traverses arranged at intervals along the strike, both within the aureole and outside it. Pitcher and Sinha (1957, p. 398) state that "suitable" lines of traverse were chosen. In fact the lines were uniformly spaced as far as exposure allowed (Pitcher, personal communication). Five traverses lie within the aureole and three outside it. Suitable sites for traverses outside the aureole are restricted by the Naran Hill Complex which cuts the schists and may have altered them, and by an anticlinal nose of limestone which almost cuts out the schists near the sea. One of the traverses (*I*) crosses an associated syncline in the schists and is of little use for estimating the composition of the schist belt.

At intervals along the traverses sampling locations 150 × 50 yd were marked out. They are separated by unequal intervals both stratigraphically and along the ground. These locations were fixed by availability of exposure and the desire to site them at equal intervals (Pitcher, personal communication).

Within the locations five specimens were collected from points "located in an arbitrary manner, though veins or particularly siliceous bands were avoided" (Pitcher and Sinha, 1957, p. 398). One specimen was collected from each of five exposures of reasonably fresh "hammerable" rock nearest to the four corners and the centre respectively, of the location rectangle (Pitcher, personal communication). For each location the five specimens were crushed and mixed in equal weights to form a sample for analysis.

The methods used for analysis are given by Pitcher and Sinha (1957, p. 399) together with the results in the form of a single analysis for each sample (Pitcher and Sinha, 1957, Table III, p. 408). The cited analyses are based on a single analysis of the specimen together with check determinations of the more variable constituents, i.e. especially alkaline oxides and MgO (Pitcher, personal communication). The accuracies of the results are indicated by a series of confidence intervals (Pitcher and Sinha 1957, p. 400) for which, however, no confidence coefficient is given.

Method I. Although modern methods have cut the time required to carry out a rock analysis considerably (Shapiro and Brannock, 1956; Riley, 1958), it is still a limiting factor in studies of this kind.

The question whether the composition of the Cleengort Pelitic Schists within the aureole differs from that outside could be answered with a minimum number of analyses in the following manner. A series of traverses normal to the strike of the schists are made at predetermined intervals, both inside and outside the aureole (avoiding the proximity of the Naran Hill complex and the anticlinal zone). During each traverse a given number of specimens are collected at predetermined intervals. The methods, difficulties and advantages of collecting at uniform and at random intervals are mentioned below (p. 163). The specimens from each traverse are bulked and analysed. The analyses are estimates of the composition of the schist belt at the traverses, being equivalent to the arithmetic mean of the analyses of the individual specimens collected on each traverse. The analyses

from traverses inside the aureole are considered as one sample and the analyses from traverses outside the aureole are considered as another sample. For each oxide the two sample means are compared by the t-test (MORONEY, 1951, p. 232–233; DIXON and MASSEY, 1951, p. 102–3). By averaging the analyses from traverses inside and outside the aureole in PITCHER and SINHA's data (1957, Table III, p. 408) two samples for such an experiment can be obtained. The results are given in Table 1. Only H_2O is present in significantly different amounts inside the aureole and outside it. The variations in the H_2O analyses for the two samples would lead less than about once in a hundred repetitions of the experiment to a difference between the means as great as or greater than that actually shown. For all other oxides, differences between the means as great as, or greater than, those shown are to be expected very much more frequently.

For SiO_2 the difference between the two means gives $t = 1{\cdot}028$ for five degrees freedom and hence a probability value of 65 per cent. That is, even if SiO_2 is present in the same concentration in the aureole and outside the aureole, during repeated sampling as above, as large an apparent difference, or larger, would be expected once in about every three trials. A confidence interval for the difference between the two means can be calculated from

$$\bar{x}_1 - \bar{x}_2 \pm t_{n_1 + n_2, \alpha} \cdot s_0 \sqrt{\left(\frac{1}{n_1} + \frac{1}{n_2}\right)}$$

where $\bar{x}_1$ is the mean of a sample of n_1 with standard deviation s_1, etc.; $100\,(1 - \alpha)$ per cent is the two-sided confidence coefficient, t is Student's t (FISHER and YATES 1948, Table III, p. 32), and

$$s_0^2 = \frac{s_1^2(n_1 - 1) + s_2^2(n_2 - 1)}{n_1 + n_2 - 2}$$

For SiO_2 and a confidence coefficient of 95 per cent the difference (SiO_2 in aureole − SiO_2 out aureole) lies between −0·89 per cent and +2·07 per cent, i.e. in about five times out of a hundred the difference between the means obtained in the manner used above would be expected to lie outside limits calculated in this way due to random variation. If the observed difference between the means for silica is a real one, the test is not able to show it, because the confidence interval includes zero. The same conclusion applies to all the oxides except H_2O. Statistically speaking the test is not powerful enough to recognize an SiO_2 difference as small as 0·6 per cent.

The test becomes more powerful when the number of analyses is increased. It is possible to calculate the number of analyses necessary to give any selected chance of recognizing as significant a difference of a certain size if it exists and on the other hand of recognizing it as non-significant if it does not exist. Supposing that it is considered desirable that failure to recognize a true difference of 0·5 per cent SiO_2 occurs only about five times in a hundred ($\beta = 95$), and that a true lack of difference is interpreted as a difference only ten times in a hundred ($\alpha = 10$), then Table 19(b) in DIXON and MASSEY (1951, p. 345, 220) indicates that eighty analyses will be necessary. If this is considered too expensive in terms of analyses a higher rate of errors must be accepted or a larger difference sought.

Table 1

	Average composition of each traverse (PITCHER and SINHA, Table IV)														
	$n = 5$					$n = 6$		Aureole: B–F		Non-aureole: G–H		t-test			
												$\bar{x}_1 - \bar{x}_2$			
	B	C	D	E	F	G	H	$\bar{x}_1$	s_1	$\bar{x}_2$	s_2	d	s_0	t $v = 5$	$t_{v,\alpha}$
SiO_2	62·74	62·76	63·50	61·54	63·00	61·73	62·50	62·71	0·721	62·12	0·544	0·593	0·690	1·028 NS	$t_{5,95} = 2{\cdot}57$
TiO_2	1·02	0·74	0·76	0·82	0·74	0·82	0·78	0·82	0·119	0·80	0·078	0·017	0·107	0·190 NS	
FeO	5·48	5·98	6·04	6·16	5·84	5·95	5·78	5·90	0·262	5·87	0·141	0·030	0·242	0·148 NS	$t_{5,99} = 4{\cdot}03$
MgO	3·62	3·68	4·16	2·52	3·10	3·38	2·90	3·42	0·626	3·14	0·410	0·276	0·590	0·560 NS	
CaO	0·66	0·60	0·78	0·46	0·50	0·50	0·45	0·60	0·128	0·48	0·035	0·125	0·116	1·290 NS	$t_{5,99·9} = 6{\cdot}86$
Na_2O	1·10	1·44	1·48	1·54	1·36	1·33	1·13	1·38	0·172	1·23	0·141	0·154	0·166	1·108 NS	
K_2O	3·72	3·36	3·24	3·68	3·60	3·50	3·65	3·52	0·210	3·58	0·106	0·055	0·193	0·034 NS	
H_2O	2·28	3·20	2·76	2·58	3·00	3·93	3·87	2·96	0·294	3·90	0·042	0·936	0·264	4·246 †	
Diff.	18·08	18·02	17·06	20·54	18·62	18·56	18·67	18·46	1·290	18·62	0·078	0·151	1·154	0·157 NS	

† Significant at 1% not at 0·1%

This method of determining the necessary number of analyses is possibly the answer sought by PITCHER in his reply to HARDIE (PITCHER and SINHA, 1957, p. 408).

HARDIE suggested to PITCHER (PITCHER and SINHA, 1957, p. 408) that all the specimens collected outside the aureole could be bulked and compared with a similar bulked sample from inside the aureole. Such an experiment may be simulated with PITCHER and SINHA's data by averaging the analyses from inside the aureole and those from outside the aureole. These averages are given in Table 1 where it can be seen that for each oxide the two averages always differ. With no knowledge of the variation of the data averaged (or bulked) it is impossible to determine whether or not these differences have any significance.

Method II. The data presented by PITCHER and SINHA are in the form of a number of analyses in each of a series of traverses. From such an array of data it is possible to learn more about the variation in composition over the area than is necessary to settle the question of whether the contact metamorphism was isochemical by method I. At the same time with the same total number of analyses there is not as great a chance of recognizing a true difference in composition between the two areas, especially if it is a small difference.

The data are suitable for a one-way analysis of variance (MORONEY, 1951, pp. 371–383; DIXON and MASSEY, 1951, pp. 121–127). The specimens collected along each traverse are considered as a representative sample of the schist belt and the one-way analysis compares the samples with a view to deciding if they could all have come from a single parent population, or if they were drawn from two or more populations with the same variances but different means. The test is an extension of the t-test used above to compare two samples.

In Table 2 the results are presented of one-way analysis of variance of PITCHER and SINHA's data omitting traverse I, which unlike the others crosses a syncline. In this table the variation of the data is shown partitioned into two components, one (the between traverses mean square) estimates the variation between the average compositions of the traverses, and the other (the within traverses mean square) estimates the variation in composition within the traverses. If the between traverses mean square is significantly greater than the within traverses mean square, and if the observations are drawn from normal distributions with the same variance, or at least do not differ too widely from this ideal (KRUMBEIN and MILLER, 1953, pp. 526–527), then there is reason to believe that the traverses were drawn from populations with different means, i.e. that the composition of the belt changes along its length.

In Table 2 only TiO_2 and H_2O show significant between traverse differences. Inspection of the original data for TiO_2 reveals that the means for traverses G and H outside the aureole lie within the range of the traverses B to F inside the aureole. Traverse B, however, appears to differ from all the other traverses. Inspection of the original data for H_2O leads to the conclusion that the significant difference is between traverses inside the aureole and traverses outside the aureole. In cases of doubt these comparisons can be made arithmetically. In Table 2(a) the between traverses mean square for TiO_2 and for H_2O are each partitioned into three components estimating variation between traverses outside the aureole, between

Table 2

		TiO_2		SiO_2		FeO		MgO		CaO		Na_2O		K_2O		H_2O		Diff.	
	v	*SS*	*MS*	*SS*	*MS*	*SS*	*MS*	*SS*	*MS*	*SS*	*MS*	*SS*	*MS*	*SS*	*MS*	*SS*	*MS*	*SS*	*MS*
Between traverses	6	0·29	0·05*	15·00	2·50	1·19	0·20	9·15	1·52	0·46	0·08	0·88	0·15	1·02	0·17	8·84	1·47†	33·46	5·58
Within traverses	30	0·55	0·018	212·49	7·08	5·36	0·17	38·47	1·24	1·29	0·043	4·52	0·15	15·00	0·50	7·94	0·26	130·36	4·34
Total	36	0·84		214·10		6·55		47·62		1·75		5·40		16·02		16·78		163·82	

* Significant at 5% not at 1%.
† Significant at 1% not at 0·1%.

traverses inside the aureole and between aureole and outside the aureole (for the method of computation see HALD, 1952, p. 436). Table 2(a) confirms the conclusions drawn above that the significant difference between the traverses for TiO_2 is due to differences between traverses inside the aureole. The TiO_2 difference is not very highly significant; as great a difference, or greater, is to be expected between two random samples drawn from the same population about five times out of a hundred. This difference would possibly be better attributed to random variation than to petrological causes if direct evidence of the latter is lacking. Table 2(a)

Table 2(a)

		TiO_2		H_2O	
	v	*SS*	*MS*	*SS*	*MS*
Between traverses inside aureole	4	0·28	0·07*	1·73	0·43
Between traverses outside aureole	1	0·00	0·00	0·02	0·02
Between aureole and outside aureole	1	0·01	0·01	7·10	7·10†
Between traverses	6	0·29		8·85	
Within traverses	30	0·55	0·018	7·94	0·26
Total	36	0·86		16·79	

* Significant at 5% not at 1%.
† Significant at 0·1%.

also confirms that the significant difference between traverses for H_2O is due to differences between traverses outside and those inside the aureole

As for the previous test, a confidence interval for the differences between the means of the within aureole analyses and the means of the without aureole analyses of the different oxides may be determined, using the within traverses mean square from Table 2 as s_0^2. For SiO_2 and a confidence coefficient of 95 per cent the difference (SiO_2 within aureole — SiO_2 without aureole) lies between —1·32 and 2·5 per cent. The confidence interval is wider than the previous one. It is based on more analyses so it is probably a better estimate. This analysis of variance gives only about the same confidence interval for differences of composition between the rocks inside the aureole and those outside the aureole, although it uses thirty more analyses; on the other hand it gives a better estimate of the variance of this difference and is therefore a better test.

Method III. Another situation of statistical interest is obtained if the locations are arranged at predetermined stratigraphic intervals of the same magnitude in all traverses, so that, for example, locations 3 in all traverses are stratigraphically equivalent. PITCHER and SINHA's data contain several notable deviations from this ideal, e.g. location 1 in traverse *E* seems to be stratigraphically equivalent to locations 2 in traverses *B*–*D*. Structural complexity and the discontinuous nature of rock exposures are the main obstacles to setting up such an experiment with stratigraphical equivalence of locations from traverse to traverse. From the

amount of equivalence Pitcher and Sinha have got, on a sampling scheme not specifically designed to give equivalence, it appears that such a sampling scheme may be a practical possibility in the area, though larger locations might be needed.

Such an array of data is amenable to a two-way analysis of variance (Moroney, 1951, pp. 348–389; Dixon and Masey, 1951, pp. 127–134). Table 3 presents the

Table 3.

		TiO_2		SiO_2		FeO		MgO		CaO	
	v	*SS*	*MS*	*SS*	*MS*	*SS*	*MS*	*SS*	*MS*	*SS*	*MS*
Between traverses	6	0·28	0·047*	16·62	2·77	1·80	0·30	9·00	1·50	0·43	0·07
Between rows of locations	4	0·28	0·07†	21·79	5·45	0·25	0·062	24·52	6·13	0·29	0·07
Residual	24	0·26	0·011	186·11	7·76	3·72	0·155	13·85	0·577	0·89	0·037
Total	34	0·82		224·52		5·77		47·37		2·23	

		Na_2O		K_2O		H_2O		Diff.	
	v	*SS*	*MS*	*SS*	*MS*	*SS*	*MS*	*SS*	*MS*
Between traverses	6	0·77	0·13	1·10	0·18	7·74	1·29	34·87	5·81
Between rows of locations	4	0·49	0·12	2·05	0·51	0·12	0·03	18·41	4·60
Residual	24	3·89	0·16	7·92	0·33	7·79	0·325	106·56	4·44
Total	34	5·15		11·07		15·65		159·84	

* Significant at 1% not at 0·1%.
† Significant at 0·1%.

results of the application of this analysis to Pitcher and Sinha's data. The several cases of lack of stratigraphic equivalence between locations of the same number in different traverses could wholly or partially invalidate the results. Locations 6 in traverses *G* and *H* have been ignored since the analysis requires the same number of locations in all traverses. The loss of these data causes the numerical differences between the between traverses mean squares in Tables 2 and 3 which otherwise would be identical for the same oxide. The within traverses mean square in Table 2 has been split into two parts in Table 3, one of which is due to a

between-rows-of-locations variation and the other, termed the residual, to the several remaining possible sources of variation (p. 171).

It is therefore possible to test not only for a significant difference between traverses but also for a significant difference between rows of locations. Where there is a significant difference between rows of locations the removal of this source of variation from the residual decreases this mean square numerically, and the previous test is shown to have been unjustified. In these cases when the between traverses mean square is tested against the residual, smaller differences between traverses become recognizable. Information about compositional variation in the succession is also gained.

In Table 3 both TiO_2 and MgO show significant between-rows-of-locations differences. Examination of the original data shows that for TiO_2 the significant between-rows-of-locations difference is due to a gradual and continuous increase in TiO_2 concentration from the limestone southward, and for MgO to a gradual decrease in concentration southward. CaO also increases southward but the total change is too small to be detected as a significant difference by the test used and the data available.

These conclusions can be checked arithmetically. A simultaneous set of confidence intervals for the maximum difference between two rows of locations means, with confidence coefficient 95 per cent, is: TiO_2, 0·05 per cent to 0·43 per cent; MgO, 0·84 per cent to 3·56 per cent; CaO, −0·19 per cent to +0·50 per cent (Scheffé, 1953, pp. 87–104). The Scheffé interval is used here instead of the smaller interval based on t, since the desire for the interval arose only after the data had been analysed; the experiment was not carried out for the purpose of obtaining this interval.

Since for SiO_2 there is no significant difference between rows of locations, it turns out that the two-way analysis of variance has no greater power to detect a significant difference between traverses than the one-way analysis of variance.

Further Consideration of Pitcher and Sinha's Data

If the sampling sites, locations and traverses are arranged at random intervals in relation to the stratigraphy the intervals being obtained, for example, from a table of random numbers and carefully measured out, then not only can the significance of differences between the various means be determined, but when the differences are significant numerical estimates can be made of the compositional variation (Dixon and Massey, 1951, p. 142). The variations along the strike (between traverses) and across the strike (between rows of locations—long range, and between specimens within locations—short range) are statistics of stratigraphical importance. If the intervals employed are uniform as measured on the ground or stratigraphically or if the sites are chosen for convenience (availability of exposure) the tests can still be made but the variances obtained are not so likely to be good estimates of the stratigraphical parameters. Regularity in sampling may react with regularity in the rock (cyclical sedimentation) to give a false estimate of variation in the rock.

Where the collection of specimens is controlled by availability of exposure in an area where beds of a certain composition, owing, perhaps, to their greater or

weaker resistance to erosion, form a higher or a lower proportion of exposures than their frequency of occurrence in the succession would warrant, the data may be difficult if not impossible to interpret both statistically and intuitively. However, in practice, specimens can only be collected from exposures. Therefore petrochemical studies of the kind considered here should evidently commence with an investigation of the nature and distribution of exposures in the area, in order that the sampling plan may be capable of interpretation. Complete sections, as in coastlines and streams are of great value. Unfortunately, Pitcher and Sinha were unable to take advantage of the coastline in their area, as the rocks there are largely covered with sand (Pitcher, personal communication).

Pitcher and Sinha have five traverses in the aureole and two outside (traverse *I* is useless for present purposes). Where a difference in composition between two areas is sought an excess of analyses in one of the areas is largely wasted: the optimum conditions are obtained with an equal number of analyses in each area (Dixon and Massey, 1951, p. 148). Pitcher and Sinha had much less room for traversing outside the aureole than inside. Statistically more useful results would have been obtained by making the same number of traverses and locations inside the aureole as outside, and applying the analyses thus saved to replication at some level in the experiment. Some possibilities in this direction are considered below.

Sampling Plans with Replication

In Table I of Pitcher and Sinha (1957, p. 399) partial chemical analyses of the five specimens collected at location 1, traverse C are given. In Table 4 (this paper) the variances for the respective oxides calculated from these data are given: they

Table 4. Data from Pitcher and Sinha's Table I

	Between specimens within location variance for Loc. 1 Traverse *C*	Resid. *MS* Table 3
SiO_2	7·05	7·76
MgO	0·77	0·58
CaO	0·018	0·037
K_2O	0·033	0·33
Na_2O	0·058	0·16

may be considered as estimates of the between specimens within locations variance. In the next column in Table 4 the residual mean square for the appropriate oxide taken from Table 3 is given. This mean square includes not only the between specimens within locations variation, but also the variation due to error in analysis, the traverses times rows of the locations interaction, and effects not allowed for in the statistical analysis.

Table 4 shows that for SiO_2, MgO and CaO, the variation between the individual

specimens collected within location 1 traverse *C* is of the same order of magnitude as the residual mean square in Table 3. Thus most of the variation of the data for SiO_2 and CaO is probably due to variation between the specimens collected within each location and bulked by PITCHER and SINHA. For MgO the variation is largely due to this factor and to a variation in composition along the traverses. For the alkaline oxides the variance between specimens within location 1, traverse *C*, is very much less than the residual mean square. If the figures given in Table 4 are good estimates of the between-specimens-within-locations variance, and the data is approximately normally distributed, there is some factor causing the data to vary other than the differences between traverses, the differences between rows of locations and the differences between specimens within locations. Examination of the original data for the alkaline oxides plotted in the form of frequency diagrams reveals the occurrence of occasional apparently incompatible values in different traverses (PICHER and SINHA, 1957, p. 403). Three traverses inside the aureole and one outside the aureole contain single values of Na_2O noticeably higher than the other values. Three traverses in the aureole contain single values of K_2O noticeably higher than the remainder; the highest of these occurs in the middle of its traverse well away from the pluton. If modal values are substituted for these incompatible values and the two-way analysis recalculated, the residual mean squares obtained are numerically similar to the appropriate variances calculated from the data for location 1 traverse *C* and given in column 1 of Table 4. Since bulked samples were analysed (the analyses represent the averages of samples of five) it seems more likely that the analyses are at fault or that the samples were contaminated before analysis than that the whole locations show such high concentrations of the respective oxides.

It is apparent that the between-specimens-within-locations variation is responsible for much of the variation in PITCHER and SINHA's data. They have attempted to reduce this factor by bulking five specimens from each location. However, the variance of the bulked samples (each is in effect the mean of five unbulked samples) is only $1/\sqrt{5}$ that of the unbulked samples. To reduce effectively in this manner the between-specimens-within-locations variation would require the bulking of a very large number of specimens at each location. Alternatively, two specimens (or more) could be collected from each location and each analysed. This replication would enable the residual mean square in Table 3 to be partitioned into a between-specimens-within-locations mean square and a residual mean square. For those oxides in which the between-specimens-within-locations variation is the main cause of variation in the data, the removal of this effect from the residual mean square would give a very much more powerful test for differences between traverses. The computations would follow the form of a three-way partially-nested analysis of variance (for an account of analyses of this type see BENNETT and FRANKLIN, 1954, Section 7.63). An experiment such as this cannot be simulated with PITCHER and SINHA's data.

For geological reasons also, it is important to take the between specimens within locations variation into account rather than attempt to reduce it by bulking as PITCHER and SINHA have done. It is possible that even though no material was added to the schists by the pluton, yet under the influence of the

elevated temperatures in the aureole homogenization might have taken place, i.e. the between-specimens-within-locations variation in the aureole might be less than that outside the aureole. The analysis of variance rests on the assumption that this is not so. A separate test would have to be carried out on the data to check for this (Brownlee, 1957, p. 38; Dixon and Massey, 1951, p. 147); these tests, are, however, only applicable to normally distributed data.

This experimental design may be extended. It is normal procedure to duplicate analyses. If the rocks are analysed in batches, as is usual with modern methods of silicate analysis, it is important that the duplicate of an analysis is not made in the same batch as the initial analysis, and it is advisable for the order in which the rocks are analysed to be a random one. If the analyses in the experiment proposed above are duplicated in this way a three-way partially-nested analysis of variance with replication may be applied to them. This experimental design resolves the residual mean square into a mean square due to analytical error (within analyses mean square) and another due to traverses times specimens within locations interaction (see Table 5). An estimate of the reproducibility of the analytical results which can be compared with the known reproducibility is thus obtained as a check on the reliability of the analyses. If the interaction turns out to be significant the cause can be ascertained from a study of the original data.

In Table 5 the table of analysis of variance and the computation formulae for a three-way partially-nested analysis of variance with replication are given. Pitcher and Sinha's data cannot be used to simulate such an experiment.

An experiment such as that described above designed to test the significance of all factors likely to cause variation is not perhaps the best test for any single one of them. It does, however, provide the information necessary for planning such a test. It can also be made to provide an estimate of the number of analyses necessary to arrive at a decision with a given probability on the significance of a particular difference.

In all the statistical models presented so far it has been assumed that if a change in composition has taken place in the aureole of the Ardara Pluton the change has affected the whole width of the Cleengort Pelitic Schists (i.e. the whole length of the traverses). If the change in composition took place only in a narrow zone next to the intrusive, unless the change in composition was very great, and therefore probably recognizable in the field, it is very likely that the statistical tests would show no significant difference between the traverses. If an examination of the data gives rise to the suspicion that such a situation exists and if the stratigraphical horizon concerned can be followed outside the aureole, one of the experimental methods mentioned above could be applied to that horizon alone. Another possible line of attack would be to compare the slopes of the regression lines of chemical composition on position in traverse for the different traverses.

Conclusions

Geological conclusions to be drawn from Pitcher *and* Sinha*'s data*

(1) The rocks inside the aureole are poorer in H_2O than those outside. The difference computed from Table 2 (see also Pitcher and Sinha, 1957,

Table 5. Three-way partially-nested analysis of variance with replication.
Table of analysis of variance.

	SS	v	$E[MS]$
Between traverses $[T]$	$\frac{1}{bcd}\sum_{i}^{a}\left(\sum_{j}^{b}\sum_{k}^{c}\sum_{v}^{d}x_{ijkv}\right)^2-\frac{1}{abcd}\left(\sum_{i}^{a}\sum_{j}^{b}\sum_{k}^{c}\sum_{v}^{d}x_{ijkv}\right)^2$	$a-1$	$\sigma^2+d\sigma^2_{T\cdot S(L)}+Bcd\sigma^2_{T\cdot R}+bcd\sigma_T{}^2$
Between rows of locations $[R]$	$\frac{1}{acd}\sum_{j}^{b}\left(\sum_{i}^{a}\sum_{k}^{c}\sum_{v}^{d}x_{ijkv}\right)^2-\frac{1}{abcd}\left(\sum_{i}^{a}\sum_{j}^{b}\sum_{k}^{c}\sum_{v}^{d}x_{ijkv}\right)^2$	$b-1$	$\sigma^2+Ad\sigma^2_{T\cdot S(L)}+Acd\sigma^2_{T\cdot R}+ad\sigma^2_{S(L)}+acd\sigma^2_R$
Between specimens within locations $[S(L)]$	$\frac{1}{ad}\sum_{k}^{c}\sum_{j}^{b}\left(\sum_{i}^{a}\sum_{r}^{d}x_{ijkv}\right)^2-\frac{1}{acd}\sum_{j}^{b}\left(\sum_{i}^{a}\sum_{k}^{c}\sum_{r}^{d}x_{ijkv}\right)^2$	$b\,(c-1)$	$\sigma^2+Ad\sigma^2_{T\cdot S(L)}+ad\sigma^2_{S(L)}$
Traverses $\times$ rows of locations $[T\cdot R]$	$\frac{1}{cd}\sum_{i}^{a}\sum_{j}^{b}\left(\sum_{k}^{c}\sum_{v}^{d}x_{ijkv}\right)^2-\frac{1}{abcd}\left(\sum_{i}^{a}\sum_{j}^{b}\sum_{k}^{c}\sum_{v}^{d}x_{ijkv}\right)^2$ $-SS$ traverses $-SS$ rows of locations	$(a-1)(b-1)$	$\sigma^2+d\sigma^2_{T\cdot S(L)}+cd\sigma^2_{T\cdot R}$
Traverses $\times$ specimens within locations $[T\cdot S(L)]$	$\frac{1}{d}\sum_{i}^{a}\sum_{j}^{b}\sum_{k}^{c}\left(\sum_{v}^{d}x_{ijkv}\right)^2-\frac{1}{abcd}\left(\sum_{i}^{a}\sum_{j}^{b}\sum_{k}^{c}\sum_{v}^{d}x_{ijkv}\right)^2$ SS traverses - SS specimens with locations	$(a-1)(c-1)b$	$\sigma^2+d\sigma^2_{T\cdot S(L)}$
Within analyses	$\sum_{i}^{a}\sum_{j}^{b}\sum_{k}^{c}\sum_{v}^{d}x^2_{ijkv}-\frac{1}{d}\sum_{i}^{a}\sum_{j}^{b}\sum_{k}^{c}\left(\sum_{v}^{d}x_{ijkv}\right)^2$ $-\frac{1}{cd}\sum_{i}^{a}\sum_{j}^{b}\left(\sum_{k}^{c}\sum_{v}^{d}x_{ijkv}\right)^2+\frac{1}{bcd}\sum_{i}^{a}\left(\sum_{j}^{b}\sum_{k}^{c}\sum_{v}^{d}x_{ijkv}\right)^2$	$abc(d-1)$	σ^2
Total	$\sum_{i}^{a}\sum_{j}^{b}\sum_{k}^{c}\sum_{v}^{d}x^2_{ijkv}-\frac{1}{abcd}\left(\sum_{i}^{a}\sum_{j}^{b}\sum_{k}^{c}\sum_{v}^{d}x_{ijkv}\right)^2$	$abcd-1$	

Chemical analyses run in random order (Model II). Specimens collected within locations at random (Model II). If traverses are located at random intervals (Model II) $A=1$, if not (Model I) $A=0$. If locations located at random intervals in traverses (Model II) $B=1$, if not (Model I) $B=0$. x_{ijkv} is the vth analysis of the kth specimen at the jth location in the ith traverse, where $i\to a$, $j\to b$, $k\to c$ and $v\to d$.

p. 403) for a confidence coefficient of 95 per cent lies between 0·78 and 1·10 per cent.

(2) Traverse *B* is richer in TiO_2 than the other traverses.

(3) TiO_2 shows a significant increase in concentration southwards from the limestone (see also Pitcher and Sinha, 1957, p. 402).

(4) MgO shows a significant decrease in concentration southwards from the limestone (see also Pitcher and Sinha, 1957, p. 402).

(5) For SiO_2, MgO and CaO the between-specimens-within-location variation is the dominant one.

(6) For Na_2O and K_2O it is suggested that the main cause of variation in the data are errors in analysis or more likely (Pitcher, personal communication) in the operation of sampling.

For each oxide the value quoted by Pitcher and Sinha differs from analysis to analysis. Some of the differences are mentioned above as significant. The remainder are not significant, but not necessarily non-existent. The differences may be real but too small to detect in the data offered by Pitcher and Sinha.

Conclusions on the use of statistics in petrochemical problems

The main conclusion to be drawn is that the experiment must be planned statistically if the maximum benefit is to be gained. The main difficulty that the experimenter will meet is that of evaluating the occurrence of exposures—how representative they are of the rocks underlying the traverses and whether they can be considered to occur at random. The planning of the experiment and the evaluation of the distribution of exposures are of course common to both statistical and intuitive experiments. The only extra work involved in the former is the arithmetic. The fruits of the arithmetical labour are numerical probabilities for the veracity of the conclusions drawn, and numerical estimates of compositional variation (stratigraphical parameters).

The greatest benefit gained from the application of statistics to such experiments is, however, the logical and rigorous thinking about the experiment, which is at the same time taught to and required of the experimenter. The statistical methods do not destroy the need for intuition; they separate and simplify the issues and present them in such a form that the intuitive decisions can be made more easily and with less possibility of error.

Acknowledgements—The author wishes to express his gratitude to Dr. Pitcher for the assistance given him and to Mr. R. L. Plackett of the Department of Applied Mathematics of the University of Liverpool for his criticisms of the paper.

References

Bennett C. A. and Franklin N. L. (1954) *Statistical Analysis.* John Wiley, New York.

Brownlee K. A. (1957) *Industrial Experimentation* (4th Ed.). H.M.S.O.

Dixon W. J. and Massey F. J. (1951) *Introduction to Statistical Analysis.* McGraw-Hill, New York.

Fisher R. A. and Yates F. (1948) *Statistical Tables.* Oliver and Boyd, Edinburgh.

Hald A. (1952) *Statistical Theory with Engineering Applications.* John Wiley, New York.

Krumbein W. C. and Miller R. L. (1953) Design of experiments for statistical analysis of geological data. *J. Geol.* **61,** 510.

Moroney H. J. (1951) *Facts from Figures.* Penguin Books, Harmondsworth.

Pitcher W. S. and Sinha R. C. (1957) The petrochemistry of the Ardara aureole. *Quart. J. Geol. Soc.* **113,** 393.

Riley J. P. (1958) The rapid analysis of silicate rocks and minerals. *Anal. Chim. Acta* **19,** 413.

Scheffé H. (1953) A method for judging all contrasts in the analysis of variance. *Biometrika* **40,** 87.

Shapiro L. and Brannock W. W. (1956) The rapid analysis of silicate rocks. *Bull. U.S. Geol. Surv.* 1036–C.

Geochimica et Cosmochimica Acta, 1959, Vol. 17, pp. 176 to 185. Pergamon Press Ltd. Printed in Northern Ireland

Origin of Be^{10} and Al^{26} in tektites

R. D. Cherry and S. R. Taylor
Department of Physics, and Department of Geology, University of Cape Town

(*Received* 2 March 1959)

Abstract—An attempt is made to show that the recently reported amounts of Be^{10} and Al^{26} in tektites can possibly be explained in terms of Urey's "comet" hypothesis for tektite origin. On the basis of our calculations we obtain a similar level of Be^{10} activity to that reported by Ehmann and Kohman (1958) but a somewhat lower figure for Al^{26} activity.

It is shown that by mixing one part of chondritic silicate, which is assumed to represent the non-volatile comet material and to contain the radioactive nuclides, with thirteen parts of arkose-like material, the overall tektite composition can be accounted for rather satisfactorarily.

1. Introduction

Ehmann and Kohman (1958) have recently reported the existence in tektites of the long-lived radioactive isotopes, $Be^{10}(t_{1/2} : 2{\cdot}7 \times 10^6$ years) and $Al^{26}(t_{1/2} : 8 \times 10^5$ years), and suggest that the level of activity indicates that tektites have spent at least 10^6 years outside the earth's atmosphere, exposed to cosmic radiation. Since Urey (1955, 1957) has calculated that a swarm of tektites would not be stable in the solar gravitational field at a distance of one astronomical unit, Kohman (1958) was led to propose that the tektites came from outside the solar system, thus ensuring a suitably long exposure to cosmic radiation. Such a postulate, however, is not in accord with data suggesting either a terrestrial, or at least solar-system origin for tektites (Barnes, 1958; Barnes *et al.*, 1958; Friedman, 1958; Taylor and Ahrens, 1959; Tilton, 1958; Urey, 1957, 1958).

In a reply to Kohman (1958), Urey (1958) lists four criteria which must be explained by any theory of origin of tektites and points out that his "comet explosion" theory (Urey, 1957) explains three of them (composition, distribution and melting). The fourth criterion (presence of Be^{10} and Al^{26}) is not explained, although Urey (1958) suggests that the comet head was a possible source. The purpose of this paper is to show that this suggestion seems to be a reasonable possibility.

2. A Comet Model

Whipple (1950, 1951) has proposed a comet model in which the comets are considered to consist of solid compounds of C, O, N and H, and finely divided dust of meteoritic composition. The composition of this dust should be closely related to that of the non-volatile material of the original dust and gas disk from which the solar system units have condensed. For reasons which are explained later (Sections 5 and 6), we obtain the best fit for the hypothesis if we take this composition to be that of the silicate phase of chondritic meteorites.

Whipple (1950, 1951) has pointed out that the C, O, N and H compounds in the comet evaporate on close approach to the sun and that the resulting comet structure has an insulating layer of meteoric dust enclosing the unstable compounds and more dust. Urey (1957) gives radii for such bodies of 10–70 km with a density of 0·01 gcm^{-3}.

After the explosion postulated by Urey (1957) resulting from the close approach of the comet to the earth, there will presumably be some mixing between the molten terrestrial material (which is propelled in all directions) and at least some of the meteoritic dust from the comet. The tektites, after solidifying and falling to earth (when a second period of melting may result) will then consist of a mixture of terrestrial material, which can reasonably be assumed to be the main component, and material from the comet head. Most of this comet material is likely to come from the insulating layer of dust in which perhaps the bulk of the meteoritic material of the comet is located: we shall now investigate the possibility of the production of Be^{10} and Al^{26} in this extraterrestrial material.

3. Production of Be^{10} and Al^{26} in Comets

We can assume that the comet material is of such an age that secular equilibrium has been reached in the production of Be^{10} and Al^{26} and thus the rate of decay is equal to the rate of production of these nuclides.* To determine this quantity, we have performed calculations along the lines followed by Reasbeck and Mayne (1955). We have used the data of Lock *et al.* (1955) on 950 MeV protons in order to obtain estimates for cross-sections and star sizes, and a figure of 0·22 particles cm^{-2} $steradian^{-1}$ sec^{-1} for the cosmic ray flux at the top of the atmosphere (Singer, 1958). Following Reasbeck and Mayne (1955) we have used an He/p ratio for star particles of $\sim$0·3. We have not, however, allowed a factor of 2 for the earth's shielding effect as they did. The comet head is assumed to be 10–70 km in diameter and will therefore act as a shield in roughly the same way as the earth.

We have used the average chondritic silicate data of Urey and Craig (1953) for the amounts of Si, Mg, Fe and O in the comet shell (see discussion in Section 6 for this choice) and on this basis have worked out the approximate rates of production of Al and Be due to cosmic radiation. Not all the Al nuclei will be Al^{26}, nor will all the Be nuclei be Be^{10}. To allow for the amounts of the other Al and Be isotopes (mainly Al^{27} and Be^{9}) we have multiplied our results by a rather arbitrary figure of 0·3; this is probably the most uncertain feature of the calculation.†

---

* On the basis of the half-lives of Be^{10} and Al^{26} about 10^7 years are necessary to reach this equilibrium: the comet dust can be assumed to have condensed early in the history of the solar system and thus have been exposed to cosmic radiation for perhaps $4{\cdot}5 \times 10^9$ years. We shall not make any allowance for effects dependent on the past history of an individual comet. For example, material in the interior of a comet with a very thick insulating layer will have become increasingly shielded with time and the secular equilibrium will no longer hold.

† Batzel *et al.* (1951) suggest that "the most probable yield for a given Z is a region two mass units wide and that the yields one mass unit on either side of this region are formed in yields about 1·5 times lower than the values in the region of maximum yield, that spallation yields two mass units removed are about ten times lower than the maximum and that yields three mass units removed are about a factor of twenty lower than the maximum." On this basis the two nuclei in the "maximum yield region" account for about 0·55 of the total yield for any Z. It seems likely that both Al^{26} (with Al^{27}) and Be^{10} (with Be^{9}) fall in "maximum yield regions" and the factor for each should therefore be $\sim(0{\cdot}55)(k)$ plus a little extra to allow for the decay of short lived isotopes of neighbouring Z. k allows for the relative yields of the two isotopes within the "maximum yield region" and might be expected to vary round about 0·5 depending on whether the isotope concerned is *e–e*, *o–e*, *e–o*, or *o–o*. Present experimental information concerning either spallation yields or the relative density of excited states of the competing isotopes (which might be expected to give an indication of the spallation yields of the ground states) is, we feel, too inadequate to give reliable estimates and we have preferred to put $k = 0{\cdot}5$. Thus we get our figure of $\sim$0·3 for the multiplying factor. It should be noted that Batzel *et al.* were concerned with 340 MeV protons; we have assumed that the same considerations hold at higher energies.

The results are given in Table 1 together with values obtained, as were those of Reasbeck and Mayne (1955), from the data of Lord (1951). Lord's results were obtained at a height of 1·1 cm Hg atmospheric pressure and could thereby include the effects of secondary particles, whereas our flux figure applies to the top of the atmosphere. One would expect Lord's data to give values of 1·5 times those obtained at the very top of the atmosphere, whereas in fact they are only about 0·9 times. This discrepancy is probably indicative of the uncertainty of our estimates. This uncertainty is further increased by the fact that effects due to lower energy protons (i.e. those below the cut-off energy operational at 55° latitude). particles in the belt of ionizing radiation discovered by the artificial satellites and

Table 1. Production rates (atoms/g per min) of Be^{10} and Al^{26} from various elements. Contributions from other elements (e.g. Al and Ca) will be present but are likely to be small (~5–10% of the total).

	Be^{10}		Al^{26}	
Parent material	Lord data	Lock data	Lord data	Lock data
Fe	0·0001	0·0001	0·0005	0·0005
Si	0·0021	0·0024	(0·0034)	0·0035
Mg	0·0025	0·0044	—	—
O	0·0125	0·0144	—	—
Total	0·0172	0·0213	0·0039	0·0040

other imponderable factors have not been taken into account. We feel that these effects would all tend to raise our estimates. Despite these uncertainties, it seems reasonable to assume that our estimates are probably correct to an order of magnitude (cf. the calculations of Sheline and Hooper (1957) who obtain a figure of ~0·03 dis/min per g for the Mn^{53} activity in iron meteorites).

The values in Table 1 are not of course the final results. They must be reduced by a factor which allows for the "mixing ratio" between the particles of the comet shell and the molten material from the earth's surface. If we assume this factor to be about 1/13 (see discussion later for this choice) we obtain final estimates of ~0·0015 dis/min per g for Be^{10} and ~0·0003 dis/min per g for Al^{26} in tektites of recent origin (<5×10^6 years). Ehmann and Kohman (1958) give values ranging from 0·0012 to 0·0052 dis/min per g for Be^{10} and from 0·003 to 0·04 for Al^{26} in tektites.* Compared with these figures, our estimates are therefore about correct for Be^{10} and too low for Al^{26}.

4. Production of Be^{10} and Al^{26} in Terrestrial Materials

We must also consider the possibility of Be^{10} and Al^{26} occurring in normal terrestrial materials. Peters (1955, 1957) has discussed the production of Be^{10}

* For the australites, the figures are 0·0030 dis/min per g for Be^{10} and 0·04 dis/min per g for Al^{26} activity.

from oxygen and nitrogen in the upper atmosphere. He quotes an experimentally observed value of $1{\cdot}56 \times 10^{10}$ Be^{10} nuclei per gram of ocean sediment and shows that this agrees well with a theoretical calculation which assumes that Be^{10} is deposited via the medium of rain-water. He assumes an annual rainfall of 90 cm, a figure which is probably ten times higher than the average rainfall in the desert area we postulate (see Section 5). Further, ocean sediment is more likely to be effective in absorbing Be than surface material in deserts. This effect is difficult to estimate but we suggest a factor of at least 2. We therefore reduce PETER's figure to $0{\cdot}88 \times 10^9$ Be^{10} nuclei/g, which gives us a disintegration rate of 0·0004 dis/min per g. Al^{26} could be produced from argon in the upper atmosphere but the amounts will probably be down by a factor of 100 on the Be^{10} figure. Thus, while the presence of Be^{10} in terrestrial samples might be accounted for by this process it does not seem a possibility for Al^{26}.

5. Composition of Tektites from Mixing of Comet and Terrestrial Materials

We shall now examine the degree of mixing required between the material of the comet head and surface material on the earth. The average composition of the tektites listed by SPENCER (1939) is given in Table 1, column 1. Unfortunately, we do not have access to the compilation of tektite analyses made by BARNES (1940). The composition of tektites shows a general resemblance to that of the more acid igneous and sedimentary rocks; this similarity has been noted by many authors. The tektites are, however, notably high in MgO and no abundant terrestrial rocks of equivalent composition are known.

MASON (1959) has pointed out that it is possible to produce material of tektite composition by igneous processes. He has selected individual analysis of igneous rocks from WASHINGTON's (1917) monumental compilation to match individual tektite analyses over the range 68·60 to 97·58% SiO_2. MASON has thus been able to contradict the assertion by UREY (1958) that: "Tektites have chemical compositions remarkably similar to those of the more acid sedimentary rocks. . . . . Such a composition is not produced by any other naturally occurring process that we know of, except perhaps in very rare and special circumstances."

The MgO content of tektites is very high for material of such high silica content. The average of those listed by SPENCER (1939) is 2·27 per cent. We have examined the superior analyses of igneous rocks listed by WASHINGTON (1917) and have plotted, in Fig. 1(a), the MgO content of all those with more than 68% SiO_2 (1250 determinations).* The arithmetic mean of the determinations (excluding those reported as "trace", "none" or "not detected") is 0·56% MgO. This is a factor of about four lower than the average MgO content (2·27%) of the tektites listed by SPENCER (1939). Fig. 1(b) shows a frequency diagram of MgO determinations in a granite (G-1) by thirty-four analysts (FAIRBAIRN *et al.*, 1951) and is included here to indicate the precision of MgO determinations at this concentration. A frequency plot of the MgO determinations in tektites is given in Fig. 1(c). It can be seen clearly that the mode for the tektites is distinctly separated from that of the igneous rocks. Fig. 2 shows the MgO determinations in (a) igneous rocks and (b) tektites

* Thirty-six analysts listed MgO as "none" or "not detected" and sixty-seven listed MgO as "trace".

plotted on a log scale. Again the two modes are separate. The negative skew shown by the MgO determinations in igneous rocks may be a real effect, but the precision of chemical determinations at these levels is poor. Ahrens (1954) estimates the

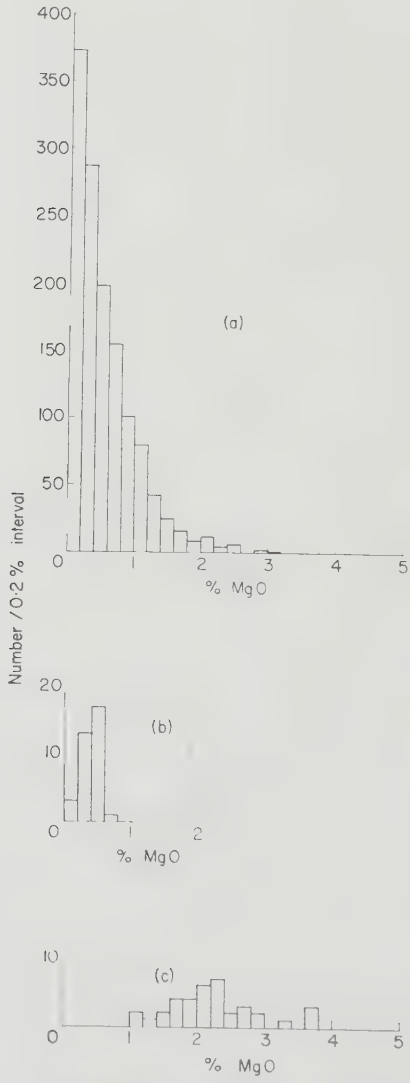

Fig. 1. (a) Histogram of MgO content in 1250 igneous rocks with more than 68% SiO_2 compiled from Washington (1917). Two determinations fall in the interval 4·0–4·20% MgO. (b) Histogram of determinations of MgO in one granite (G-1) by thirty-four analysts (Fairbairn *et al.*, 1951). (c) Histogram of MgO content in twenty-six tektites listed by Spencer (1939). A 0·2 per cent interval is used.

Fig. 1(a) after Washington(1917).

relative deviation at the 0·3% MgO level to be 32 per cent and it is likely to be much higher at 0·01% MgO level.

It can be seen from Fig. 1 and 2 that there is a certain amount of overlap

between the tektite determinations and those from the igneous rocks. Thus it is possible to match individual igneous rock and tektite determinations. Although it is not impossible to produce material of tektite composition by igneous processes, the statistical evidence from the MgO contents given above indicates that this is an infrequent event, although more common than implied in UREY's statement quoted above.

SPENCER (1933) in discussing the origin of tektites by fusion of terrestrial material by meteorite impact notes that "the terrestrial rock at the time of fall

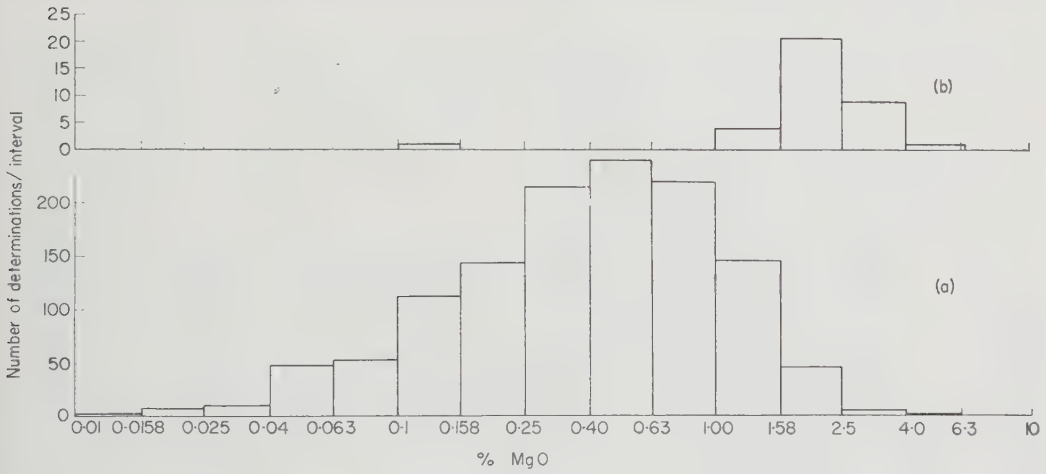

Fig. 2. (a) Histogram of MgO content of 1250 igneous rocks with more than 68% SiO_2 plotted on a log scale. (b) Histogram of MgO content of twenty-six tektites plotted on a log scale. A power factor of 1·58 is used to give the interval.

must be of the right kind, such as sandstone or quartzite, or, perhaps best of all, clean desert sand. The composition of tektites indicates that a certain amount of feldspar, mica or clayey material was present in the rock (arkose or siltstone)."

The only common sedimentary rocks* containing high SiO_2, Al_2O_3 and K_2O are the arkoses and an average arkose composition is listed in Table 2 column 2. (PETTIJOHN, 1957, p. 324). It can be seen to bear a general resemblance except that MgO is very low compared with the tektite. In column 3, Table 2 is given the average of the silicate phase of chondrites (high and low groups) from UREY and CRAIG (1953, Table 4) with new figures for Na_2O and K_2O from EDWARDS (1955). Since the correction is very small we have not recalculated the other constituents, so that the sum becomes 99·58.

In column 4, Table 2, is given the composition of a mixture of one part chondritic silicate (column 3) with thirteen parts of arkose. It can be seen that this bears a rather close resemblance to the tektites, containing, in particular, significant amounts of SiO_2, K_2O and MgO. This composition is very difficult to produce by conventional geological processes. The outstanding anomaly is that K_2O is too

* Granite has too low a silica content (average: 70·18% SiO_2; BARTH, 1952, Table 33, p. 69) for it to be a satisfactory source material for tektites.

high by a factor of 2. This can be adjusted fairly readily. In the five arkose analyses given by Pettijohn (1957) CaO varies from 0·15–3·09%, Na_2O from 0·50 to 3·30% and K_2O from 3·35 to 6·16%. Total modal feldspar ranges from 30 to 64%. The K_2O : Na_2O : CaO averages in the tektite indicate a theoretical Or : Ab : An ratio of 14·4 : 11·9 : 12·7 or rather close to unity. If we assume an arkose to contain 50% quartz and 50% feldspar with Or, Ab and An components equal, we obtain the composition given in Table 2, column 5. If this is mixed with the chondritic silicate (column 3) we get the composition in column 6 which gives more reasonable alkali figures. If we add 3·73% FeO to this theoretical arkose we

Table 2. Comparison of composition of tektites with various mixtures of chondrite silicate with arkose or arkose-like material. The average tektite composition is given in column 1. This should be compared with columns 4, 6, 8 and 10.

	1	2	3	4	5	6	7	8	9	10
SiO_2	**73·08**	76·37	47·04	**74·28**	79·40	**77·09**	76·44	**74·34**	75·57	**73·53**
Al_2O_3	**12·69**	10·63	3·09	**10·09**	12·50	**11·83**	12·03	**11·39**	11·38	**10·78**
FeO*	**4·56**	3·12	15·40	**4·00**	—	**1·10**	3·73	**4·56**	2·36	**3·29**
MgO	**2·27**	0·23	29·48	**2·32**	—	**2·11**	—	**2·11**	0·72	**2·78**
CaO	**2·55**	1·30	2·41	**1·38**	3·35	**3·28**	3·23	**3·17**	1·69	**1·74**
Na_2O	**1·41**	1·84	0·90	**1·77**	1·95	**1·90**	1·88	**1·79**	2·45	**2·28**
K_2O	**2·43**	4·99	0·10	**4·64**	2·30	**2·14**	2·21	**2·06**	3·35	**3·12**
Cr_2O_3†	**0·006–0·055**	—	0·45	**0·032**	—	**0·032**	—	**0·032**	—	**0·032**

* Total iron expressed as FeO.
† Preuss (1935), see text.

1. Average of thirty-six analyses of tektites (Spencer, 1939, Table 1).
2. Average arkose (Pettijohn, 1957, Table 56, anal. F).
3. Average silicate phase of chondrites (Urey and Craig, 1953, Table 4) Na_2O and K_2O from Edwards (1955).
4. Mixture of thirteen arkose (col. 2) and one part chondritic silicate (col. 3).
5. Composition of a mixture of 50% quartz and 50% feldspar (Or = Ab = An).
6. Mixture (13/1) of quartz–feldspar (col. 5) and chondritic silicate (col. 3).
7. Composition of a 1 : 1, quartz: feldspar mix containing 3·73% FeO.
8. Mix (13/1) of column 7 with chondritic silicate (col. 3).
9. Torridonian arkose (Pettijohn, 1957, p. 324, Table 56, anal. C).
10. Mixture of thirteen parts Torridonian arkose (col. 9) with one part chondritic silicate (col. 3).

get the composition given in column 7. This mixed on a 13/1 mix with the meteoritic silicate results in the composition in column 8. This is very close to column 1 in composition. We feel that few geologists would take exception to the composition listed in column 7 which could represent a sand with equal amounts of quartz and feldspar, with a little iron oxide cement. It is, in fact, rather close in composition to the widespread Torridonian arkose listed by Pettijohn (1957, p. 324) and given here in column 9. In column 10, the result is given of mixing thirteen parts of Torridonian arkose with one part of chondritic silicate (column 3). The result is again very similar to the average tektite composition given in column 1.

It should be noted that the tektites listed by Spencer (1939) vary somewhat in composition. For example, SiO_2 ranges from 68·00% to 80·73% and MgO from

1·22% to 4·05% (excluding one very low value of 0·11%). Using the MgO content as the mixing index, we obtain a standard deviation spread from 9 to 19 in the mixing ratio. On the basis of the comet hypothesis, non-uniformity in composition of the tektites can reasonably be expected. The mixing of the two materials might be expected to vary depending on distance from the centre of the explosion, and one group of tektites might show significant differences from another group.

Urey (1957) did not estimate what depth of material would be affected by the explosion, beyond stating that a very broad shallow crater might result. This would be very difficult to detect. If the depth is very small (less than a few metres) we must assume that the explosion took place over an area without thick soil cover, since it is not possible to account for the tektite composition if much material of the composition of soil was involved.

Thus we need an area without soil cover and with material of arkose composition at the surface. These conditions would be fulfilled quite readily by a combination of an arid climate and a granite terrain, since arkose is common as a surface mantle under these circumstances. These are widespread enough to avoid the necessity to postulate a special or unique geological environment. It does not appear unreasonable that these conditions were existent in Australia at the time of formation of the australites.

These conditions are consistent with the low water content of tektites reported by Friedman (1958, p. 320) who states that "the difficulty of removing water may have restricted tektite formation by Urey's process to initially dry sediments found on a desert surface." Friedman's paper provides strong supporting evidence for Urey's hypothesis.

6. Composition of Comet Dust

We will now examine the assumption that the material in the comet head has the composition of the silicate phase of chondrites. We began to make these calculations using the average composition of cosmic non-volatile material given by Suess and Urey (1956) and also the data given by Ringwood (1959) for completely oxidized non-volatile material. Both these estimates take into account small but significant amounts of meteoritic metallic phase. Ringwood's average, for example, contains 2·27% NiO.

If material containing this amount of nickel had been mixed we could expect tektites to contain large amounts of Ni (>1000 p.p.m.). The only data available to us are some old spectrographic determinations by Preuss (1935). For tektites he gives a range of 20 to 350 p.p.m. NiO and 60 to 550 p.p.m. Cr_2O_3. Through the courtesy of Dr. Crompton, South African Museum, Cape Town, we obtained an australite. A semiquantitative spectrographic analysis showed that it contained about 40 p.p.m. Ni, 50 p.p.m. Cr and 400 p.p.m. Zr. These figures are based on comparison with the standard diabase, W-1 and granite, G-1, using the values recommended by Ahrens and Fleischer (1959). These figures indicate that Preuss' data is probably of the right order of magnitude and rule out the possibility of mixing in meteoritic metal phase. We were thus constrained to use the silicate phase of chondrites as the most reasonable approximation to the composition

of the material in the comet head. It should be noted that the production rates of Be^{10} and Al^{26} calculated using these three sets of data are very similar.

It is of interest to note that the amount of Ni and Cr in tektites, although low, is much more than could reasonably be expected in an arkose, by a factor of 5 or 10 (Krauskopf, 1955), and that the Cr content, and probably Ni as well, can be derived from the chondritic silicate (cf. columns 1, 2, 3 and 4 of Table 2). The comparatively large amount of zirconium found is consistent with derivation from an arkose type sediment.

7. Conclusions

On the basis of the above discussions on chemical composition and radioactive contents of tektites, we feel that the Urey "comet" hypothesis can be considered to explain the relevant facts satisfactorily. The one discrepancy is the Al^{26} content, but we would point out that, as mentioned earlier, our estimates are likely to be low. We would require a factor of 10 or greater to explain the discrepancy; while large, this is not by any means impossible. Although the assumptions in the Urey hypothesis are many, it seems inherently more plausible than the theories of Kohman (1958), O'Keefe, *et al.* (1958) (see reply by Barnes *et al.*, 1958) and other older postulates. These have been adequately summarized by Barnes (1958). The most reasonable rival hypothesis to Urey's comet proposal is that tektites are derived from the disintegration of a planet similar to the earth. In order to provide the observed Be^{10} and Al^{26} activities, it would be necessary for the tektites to spend up to 10^7 years in transit to the earth. We should like to stress the desirability of Ehmann and Kohman's work being repeated with a wide variety of tektites from different areas. Quite apart from providing a check on theories of tektite origin, radioactivity data from large numbers of samples would provide fuel for future quantitative studies. The provision of precise and accurate determinations of major and trace elements on the various groups of tektites would solve many of the problems raised in this paper.

References

Ahrens L. H. (1954). A note on the relationship between the precision of classical methods of rock analysis and the concentration of each constituent. *Mineral. Mag.* **30,** 467–470.

Ahrens L. H. and Fleischer M. (1959) Report on trace constituents in standard granite G-1 and standard diabase W-1. *Bull. U.S. Geol. Surv.* In press.

Barnes V. E. (1940) North American tektites. *Univ. Tex. Publ.* 3945, 477–656.

Barnes V. E. (1958) Properties of tektites pertinent to their origin. *Geochim. et Cosmochim. Acta.* **14,** 267–278.

Barnes V. E., Kopal Z. and Urey H. C. (1958) Origin of tektites. *Nature, Lond.* **181,** 1457–1458.

Barth T. F. W. (1952) *Theoretical Petrology.* John Wiley, New York.

Batzel R. E., Miller D. R. and Seaborg, G. T. (1951) High energy spallation products of copper. *Phys. Rev.* **84,** 677.

Begemann F. and Libby W. F. (1957) Continental water balance, ground water inventory and storage times, surface ocean mixing rates and world-wide water circulation patterns from cosmic-ray and bomb tritium. *Geochim. et Cosmochim. Acta* **12,** 227–296.

Edwards G. (1955) Sodium and potassium in meteorites. *Geochim. et Cosmochim. Acta* **8,** 285–294.

Ehmann D. and Kohman T. P. (1958) Cosmic-ray induced radioactivities in meteorites. II. Al^{26}, Be^{10} and Co^{60} in aerolites, siderites and tektites. *Geochim. et Cosmochim. Acta* **14,** 364.

Fairbairn H. W. *et al.* (1951) A co-operative investigation of precision and accuracy in chemical, spectrochemical and modal analyses of silicate rocks. *Bull. U.S. Geol. Surv.* 980.

Friedman I. (1958) The water, deuterium, gas and uranium content of tektites. *Geochim. et Cosmochim. Acta* **14,** 316–322.

Kohman T. P. (1958) Are tektites extra-solar system meteorites? *Nature, Lond.* **182,** 252–253.

Krauskopf K. B. (1955) Sedimentary deposits of rare metals. *Econ. Geol.* Fiftieth Anniversary Volume, 411–463.

Lock W. O., March P. U., Muirhead H. and Rosser W. G. V. (1955) Nuclear interactions of 950 MeV protons. *Proc. Roy. Soc.* A **230,** 215–221.

Lord J. J. (1951) The altitude and latitude variation in the rate of occurrence of nuclear disintegrations produced in the stratosphere by cosmic rays. *Phys. Rev.* **81,** 901–909.

Mason B. H. (1959) Chemical composition of tektites. *Nature, Lond.* **183,** 254–255.

O'Keefe J. A., Varsavsky C. M. and Gold T. (1958) Origin of tektites. *Nature, Lond.* **181,** 172–174.

Peters B. (1955) Radioactive beryllium in the atmosphere and on the earth. *Proc. Indian Acad. Sci.* **41,** 67.

Peters B. (1957) Uber die Anwendbarkeit der Be^{10} -Methode zur Messung kosmischer Strarhlungsintensitat und uber Ablagerungsgeschwindigkeit von tiefsee Sedimenten vor einigen Millionen Jahren. *Z. Phys.* **148,** 93–111.

Pettijohn F. J. (1957) *Sedimentary Rocks* (2nd Ed.) Harper.

Preuss E. (1935) Spektralanalytische Untersuchungen der Tektite. *Chem. d. Erde* **9,** 365–418.

Reasbeck P. and Mayne K. I. (1955) Cosmic radiation effects in meteorites. *Nature, Lond.* **176,** 733–734.

Ringwood A. E. (1959) On the chemical evolution and densities of the planets. *Geochim. et Cosmochim. Acta.* **15,** 257–283.

Sheline R. K. and Hooper J. E. (1957) Probable existence of radioactive Mn^{53} in iron meteorites. *Nature, Lond.* **179,** 85–87.

Singer S. F. (1958) *Progress in Elementary Particle and Cosmic Ray Physics.* Vol. 4, p. 275.

Spencer L. J. (1933) Origin of tektites. *Nature, Lond.* **131,** 117.

Spencer L. J. (1939) Tektites and silica glass. *Mineral. Mag.* **25,** 425–440.

Suess H. E. and Urey H. C. (1956) Abundances of the elements. *Rev. Mod. Phys.* **28,** 53–74.

Taylor S. R. and Ahrens L. H. (1959) Significance of K/Rb ratios for theories of tektite origin. *Geochim. et Cosmochim. Acta* **15,** 370–372.

Tilton G. R. (1958) Isotopic composition of lead from tektites. *Geochim. et Cosmochim. Acta* **14,** 323–330.

Urey H. C. (1957) Origin of tektites. *Nature, Lond.* **179,** 557.

Urey H. C. (1958) Origin of tektites *Nature, Lond.* **182,** 1078.

Urey H. C. and Craig H. (1953) The composition of the stone meteorites and the origin of the meteorites. *Geochim. et Cosmochim. Acta* **4,** 36–82.

Washington H. S. (1917) Chemical analyses of igneous rocks. *Prof. Pap. U.S. Geol. Surv.* 99.

Whipple F. L. (1950) A comet model. I: The acceleration of Comet Encke. *Astrophys. J.* **111,** 375.

Whipple F. L. (1951) A comet model. II: Physical relations for comets and meteors. *Astrophys. J.* **113,** 464.

Geochimica et Cosmochimica Acta, 1959 Vol. 17, pp. 186 to 200. Pergamon Press Ltd. Printed in Northern Ireland

A geochemical study of the shales of the Lower Cambrian Manganese Shale Group of the Harlech Dome, North Wales

P. A. Mohr
University College of Addis Ababa, Ethiopia

(*Received* 4 *March* 1959)

Abstract—The shales of the Manganese Shale Group are featured geochemically by their relatively high manganese content, the predominance of ferrous over ferric iron, the sympathetic behaviour of cobalt, nickel, chromium, and vanadium with total iron, an inverse relationship of strontium and barium and a direct relationship of boron and barium. Evidence is presented to indicate that the source rocks of the Manganese Shales were acid gneisses.

Introduction

A study has been made of the geochemical variations in the shales of the Manganese Shale Group which forms part of the Harlech Grits Series, both across their basin of deposition and throughout their stratigraphical column. Such a study directly involved new data being obtained on the geochemistry of shales, and also the possibility of interpreting the source and conditions of deposition of the original sediments.

The choice of the Manganese Shale Group was decided by four factors:

(1) The sediments were deposited in a basin separate from other areas of contemporaneous sedimentation, and as such are well suited to the programme outlined above.

(2) The edges of the original basin of deposition appear to correspond fairly closely with the present outcrop round the Harlech Dome (Woodland, 1938a).

(3) The Manganese Shale Group shows a remarkably constant lithology of typical fine-grained shale over the whole of its exposure and also throughout the greater part of its stratigraphical column (concerning the latter an important exception is the occurrence of the Manganese Ore and associated rocks, the geochemistry of which has been summarized in Mohr, 1956).

(4) The geochemistry of the original sediments is unlikely to have been greatly affected by post-depositional processes, the metamorphism which they have undergone being of the lowest chlorite zone (except at Hendre, see Woodland, 1938b).

Specimens from the same horizon occurring at St. Tudwal's Peninsula, Caernarvonshire, have been included in this study.

Field Relationships

The detailed stratigraphy and geological history of the Cambrian rocks of the Harlech Dome have been described by Matley and Wilson (1946). The

Manganese Shale Group, with which this paper is concerned, is divided as follows:

Harlech Dome:

Upper Manganese Shales	600 ft (average thickness)
Manganese Grit	40 ft
Mudstones	40 ft
Bluestone Grit	3 ft
Bluestone	6 ft
Manganese Ore	10 in.
Pyritiferous Mudstone	2 in.
Lower Manganese Shales	30 ft

St. Tudwal's:

Grits with interbedded mudstones showing "manganese" weathering	450 ft
Grits and mudstones very rich in manganese	50 ft

Method of Sampling

Samples of shale from the Lower and Upper Manganese Shales were taken from six localities round the Harlech Dome: the road-section at Llechwedd-du-bach near Harlech (code letters HA); the western slopes of Moelfre (MO); Cell Fechan, near Barmouth (BA); the north-east shoulder of Diphwys (DI); the south-west slopes of Y Garn (YG); the river section at Afon Gamlan (AG). The samples were collected at as regular intervals as exposures allowed from the base to the top of the Manganese Shale Group. The vertical interval of sampling was 50–100 ft, according to locality, throughout the total thickness of shales. Samples with the code number 1 were taken from the very base of the Lower Manganese Shale, and the numbers increase up the stratigraphical column (at Afon Gamlan the topmost shales are cut out by a sill). A similar plan was followed at St. Tudwal's (ST).

Care was taken to make the sampling as representative as possible, each shale sample being taken as a number of fresh pieces obtained within an horizon of about 1 ft and along about 10 ft of the strike.

Owing to the time-factor not all the specimens collected could be analysed and a selection was made based on a preliminary petrographic study.

Petrography

Macroscopically the shales are rather dark, uniformly grey–green rocks often showing a submetallic sheen on fracture planes. They are very fine-grained and compact, though having a tendency to fissility along the bedding planes. The effect of cleavage is visible in some specimens.

Microscopically the shales are seen to consist essentially of detrital quartz grains and white mica flakes in an extremely fine-grained matrix of recrystallized chlorite and sericite, the latter orientated sub-parallel to the bedding plane. The

quartz grains have an average diameter of 0·05 mm and are most commonly subangular. White mica flakes vary considerably in abundance from specimen to specimen but are always present, and when very abundant the fissility of the rock is markedly increased. The flakes vary in length, from 0·2 to 0·04 mm. The minute laths and flakes of chlorite and sericite whose intergrowth forms the matrix of the rock have a grain-size of from 0·05 to 0·005 mm. Accessory minerals vary considerably both in type and abundance even within a single specimen. Detrital grains of badly weathered orthoclase and remarkably fresh oligoclase occur in most specimens, but quartz always predominates exceedingly over feldspar. Magnetite grains are abundant in certain bands as small "placers", less commonly ilmenite also. Smaller euhedral grains of magnetite scattered sparsely throughout the rock are probably authigenic. Large patches of recrystallized, deep-green chlorite, usually strongly pleochroic and showing anomalous interference colours, occur in some of the shales. Small rounded zircons occur in most of the shales, especially in the magnetite-rich bands, but rutile, garnet, pyrite and tourmaline are more rare. Very rare are barytes, haematite, calcite, epidote and badly altered grains of biotite and hornblende.

The proportion of detrital to authigenic minerals varies somewhat for different specimens, and for bands within a given specimen, but generally the volume proportions are about equal.

Chemistry

(a) *Major elements*

Eight specimens of Manganese Shale have been analysed by gravimetric methods for the major elements, and in addition a specimen of Llanbedr Slate (LS). (The Llanbedr Slate occurs below the Rhinog Grits which themselves underlie the Manganese Shale Group.) The results are given in Table 1.

Furthermore, total iron (as Fe_2O_3) and MnO have been determined on seven additional shales, and all the results obtained for these two oxides are given in Table 2, with the calculated Mn/Fe ratios.

Taking the seven typical Manganese Shales HA 5A, HA7, HA9, BA8, YG1, and AG1 (HA5B is a fine-grained grit rich in carbonate), an average composition can be calculated and is compared with the data of some previous workers in Table 3. The Manganese Shale composition differs significantly from other data on shales in showing high MnO, total iron, TiO_2 and Al_2O_3, and low CaO, MgO, P_2O_5, and CO_2. FeO predominates over Fe_2O_3. Assuming the averages of Clarke and of Nanz reflect a characteristic environment for shales the following deductions can be made concerning the deposition of the Manganese Shale:

Low CaO, P_2O_5 and CO_2, i.e. low $CaCO_3$ and $Ca_3(PO_4)_2$, indicate the scarcity or absence of living organisms. The high TiO_2 and Al_2O_3 may be related, the greater part of the titanium in the sedimentary cycle entering the clay minerals of the hydrolysate sediments, this predominating quantitatively over the titanium bound in detrital minerals such as ilmenite and rutile. The ratio Ti/Al in marine hydrolysates is normally about 1/20 (Goldschmidt, 1954). It is rather higher in the Manganese Shale, 1/16·6, possibly due to the detrital ilmenite frequently observed in thin-section. High Al_2O_3 in the Manganese Shale signifies that the

Table 1. Analyses of eight Manganese Shale and one Llanbedr Slate specimen

	HA5B	HA5A	HA7	HA9	MO1	BA8	YG1	AG1	LS
SiO_2	67·84	61·50	56·44	60·03	53·99	60·80	62·32	58·41	55·08
TiO_2	0·55	0·92	1·07	1·82	0·82	0·80	1·28	1·23	1·11
Al_2O_3	7·84	16·02	18·54	19·19	21·49	18·07	15·75	22·22	22·55
Fe_2O_3	1·22	2·93	2·82	0·96	1·20	3·71	3·63	1·91	7·17
FeO	5·32	7·12	8·21	5·77	5·24	4·77	6·68	4·68	3·12
MnO	3·63	1·15	1·27	0·45	5·73	0·83	0·60	0·61	0·16
MgO	1·10	1·93	2·45	1·98	1·08	1·48	2·11	1·61	2·45
CaO	4·01	0·64	0·84	0·17	2·02	0·88	0·47	0·32	0·51
Na_2O	1·68	1·84	1·08	0·91	1·04	1·05	1·22	0·75	0·98
K_2O	1·01	2·63	2·24	4·39	2·80	4·51	3·03	4·54	3·37
P_2O_5	0·03	0·04	tr.	0·09	0·04	0·03	nil.	0·01	n.d.
H_2O+	1·71	3·48	4·23	3·06	2·53	3·02	2·73	3·62	3·76
H_2O-	0·26	0·23	0·54	0·40	0·35	0·13	0·03	0·13	0·13
CO_2	4·10	nil.	0·36	0·05	1·77	0·28	nil.	nil.	0·04
C	n.d.	n.d.	n.d.	0·42	n.d.	n.d.	n.d.	n.d.	n.d.
S	nil.	tr.	n.d.	0·04	0·04	nil.	n.d.	0·01	n.d.
BaO	0·02	n.d.	n.d.	nil.	0·07	0·09	n.d.	0·16	n.d.
ZrO_2	0·04	nil.	n.d.	n.d.	n.d.	nil.	n.d.	nil.	n.d.
−O for S				−0·02	−0·02				
Total	100·36	100·39	100·09	99·71	100·19	100·45	99·85	100·21	100·43

Table 2. Total iron (as Fe_2O_3) and MnO in fifteen Manganese Shale and one Llanbedr Slate specimen

	Total iron (Fe_2O_3) (%)	MnO (%)	Mn/Fe
HA1	7·70	1·21	0·174
HA5A	10·84	1·15	0·118
HA7	11·95	1·27	0·118
HA9	7·36	0·45	0·068
HA11	10·01	0·59	0·065
MO1	7·02	5·73	0·903
MO7	7·12	0·74	0·115
MO12	8·36	0·85	0·112
BA1	6·22	0·60	0·106
BA8	9·01	0·83	0·102
BA10	7·43	0·45	0·067
YG1	11·98	0·58	0·060
YG5	6·85	0·62	0·100
AG1	7·11	0·61	0·095
HA5B	7·13	3·63	0·601
LS	10·63	0·16	0·016

sediments were deposited from waters carrying comparatively large amounts of clay minerals. This in turn signifies a rather intensive weathering of the source rocks (Rankama and Sahama, 1949).

Low MgO in the Manganese Shale may be related to the low CO_2, magnesium being transported in solution predominantly as the bicarbonate (Rankama and Sahama, 1949, give an average figure of 1·48% MgO for argillaceous rocks). The

Table 3. Average composition of the Manganese Shale (seven analyses), and other shales

	(1)	(2)	(3)	(4)
SiO_2	59·07	58·38	60·15	58·32
TiO_2	1·13	0·65	0·76	0·98
Al_2O_3	18·75	15·47	16·45	20·00
Fe_2O_3	2·45	4·03	4·04	2·01
FeO	6·07	2·46	2·90	4·98
MnO	1·52	tr.	tr.	0·22
MgO	1·81	2·45	2·32	1·85
CaO	0·76	3·12	1·41	0·66
Na_2O	1·13	1·31	1·01	1·26
K_2O	3·45	3·25	3·60	4·49
P_2O_5	0·03	0·17	0·15	0·15
H_2O+	3·24	3·68	3·82	4·10
H_2O-	0·26	1·34	0·89	
CO_2	0·35	2·64 *	1·46 †	0·43
	100·02	100·46	100·46	100·02

* Includes: SO_3 0·65, C 0·81, BaO 0·05.
† Includes: C 0·88, BaO 0·04.

(1) Average seven Manganese shales.
(2) Average seventy-eight shales (Clarke, 1924).
(3) Average fifty-one Palaeozoic shales (Nanz, 1953).
(4) Chlorite–muscovite phyllite, Stavanger (Goldschmidt, in Tilley, 1926).

data of Table 1 show that MgO varies directly with total iron in the Manganese Shale, indicating a common mode of transportation, undoubtedly as bicarbonates. Mg/Fe for the Manganese Shale averages 0·170.

The great predominance of FeO over Fe_2O_3 is almost certainly original, i.e. represents the oxidation state of iron at the time of deposition, though the low-grade dynamic metamorphism which has affected the rocks must be taken into consideration. It is considered by some previous workers that such metamorphism causes a reduction in the state of iron in sediments (see Tilley, 1926; Barth, 1936; Rankama and Sahama, 1949). In the Manganese Shale, however, the metamorphism is of such low grade as to be considered to have had a negligible effect in this respect, and the iron was probably originally deposited mostly in the ferrous state as indicated by the present chemical composition. Krumbein and Garrels (1952) state that diagenetic effects of sufficient magnitude to mask

the original Eh–pH conditions of sedimentation are relatively rare amongst the large bulk of sedimentary rocks, especially where organic matter is absent. It is noteworthy that certain bands in the Manganese Ore bear much haematite, the reduction of iron by metamorphism not being evident in this case.

The explanation of the predominance of FeO over Fe_2O_3 cannot be validly ascribed to peculiar composition of the Cambrian atmosphere (James, 1954); neither to the environment being restricted and non-marine if consideration is given to the geosynclinal nature of the basin of deposition and also to the geochemical data obtained for boron in the shales. Iron is chiefly transported as Fe^{2+}, in lesser amounts as colloidal $Fe(OH)_3$, and is deposited under normal marine conditions (pH 7·8; Eh +0·1 to +0·3) in the ferric state. In the Harlech geosyncline it seems that pH and/or Eh were lower than normal, and a slightly lower pH would also account for the paucity of carbonates in the Manganese Shale.

Most of the iron in the Manganese Shale probably occurs as Fe^{2+} in the chlorite with lesser amounts as both Fe^{2+} and Fe^{3+} in the magnetite.

In the Manganese Shale total iron (9·21% Fe_2O_3) is enriched 1·4 times compared with Rankama and Sahama's average value for shales of 6·73%. The relative enrichment of MnO is even greater, 1·52% MnO in the Manganese Shale compared with Rankama and Sahama's value of 0·06%, an enrichment of twenty-five times. This general enrichment of manganese is characteristic of the rocks of the Manganese Shale Group. The average Mn/Fe ratio for fourteen manganese shales is 0·157 compared with Goldschmidt's (1954) value for shales of 0·013. The specimen of Llanbedr Slate gave MnO 0·16% and Mn/Fe 0·016 so that it seems that large quantities of manganese were not available until suddenly with commencement of the deposition of the Lower Manganese Shale. The absolute enrichments of Mn and Fe indicate peculiar weathering conditions of source rocks of a particular type (see Mohr 1956, summarized from Mohr, 1955). Al_2O_3 shows a general decrease with increasing SiO_2 as would be expected where the silica occurs mainly as detrital quartz rather than as derived from a colloidal gel accompanying the clay minerals. K_2O varies directly with Al_2O_3 showing that the K^+ ions were sorbed on the clay minerals deposited.

In the Manganese Shale an inverse relationship is found to exist between the amounts of clay minerals and calcium carbonate deposited, and this shows up especially well in certain minor element associations, discussed below.

(b) *Minor elements*

Accurate quantitative analysis for minor elements was performed using a Hilger Quartz Spectrograph with anode excitation of the arc. Variable internal standardization was employed using the "separation at constant blackening value" method ($\log d_0/d = 1{\cdot}0$) to obtain $\log I$ values (see Mitchell, 1948).

Fe was the variable internal standard used for Co, Ni, Cr and V; Ca was used for Sr and Ba; Si was used for B, Zr, Cu; Be and Li were determined semiquantitatively. The analyses are given in Table 4, and discussion of them follows:

(i) *Cobalt and nickel.* The average values for fourteen manganese shales are: Co, 27 p.p.m.; Ni, 68 p.p.m.; Co/Ni, 0·40. Rankama and Sahama (1949) give values for shale of Co, 8 p.p.m., and Ni, 24 p.p.m. However, Lundegardh (1946, in

Rankama and Sahama, 1949) obtained much higher values for Swedish shales of Co, 30–60 p.p.m., and Ni, 70–150 p.p.m.; Shaw (1954) found averages of Co, 16·8 p.p.m. and Ni, 80·5 p.p.m. for thirteen Devonian pelites from New Hampshire, U.S.A.

The Co/Ni ratio of 0·40 for the Manganese Shale accords exactly with the value suggested for hydrolysate sediments by Goldschmidt (1954), though the data of later workers indicates a rather lower value (see Leutwein 1951; Shaw, 1954).

Bradshaw (1954) has plotted histograms for many minor elements, including Co and Ni, in both marine and fresh-water shales. It is found that the Manganese

Table 4. Minor elements in the Manganese Shale (p.p.m.)

	HA1	HA5B	HA5A	HA7	HA9	HA11	MO1	MO7	MO9	MO12	BA1	BA4
B	200	20	125	110	155	50	110	105	150	95	135	105
Be	<2	<2	<2	<2	2	2	3	<2	<2	<2	3	<2
Cr	95	33	70	78	79	65	55	79		60	67	
V	165	60	180	185	180	160	120	160		130	150	
Li				15	90							
Ni	55	35	66	152	48	89	53	71		68	36	
Co	22	6	45	68	28	33	28	26		32	11	
Zr	200	200	175	175	200	250	200	150		200	200	
Cu	40	75	40	75	30	20	30	75		300	50	
Sr	65	130	65	125	60	80	85	95	120	60	45	100
Ba	1050	190	520	590	710	575	600	540	670	600	1050	1520

	BA8	BA10	DI1	DI4	YG1	YG5	YG9	AG1	AG4	ST3	ST9	Y1	LS
B	135	175	110	105	60	110	75	70	55	70	55	55	180
Be	<2	<2	<2	<2	<2	<2	<2	<2	<2	<2	<2	<2	5
Cr	89	98			80	81		74					105
V	215	200			150	145		190					250
Li	120							2					250
Ni	71	48			107	41		49					73
Co	35	<2			25	16		13					18
Zr	150	450			300	175		300					175
Cu	5	40			150	50		100					100
Sr	90	65	80	160	45	100	14	26	90	75	90	160	110
Ba	900	1320	770	345	740	530	540	2240	275	210	550	485	410

Y1 basal shale from Llyn Eiddew Mawr.
Spaces blank equals "not determined".

Shale histograms bear a greater resemblance to those of Bradshaw's marine shales than to the fresh-water shales. The Co histogram for the Manganese Shale shows a very sharp peak, and this is characteristic of many minor elements in the Manganese Shale, indicating small spread for individual shales and confirming the remarkably constant lithology of the latter.

Considering regional values the Moelfre and especially the Harlech rocks have noticeably higher Co contents than shales from other parts of the Harlech Dome. The significance of this fact is related to the differing sedimentary cycles of Co and Ni. Whereas Ni tends to remain in the solid products of weathering as hydrosilicates, Co dissolves as the bicarbonate or forms the colloidal hydroxide. Once

Ni gets into solution, however, the Ni^{2+} ion is much more stable that the ions Co^{2+}, Fe^{2+}, and Mn^{2+}. Thus whereas the three latter ions would tend to be more easily precipitated from solution nearer the source of incoming waters, Ni would be deposited in a more constant manner over the whole basin of deposition. This is observed in the Manganese Shale where higher Co (and Fe and Mn) but not Ni values are obtained for rocks from the north-west of the Harlech Dome, indicating a source of sediments to the north-west.

It is important that in discussing the relative behaviour of Co and Ni consideration should be given to the mineralogy of the analysed specimens. There is evidence that whilst Ni varies with the observed chlorite content of the shales it is also influenced, sometimes considerably (e.g. YG1 and BA8), by the amount and type of detritus, especially iron ore. On the other hand Co tends to be more abundant in the finer-grained shales than in those rich in detritus. However, detailed petrographic study has shown that mineralogy alone cannot account for the Co enrichment in the rocks of the north-west region. The data point to source rocks to the north-west of the Harlech Dome providing solutions rich in the ferrides.

When plotted against total iron Ni, and especially Co, show a marked direct relationship. As the major elements Mg and Fe themselves show a direct relationship it is not possible to distinguish which of these two elements they might preferentially be following. Ahrens (1953) states that the coherence of Ni and Mg in the sedimentary cycle is poor, but both elements form hydrosilicates on weathering and the roles of these two very stable ions in solution seem only to diverge in the presence of CO_2. A study of Co/Fe, Ni/Fe, Co/Mg and Ni/Mg ratios for the Manganese Shale indicates a very close coherence of Co and Fe, and one less close of Ni and Fe though there is here probably some affinity of Ni for Mg.

The data for the Llanbedr Slate specimen tend to confirm that Co and Ni are following both oxidation states of Fe, not solely the ferrous. There is no relationship of Co and Ni with Mn in the Manganese Shale, indicating that the cycle of Mn differs from those of the other ferrides.

(ii) *Chromium*. The average content of fourteen manganese shales is 76 p.p.m. Cr. This compares with Rankama and Sahama's figure for shales of 410–680 p.p.m. Cr. For thirteen Devonian pelites Shaw obtained an average of 116 p.p.m. Cr. Goldschmidt states that the average Cr content of shales is probably about 200 p.p.m., and, together with the data of Bradshaw and of Leutwein, it would seem that the figure given by Rankama and Sahama is too high.

As for Co, there is a very sharp peak in the Cr histogram of the Manganese Shale, again indicating a very constant type of sediment both vertically and horizontally.

Cr is found to follow closely total iron in the Manganese Shale. It can occur in two host-minerals: associated with the Fe_2O_3 of the detrital magnetite; derived from solution, in the chlorite where it is substituting probably with Fe^{3+} for 6-co-ordinated Al (Rankama and Sahama, 1949). It is noteworthy that the Llanbedr Slate specimen, rich in haematite, has a high Cr content and the same applies to a lesser extent to specimen HA1. Specimens BA8 and BA10, again with higher than average Cr contents, contain detrital ferromagnesian minerals.

(iii) *Vanadium*. The average content of fourteen manganese shales is 165 p.p.m. V. This compares with other data for shales of 120 p.p.m. V (Rankama and Sahama), 109 p.p.m. V (Shaw), and 200 p.p.m. V (Goldschmidt). Thus the V content of the Manganese Shale is a normal figure, and again its histogram shows a sharp peak.

Whilst V appears to follow total Fe it is probably, like Cr, more closely associated with Fe^{3+}. Magnetite is a typical host for V, and indeed authigenic magnetite in the Manganese Ore has been found to show an enrichment of V over the ore-matrix of twenty times. Goldschmidt states that V is also concentrated in the hydrolysates by sorption on clay minerals in the form of V^{3+}, indicating possible affinity of V with Al. It is most unlikely that the Eh of the waters of deposition of the Manganese Shale sediments was ever high enough to have allowed the existence of the V^{5+} ion. It thus seems that V was transported bound in detrital magnetite and also in solution as the V^{3+} ion.

Like Cr, V is enriched in the Llanbedr Slate specimen, and to some extent in specimens BA8 and BA10. Again like Cr, V shows no definite variations in concentration either vertically or horizontally throughout the Manganese Shale.

(iv) *Strontium and barium*. The average values for twenty three manganese shales, including two specimens from St. Tudwal's, are compared with the data of other workers below:

	Sr (p.p.m.)	Ba (p.p.m.)	Sr/Ba
Average twenty three manganese shales	85	750	0·114
Shale (Noll, 1934 from Rankama and Sahama, 1949)	170	630	0·27
Shale (von Englehardt, 1936 from Rankama and Sahama)	—	460	—
Al-rich schists (Sahama, 1945 from Rankama and Sahama)	160	690	0·23
Thirteen Devonian pelites (Shaw, 1954)	524	—	—

It is seen that the Manganese Shale is rather richer in Ba and poorer in Sr than most other shales. The remarkable feature of the individual Manganese Shale data, reflected broadly also in the above table, is the inverse relationship of Sr and Ba. The reason for this relationship lies in the sedimentary cycles of these two elements which are quite different.

Sr follows Ca to a certain extent, occurring in the carbonate precipitates, though the average Sr/Ca ratio for the Manganese Shale, 0·018, is lower than in sea-water, 0·03 (Rankama and Sahama), indicating that relatively more Sr remained in solution. A second source of Sr in shales is in detrital minerals such as plagioclase. In the Manganese Shale it seems that these two sources of Sr were usually about equally important, the calcium carbonate content being very low. Ba, on the other hand, is strongly concentrated in the hydrolysates due to the low ionic

potential of the Ba^{2+} ion. In this manner nearly all the Ba entering the basin of deposition is rapidly precipitated relatively close inshore to the entering solutions, the amount of Ba that remains in sea-water to be available for chemical precipitation being negligible. Detrital minerals bearing Ba such as orthoclase and biotite are rather uncommon in the Manganese Shale and in any case the amounts of such Ba would be negligible compared with that contained in the hydrolysates.

Now it is obvious that if the proportion of detritus in a sediment increases then the proportion of hydrolysate clay minerals must decrease, and vice versa. The amount of chemical precipitation might be expected to be independent of either of these two factors, but in the Manganese Shale it varies directly with the amount of detritus, especially well shown in specimen HA5B. Rankama and Sahama quote values showing that the CO_2 content of sandstones is considerably higher than that of shales. Thus the mineral hosts of Sr and Ba vary inversely in amount, detrital and chemical vs. hydrolysate sedimentation, and therefore shales derived from similar source material and deposited in a single basin of deposition would be expected to show an inverse Sr–Ba relationship.

Concerning Sr and Ba values in the individual manganese shales the most significant fact is the lower Sr and higher Ba at the base of the Manganese Shale Group compared with the average value:

	Sr (p.p.m.)	Ba (p.p.m.)
Average twenty three manganese shales	85	750
Average of specimens HA1, MO1, BA1, DI1, YG1, AG1	60	1075

The relation of this fact to palaeogeography is discussed later.

The shales from Cell Fechan are noticeably richer in Ba than those from other localities of the Harlech Dome, the four specimens analysed averaging 1200 p.p.m. Ba. There is some detrital orthoclase visible in thin-sections of these rocks but whether this carries the extra Ba is unknown. In the two Barmouth shales analysed for major elements K is also high. The specimens from St. Tudwal's show no significant differences from the Manganese Shale other than low Ba due to their coarser texture.

Ba/K ratios for the individual manganese shales show a very close geochemical coherence of the two elements (average value Ba/K, 0·034). Sr/Ca ratios vary rather more widely and average 0·018 (Goldschmidt gives an average value for shales of 0·02). The Llanbedr Slate specimen shows its greatest geochemical divergences from the Manganese Shale in its high Sr/Ca ratio (0·031) and low Ba/K ratio (0·015).

(v) *Boron.* The average content of twenty-three manganese shales is 105 p.p.m. B. Goldschmidt and Peters (Rankama and Sahama, 1949) obtained an average value for shales of 310 p.p.m. B. Landergren (1945) analysed 359

Swedish Cambrian slates and found an average content of 100 p.p.m. B. The work of these two sets of authors has shown that the B content of hydrolysates depends on the salinity of the waters of deposition.

According to Landergren normal marine sediments average 150 p.p.m. B. However, when applying this figure to sedimentary rocks two important factors must be considered. First that B is a very mobile element under metamorphism, and the Harlech Grits Series has undergone metamorphism though of the lowest grade; secondly, according to Landergren, B content varies inversely with the grain-size of the sediment, and thus directly with Al content. The reason for this concerns the mode of occurrence of B in shales. By far the most important hosts to B in sediments are the colloidal clay minerals on which it is sorbed. Therefore increase in the amount of detritus in a sediment will proportionately lower its B content, other conditions being equal. The only detrital mineral which carries significant quantities of B is tourmaline and this is extremely rare as a detrital mineral in the Manganese Shale.

The sorption of B in the hydrolysates of the Manganese Shale is most strikingly proved by the remarkably close direct relationship of B and Ba in these rocks. The present mode of occurrence of B in the Manganese Shale is observed to be in the form of exceedingly minute authigenic tourmalines, though some B may still be contained in the chlorite and sericite matrix derived from the original clay minerals.

Regarding the salinity of the waters in which the Manganese Shale was deposited the data for B seems to indicate, following previous authors, that the deposition was in an marine environment, though the B histogram for the Manganese Shale shows its peak at a slightly lower value than that of Bradshaw for fully marine shales. This may be due to the grain-size factor, or to the waters of deposition being brackish rather than fully marine, or to the very low grade metamorphism, or the much debated possibility that the salinity of the oceans has changed since the end of the pre-Cambrian (see Conway, 1942; Landergren, 1945; Goldschmidt, 1954).

The basal shales of the Lower Manganese Shale show a slightly higher B content than the average, 115 p.p.m. This small enrichment, which is masked by the low values for B in shales from the south-east of the Harlech Dome, might be predicted from the similar enrichment of Ba. The St. Tudwal's rocks show low B which is undoubtedly associated with their coarser texture.

(vi) *Zirconium*. The average content of fourteen manganese shales is 230 p.p.m. Zr. This is considerably higher than the value of 120 p.p.m. Zr given by Rankama and Sahama for shales. Shaw's average for thirteen Devonian pelites was 191 p.p.m. Zr, and for Thuringian slates Leutwein found <100 p.p.m. Zr. The high value in the Manganese Shale may be associated with intensive weathering conditions at the source rocks.

Detrital zircon is frequently observed in thin-section of the Manganese Shale but, as the work of Goldschmidt suggests, a considerable proportion of the contained Zr has probably been incorporated from solution into the hydrolysates. Thus in specimen BA10, where zircon is observed to be a very rare accessory mineral, analysis proves 450 p.p.m. Zr.

(vii) *Copper*. The average content of fourteen manganese shales is 70 p.p.m. Cu. Previous workers have obtained values of 192 p.p.m. Cu (Carrobbi and Pieruccini for Italian argillaceous sediments, in Rankama and Sahama, 1949), and 23 p.p.m. Cu (Shaw, 1954). Clarke (1924) showed that marine sediments tend to contain higher Cu than do fresh-water sediments, but it seems likely that the type of source rock also has an important influence.

Most of the Cu in the sedimentary cycle is concentrated in the reduzates (with sulphides, as is well shown in the Pyritiferous Mudstone; see Mohr, 1956), but some is sorbed in hydrolysate sediments. This second mode of occurrence is sufficient to account for the Cu content of the Manganese Shale, the amount contained in detrital iron ore and ferromagnesian minerals probably being negligible by comparison.

Specimens YG1 (150 p.p.m. Cu) and MO12 (300 p.p.m. Cu) are both seen to contain abundant patches of recrystallized deep-green chlorite, which thus probably contains the Cu. Specimen BA8 (5 p.p.m. Cu) is remarkably deficient in chlorite for a manganese shale.

Like Zr, Cu shows no significant variations either vertically or horizontally throughout the Manganese Shale.

(viii) *Beryllium*. The average content in the Manganese Shale is about 1 p.p.m. Be. Goldschmidt and Peters (Rankama and Sahama, 1949) obtained an average value for shales of 3·6 p.p.m. Be.

Rankama and Sahama state that Be accompanies Al in the sedimentary cycle on account of the similarity of the ionic potentials of the two elements, and that Be is thus mainly incorporated in the hydrolysates. The highest value obtained in the present work, 5 p.p.m. Be in the Llanbedr Slate, is associated with a high Al_2O_3 content of 22·55 per cent.

(ix) *Lithium*. This element was determined on only five specimens, those analysed showing divergent values. However, the average is probably close to values previously obtained for shales of 46 p.p.m. Li (Rankama and Sahama, 1949) and 55 p.p.m. Li (Shaw, 1954).

If Li is following Mg, data are insufficient to prove it. However, the specimen of Llanbedr Slate shows a high content of Li (250 p.p.m.) associated with a relatively high MgO of 2·45%.

(x) *Other elements*. With the exceptions of Ga, Rb and Pb, which were not determined, all other elements lay beneath the limits of detection with the methods used.

Conclusions

The most important geochemical facts emerging from the study of the Manganese Shale are as follows: (i) the sympathetic variations of the ferrides except for Mn; (ii) the inverse relationship of Sr and Ba; (iii) the direct relationship of B and Ba.

Concerning the major elements, a comparison can be made first with the average shale composition calculated by Clarke (1924) according to whether the individual oxides in the average Manganese Shale are higher or lower than Clarke's figures. These are given in Table 5, column 3. Secondly, Kennedy (1951), working on pelitic Silurian sediments in the Scandinavian Caledonian

chain, has correlated change in chemical composition with maturity of sediments, and his findings are applied to the Manganese Shale in Table 5, column 4.

The data indicate the Manganese Shale sediments to be relatively mature, and this is interpreted as due to the source rocks being of such types as ancient gneisses and schists (e.g. rocks similar to the Mona Complex of Anglesey, as postulated by Woodland, 1938a, and others), rather than that the sediments were far travelled.

Table 5. The maturity of the Manganese Shale sediments relative to Clarke's average shale (see text)

	(1)	(3)	(3)	(4)
SiO_2	59·07	58·38	+	+
TiO_2	1·13	0·65	+	+
Al_2O_3	18·75	15·47	+	+
Fe_2O_3	2·45	4·03	−	−
FeO	6·07	2·46	+	−
MnO	1·52	tr.	+	+
MgO	1·81	2·45	−	−
CaO	0·76	3·12	−	−
Na_2O	1·13	1·31	−	−
K_2O	3·45	3·25	+	+
P_2O_5	0·03	0·17		

(1) Values for average Manganese Shale (from Table 3).
(2) Values for average shale (Clarke, 1924, from Table 3).
(3) Divergence of values in column (1) from those in column (2), whether higher (+) or lower (−).
(4) Kennedy's (1951) trends for increasing maturity of sediments, whether higher percentage of oxide (+) or lower (−).

Concerning the minor elements and their relationship to source rock type, Table 6 summarizes the facts which are interpreted (mainly following Rankama and Sahama, 1949) as suggesting weathering of acidic rocks, probably acid gneisses to bring the hypothesis into conformity with the deductions made above from major elements data.

Palaeogeography

Data on the major elements are insufficient to establish any definite trends either vertically or horizontally throughout the Manganese Shale, though possibly the rocks of the north-west of the Harlech Dome are slightly higher in MnO and total iron. The following significant facts emerge from the minor element study:

(i) High Co and thus Co/Ni in the rocks from the north-west of the Harlech Dome, possibly associated with high Mn and Fe. This suggests an important source of ferride-rich solutions to the north-west of the Harlech Dome, especially for Co and Mn.

(ii) The lower Sr and higher Ba in the basal Manganese Shale. This possibly indicates a shallower basin of deposition at the beginning of Manganese Shale Group times, with less chemical precipitation occurring owing to stronger bottom

Table 6. Relation of minor element concentrations to type of source rock, based mainly on data from Rankama and Sahama (1949).

Element	Trend in Mn Shale	Type of source rock to give trend mentioned
Co	high	Basic, but high Co/Ni indicates acidic
Ni	low	acidic
Cr	low	acidic
V	normal	—
Sr	low	acidic?
Ba	high	acidic
B	low	Largely independent of source rock
Zr	high	acidic
Cu	low	acidic

current flow, together with hydrolysate sedimentation taking place relatively nearer the incoming solutions and sorbing Ba from solution.

(iii) The rather lower than normal B content for shales. If significant, it may suggest a basin of deposition connected with the ocean but partially enclosed, thus giving a somewhat lower salinity than for a fully marine environment due to inflowing fresh-waters. The lower B values to the east may suggest another source of sediments in that direction, as postulated by Woodland (1938a).

(iv) The otherwise remarkably constant minor element concentrations both vertically and horizontally throughout the Manganese Shale. This indicates similar source rocks and conditions of weathering, transportation and deposition throughout Manganese Shale times, with free circulation of ions in the waters of the basin of deposition.

(v) The similar Sr, Ba and B contents of the St. Tudwal's rocks compared with the Manganese Shale, allowance being made for differing textures. This suggests that the Harlech basin of deposition extended to the present St. Tudwal's Peninsula region to the west. This theory is strongly supported by geochemical data on the Manganese Ore (Mohr, 1956).

(vi) The much lower MnO content of the Llanbedr Slate specimen compared with the Manganese Shale. It seems that the source of large quantities of Mn, or its means of concentration, was not available until suddenly with commencement of deposition of the Lower Manganese Shale.

Acknowledgements—This work was done at Manchester University under the supervision of Prof. W. A. Deer and Dr. G. D. Nicholls, to whom the writer acknowledges his debt.

References

Ahrens L. H. (1953) The use of ionization potentials. II: Anion affinity and geochemistry. *Geochim. et Cosmochim. Acta* **3**, 11.

Barth T. (1936) Petrology of Palaeozoic rocks from Duchess Co., New York. *Bull. Geol. Soc. Amer.* **47**, 775–850.

Bradshaw B. A. (1954) Personal communication.

Clarke F. W. (1924) *Data of Geochemistry.*

Conway E. J. (1942) The chemical evolution of the ocean. *Proc. Roy. Irish Acad.* **48,** 174–212.
Goldschmidt V. M. (1954) *Geochemistry.* (Edited by Muir A.) Oxford University Press.
James H. L. (1954) Sedimentary facies of iron-formation. *Econ. Geol.* **49,** 244–246.
Kennedy W. Q. (1951) Sedimentary differentiation as a factor in the Moine–Torridonian correlation. *Geol. Mag.* **88,** 257–266.
Krumbein W. C. and Garrels R. M. (1952) Origin and classification of chemical sediments in terms of pH and oxidation-reduction potentials. *J. Geol.* **60,** 23.
Landergren S. (1945) The distribution of Boron in some Swedish sediments, rocks and iron ores. *Ark. Kemi Min. Geol.* **19,** No. 26, 1–31.
Leutwein F. (1951) Geochemische Untersuchungen an den Alaun-und Kieselschiefern Thuringens. *Arch. Lagerst. Forsch* **82,** 7–47.
Matley C. A. and Wilson T. S. (1946) The Harlech Dome, North of the Barmouth Estuary. *Quart. J. Geol. Soc.* **71,** 1–40.
Mitchell R. L. (1948) The spectrographic analysis of soils, plants, and related materials. *Commonwealth Bureau of Soil Science Technical Communication,* No. 44, 20–33.
Mohr P. A. (1955) *A Geochemical Study of the Lower Cambrian Manganese Shale Group of the Harlech Dome.* Unpublished thesis, University of Manchester.
Mohr P. A. A geochemical study of the Lower Cambrian manganese ore of the Harlech Dome, North Wales. Symposium sobre yacimientos de manganeso. *Proc. Twentieth Congr. Geol. Int., Mexico, 1956,* 273–289.
Nanz R. H. (1953) Chemical composition of pre-Cambrian slates with notes on the geochemical evolution of lutites. *J. Geol.* **61,** 58.
Rankama K. and Sahama T. G. (1949) *Geochemistry.* Chicago University Press.
Shaw D. M. (1954) Trace elements in pelitic rocks. I: Variation during metamorphism. *Bull. Geol. Soc. Amer.* **65,** 1151–1166.
Tilley C. E. (1926) On mineral transformations in crystalline schists. *Mineral. Mag.* **21,** 37 and 40.
Woodland A. W. (1938a) Unpublished thesis.
Woodland A. W. (1938b) Petrological studies in the Harlech Grits Series of Merionethshire. *Geol. Mag.* **75,** 369–375.

Geochimica et Cosmochimica Acta, 1959, Vol. 17, pp. 201 to 208. Pergamon Press Ltd. Printed in Northern Ireland

Some aspects of the marine geochemistry of uranium

Mitsunobu Tatsumoto and E. D. Goldberg
University of California, Scripps Institution of Oceanography, La Jolla, California

(*Received* 31 *March* 1959)

Abstract—The uranium concentrations in marine calcareous material of a biological origin varied between 0·0X and 0·X p.p.m. with the exception of corals which had concentrations of several p.p.m. The aragonitic oolites and aragonite precipitated from sea-water had values similar to those of the corals. A geochronology based on the growth of ionium (thorium-230) from uranium is applicable not only to corals, as previous investigators have pointed out, but also to oolites. Several examples of "oolite ages" are given. The uranium content of ferromanganese minerals from pelagic deposits is of the order of from 4 to 5 p.p.m.

Several problems concerned with our studies on marine sediments have prompted investigations of the uranium contents of various oceanic mineral deposits. First of all, it was of interest to ascertain what extensions of the uranium–ionium dating technique applied by Barnes *et al.* (1956) to corals might be found in other carbonates of the marine environment. Secondly, the ionium/thorium chronology for pelagic sediments developed by Goldberg and Koide (1958) demands a knowledge of the uranium content of the sample under consideration in order to know the amount of uranium-supported ionium. Finally, an extended knowledge of the distribution of uranium among the components of marine sediments is of general utility to the marine geochemist.

Experimental

Uranium assay of calcareous samples

An amount of sample containing at least 0·5 μg of U is dissolved in concentrated nitric acid. Any organic matter is destroyed by the addition of concentrated perchloric acid, followed by heating to perchloric acid fumes. Ferric iron (10 mg) is added to the diluted acid sample to carry down any uranium on a ferric hydroxide floc formed by the addition of gaseous ammonia. The precipitate is converted to a sulphate solution, which is the most satisfactory form for the uptake of uranium in the subsequent anion-exchange process, by the addition of concentrated sulphuric acid.

The pH is then adjusted to a value between 1·0 and 1·5 with 5 M sodium hydroxide. A sufficient amount of 6% sulphurous acid is added to completely reduce the ferric iron to the divalent state, a form which does not adhere to the ion-exchange column. The solution is then passed through an IRA 400 (80-100 mesh) resin in the sulphate form at a rate of approximately one drop per second with the resulting adsorption of uranium on the column (Fisher and Kunin, 1957). The column is subsequently rinsed with 50 ml of a 0·1 M sodium sulphate solution containing 5 ml of 6% sulphurous acid and then with 50 ml of hot water.

The uranium is eluted with 40 ml of hot 1 M perchloric acid into a 50 ml beaker and then the eluant is evaporated to fumes of perchloric acid. At this

point 2 ml of concentrated nitric acid are added and the solution evaporated to dryness. (These last steps destroy any organic matter taken up by the eluant from the resin.) The residue is taken up in 1 ml of 25% HNO_3, transferred to a 10 ml volumetric flask; the beaker is rinsed with 4 ml of water which is added to the flask, followed by the addition of 1 ml of 0·1 M ammonium tartrate, 1 ml of 0·2% EDTA and 3 ml of the reagent solution (0·2 g of dibenzoylmethane dissolved in 300 ml of redistilled pyridine). The absorbance is measured at 415 mμ against a reagent blank, in 10 cm cells 30 min after the addition of the reagents (YOE *et al.*, 1953).

Table 1. Uranium analyses on Mississippi limestone

Sample	Uranium found
1	1·11
2	1·07
3	1·07
4	1·09
5	1·04
6	1·02
7	1·06
8	1·09
	Average value 1·07 ± 0·03

Other results (SACKETT, 1958)

Fluorimetric method	1·02 ± 0·05
Activation analysis	1·07 ± 0·05
Isotope dilution	1·04 ± 0·06

The EDTA solution was used to mask any trace amounts of iron that might have been carried through the procedure or picked up while the tartrate solution was added to prevent the development of any zirconium (or hafnium) dibenzoylmethane colour, especially in the case of ferromanganese minerals which contain an appreciable amount of zirconium.

Pyridine was used in the final step both as a pH buffering agent and also as a solvent for the dibenzoylmethane. Previous workers have encountered pH adjustment difficulties in this colorimetric technique which can be eliminated by the use of pyridine. The "measured pH" in the final solution was 5·85 ± 0·05.

Uranium assay of ferromanganese minerals

An amount of sample containing at least 0·5 μg of U is dissolved in concentrated hydrochloric acid and any residue is removed by centrifugation. The iron is precipitated as the hydroxide upon the addition of gaseous ammonia to the solution and the resultant precipitate is dissolved in nitric acid. A second iron hydroxide precipitation is made and the precipitate again is taken up in nitric acid (0·7 ml) and diluted with 10 ml of water. Ammonium nitrate is then added

(19 g) as a salting-out reagent and the uranium is extracted twice into 10 ml portions of ethyl acetate. The ethyl acetate solution is evaporated to dryness, the residue taken up with sulphuric acid, fumed and the resultant solution is carried through the ion-exchange resin as above.

Accuracy and precision of the results

Analyses were made on a Mississippi limestone, previously used by Professor H. A. Potratz of Washington University, as a standard in his uranium work. Table 1 gives values found in this and other laboratories.

In the analyses of calcareous materials a precision and accuracy of plus or minus 5 per cent was realized. However, results on the ferromanganese minerals are undoubtedly less accurate owing to the ethyl acetate extraction step which is not 100 per cent efficient. The use of U^{233} as a yield tracer would certainly refine these analyses. Owing to the fact that low level α-counting and processing was going on in the same laboratory, advantage was not taken of this technique.

Results

The uranium contents of a group of calcareous organisms are given in Table 2 along with the crystal form of the shell. Table 3 gives the uranium concentrations in a series of oolites, an aragonitic deposition of calcium carbonate, apparently of a non-biological nature. Two corals, *Diploria labrinthiformis* and *Montastrea annularis*, collected at Windleys Key, Florida, are included for comparison. Both of these species are mixtures of calcite and aragonite. Probably, aragonite was originally laid down by the animals, inasmuch as modern specimens analysed pure aragonite. The conversion was apparently accompanied by the loss of uranium and/or ionium, as the uranium–ionium ages for these corals differ by nearly a factor of 2 (see Table 3 and accompanying text) and the samples were taken from the same 6 ft block of essentially one single age (Ginsburg, personal communication).

Uranium analyses were also made upon calcium carbonate samples precipitated from sea-water, which was previously filtered, and these results are collected in Table 4. These samples were all aragonite. Finally, in Table 5, are listed the uranium contents of some manganese nodules from both the Atlantic and Pacific Oceans.

Discussion

The uranium concentration in marine oolites (average value of 3 p.p.m.) compares favourably with the values found in the laboratory precipitation of aragonitic calcium carbonate. This result provides another argument for the inorganic origin of these calcareous sands (a review of this problem may be found in Revelle and Fairbridge, 1957; recent investigations by Lowenstam and Epstein, 1957, on the isotopic analyses of carbon and oxygen in carbonates from the marine environment also point to a non-biological origin of oolites). Further, the high uranium values in corals (2·9–5·5 p.p.m.), initially observed by Barnes *et al.* (1956), are confirmed in two further cases.

These results parallel to some extent the accumulation of strontium in marine

Table 2. Uranium contents of marine calcareous specimens

Sample	Class	Location	Uranium (p.p.m.)	Crystal type
Dendraster excentricus	Echinoidea	La Jolla, Calif.	0·17	Calcite
Dendraster laevis	Echinoidea	South Coronada Isle, Mexico	0·18	Calcite
Tetraclita squamosa	Cirripedia	La Jolla, Calif.	0·041	Calcite
Protothaca staminea	Pelecypoda	La Jolla, Calif.	0·21	Aragonite
Littorina planaxis	Gastropoda	La Jolla, Calif.	0·012	Aragonite
Acmeca limatula	Gastropoda	La Jolla, Calif.	0·067	Aragonite
Olivella biplicata	Gastropoda	La Jolla, Calif.	0·022	Aragonite
Littorina scutulata	Gastropoda	La Jolla, Calif.	0·028	Aragonite
Trochus niloticus	Gastropoda	Outer reef, Palau	0·009	Aragonite
Mytilus edulis	Pelecypoda	Dutch Harbor, Alaska	0·046	Arag. + calcite
Mytilus californianus	Pelecypoda	La Jolla, Calif.	0·021	Arag. + calcite
*Pseudochama**	Pelecypoda	La Jolla, Calif.	0·013	Arag. + calcite
Haliotis corrugata	Gastropoda	La Jolla, Calif.	0·013	Arag. + calcite
Haliotis cracherodii	Gastropoda	La Jolla, Calif.	0·014	Arag. + calcite
*Bryozoa**	Bryozoa	On the surface of Haliotis corrugata	0·47	Arag. + calcite
Tegula fonebralis	Gastropoda	La Jolla, Calif.	0·004	Arag. + calcite
Acathina spirata	Gastropoda	La Jolla, Calif.	0·032	Arag. + calcite
Ianthina	Gastropoda	Open Pacific Ocean	0·044	Arag. + calcite
Diploria labrinthiformis	Anthozoa	Key Largo Limestone, Windleys Key, Florida	2·5	Aragonite
Montastrea annularis	Anthozoa	Key Largo Limestone, Windleys Key, Florida	3·2	Aragonite

* Contained detrital sand and/or silt particles.

calcium carbonates. Oolites contain somewhat above 2 per cent strontium carbonate (Lowenstam and Goldberg quoted in Revelle and Fairbridge, 1957) likewise the aragonite precipitated from sea-water in our laboratory contains an identical amount of $SrCO_3$. Thompson and Chow (1955) summarize similar findings of strontium carbonate concentrations in corals from work in their own and other investigators' laboratories.

Whereas strontium is much more readily accommodated in the aragonitic as opposed to the calcitic structure (Thompson and Chow, 1955) in biological calcareous specimens, the uranium in our limited set of analyses does not seem to show such an evident preference (excluding of course the corals).

The presence of substantial amounts of uranium in the oolites directed this investigation to the possible use of these minerals in age determinations by the uranium ionium parent daughter relationships. Such a chronology would be

Table 3. Uranium and ionium contents and "U-Io ages" of oolites

Sample	Uranium (p.p.m.)	Thorium (p.p.m.)	Ionium (uranium equivalents)	Age (years)
Bahamas Banks North of Joulters Cay in area of submarine sand channels and deltas; 30-50 mesh fraction.	3·3	n.d.*	0·00	Recent
Laguna Madre LM-193B, from API 51 project; $\frac{1}{4}$-$\frac{1}{2}$ mm fraction. Sample contained a residue of 21·3% quartz and feldspars after acid dissolution.	0·83	2·0	0·92	—
Bahama Bank, about 1 mile SE of South Point, Cat Cay; 79°15′ W; 29°30·5′ N.	3·4	n.d.	0·00	Recent
Bahama Bank, 2 miles S of South Cat Cay, Miami, dredged from below sea level in Topine Brothers Rock Pit on Stock Island, near Key West.	3·1	n.d.	0·23	9,000
Friable oolite from a soil horizon in Queens Staircase, Nassau, N.P.	3·8	n.d.	3·4	260,000
Great Salt Lake, Stansbury Point, quartz residue of 6·8%, following acid dissolution.	3·5	n.d.	2·6	160,000
Coral, Key Largo Limestone, *Montastrea annularis*.	5·8	1·2	1·3	—
Coral, Key Largo Limestone, *Diploria labrinthiformis*.	3·2	n.d.	2·1	130,000
	2·5	n.d.	2·0	230,000

* n.d., not detected; less than 0·05 p.p.m., see text.

Table 4. Uranium in calcium carbonates, aragonitic, precipitated in the laboratory from sea-water

Sample	Uranium in $CaCO_3$ (p.p.m.)
1. CO_2 passed through water under heat treatment; following cooling, NH_3 is passed through the system. Final pH = 7·6. A small amount of calcium sulphate contaminated this sample.	2·6
2. Similar to above but final pH was 7·9.	3·2
3. Similar to above but final pH 7·95. Sample (1), $CaCO_3$ floating at surface	3·2
Sample (2), $CaCO_3$ adhering to walls of vessel.	4·6

Table 5. The uranium contents of some manganese nodules

Nodule description	Uranium concentration (p.p.m.)
Horizon nodule, from 40°14′ N and 155°15′ W at a depth of 5500 m.	3·9, 3·6, 3·6
Nodule from Downwind Core DWBG47 taken at 36°33′ S and 137°24′ W at a depth of 4700 m.	4·6
Nodule from Downwind Core DWBG52 taken at 40°36′ S and 132°49′ W at a depth of 5120 m.	3·6
Nodule from Downwind Dredge DWHD taken at 37°04′ S and 81°50′ W collected from a depth of 4000 m.	4·0
Nodule from Lamont Theta Trawl no. 4 taken at 29°18′ N and 57°20′ W at a depth of 5400 m.	5·0

useful over the time period of zero to a half million years (Fig. 1). Two prerequisites primarily govern the application of U–Io dating to minerals: first of all, there can be no alterations to the mineral which would result in the addition or removal of uranium, ionium or the intermediate radionuclides in this naturally occurring radioactive series; and secondly, there can be no unsupported ionium initially present in the sample. A ready test of the second qualification may be found in the presence of any thorium, if it is assumed that any unsupported ionium would come from the sea-water. The deduced ratio of ionium to thorium (in units of disintegration per time interval) in sea-water can be of the order of 35 (GOLDBERG and KOIDE, 1958). Hence, any significant amounts of thorium in such samples would negate any derived age.

Table 3 presents thorium, in units of parts per million by weight, and ionium, in equivalents of uranium, concentrations in some oolites and corals. These thorium isotopes were assayed radiometrically by a previously described technique (GOLDBERG and KOIDE, 1958). Five of the seven samples were free of thorium within the limits of error, while the oolites from Laguna Madre and from the Great Salt Lake had thorium contents of about 1 p.p.m. and are undatable by this technique (see below). Two of the samples from Bahama Bank gave zero age, reasonable numbers inasmuch as the samples came from the surface of the sedimentary deposits. The remaining samples, including two corals, show a spectrum of ages from 9000–260,000 years. These results, although not forming a part of a geologic problem, are not in conflict with known geologic evidence (R. N. GINSBURG, personal communication). An estimate of the lower limit of age detection and the influence of thorium isotopes, accumulated from sea-water by the calcium carbonate, on the results can be ascertained in the following ways. For a 2 g sample, in which the thorium isotopes are recovered with a 100 per cent efficiency, 60 net counts over background are detectable in a 600 min counting period in our instrumentation. This is equivalent to 0·2 disintegrations per min, correcting for our geometry of 52 per cent. Assuming 3 p.p.m. of uranium in the sample, the ratio of activity of ionium to uranium is 0·05 which results in a minimum age of detection of around 6000 years. Larger samples, obviously, would

reduce this figure and there is no experimental reason to prohibit processing samples in the hundreds of grammes.

A thorium contamination of 0·05 μg, in a 2 g sample, represents an ionium equivalent of 0·3 μg of uranium, assuming an ionium–thorium activity ratio of 35. This thorium value represents about the lower limit of detectability and an error in the age of 6000 years. However, 2·0 μg of thorium in a 2 g sample gives spurious ages of tens of thousands of years.

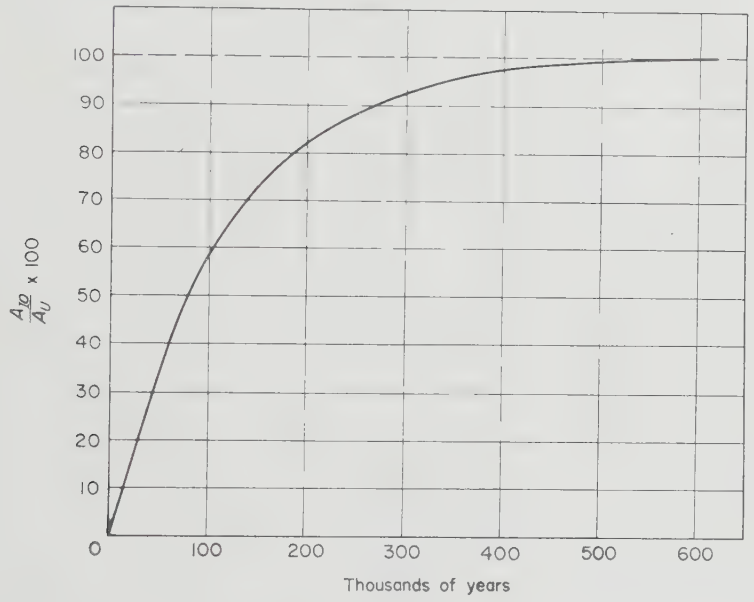

Fig. 1. The growth of ionium from its parent uranium as a function of age.

The uranium concentrations in the ferromanganese minerals (Table 5) are of the order of 4–5 p.p.m. and are markedly lower than the corresponding thorium concentrations of 30–100 p.p.m. (Goldberg and Picciotto, 1955). Assuming that these minerals obtain their constituents from the dissolved chemical species in sea-water, there is a marked fractionation against uranium compared to thorium, for the uranium content of sea-water is of the order of several parts per billion whereas the thorium is less than five-hundredths of a part per billion. This situation probably arises from the fact that the thorium is in solution in the tetravalent state while the uranium is in the hexavalent state, possibly complexed with carbonate as the uranyl ion (Starik and Kolyadin, 1957).

Acknowledgements—The writers gratefully acknowledge samples from Dr. R. Ginsburg, Shell Oil, Miami; Dr. G. Rusnak of the Scripps Institution of Oceanography; and Dr. P. H. Monaghan of the Humble Oil and Refining Company. This study was sponsored by the Office of Naval Research under contract with the University of California.

References

Barnes J. W., Lang E. J. and Potratz H. A. (1956) Ratio of ionium to uranium in coral limestone. *Science* **124**, 175–176.

Goldberg E. D. and Picciotto E. (1955) Thorium determinations in manganese nodules. *Science* **121,** 613–614.

Goldberg E. D. and Koide M. (1958) Ionium–thorium in deep-sea sediments of the Pacific. *Science* **128,** 175–176.

Fisher S. and Kunin R. (1957) Use of ion exchange resins for determination of uranium in ores and solutions. *Analyt. Chem.* **29,** 400–402.

Lowenstam H. A. and Epstein S. (1957) On the origin of sedimentary aragonite needles of the Great Bahama Bank. *J. Geol.* **65,** 364–375.

Revelle R. and Fairbridge R. (1957) Carbonates and carbon dioxide. *Treatise on Marine Ecology and Paleoecology* Vol. 1, pp. 239-96. Memoir 67, Geological Society of America.

Sackett W. (1958) Thesis, University of Washington, St. Louis, Mo.

Starik I. E. and Kolyadin L. B. (1957) The conditions of occurrence of uranium in sea-water. *Geochymia* 204–13.

Thompson T. G. and Chow T. J. (1955) The strontium/calcium atom ratio in carbonate-secreting marine organisms. *Deep-Sea Res.* Suppl. **3,** 20–39.

Yoe J. H., Will F. and Black R. A. (1953) Colorimetric determination of uranium with dibenzoylmethane. *Analyt. Chem.* **25,** 1200–1204.

Geochimica et Cosmochimica Acta, 1959, Vol. 17, pp. 209 to 213. Pergamon Press Ltd. Printed in Northern Ireland

Manganese and nickel on the ocean floor

H. Pettersson
Oceanografiska Institutet, Göteborg 4, Sweden

(*Received* 4 *April* 1959)

Of all the elements found in deep-sea deposits few have a more puzzling distribution than the two ferrides, manganese and nickel. Both of them are present in higher concentrations than in igneous continental rocks. However, it is their horizontal and vertical distribution in ocean sediments, as revealed by the study of long sediment cores, which appear most enigmatic and seem to indicate that their origin may be different from that of the other elements. These traits appear most pronounced after a study of the long sediment cores raised from the Swedish Deep-Sea Expedition with the *Albatross* in 1947–1948.

In ordinary igneous rocks from the continents the average content of manganese is estimated at 0·1 per cent or 1000 p.p.m. In hydrolysates the average content is 620 p.p.m., whereas in red clay, according to Clarke and Steiger, the average content is 7670 p.p.m. Landergren's (1954) more recent value is 9430 p.p.m. In general the red clay samples have a much higher manganese content in the Pacific than in the Atlantic Ocean. However, of much greater interest than the *average* values, derived from a large number of samples analysed, are the *individual* values found in different samples from the same core.

By careful determination by means of the spectrograph on samples taken from a long core from the Romanche Deep in the equatorial Atlantic (lat. S 00°07′ long. W 18°12′, depth 7315 m, length of core 14·1 m) Landergren finds the average value from 140 samples, taken at intervals of 10 cm, to be 2400 p.p.m. of manganese. The individual values show very large variations, from a minimum of 700 p.p.m. to a maximum of 18,000 p.p.m., i.e. in the ratio of 1 : 26. Over a distance of 10 cm the content will fall from 18,000 to 900.

The curve taken from Landergren's paper, here reproduced as Fig. 1, presents very sharp and distinct maxima, separated by equally pronounced minima. Equally strong and abrupt variations in the manganese content were found in a number of long cores from the equatorial Pacific Ocean, analysed in Göteborg by Berrit and Rotschi (1956). It is obviously desirable to find an explanation for these extraordinary variations in the manganese content.

The great master of deep-sea sedimentology, Murray (1876), declared the manganese in the deep-sea deposits and also the red clay itself to be derived from a subaqueous decomposition of volcanic debris. Other authors of that time assumed the manganese in the sediment to be derived from the sea-water. Clarke in his review of the different hypotheses finds that by Murray to be the most probable. In recent times the main objection to the volcanic origin of suboceanic manganese has come from another master of deep-sea sedimentology, Correns (1937) of Göttingen. From his study of the Atlantic cores raised from the *Meteor*

expedition he concludes, that the excess manganese present in deep-sea sediments is largely derived through a biological extraction from the sea-water and a subsequent settling on to the ocean floor with calcareous shells.

In an earlier paper the present writer has voiced some objections to this view, mainly from a quantitative standpoint Pettersson, 1945). Still earlier (Pettersson, 1931) in a short paper published in Swedish, the writer suggested, that at volcanic eruptions on the ocean floor, chemical reactions on a vast scale between the magma and the highly compressed sea-water may be expected to take place, leading to a release of mineral acids. The same explanation may account for extensive layers of red clay over areas where no influence from Arctic or Antarctic bottom currents can be evoked, but where there is instead an abundance of volcanic minerals and glass dispersed in the sediment.* Also Correns, in his report, expresses similar views, without expressly indicating mineral acids as operative: "Die submarine Verwitterung hat sich also in diesem Beispiel im besten Falle auf das Glas beschränkt, wenn es sich nicht überhaupt um einen reinen Auslaugungsvorgang bei der Reaktion des heissen Magmas mit dem Meerwasser handelt."

From this view of the volcanic debris on the ocean floor as a possible source of suboceanic manganese Goldberg and Arrhenius (1957) in a joint paper take exception: "In view of the obvious" (?) "necessity of separating the source of the manganese from the deposits the emphasis on volcanic debris on the ocean bottom does not any longer seem to be necessary".

This somewhat apodictic statement is in contrast with views earlier expressed by one of the authors (Arrhenius) who in his important contribution to the *Reports of the Swedish Deep-Sea Expedition* (Vol. V., 1, p. 112) states: "The higher concentration of manganese in its turn is believed to have its origin in decaying volcanic matter in this area", and, in another place: "Especially in regions of volcanic activity amounts of manganese appear to be released by the submarine weathering of igneous rocks and to be separated from the iron through selective diffusion and precipitation."

Although Landergren (1954) abstains from pronouncing a verdict upon the different theories for the origin of suboceanic manganese, he writes (*ibid.* p. 142). "One inclines to assume that the source of this ferride" (manganese) "is to a great extent different from that of the other ferrides".

Berrit (1955), discussing the abnormally high values for manganese found in different *Albatross* cores, writes: "On peut se demander si ces valeurs exceptionelles de la teneur en manganese ne sont pas à rattacher à une activité volcanique et à l'erosion sous-marine, si la seule source du manganese est continental, ou s'il n'existe pas une autre source sous-marine, liée au volcanisme."

* Added to recent discoveries of numerous volcanic peaks, "guyots" in the Pacific Ocean we have now the evidence from seismic investigations by Gaskell, Hill and Swallow (1958) proving the widespread occurrence of submarine lava beds below the unconsolidated sediments in the Pacific and Indian Oceans, supporting the views of the dominant influence on the ocean floor from submarine volcanic activity.

In the joint paper by Arrhenius and Goldberg (1957), p. 195, it is stated that the belief in the relatively high manganese contents of the foraminifera reported by Correns have been confirmed recently (Arrhenius, *et al.*, in preparation) by analyses of planktonic foraminifera caught by tow-net, So far no quantitative data on this find have reached the present author.

Instead of referring at length to the different views brought forward on this theme the present writer will refer only to the two figures showing the vertical distribution of manganese in two cores, one (Fig. 1) from the central Atlantic Ocean (LANDERGREN), the other in Fig. 2 from the west Pacific Ocean (*Albatross* core no. 100) analysed by BERRIT and ROTSCHI (1956). "According to the present author the very prominent maxima of manganese in these two cores are due to volcanic outbreaks in the near locality. It would be most interesting to know

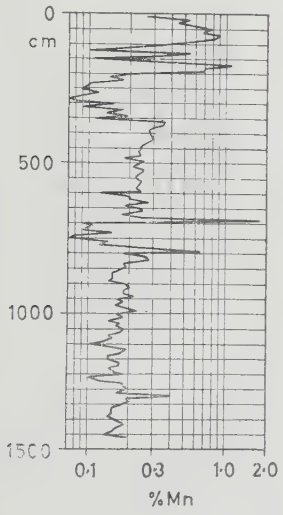

Fig. 1.

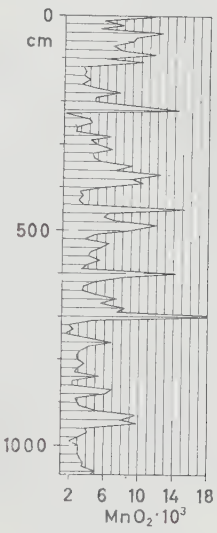

Fig. 2.

how these remarkable curves are to be explained by the theories of biological extraction or of chemical precipitation from sea-water!"

Nickel. In ordinary igneous rocks from the continents the average content of nickel according to SANDELL and GOLDICH (1943) is 80 p.p.m. or 0·008 per cent. According to spectrographic analyses by LANDERGREN on 140 samples taken from the core from the Romanche Deep, their average content is 138 p.p.m. or 0·0138 per cent for the whole core. Just as in the case of manganese there are striking variations along the core in nickel content, from a maximum of almost 0·1 per cent or 990 p.p.m., to minima of 20 p.p.m. in the ratio of almost 50 : 1. On the other hand in a core from the equatorial Pacific Ocean analysed by ROTSCHI (1951) there were variations in the nickel content from a maximum of 624 p.p.m. to a minimum of 24 p.p.m., i.e. in the ratio of 26 : 1 (compare Figs. 3 and 4).

In order to explain the relatively large content of nickel in deep-sea deposits PETTERSSON and ROTSCHI (1952) suggested that the excess nickel may be of cosmic origin. The maxima of nickel found in different levels of the cores might then be explained as due to an unusually heavy incidence from the cosmos.

Against this interpretation SMALES and WISEMAN (1955) objected that the relatively low values for cobalt and copper found by them in the nickel from a deep-sea core make it unlikely that the suboceanic nickel is of cosmic origin. The acknowledged master of meteor studies, ÖPIK (1956), took exception to this

view stating (p. 116): "A reconsideration of Smales' and Wiseman's results show that they are not so negative at all, the apparent contradiction being partly due to the arithmetic of presentation . . ."

Assuming an admixture of 1·25 per cent of cosmic substance to the sediment, with 2 per cent nickel content, Öpik finds that the relative abundance of nickel and copper agree very well with the hypothesis of cosmic (meteoritic) origin: "Smales and Wiseman compared only the abundance ratios of the red clay with

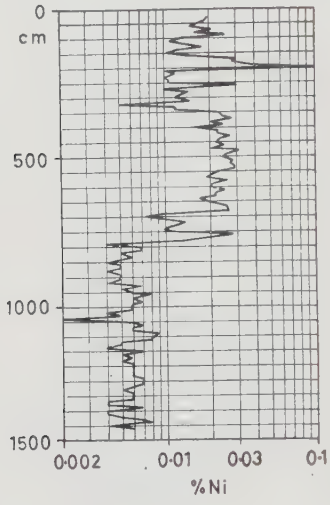

Fig. 3.

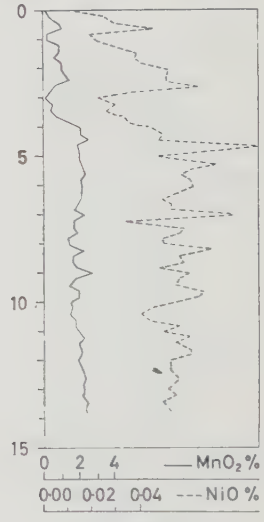

Fig. 4.

those of the two parent substances, without calculating how they would result in a mixture. Their analyses actually support the hypothesis of cosmic origin, with the possibility that cobalt is more abundant in the zodiacal dust than in the meteorites." Öpik sums up his reasoning with: "Pettersson's hypothesis of the cosmic origin of the deep-sea nickel has gained considerable support."

Recently Goldberg (1954) has propounded a theory for the "scavenging" of various trace elements into the sediments like nickel by the hydrated oxides of manganese and iron. In support of this view Goldberg quotes results from analyses made here in Göteborg on some Pacific sediments, from which he infers that the ratio Mn/Ni is remarkably constant, varying only between 38 and 53, with the exception of two cores in which it is considerably higher. These two exceptions Goldberg explains from an admixture of volcanic glass, palagonite and phillipsite to the two cores, giving them higher values for the ratio manganese to nickel.

This appears as a typical misuse of *average* values from core analyses. Scrutinizing instead the analyses of *individual* samples, from which the table quoted by Goldberg was computed, one finds very considerable variations of the Mn/Ni ratio in these cores, variations which refute Goldberg's hypothesis of a constant Mn/Ni ratio.

From the assumption that the hydroxides of manganese and nickel act as

scavengers for nickel, one must expect a close correlation between the content of nickel and of the two other ferrides in our cores. This is certainly not the case, as a scrutiny of the results published by LANDERGREN and by BERRIT and ROTSCHI proves.

The writer, therefore, finds no reason to abandon his earlier published view, that the origin of the two elements here discussed in the deep-sea sediments is different from that of the other ferrides, especially as regards the anomalously high values for manganese and nickel contents, the former being largely due to suboceanic volcanic action, the latter due to contributions from the cosmos.

REFERENCES

BERRIT G. R. (1955) Etude des Teneurs en Manganese etc. *Medd. Oceanogr. Inst.* **23,**

BERRIT G. R. and ROTSCHI H. (1956) *Reports Swedish Deep-Sea Expedition* Vol. VI, Fasc. 2.

CORRENS C. (1937) Die Sedimente d.Äq, Atl. Oceans. *Wiss. Ergebn. dtsch. atlant. Exped. 'Meteor'.* **3,** 3.

CORRENS C. (1941) Beiträgez. Geochem. d. Eisens und Mangans. *Nachr. Akad. Wiss. Göttingen.*

GASKELL T., HILL M. and SWALLOW J. (1958) Seismic investigations. *Phil. Trans.* **251,** 23-63.

GOLDBERG E. (1954) Marine geochemistry etc. *J. Geol.* **62,** 254.

GOLBDERG E. and ARRHENIUS G. (1957) Chemistry of pacific pelagic sediments. *Geochim. et Cosmochim. Acta* **13,** 153.

LANDERGREN S. (1954) *Reports Swedish Deep-Sea Expedition* Vol. VII, Fasc. 2. Göteborg.

MURRAY J. (1876) *Proc. Roy. Soc. Edin.* **9,** 255.

ÖPIK E. J. (1956) Interplanetary dust etc. *Astr. J.* **4,** 116.

PETTERSSON H. (1931) Djuphavets radiumhalt. *Ymer.* **51** 36.

PETTERSSON H. (1945) Iron and manganese on the ocean floor. *Medd. Oceanogr. Inst.* **7,**

PETTERSSON H. and ROTSCHI H. (1952) *Geochim. et Cosmochim. Acta* **2,** 81.

Reports of the Swedish Deep-Sea Expedition Vol. II, IV and V. Göteborg.

ROTSCHI H. (1951) Etude des teneurs en fer etc. *Centre de Recherches et d'Études* 2-22.

SANDELL E. and GOLDICH S. (1943) *J. Geol.* **51,** 161-189.

SMALES A. and WISEMAN J. (1955) *Nature, Lond.* **175,** 464.

Geochimica et Cosmochimica Acta, 1959, Vol. 17, pp. 214 to 225. Pergamon Press Ltd. Printed in Northern Ireland

The change in solubility of calcium carbonate with temperature and carbon dioxide content*

P. K. Weyl
Shell Development Company, Houston, Texas

Abstract—The solubility of calcite and aragonite in carbonic acid has been determined over a CO_2 concentration range from 10^{-4} to 10^{-3} molal and a temperature range from 10° to 70°C. The measurements were made in the absence of a gas phase in a newly developed conductometric solubility apparatus. The temperature derivative of solubility of calcite at constant CO_2 concentration varies from -10^{-6} to -3×10^{-5} molal/°C, being a maximum for the highest CO_2 concentration and temperature. The derivative of the solubility of calcite with respect to CO_2 concentration at constant temperature has a value approximately 1 at very low CO_2 concentrations and decreases as the CO_2 concentration rises.

At low CO_2 concentrations, the solubility of aragonite is the same as that of calcite within the experimental errors. At a CO_2 concentration of 10^{-3} molal, aragonite is about 11 per cent more soluble than calcite.

Introduction

In a recent paper (Weyl, 1958), the writer has investigated the solution kinetics of calcite. It was shown that under normal geologic conditions, the water in the pores of a limestone is always saturated with respect to calcite. Solution or precipitation can therefore only take place as the solubility changes because of changes in temperature, pressure, or chemical composition of the moving water.

Recently, Graf and Lamar (1955) have reviewed the literature on calcium carbonate. In the previous work, the solubility of calcium carbonate in equilibrium with a fixed partial pressure of CO_2 was determined. In these experiments, as the temperature is changed, the amount of CO_2 dissolved in the water changes. As water moves through the pores of a permeable limestone, it is generally not in contact with a gas phase so that no exchange of CO_2 can take place. It is therefore of interest to determine directly how the solubility of calcium carbonate changes with temperature for a given initial concentration of CO_2 in the water. The change of solubility with initial CO_2 concentration can be obtained by repeating the measurements with different initial concentrations.

The main problem in measuring the solubilities of slightly soluble substances is to attain saturation rapidly and to know when saturation has been reached. To permit continuous monitoring of the solution process without disturbing the system, the conductometric method, first developed by Kohlrausch (1903) and used by Baeckstroem (1921) to measure the solubility of calcite and aragonite, was employed.

If the experiment is not expeditiously designed, the time required to reach equilibrium can be very long; thus Shternina and Frolova (1952) required 30 days and Baeckstroem (1921) 100 hr. In order to minimize the time, it is necessary to know the rate-determining mechanism. The writer has shown (Weyl, 1958) that the rate of solution of calcite is determined by the rate of diffusion of the solute away from the solid liquid interface, where the solution is always

* Publication No. 186, Shell Development Company, Exploration and Production Research Division, Houston, Texas.

saturated. To decrease the equilibration time, it is thus necessary to reduce the distance the solute has to diffuse. This can be done either by stirring, or by passing the solution through a pack of small crystals of the solid phase, so that the diffusion distance is limited to the effective radius of the pores in the pack. The latter method was chosen in this experiment.

Apparatus

To determine the solubility of calcium carbonate conductometrically, a special solubility apparatus was developed. This apparatus has been described in detail in a previous publication (Weyl, 1957).

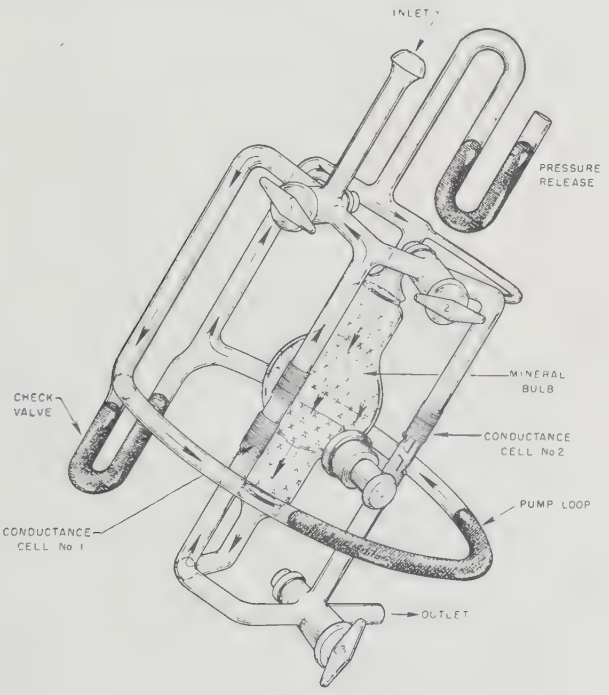

Fig. 1. Solubility apparatus.

Fig. 1 is a perspective drawing of this solubility apparatus, which consists of two conductance cells, a bulb filled with the mineral under investigation, and a pump for circulating the solution. The entire apparatus is made out of glass and can be completely filled with the solution under investigation.

The pump circulates the solution through the mineral bulb, where solution or precipitation takes place, and then through conductance cell no. 1 and back again. The process of equilibration can be continuously monitored by measuring the conductance in cell no. 1. Conductance cell no. 2, which can be isolated from the system by stopcocks nos. 2 and 3, is provided to determine the change of conductance with temperature of a solution of constant concentration. Stopcock no. 1 permits sealing the apparatus after filling. To provide for differential thermal expansion, a mercury-sealed pressure release is provided.

The constant temperature bath

The conductance apparatus in its mount is immersed in an oil thermostat, so that the circulating solution is maintained at a constant temperature. The bath consists of a 12 in. diameter by 12 in. deep Pyrex jar with heater, stirrer, cooling coils and thermo-regulator. The temperature is maintained constant to within $\pm 0{\cdot}05$°C over a range from 10° to 70°C. For the lower temperatures, ice water is circulated through the cooling coils.

The conductance bridge

The conductance bridge employed is a Model 250-DA Impedance Bridge manufactured by Electro-Measurements, Inc. All the measurements were made at a frequency of 1000 c/s. The quoted accuracy of the bridge is $\pm 0{\cdot}5$ per cent. The reproducibility of the measurements was about $\pm 0{\cdot}1$ per cent.

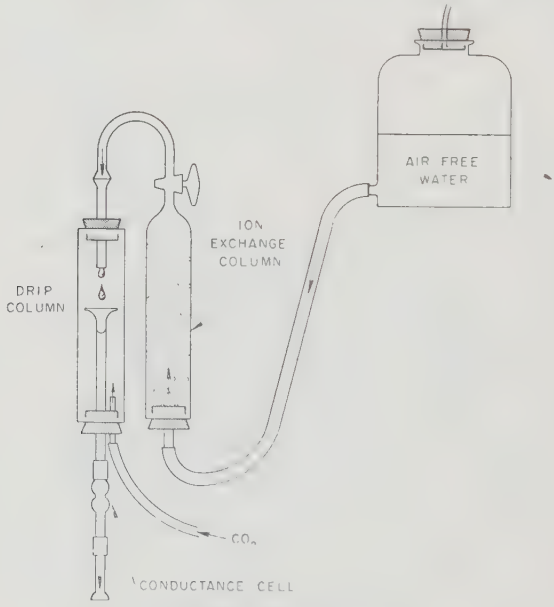

Fig. 2. Carbonic acid column.

Procedure of Measurements

The conductance cell is cleaned and filled with distilled water. Crystals of the mineral under investigation of size fraction from 20 to 35 mesh are washed into the mineral bulb through the tapered opening. During this operation, care must be taken that no air bubbles are trapped in the pack. The opening is closed with the glass stopper, and again no air must be trapped. The pumping loop and check valve are now filled with an appropriate amount of mercury to ensure pumping action. The cell is mounted in a horizontal position so that the mercury does not seal the solution in the loop.

Carbonic acid of known concentration is flowed into the cell to displace all the original water. Fig. 2 shows how the carbonic acid is prepared. Since the cell will later be raised to a temperature of 70°C, it is important that the water used

be deaerated by boiling under reduced pressure to ensure that no gas will come out of solution when the cell is heated. To purify the distilled water further, it is passed through a column filled with Rohm and Haas Amberlite MB-1 mixed cation and anion exchange resin. After leaving the resin, the water passes through only glass or Teflon couplings to prevent contamination.

To prepare carbonic acid, the purified water is dripped through CO_2 gas. By adjusting the height through which the water drips, the CO_2 concentration can be varied from less than 10^{-3} to more than 10^{-2} molal. The concentration of the carbonic acid is determined by measuring its conductance. For this purpose an Industrial Instruments pipette conductivity cell model G05 is attached to the end of the drip column. After leaving the conductivity cell, the carbonic acid is made to flow through the solubility apparatus until all the water in it has been replaced. When the cell is filled, sufficient mercury is put into the pressure release tube to seal it from the atmosphere. After a limited amount of pumping, and before the solution has become saturated, stopcocks nos. 2 and 3 are closed so that cell no. 2 is isolated from the system.

The solubility apparatus is now placed on its mounting, and the entire assembly is immersed in the oil thermostat. The cell is rotated to produce pumping, and the resistance of the solution in the cells is measured from time to time until equilibrium is reached. Fig. 3 is a typical plot of the resistance values obtained. These measurements were made at 25°C. The temperature was approached from above and below to make sure that equilibrium had been attained. The resistance of cell no. 2 gives an indication of the temperature, while the ratio of the two resistances indicates the change in solubility. The two determinations of solubility differ by about 0·25 per cent, which is well within the experimental error. Baeckstroem found differences of about 1 per cent when he approached equilibrium from above and below.

After equilibrium had been reached, the temperature of the bath was changed and a new determination was made. Data were obtained at 10°, 25°, 40°, 55° and 70°C. After one run was completed, the carbonic acid in the solubility apparatus was replaced by carbonic acid of a different concentration.

To determine the amount of supersaturation that can be tolerated before calcium carbonate precipitates in absence of a solid phase, the solution in both cells was brought to saturation at 10°C, where the solubility was greatest. Cell no. 2 was then isolated, and the apparatus was slowly heated to 70°C.

Calculation of the Solubility

Calculation of the carbon dioxide concentration in the feed water

The water used in filling the solubility apparatus contains only dissolved CO_2, carbonate, bicarbonate, hydrogen and hydroxide ions. At the CO_2 concentrations used, the concentrations of the various constituents have the following relationship:

$$[H_2CO_{3\,aq.}] \gg [H^+] = [HCO_3^-] \gg [CO_3^{2-}], [OH^-]. \quad (1)$$

The first ionization constant of carbonic acid is

$$k_1 = [H^+][HCO_3^-]/[H_2CO_{3\,aq.}] = [H^+]^2/[H_2CO_{3\,aq.}]\,. \quad (2)$$

Since the conductance of the solution is proportional to the hydrogen ion concentration, the square of the conductance will be proportional to the concentration of dissolved CO_2.

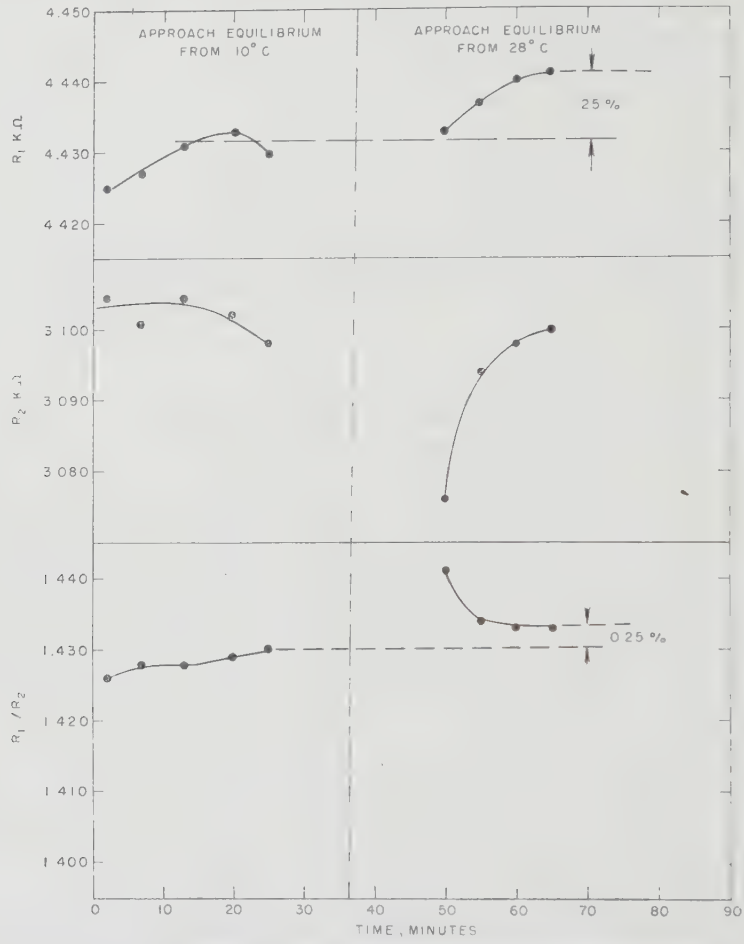

Fig. 3. Approach of equilibrium in conductance measurement.

To obtain the proportionality constant at any one temperature, the following relationship is used:

$$C = \sigma^2 C_s/\sigma_s^2 \tag{3}$$

where C is the concentration, C_s is the concentration of a saturated solution, and σ and σ_s are the specific conductances of the solution and the saturated solution, all taken at the same temperature. Table 1 lists the required data as obtained from the literature.

Fig. 4 is a plot of the ratio C_s/σ_s^2 vs. temperature. The validity of equation (3) has been checked against data obtained by Shedlovsky and MacInnes (1935). For a range of concentrations from 2 to 33 $\times$ 10^{-3} molal, the ratio of C/σ^2 at 25°C differed from the above tabulated value of C_s/σ_s^2 by no more than 2·5 per cent.

Table 1

T (°C)	σ_s (ohm/cm $\times 10^5$)	C_s (molal $\times 10^3$)	C_s/σ_s^2 [molal (ohm cm)$^2 \times 10^{-7}$]
20	4·53	38·4	1·87
25	4·71	33·7	1·52
30	4·86	28·7	1·215

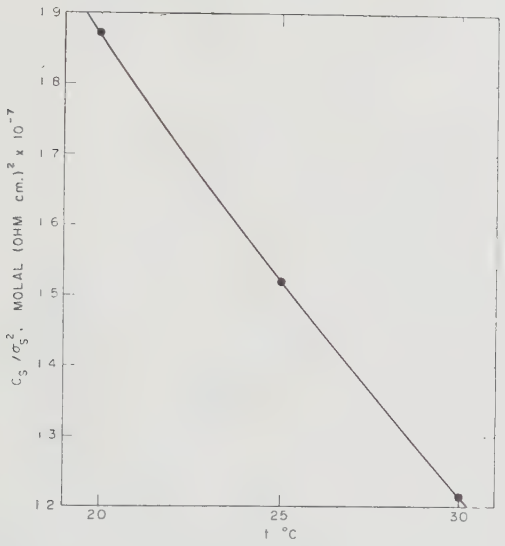

Fig. 4. The ratio of the concentration to the square of the specific conductance for carbonic acid.

This error combined with an error of 1 per cent in the specific conductance shows the error in the CO_2 concentration to be no more than 4 per cent.

Calculation of the calcium ion concentration

As calcite dissolves in the carbonic acid, the H_2CO_3 aq. dissociates until, for the concentrations here considered, there are two bicarbonate ions for every calcium ion. The solution can thus be considered as a calcium bicarbonate solution.

The molal conductance of calcium bicarbonate at 25°C as a function of concentration has been determined by Baeckstroem (1921) and Kendall. Their data over the concentration range of interest are plotted in Fig. 5. To determine the concentration it is then necessary to convert the conductance data at a series of temperatures to the conductance at 25°C. To obtain the ratio of the conductance at temperature T to the conductance at 25°C, the resistance of a solution of constant weight concentration is measured in cell no. 2. The specific conductance at 25°C is then found from the following formula:

$$\sigma(25) = K_1 R_2(T)/R_1(T)R_2(25) \qquad (4)$$

where $\sigma(25)$ is the specific conductance at 25°C of a solution having the same weight concentration as the saturated solution, K_1 is the cell constant of conductance cell no. 1, $R_1(T)$ is the resistance of cell no. 1 filled with a saturated solution at temperature T, and $R_2(T)$ and $R_2(25)$ are the resistances of cell no. 2 filled with a solution of constant weight concentration at temperatures T and 25, respectively.

For this expression to be valid, it is necessary that the ratio of $R_2(25)/R_2(T)$ be independent of the concentration. Fig. 6 is a plot of this ratio for a number of

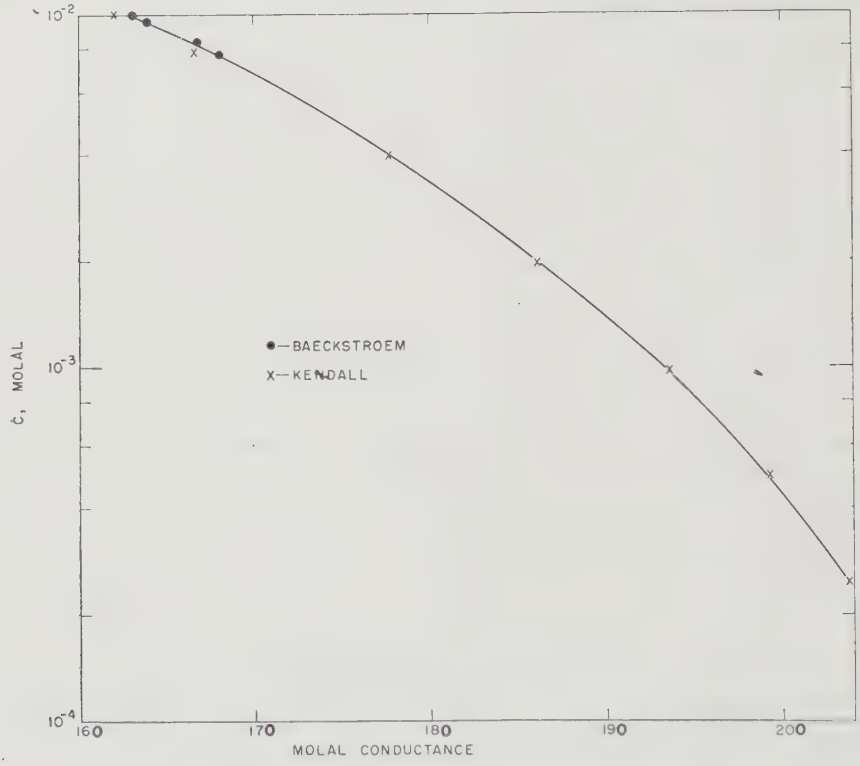

Fig. 5. Molal conductance of calcium bicarbonate at 25°C.

undersaturated and supersaturated solutions. It can be seen that the ratio is indeed independent of the concentration within the experimental errors.

With equation (4), an accurate determination of the temperature is not required, for the solubility changes only little with temperature. To obtain the concentration of the saturated solution, the specific conductance corrected to 25°C is divided by the molal conductance of a solution of the required concentration at 25°C. This calculation is carried on by a number of successive approximations. The concentration is first guessed, and the appropriate molal conductance is read off Fig. 5. Dividing the specific conductance by this molal conductance gives a new value for the concentration. This gives a better approximation for the molal conductance, in turn giving a new concentration. As a change in concentration from 10^{-2} to 10^{-3} molal only changes the molal conductance 17 per cent, a final value of the concentration is rapidly reached.

Results

The results of six determinations with calcite and two with aragonite are listed in Table 2.

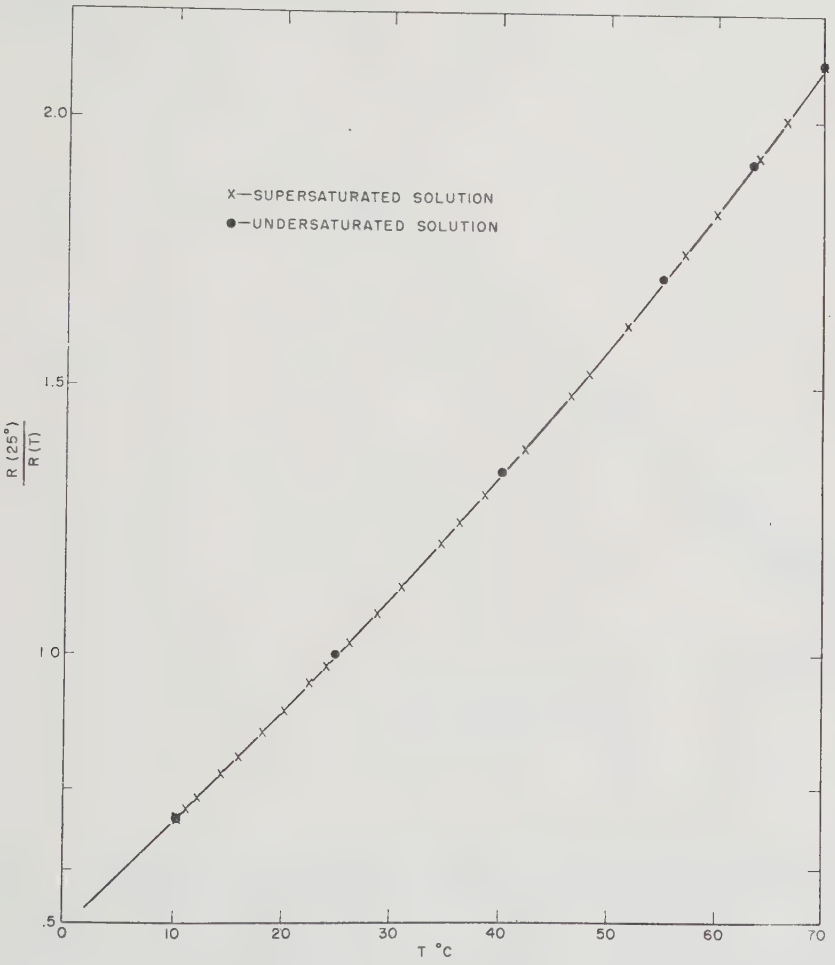

Fig. 6. Change of conductance of calcite solutions in carbonic acid with temperature.

Calcite

The calcite used was optical grade Iceland spar from Mexico. The data are plotted in Fig. 7. The errors are about 4 per cent in the CO_2 concentration and 1 per cent in the calcium ion concentration. Three points at 25°C from the data of Shternina and Frolova (1952) are in good agreement with the data.

The temperature derivative of solubility with constant initial CO_2 content is plotted in Fig. 8. The derivative is negative, indicating a decrease of solubility with increasing temperature. Increasing the temperature or the CO_2 content increases the magnitude of the derivative. The derivative varies from about -10^6 to -3×10^{-5} molal/°C. The error in the derivative is about 10 per cent at

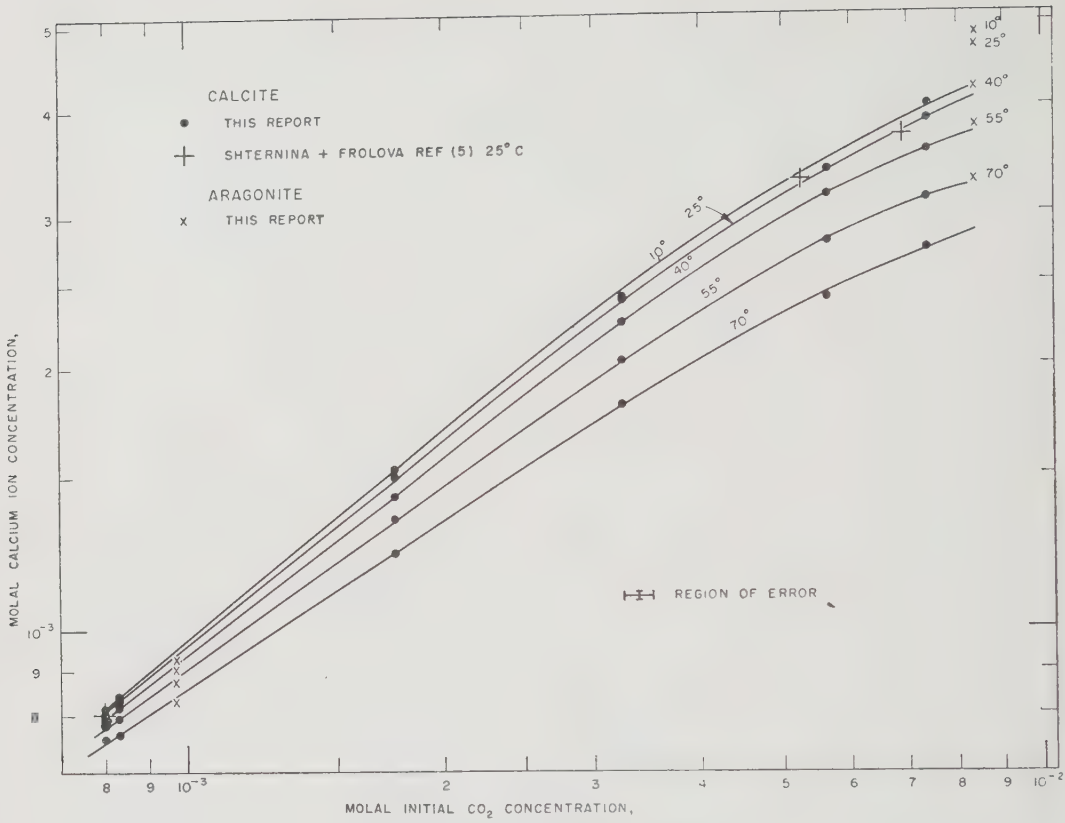

Fig. 7. Solubility of calcium carbonate.

Table 2. Molal solubility of calcite and aragonite in carbonic acid

	$C\ CO_2 \times 10^3$	$C\ Ca^{2+} \times 10^3$				
		10°	25°	40°	55°	70°
Calcite	0·80	0·812	0·808	0·795	0·776	0·748
	0·83	0·838	0·829	0·814	0·789	0·754
	1·76	1·53	1·50	1·43	1·34	1·23
	3·28	2·43	2·40	2·25	2·05	1·82
	5·67	3·38	3·37	3·15	2·78	2·41
	7·40	4·00	3·86	3·53	3·12	2·74
Aragonite	0·975	0·925	0·916	0·902	0·873	0·824
	8·34	4·83	4·70	4·21	3·80	3·29

the highest temperatures, while the error at the lower temperatures is considerably larger.

The change of solubility of calcite with addition of CO_2 at constant temperature is plotted in Fig. 9. For low CO_2 concentrations, the derivative approaches

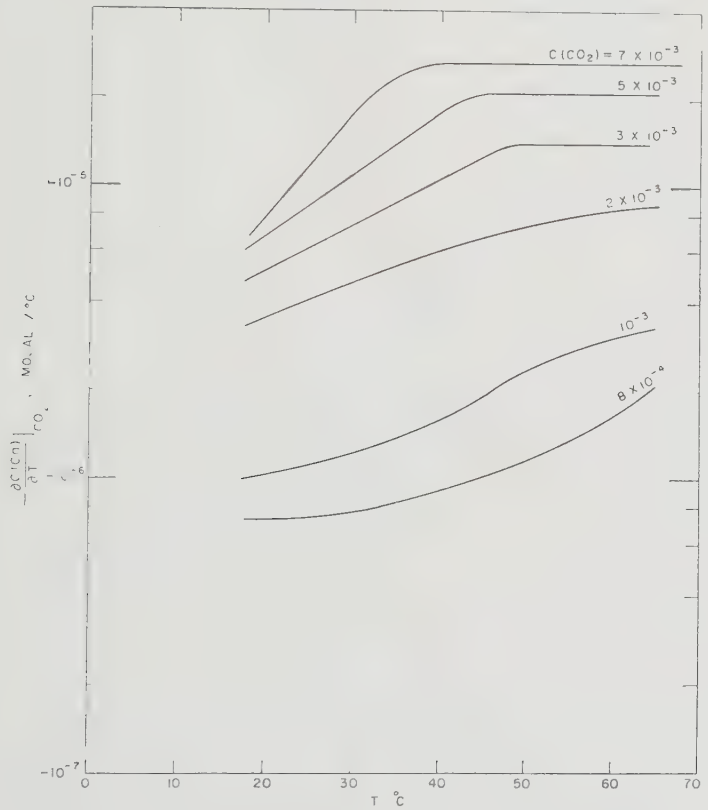

Fig. 8. Temperature derivative of solubility of calcite at constant initial CO_2 concentration.

unity. Increasing the temperature or the CO_2 pressure decreases the value of the derivative. The value of the derivative is accurate to about 10 per cent.

An 11 per cent supersaturated solution at 70°C, obtained by slowly heating a solution saturated at 10°C to 70°C in 2·5 hr, did not result in precipitation.

Aragonite

The aragonite used was white crystalline material from Agrigento, Sicily. Two determinations were made at CO_2 concentrations of 0·975 and 8·34 $\times$ 10^{-3} molal. The data are plotted in Fig. 7. The data for the low CO_2 concentration do not differ significantly from the data for calcite, while the solubility of aragonite at the higher CO_2 concentration is significantly greater. The ratio of the solubility of aragonite to the solubility of calcite at a CO_2 concentration of 8·3 $\times$ 10^{-3} molal is about 1·14 $\pm$ 0·02 for the temperature range from 10° to 70°C. For saturated

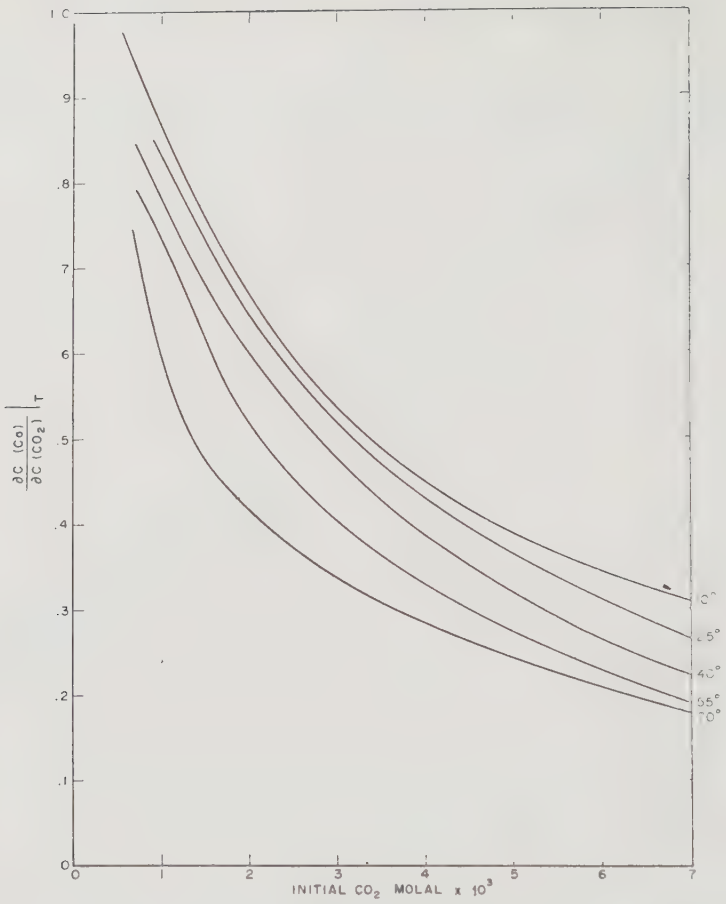

Fig. 9. Change of solubility of calcite with addition of CO_2 at constant temperature.

solutions in equilibrium with 1 atm. of CO_2. Baeckstroem (1921) obtained a ratio of 1·12, 1·13 and 1·145 at temperatures of 9°, 25° and 35 °C, respectively.

A 35 per cent supersaturated solution at 70°C, obtained by slowly heating a solution saturated at 10°C to 70°C in 6·5 hr, did not result in precipitation.

Acknowledgement—Most of the experimental work herein described was done by Mr. D. C. Berkshire.

References

Baeckstroem H. L. J. (1921) Ueber die Affinitaet der Aragonit-Calcit Umwandlung. *Z. phys. Chem.* **97,** 179.

Graf D. L. and Lamar J. E. (1955) Properties of calcium and magnesium carbonates and their bearing on some uses of carbonate rocks. *Econ. Geol.* Fiftieth Anniversary Volume, pp. 639–713.

Kohlrausch F. (1903) Ueber gesaettigte waessrige Loesungen schwerloeslicher Salze. *Z. phys. Chem.* **44,** 197.

Shedlovsky T. and MacInnes D. A. (1935) The first ionization constant of carbonic acid. *J. Amer. Chem. Soc.* **57,** 1705.

Shternina E. B. and Frolova E. V. (1952) The solubility of calcite in the presence of CO_2 and NaCl. *Izv. Sektor. Fiz-Khim. Anal., Obshch. Neorg. Kim., Akad. Nauk SSSR* **21,** 271–287; A. T. S. Translation No. 34H9R.

Weyl P. K. (1957) Apparatus for the conductometric determination of solubility. *Rev. Sci. Instrum.* **28,** 722–723.

Weyl P. K. (1958) The solution kinetics of calcite. *J. Geol.* **66,** 163–176.

Geochimica et Cosmochimica Acta, 1959, Vol. 17, pp. 226 to 233. Pergamon Press Ltd. Printed in Northern Ireland

Determination of uranium equilibrium in rocks using α and fission fragment radiography*

J. D. Grace and T. F. Bates
The Carter Oil Company, Riverton, Wyoming
and
Department of Mineralogy, Pennsylvania State University,
University Park, Pennsylvania

(*Received* 4 *February* 1959)

Abstract—A technique has been developed that permits the determination of uranium–daughter product equilibrium in polished sections by combining α and fission fragment radiography. The procedure consists of placing an uncovered rock section in contact with, first, an α-sensitive emulsion to record the α-particle emission from uranium and its eight α-emitting daughter products, and second, an emulsion sensitive to fission fragments (but not α-particles) to record the tracks of fission fragments produced from U^{235} when the slide is bombarded with thermal neutrons. A sample with approximately 100 p.p.m. of uranium in equilibrium emits about 570 α-tracks/cm² per day in an autoradiograph, and about 10,000 fission fragment tracks/cm² per hr, when exposed to a neutron flux of $2{\cdot}25 \times 10^{10}$ neutrons/cm² per sec. A sample deficient in uranium daughter products will release relatively more fission fragment tracks than α-tracks, and the opposite is true if the sample has a deficiency of uranium with respect to daughter products.

The technique has the advantages of being non-destructive, applicable on a micro scale, and suitable for use on samples having uranium contents as low as 10 p.p.m.

Introduction

In the determination of uranium content and distribution in natural specimens, results obtained with most types of electronic equipment are seriously affected if the uranium and its daughter products are not in equilibrium. Similarly α-track autoradiographic methods, although very useful in studying the distribution of all α-emitters in the specimen, do not reveal the amount and distribution of uranium if disequilibrium exists. Curie and Faraggi (1951) have shown how fission fragment radiography can be effectively used to determine the uranium content and distribution irrespective of the extent of disequilibrium in the sample. Bates, Wright and Skipper (in press) have provided additional information on the application of the method to the qualitative study of the distribution of uranium^{-235} in thin sections of rocks containing very small as well as large amounts of this element. The technique described herein shows how α and fission fragment radiography can be combined to determine the nature and extent of the equilibrium relationships between uranium and its daughter products.

The procedure consists of obtaining first an α- autoradiograph and then a fission fragment radiograph from the same sample. A comparison of track number and distribution in the two patterns provides the appropriate information as to the state of equilibrium in the specimen as a whole and the microscopic distribution of uranium as related to that of the daughter products. The procedure has the advantages of being non-destructive, applicable on a micro scale, and makes it

* Contribution no. 58–49, Mineral Industries Experiment Station, The Pennsylvania State University, University Park, Pennsylvania.

possible to relate uranium and daughter product distribution, independently, to the mineralogical and petrographic properties of the specimen. On the other hand the technique is not effective for these purposes in rocks containing appreciable thorium since α-tracks from this element and its daughter products will cloud the uranium–uranium daughter product picture. Fortunately the effect of thorium is reduced since its decay constant is less than one-third that of uranium and since there are fewer α-emitting daughter products in the thorium series.

Table 1. Alpha and fission fragment track data

Sample	1 U	2 eU	3 U/eU	4 α exp. (days)	5 α-count	6 α/cm² per day	7 Reactor exp. (hr)	8 Fission fragment count	9 Fission fragment cm² per hr	10 col. 6(x100) / col. 9
Group I										
005	0·0207	0·0002	103	20	112	286	6·5	514	18,615	1·536
025	0·0836	0·0003	279	20	504	1286	0·5	184	86,627	1·485
125	0·4210	0·0026	162	5	601	6136	0·5	852	401,122	1·530
Group II										
361	0·0137	0·0163	0·84	20	229	584	6·5	281	10,177	5·738
455	0·0528	0·0568	0·93	5	274	2798	0·5	104	48,963	5·715
461	0·0203	0·0209	0·97	5	113	1154	0·5	44	20,715	5·571
Group III										
1577	0·2478	0·2170	1·14	5	974	9945	0·5	661	311,199	3·196
9300	0·0511	0·4750	0·11	5	826	8433	0·5	139	65,441	12·886
9301A	0·0997	0·0726	1·37	5	397	4053	0·5	242	113,934	3·557
Group IV										
2-112	0·0142	0·0133	1·07	60	656	558	6·5	282	10,213	5·464
2-113	0·0084	0·0129	0·65	60	621	528	6·5	247	8,946	5·902
2-114	0·0092	0·0115	0·80	60	645	549	6·5	261	9452	5·808
3-115	0·0054	0·0075	0·72	60	428	364	6·5	179	6483	5·615
3-116	0·0075	0·0113	0·66	60	540	460	6·5	196	7098	6·481
3-118	0·0039	0·0094	0·41	60	306	260	6·5	98	3549	7·326
4-120	0·0091	0·0118	0·77	60	642	546	6·5	243	8800	6·205
4-121	0·0061	0·0101	0·63	60	512	436	6·5	194	7026	6·206
4-122	0·0023	0·0071	0·32	60	277	236	6·5	75	2716	8·689
Group V*										
154·3	0·0112	0·0125	0·90	60	153	520	6·5	247	8945	5·813
157·9	0·0090	0·0127	0·71	60	150	510	6·5	259	9380	5·437
158·2	0·0080	0·0114	0·70	60	146	496	6·5	237	8583	5·779
194·6	0·0101	0·0135	0·75	60	166	564	6·5	290	10,502	5·370
197·5	0·0058	0·0106	0·55	60	132	449	6·5	187	6772	6·630
198·7	0·0146	0·0115	1·27	60	141	490	6·5	272	9851	4·974
206·5	0·0091	0·0129	0·71	60	160	544	6·5	253	9162	5·938
209·4	0·0079	0·0101	0·78	60	166	564	6·5	269	9742	5·789
210·4	0·0077	0·0099	0·78	60	155	527	6·5	241	8728	6·038

* On these samples track counts were taken at the top and bottom of each thin section. The figures given in this table are the average counts for the section as a whole.

Samples Investigated

In order to provide a variety of equilibrium conditions to determine the possible range of the technique, five groups of samples were chosen for the study.

Group I, as listed in Table 1, consists of standard samples prepared by soaking 1 cm² of high gloss paper in an aqueous solution of uranium acetate of known concentration. The paper was placed on a plastic slide and exposed to the emulsions in the same manner as in the case of the rock sections. These samples were employed primarily because they were known to be out of equilibrium as no appreciable quantity of the daughter elements could have formed since the date of manufacture.

The group II samples are specimens of uraniferous microcrystalline quartz

vein material collected by Dr. H. D. Wright of the Department of Mineralogy, The Pennsylvania State University, from the Boulder Batholith Region of western Montana. They are presumed to be in equilibrium since uranium and radium determinations made for Dr. Wright revealed this to be the case for two other samples of the group.

The samples of group III are hydrothermal sulphide minerals also collected by Dr. Wright from waste piles near Central City, Colorado. These samples are believed to be in disequilibrium because of their long exposure to weathering; and because Phair and Levine (1953) have shown that such is the case for other samples from these waste piles.

The samples listed in the table in group IV are outcrop samples of the uraniferous Chattanooga shale collected from the Youngs Bend area near Smithville, Tennessee. The samples were badly weathered and were included in order to determine whether exposure had produced a different state of equilibrium than that exhibited by group V material.

The samples in the last group (V) were randomly selected from three cores of the "top black" unit of unweathered Chattanooga shale, also near Smithville, Tennessee. The specimens are extremely hard and compact, show no effects of metamorphism or ground water action, and are considered to be in equilibrium. A description of this material has been given elsewhere by Bates and Strahl (1957).

Techniques

Production of Radiographs

Preparation of samples

Each sample was cut in half and one portion was used for performing fluorimetric uranium determinations and β–γ counts for equivalent uranium determinations on each sample. The second half was cemented to a plastic slide, used instead of glass to avoid unwanted activation of some of the elements in the glass during exposure in the nuclear reactor. The sections were then ground and polished to a smooth surface by standard procedures, taking care to change the grinding powder after each slide was completed in order to avoid contamination. Rather than attempting to make thin sections of constant thickness, a uniformly thick source for α-emission was assured by making sections thicker than 50 μ, the maximum range of α-particles in rock material.

The nine samples from the shale cores were mounted with the bedding perpendicular to the length of the slide and with the direction of the stratigraphic top of the section known so that the comparison of α and fission fragment tracks at the top vs. the bottom of each section would reveal any disequilibrium that might exist within the section.

Emulsions

A wide variety of commercially produced nuclear emulsions are available with varying sensitivity for recording nuclear particles (See Yagoda, 1949; and Boyd, 1955). For this study, 50 μ Ilford C. 2 emulsion on 1 × 3 in. glass plates was used for recording α-particles. Kodak experimental NTC emulsion in gel

form, obtained through the courtesy of Dr. W. F. Swann of the Eastman Kodak Company, was used for the preparation of emulsion plates for recording fission fragment tracks. Plastic slides, identical with those used for mounting the samples, were coated with the emulsion using techniques similar to those developed by Edwards (1955). The NTC emulsion does not detect α-particles.

Exposure

After preparation, the polished sections were placed in direct contact with the Ilford C.2 emulsion, with the labels of both slides coincident to facilitate relating the α-activity of the samples to their mineral composition and texture. The emulsion and sample pair were then placed in a light-tight box and exposed for a duration of time inversely proportional to the estimated activity of the specimen.

After exposure the α-plate was removed and the section placed in direct contact with the prepared NTC emulsion in order to record the fission fragments released from the sample during neutron bombardment. The two slides were clamped together and wrapped in light-tight paper to facilitate handling during shipment to the Los Alamos Reactor where, under the direction of Dr. N. Nereson of the University of California, the samples were exposed to a flux of $2{\cdot}5 \times 10^{10}$ neutrons/cm^2 per sec. The samples of relatively low uranium content has a $6\frac{1}{2}$ hr exposure at the given flux and the samples of greater radioactivity were given a $\frac{1}{2}$ hr exposure.

Eradication of γ-ray "fog"

During the exposure of the sample in the nuclear reactor, the γ-radiation associated with the production of neutrons produces a latent image in the emulsion. Development results in a darkening or background "fog" which makes observations of the fission fragment tracks difficult. The fogging is particularly prominent when it is necessary to use long exposures for samples of low radioactivity.

Several methods of reducing the amount of fogging have been described by Liebermann and Barschall (1943), Faraggi *et al.* (1952), and others. For this study a method described by Goldstein and Sherman (1952), based on the principle of Herschel effect, was found to be fast and convenient. The technique involves infra-red irradiation of the photographic emulsion after the latter is exposed to neutron bombardment but before development. The infra-red radiation preferentially reduces the weakly ionized latent image caused by γ-radiation, relative to the latent image produced by the stronger ionizing radiation of the fission fragments.

Experimentally the procedure consisted of placing the "reactor-exposed" emulsions in a light-tight box having a Wratten 88 infra-red filter at one end. Light from a 500 W source placed 50 cm from the box was passed through the filter on to the emulsion. It was found that emulsions exposed in the reactor for $6\frac{1}{2}$ hr needed an infra-red exposure of 10 min to reduce the background fog sufficiently to observe the fission fragment tracks. The samples exposed for $\frac{1}{2}$ hr in the reactor needed only a 4 min infra-red exposure.

Photographic processing

Kodak D-19 developer was found to be satisfactory for producing legible tracks with a minimum of interference from background fog. The Ilford C.2 α-recording emulsions were developed for 4 min while the fission fragment-sensitive NTC emulsions were given a 3 min development. The shorter time is sufficient for developing the tracks from the high energy fission fragments yet helps to inhibit the development of background fog.

Microscopic Evaluation

After processing both the Ilford C.2 α-emulsion and the Kodak NTC fission-sensitive emulsion obtained on a given sample, the films were ready for microscope examination in order to determine the number of tracks recorded. All the emulsions were examined with a Zeiss microscope equipped with a mechanical stage. For track-counting purposes it was found that the use of a binocular eyepiece and soft green light helped reduce eyestrain.

A magnification of five hundred proved to be satisfactory for counting the α-tracks registered in the Ilford C.2 emulsions. The area of emulsion viewed in each field at this magnification is 0·0816 mm^2. A total of twenty-four such fields, arranged in a grid pattern were counted on each emulsion to give a representative number of tracks emitted from the samples of groups I, II, and III. The emulsions from the samples of group IV were counted by taking six fields of view covering a total area of approximately $1 \times \frac{1}{2}$ mm at the opposite ends of the emulsion which in turn correspond with the stratigraphic top and bottom of the sample. From these values the number of α-tracks/cm^2 per day was calculated (column 6, Table 1).

The short range fission fragment tracks were counted by using a one hundred power oil immersion objective, coupled with a ten power ocular for a total magnification of approximately one thousand. The area of the field of view at this magnification is 0·0177 mm^2. The fission fragment tracks were counted by using a twenty-four field grid pattern similar to that used in the α-track counting, and the counts were converted to fission fragment tracks per cm^2. This figure in turn was divided by the exposure time of the sample in the nuclear reactor to give the number of fission fragments per cm^2 per hr exposure (column 9, Table 1).

The ratio of column 6 (multiplied by 100 for convenience) to column 9 is presented in column 10 and is referred to as the α/fission fragment ratio.

Analysis of Data

The data obtained on the twenty-seven samples investigated are presented in Table 1. The last column gives the ratio of α to fission fragment tracks obtained in the emulsions under the conditions described previously.

Materials believed from other considerations to be in equilibrium, namely samples of groups II and V, give ratios averaging approximately 5·7. Since the amount of thorium in these samples is known to be too small to affect the ratio seriously, this value is taken to be representative of natural situations wherein neither uranium nor its daughter products have been preferentially leached from or added to the rock.

Calculation of the "equilibrium value" of the ratio on the basis of uranium vs. eU data is illustrated in Fig. 1, which shows the α/fission fragment ratio vs. the chem.U/eU ratio for each sample plotted on a log–log scale. Correlation between the two variables is high ($r = 0{\cdot}91$), and the regression equation [$\log y = 0{\cdot}847 - 0{\cdot}3072 \log(x + 1)$] gives a value of 5·689 for the α/fission fragment ratio at equilibrium conditions (as represented by U/eU = 1·0).

In considering the deviations of points from the regression line in Fig. 1 it will be noted that the weathered sulphide samples (group III) show a greater

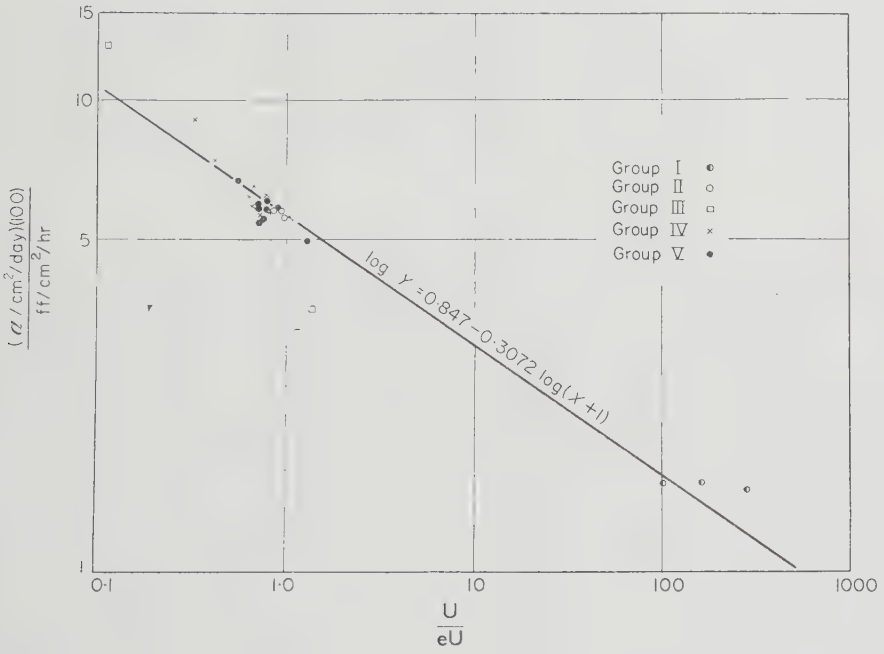

Fig. 1. Equilibrium conditions of the the samples as indicated by track vs. Chem. U/eU data.

departure than the others. This may be attributed to several possible causes, of which the most important is the difficulty of obtaining representative track counts and comparable U and eU determinations from samples which have a very heterogeneous distribution of the radioactive constituents. Actually, the apparent discrepancy brings out an important advantage of the track method, namely that it provides an effective means of studying microscopic variations which cannot be "resolved" by techniques requiring larger or pulverized samples.

The samples of group I, which are those prepared from uranium acetate and therefore contain a minimum of daughter products, give an average value of 1·52 for the ratio of α to fission fragment tracks. Under the conditions of experiment involved, this figure is believed to approach the limiting value for that type of disequilibrium in which uranium is in excess of its daughters. Disequilibrium of this type is also represented by the ratios obtained for the natural weathered sulphide samples NO. 1577 and NO. 9301A, and for Chattanooga shale sample NO. 198·7.

In samples where the thorium content is not significant, such as those described here, ratios greater than that of approximately 5·7 for the equilibrium situation would result from preferential removal of uranium or selective enrichment or this part of the rock with daughter products produced elsewhere. The third weathered sulphide specimen, NO. 9300, shows the greatest amount of disequilibrium of this type. In the case of this particular sample it has been shown previously (Bates, Wright and Skipper, in press) that abundant star-clusters of α tracks due to radium provide a striking difference between the α and the fission-fragment track patterns.

A few of the shale samples such as NO. 3–118 and NO. 4–122, give high ratios; and the average of the outcrop shale samples (group IV), 6·410, is appreciably greater than that of the core material (group V), 5·752. However, an analysis of variance reveals that the difference between these two groups as compared with the variance within the groups is not significant at the 0·05 per cent level.

Summary and Conclusions

By comparing α-autoradiographs and fission-fragment radiographs of thin polished sections of uraniferous rocks and counting a representative number of each type of tracks in the two different radiographs produced from the same section, an evaluation can be made of the state of equilibrium that exists on a micro scale between uranium and its daughter products. The method is non-destructive and can be applied equally well to materials of low or high uranium content. The technique involves comparison of the α-autoradiograph, produced in the usual way, with a fission-fragment radiograph obtained by bombarding the U^{235} in the emulsion-coated specimen with thermal neutrons from a reactor. γ-Fogging of the reactor-irradiated film is partially eradicated by exposure of the latent image to infra-red radiation prior to development of the emulsion.

A study was made of twenty-four natural and three synthetic specimens having uranium contents ranging from 39 to 4,210 p.p.m. Under the conditions of the experiment samples in equilibrium gave a value of 5·7 for the ratio of α tracks $(\times 100)/cm^2$ per day of exposure to fission fragment tracks/cm^2 per hr of exposure. Other specimens in which weathering had caused preferential movement of uranium with respect to its daughter products, or vice versa, gave ratios varying from 12·89 to 3·19. Nine weathered outcrop samples of Chattanooga shale were found to be not significantly different from nine, apparently unweathered, core samples as far as the state of equilibrium is concerned, indicating lack of preferential removal of uranium with respect to its daughter products.

References

Bates T. F. and Strahl E. O. (1957). Mineralogy, petrography, and radioactivity of representative samples of Chattanooga Shale. *Bull. Geol. Soc. Amer.* **68**, 1305–1314.

Bates T. F., Wright H. D. and Skipper S. J. Geological studies of uraniferous minerals and rocks by fission fragment radiography. *Proc. Twentieth Int. Geol. Congr., Mexico City, 1956.* In press.

Boyd G. A. (1955) *Autoradiography in Biology and Medicine.* Academic Press, New York.

Curie I. and Faragci H. (1951) Autoradiographie par neutrons. Dosage separe de l'uranium et des thorium dans les mineraus. *C. R. Acad. Sci., Paris* **232**, 959–961.

Edwards L. C. (1955). Nuclear plate coating device for autoradiography. *Rev. Sci. Instrum.* **26**, 515–516.

Faraggi H., Bennet A. and Cohen M. J. (1952) Irradiation et development des emulsions nucleaires exposées à des lux intenses de neutrons thermiques, accompagnés de rayons r. *J. Phys. Radium* **13**, Suppl. 7, 105A–111A.

Goldstein A. M. and Sherman C. H. (1952) The Herschel effect and selective erasing of nuclear emulsions. *Rev. Sci. Instrum.* **23**, No. 6, 267–271.

Liebermann L. N. and Barschall H. H. (1943) A method for removing microscopic fog from photographic plates. *Rev. Sci. Instrum.* **14**, No. 4, 89–90.

Phair G. and Levine H. (1953) Notes on the differential leaching of uranium, radium and lead from pitchblende in H_2SO_4 solutions. *Econ. Geol.* **48**, 358–369.

Yagoda H. (1949) *Radioactive Measurements with Nuclear Emulsions*. John Wiley, New York.

Geochimica et Cosmochimica Acta, 1959, Vol. 17, pp. 234 to 247. Pergamon Press Ltd. Printed in Northern Ireland

Magnetic susceptibility of tektites and some other glasses*

F. E. Senftle and A. Thorpe
U.S. Geological Survey, Washington 25, D.C. and Howard University, Washington, D.C.

(*Received* 9 *April* 1959)

Abstract—The magnetic susceptibility at several magnetic field strengths of about thirty tektites from various localities have been measured. The susceptibility ranges from 2×10^{-6} to about $7{\cdot}9 \times 10^{-6}$ e.m.u./g. Tektites from a given locality have similar susceptibilities. The intensity of magnetization of all the tektites measured is zero or very small.

For comparison, the same measurements have been made on about thirty obsidians. The magnetic susceptibilities cover approximately the same range, but the intensity of magnetization of the impurity was found to be much higher. By heating the obsidians to 1450°C the intensity of magnetization was reduced to zero.

From the above data, it is shown that the tektites must have been heated well above 1400°C, and that essentially all the iron is in solution. On the other hand, the evidence shows that obsidians have not been heated much above this temperature, and that there is a significant amount of undissolved iron in the glass, probably as magnetite. Further, if tektites are extraterrestrial, they probably entered the earth's atmosphere as a glass.

Introduction

Small glass objects of certain types, found in widely separated localities on the face of the earth have been called tektites. There are currently two schools of thought on the origin of tektites, one that they are terrestrial, the other extraterrestrial. It was hoped at the start of this work that a study of the magnetic properties might add evidence to favour either one theory or the other, although not necessarily offer a proof. If the source is outside the earth, tektites can perhaps yield interesting information about materials from outer space. Current emphasis on space studies has stimulated a considerable increase in the investigation of tektites during the past few years.

Although many properties have been studied, there has been no systematic investigation of the magnetic susceptibility of tektites and their comparison with the magnetic properties of other natural glasses. So far as is known the magnetic susceptibility of only one tektite has ever been measured. Sigamony (1944) measured the susceptibility of a tektite from Billiton Island and his results are listed in Table 1. A resumé of the past work and some of the important recent work on these strange objects has been published as a result of a Symposium on Tektites (Friedman *et al.*, 1958; Friedman, 1958a).

Experimental Procedure

The magnetic susceptibility measurements were made on a modified Curie–Cheneveau balance developed by Senftle *et al.* (1958). Only about 1 mg of sample was required, and for most measurements only a single fragment of the sample was used in order to reduce the possibility of surface contamination. The surfaces of the glasses were cleaned by soaking overnight in cold HCl to remove any possible external ferromagnetic contamination. After the specimens were

* Publication authorized by the Director, U.S. Geological Survey.

Table 1. Magnetic susceptibility of tektites and other similar glasses

Sample no.	Locality	Magnetic susceptibility ($\times 10^{-6}$ e.m.u./g)	Intensity of magnetization ($\times 10^{-4}$ e.m.u./g)
42-1	Philippines, Busuanga	7·3	0
96-6	Philippines, Balacan	7·6	0
43-3	Philippines, Rizal	6·8	0
43-3	Same as above except heated to 1450°C	6·6	0
43-6	Philippines, Rizal	7·0	0
96-2	Philippines, Luzon	6·5	0
96-7	Billiton Island, Indonesia	7·2	0
*	Billiton Island, Indonesia	7·8	0
96-11	Java	7·6	0
RS-6	Java	7·7	0
RS-7	Java	7·0	0
RS-8	Java	7·9	0
RS-9	Java	6·9	0
RS-10	Java	6·7	0
40-15	French Indo-China	7·3	0
42-2	French Indo-China	5·4	0
96-10	French Indo-China	6·3	0
43-7	Texas	6·5	0
27-17	Texas	5·4	0
27-17	Same as above except heated to 1450°C	5·4	0
RS-2	Eastern portion, Lee County, Texas	5·2	0
RS-3	Near Bedias, Grimes County, Texas	4·2	0
RS-4	Near Muldoon, Fayette County, Texas	5·0	0
RS-5	Near Bedias, Grimes County, Texas	5·4	0
97-2	Australia	5·8	0
43-4	Perth, Australia	6·0	0
H-1	Australia	6·9	0
H-2	Australia	5·9	0
H-3	Australia	6·2	0
96-9	Thailand	5·1	0
97-9	Bohemia	2·3	0
3060-1	Bohemia	3·0	0
1396	Georgia	3·6	0
41-15	Peru†	0·41	3·8
43-5	Libyan Desert†	−0·20	0
97-1	Aouelloul, Adrar, French West Africa‡	3·8	0

* Measured by A. Sigamony (1944). No sample number designated.
† Considered by some not to be a true tektite.
‡ Impactite.

thoroughly washed and dried, they were placed on the balance and the final measurements made in a helium atmosphere at room temperature (29°C). All measurements were referred to a platinum standard, $\chi = (0{\cdot}962_8 \pm 0{\cdot}0015) \times 10^{-6}$ e.m.u./g (29°C).

The magnetic susceptibility of each specimen was measured at several field

strengths. The apparent magnetic susceptibilities were plotted against the reciprocal field at each field strength to check for ferromagnetic impurity after the manner of Owen (1912) and Honda (1910). For the field strengths used (>3900 G) the apparent susceptibility, χ_a, is given by

$$\chi_a = \chi_t + \frac{\sigma}{H} \tag{1}$$

where H is the field strength and σ is the intensity of magnetization per gramme of the ferromagnetic impurity in the sample. The true magnetic susceptibility, χ_t, could thus be evaluated by extrapolating to $1/H = 0$. In all cases where $\sigma > 0$ a

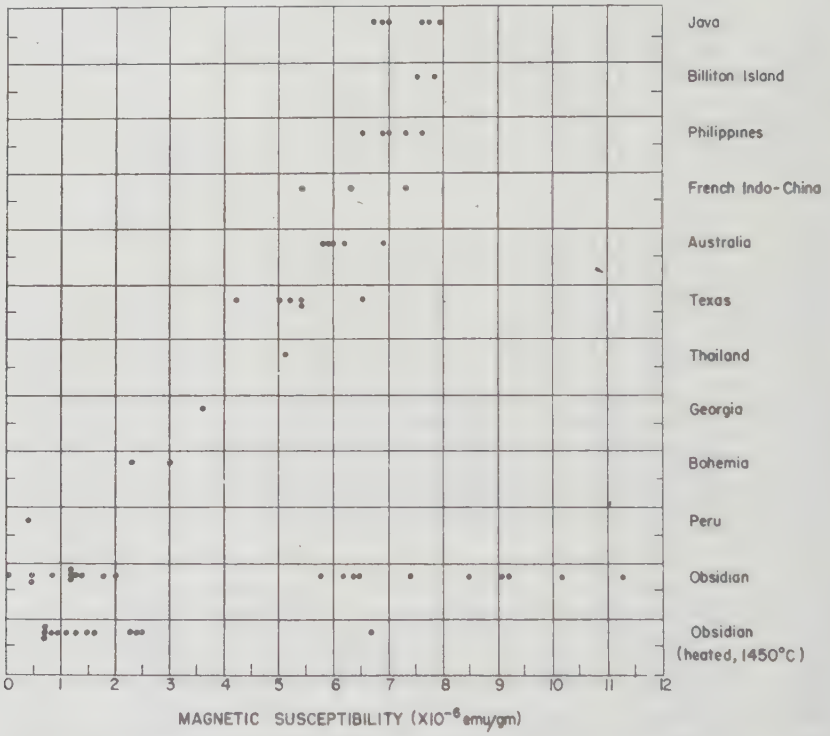

Fig. 1. Relative magnetic susceptibility of the tektites and obsidians measured.

least squares analysis was made to obtain the extrapolated value of the magnetic susceptibility. The intensity of magnetization, i.e. the slope of these curves is a measure of the ferromagnetic impurity and is affected by the past thermal history of the sample. For this reason it was also measured for each specimen.

The susceptibility measurements at each field strength are accurate to about 1 per cent. However, because of the compositional variation in the sample and errors in the extrapolation to $1/H = 0$, the errors are of the order of 2 or 3 per cent.

Results

The magnetic susceptibilities of tektites, obsidians and a variety of other earth glasses are shown in Tables 1–4. The results for each class of materials are different

and are discussed below in some detail. The tektite and obsidian data are summarized in Fig. 1. Most of the specimens have been obtained from FRIEDMAN and are described in more detail by him (FRIEDMAN, 1958b, and FRIEDMAN and SMITH, 1958). Those not described in these publications are detailed at the end of this paper.

Tektites

The magnetic susceptibilities of tektites range from about 2×10^{-6} e.m.u./g for a specimen from Bohemia to $7{\cdot}9 \times 10^{-6}$ e.m.u./g for a Java tektite. If one considers the Peruvian specimen and Libyan Desert glass as true tektites this would extend the range to lower values. In general those tektites of a given type have susceptibilities which fall reasonably close to each other. The samples from Java and Billiton Island have susceptibilities similar to the philippinites and this similarity may be taken as evidence that they are from the same source. On the other hand one can see that both the specimen from Georgia and the moldavites show unusually low magnetic susceptibilities. This similarity may likewise be construed as evidence that the Georgia specimen is a moldavite, but the geographical separation of their locations makes a common source theory somewhat questionable, especially if a terrestrial theory of formation is held. Absorption spectra of COHEN (1958) also show similarities between these two types of tektites.

One of the most striking features of the tektites as a group is their extremely low intensity of magnetization. This field independence indicates the absence of a ferromagnetic impurity phase. Although most tektites analysed to date show several per cent iron, the lack of ferromagnetism is not surprising if one considers the nature of a tektite. Since they are glasses and hence true liquids the impurity atoms should be in solution and completely ionized. At low concentrations dissolved ions are paramagnetic or diamagnetic, but as far as is known never ferromagnetic. For ferromagnetism one must have elemental aggregates in order to form a ferromagnetic "domain". One is therefore led to either one of two conclusions, (1) the iron in tektites is completely in solution or (2) the iron is in an iron compound, such as magnetite, the particles of which must be extremely small, i.e. "sub-domain" in size.

Since iron is the principal paramagnetic ion present in tektites, it is of interest to attempt a rough calculation of the susceptibility of the various tektite types. To do this one can use the Stoner–Van Vleck formula for atomic ferrous and ferric paramagnetic susceptibilities,

$$\chi_c = \frac{N\beta^2}{3kT}[4S(S+1) + L(L+1)] \tag{2}$$

where N is Avogadro's number, β is the unit Bohr magneton, k is Boltzmann's constant, and T is the absolute temperature. S and L are the spin and orbital quantum numbers. Since L is quenched, the spin only formula was used in calculating the magnetic susceptibility of ionic iron. The total susceptibility, χ, is therefore found by using the relation

$$\chi = (\chi_c \cdot \mathrm{Fe})_{\mathrm{Fe}^{2+}} + (\chi_c \cdot \mathrm{Fe})_{\mathrm{Fe}^{3+}} + \chi_g \tag{3}$$

where Fe is the percentage ferrous or ferric iron in the glass and χ_g is the magnetic susceptibility of the base glass, i.e. the glass without any iron.

From the average FeO and Fe_2O_3 analyses of each type presented by Barnes (1940), we have estimated the approximate susceptibility of the base glass for each tektite type using the magnetic susceptibility of the average indochinite base glass as a reference. We also assumed the observed susceptibility of the indochinite glass to be correct and calculated the base glass susceptibility which would give the correct value of χ. The susceptibility of the base glass for the other tektite

Table 2. Comparison of the calculated and observed magnetic susceptibilities

Type	Average FeO (from analyses given by Barnes, 1940) (%)	Average Fe_2O_3 (from analyses given by Barnes, 1940) (%)	Contribution of magnetic susceptibility of base glass (calculated on basis of the indochinite base glass) ($\times 10^{-6}$ e.m.u./g)	Average observed magnetic susceptibility ($\times 10^{-6}$ e.m.u./g)	Calculated magnetic susceptibility ($\times 10^{-6}$ e.m.u./g)
Bediasites	4·00	0·41	$-0{\cdot}87_8$	$5{\cdot}2_9$	$5{\cdot}3_7$
Philippinites	4·19	1·47	$-0{\cdot}87_3$	$7{\cdot}0_4$	$7{\cdot}0_4$
Moldavites	2·24	0·15	$-0{\cdot}88_8$	$2{\cdot}6_5$	$2{\cdot}7_4$
Indochinites	4·98	0·19	$-0{\cdot}87_3$	$6{\cdot}3_3$	$6{\cdot}3_3$*
Australites	4·25	0·50	$-0{\cdot}87_6$	$6{\cdot}1_6$	$5{\cdot}8_8$
Billitonites and associated tektites	5·27	0·74	$-0{\cdot}86_7$	$7{\cdot}5_0$	$7{\cdot}7_3$
Libyan Desert glass	0·23	0·11	$-0{\cdot}90_7$	$-0{\cdot}20$	$-0{\cdot}3_9$
Java tektites	4·46	0·83	$-0{\cdot}87_3$	$7{\cdot}3_0$	$6{\cdot}7_8$†

* Reference value, assumed the same as observed value.
† Based on analyses on a single sample given by Barnes (1940).

types was estimated by adjusting this value proportionally according to the percentage of all other impurity, i.e. 100 minus percentage total iron. The estimated susceptibilities of the base glass are shown in Table 2. The indochinites were picked for a reference because the average analyses seemed to be representative of tektites in general.

The results of the calculated and observed magnetic susceptibilities (Table 2) agree reasonably well when one considers that the iron analyses are only average values and do not correspond to the exact specimens on which the susceptibilities were measured. The fact that one can estimate the susceptibility from the chemical ferrous and ferric iron analyses lends support to the view that the iron is present primarily in the ferrous state. Absorption spectra of tektites measured by Cohen (1958) also show that the iron is in the ferrous state although similar spectral measurements have been interpreted by Stair (1955) as showing the iron primarily in the ferric state. Further the agreement between the calculated and experimental susceptibilities indicates essentially complete solution of the iron. If the iron were

present as "sub-domain" size particles of iron-bearing compound, the paramagnetic susceptibility would be such as to make it extremely doubtful whether one could get so good an agreement.

If the iron is completely dissolved one would expect little change on heating. Even the dark colour of tektites would not change. The approximately 4–5 per cent ionic iron is sufficient to give the dark colour. To substantiate this reasoning two tektites (27-17 and 43-3) were heated to about 1450°C for about 10 min in a vacuum. As expected the colour and the magnetic properties remained unchanged.

To check the uniformity of the magnetic susceptibility of a given tektite, several measurements were made across single specimens. Fig. 2(a) shows a slice from the indochinite, 40-15, showing the location of the chip taken for the measurement and the magnetic susceptibility. In this particular specimen only a 4 per cent variation was noted. This tektite is considered quite homogeneous when compared to a similar test on obsidian glass. Fig. 2(b) shows a flanged tektite from Australia, H-1. Again the values obtained do not vary widely. The reheated flange has a slightly higher value of χ, but this is not considered significant.

The Aouelloul glass from Adrar, French West Africa, although considered by some to be an impactite has been included in the list of tektites because of its similarity to these specimens. The magnetic susceptibility is not unlike that found for a moldavite or the tektite from Georgia. What is more impressive, however, is the complete lack of any detectable ferromagnetic impurity which again indicates a high melting temperature. Smith and Hey (1952), in discussing this same glass, have called attention to the similarity in composition between the Aouelloul glass, a moldavite, and the local sandstone. They further suggest that it may well be an impactite formed by mixing of a molten tektite of moldavite composition with the local sandstone. The magnetic data, indeed, would seem to confirm this hypothesis.

The specimen from Peru apparently is questionable as a true tektite. Cohen (1958) and others believe that this americanite is a rare type of obsidian. The magnetic susceptibility of this specimen is certainly lower than for most tektites, but this can readily be explained by the low iron content (Linck, 1926). However, a small amount of ferromagnetic impurity is shown by the low intensity of magnetization. Although the field dependence is not large, it is significant especially for a specimen with such a low susceptibility. Undoubtedly this specimen contains some "magnetic domains", i.e. undissolved ferromagnetic compounds, and in this respect it looks as if it might be an obsidian.

Obsidian

Acid igneous glasses closely resemble in many ways the average tektite. For this reason, it was interesting to examine more closely the magnetic properties of obsidian. The range of the magnetic susceptibilities of the obsidian samples (Table 3 and Fig. 1) in general overlaps that of the tektites, and extends both above and below the tektite range in a few of the specimens. Also from Fig. 1 it is shown that the data on the individual samples appears to fall into two groups, one below a susceptibility of 2×10^{-6} e.m.u./g and the other from 6 to 11×10^{-6} e.m.u./g.

One of the very marked differences found between these two glasses is the much larger intensity of magnetization, σ, determined for obsidians. As stated previously

Table 3. Magnetic susceptibility of obsidians

Sample no.	Locality	Before heating		After heating to approximately 1450°C	
		Magnetic susceptibility ($\times 10^{-6}$ e.m.u./g)	Intensity of magnetization ($\times 10^{-4}$ e.m.u./g)	Magnetic susceptibility ($\times 10^{-6}$ e.m.u./g)	Intensity of magnetization ($\times 10^{-4}$ e.m.u./g)
67-4	Xalpazquillo Pueblo, Mexico.	0·28	89	0·88	0
70-11	Ongarato (North Island), New Zealand (38°23′ S, 175°56′ E).	8·5	230	1·3	0
70-9a	Mayor Island, North Shore, New Zealand (37°18′ S, 176°15′ E); at tide mark.	6·5	0	6·7	0
70-9b	Same as above, except well above tide mark.	5·8	0	—	—
53-9	Olancha, Keeler quadrangle, California (36°20′ N, 117°50′20″ W).	1·8	77	0·97	0
52-21	Lower Lake, Clear Lake area, California, Secs. 16 and 17, T. 13 N. 7 W, M.D. (39°0′ N, 122°40′ W).	1·2	193	1·6	0
39-1	Mono Craters, Obsidian Cliff, California.	6·4	387	—	—
53-7	Mono Craters, Obsidian Cliff, California.	2·0	190	1·5	0
47-13	Big Glass Mountain, California.	0·85	364	2·4	2·6
2-5	Big Glass Mountain, California.	0·49	249	2·3	0
51-16	Little Glass Mountain, California.	0·07	506	2·5	0
3024-7	Superior, Arizona.	0·49	10	0·72	1·7
65-8	Thomas Range, Utah.	10	1000	1·1	15
65-3	Steamboat Springs, Nevada.	11	1040	0·71	7·4
67-2a	Bear Head, New Mexico.	9·2	1760	0·74	0
2-2	Peralta Canyon, Jemez Mountains, New Mexico.	1·4	69	—	—
39-2	Obsidian Cliff, Yellowstone Park, Wyoming (44°49′48″ N, 110°43′35″ W).	9·1	888	—	—
3023-3	Prestahnukur, Iceland (64°35′15″ N, 20°42′ W).	7·4	238	—	—
15-2	Lisht, Egypt.	6·2	84	—	—
27-7i-1	Naupe, Guayas Province, Ecuador.	1·2	112	—	—
27-7i-2	Naupe, Guayas Province, Ecuador.	1·3	308	—	—
27-7i-3	Naupe, Guayas Province, Ecuador.	$\geqslant 10^{-6}$*	$\geqslant 10^{-4}$*	—	—

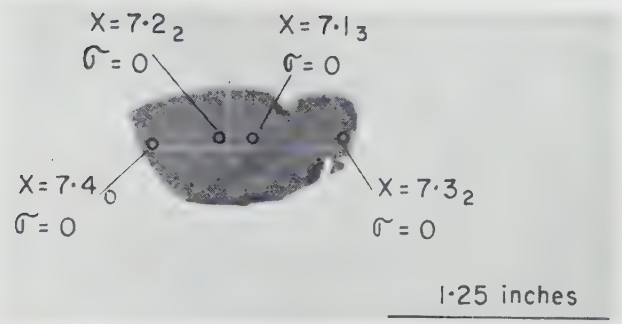

Fig. 2(a)

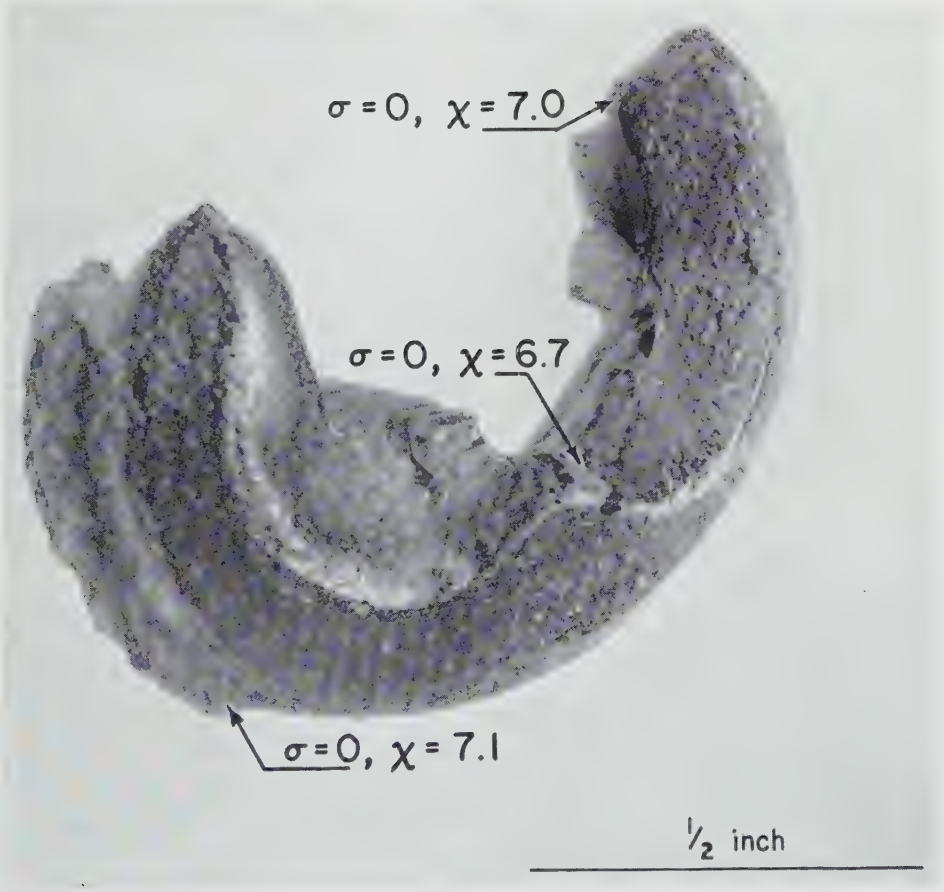

Fig. 2(b)

Fig. 2. (a) The magnetic susceptibility and intensity of magnetization at different locations across a tektite from Indochina (sample 40-15). (b) The magnetic susceptibility and intensity of magnetization of the reheated flange and at points within an Australian tektite (sample H-1).

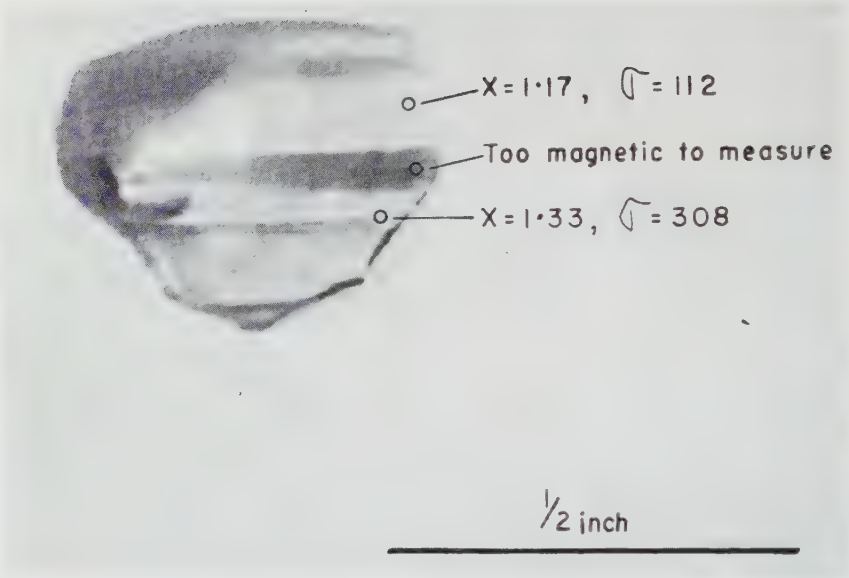

Fig. 3. Banded obsidian artifact showing the changes in the magnetic susceptibility and intensity of magnetization due to magnetic inclusions within the bands.

susceptibilities which are field dependent are indicative of ferromagnetic impurity which undoubtedly is due to undissolved iron compounds. Specimens of each obsidian which had been heated for several minutes at 1450°C in a vacuum in an induction furnace were measured. The results are also shown in Table 3, and summarized in Fig. 1. 1450°C is well beyond the melting region of the glass and is hot enough for most undissolved impurities to go into solution. Any undissolved iron would thus dissolve and the dispersed iron ions would lose their ferromagnetism. As expected, when the samples were heated, substantial reduction of the intensity of magnetization was observed. Where the intensity of magnetization is still slightly greater than zero, it can be assumed that there still remains a small amount of undissolved iron even after heating to 1450°C for a few minutes. The heated obsidian also shows a marked attenuation in magnetic susceptibility (see Fig. 1), especially for those obsidians which originally had susceptibilities greater than about 6×10^{-6} e.m.u./g.

It is generally thought that iron crystallizes out of obsidian probably in the form of magnetite and the usual grey black colour is attributed to microscopic magnetite particles. A good example of this, and one suitable for study, was found in sample 27-7i. This was a specimen of a sharply banded obsidian artifact (Fig. 3). The bands were made up of myriads of exceedingly small black particles. The unbanded area was glass clear but under the microscope a sparse population of slightly larger black particles was observed. The magnetic susceptibility, χ, of the clear glass (27-7i-1) was low and the intensity of magnetization, σ, indicated that these inclusions contained enough iron to form some ferromagnetic domains. The portion 27-7i-2 was similar to 27-7i-1 except it also had a very thin black striation made up of many microscopic black particles. As might be expected both χ and σ were higher showing that more iron was in an undissolved state. That portion of the specimen taken within the heavy black band, 27-7i-3, was so ferromagnetic that it could not be measured on our balance.

When obsidians are heated to 1450°C we find that generally the fine and coarser black particles disappear and σ approaches zero. This phenomenon, of course, is accompanied by a change in colour. The original black glass becomes a tinted transparent glass on thin edge and grades to a grey or black on thicker specimens. The lower iron content of most obsidian probably accounts for the greater bleaching effect on heating as contrasted with the somewhat darker colour retained by the tektites when heated. With one exception, the magnetic susceptibility is also lower (see Fig. 1) than in the unheated specimens when the susceptibility is above 6×10^{-6} e.m.u./g. The lower mean susceptibility is compatible with the known average chemical analysis of iron in obsidian, assuming all of the iron is in solution. For those obsidian specimens containing a large amount of ferromagnetic impurity, and where the susceptibility is less than 2×10^{-6} e.m.u./g, it becomes exceedingly difficult to measure the susceptibility accurately. Therefore, little significance is attached to the fact that in some specimens the susceptibility actually increased after heating (e.g. specimen 2-5 or 51-16). From this data one must assume an undissolved iron mineral in most obsidians which has gone into solution on heating to 1450°C.

The sample, 70-9, from Mayor Island, New Zealand is the only obsidian found

completely free of ferromagnetic impurity. This is surprising especially as the iron content reported by Marshall (1936) is 1·17 per cent Fe_2O_3 and 2·05 per cent FeO, values which are slightly higher than for the average obsidian. On heating to 1450°C the magnetic properties of this specimen remained essentially unchanged. As the magnetic susceptibility is field independent, the iron must be completely in solution, and in this respect this obsidian is similar to a tektite. This field independence might be explained if the molten lava chilled fast enough to preclude the possibility of iron coming out of solution. It is difficult to see why an obsidian with this iron content should retain all of the iron in solution except by rapid cooling.

Miscellaneous glasses

A few other terrestrial glasses have also been measured for the purpose of comparison (Table 4). The intensities of magnetization of the Hawaiian basaltic

Table 4. Magnetic susceptibility of miscellaneous samples

Sample no.	Locality	Magnetic susceptibility ($\times 10^{-6}$ e.m.u./g)	Intensity of magnetization ($\times 10^{-4}$ e.m.u./g)
67-3	Basalt glass, Hawaii (1954 flow).	17·0	0
67-3-S	Basalt glass, Hawaii (1919 flow).	17·0	0
40-13	Welded tuff, Idaho.	11·0	939
4C-13a	Welded tuff, Idaho (heated to 1450°C).	2·3	0
98-5	Beer bottle glass.	−0·09	—
93-4	Atom bomb glass, Alamogordo, New Mexico.	2·8	6·63
S-7	Oak Springs tuff, Rainier Tunnel, Nevada, before nuclear blast.	2·8	456
S-6	Atom bomb glass, produced by Rainier bomb test.	3·5	80
S-2	Brown sandstone, Imboden, Wise County, Virginia.	2·0	32·9
S-3	Black sintered sandstone, Imboden, Wise County, Virginia.	~0·4(?)	1270·0
S-4	Fused sandstone, black vitreous texture, Imboden, Wise County, Virginia.	$\geqslant 10^{-6}$*	$\geqslant 10^{-4}$*
S-1	Completely fused sandstone, translucent light brown glass, Imboden, Wise County, Virginia.	6·4	0
RS-1	Fulgurite, location unknown.	3·3	151

* Too magnetic to measure on our balance.

glasses from the 1919 and 1954 flows are zero and thus are similar to tektites, but the susceptibilities are higher than any tektite measured. The high susceptibility is to be expected from their greater iron content (2·06 per cent Fe_2O_3, 9·03 per cent FeO, Macdonald, 1949). The change in the intensity of magnetization of the welded tuff from Idaho after heating to 1450°C is also another good example of the effect of undissolved iron.

In September of 1958, a power line failure occurred near Imboden, Wise County, Virginia, which resulted in the fusion of about 40 ft^3 of sandstone about the base of a steel power line tower. Magnetic susceptibility measurements were made on the unmelted rock and also at different levels of heating as one progressed into the area where the molten rock actually flowed. The unmelted sandstone, S-2, had a normal susceptibility, but the black sintered, S-3, and vitreous material, S-4, contained too much iron, probably from melting of the tower, to get reliable results. A microscopic examination of the light brown glass, S-1, from what was the hottest region showed minute globules formed from molten iron. However, by hand-picking a few pieces free of such particles, glass was obtained with zero intensity of magnetization. The magnetic properties of this glass are strikingly similar to those of a tektite.

The glass formed by the experimental atom bomb at Alamogordo, New Mexico has a low, but positive, value of σ showing a small amount of undissolved iron. Ross (1948) estimates a temperature greater than 1470°C for this glass and one would think the iron might be completely dissolved. However, this temperature was of such brief duration that sufficient time for complete mixing and solution was not available. The ferromagnetism in the tuff, S-6 and S-7, before and after the Rainier nuclear shot shows a similar pattern. There is a substantial reduction in the undissolved iron but this is not complete.

Most of these odd glasses were measured to show the effects of heating, and of ferromagnetic impurities in the undissolved and ionic state.

Discussion and Conclusions

In order to discuss the foregoing magnetic measurements on glasses it is pertinent to review briefly some experimental results obtained recently on synthetic glasses. Abou-El-Azm (1954) has recently studied the magnetic properties and the iron content of a variety of glasses ranging between 60 and 80 per cent SiO_2. When he added 1 per cent Fe_2O_3, he found a slow reduction of the ferric to ferrous iron at high temperatures. The rate of reduction increased between 1300° and 1400°C and increased rapidly above 1400°C. As Fe_2O_3 is known to decompose in air at 1385°C, Abou-El-Azm reasoned that decomposition is undoubtedly what is taking place in the glass. In glass decomposition starts at a slightly lower temperature and he attributes this to increased contact between the alkali ions and the ferric oxide in the molten glass. The temperature at which the increase began was actually around 1390°C for a 70 per cent SiO_2 glass, and could be lowered slightly by increasing the proportion of alkali in the glass. During the reduction process Fe_3O_4 is formed along with FeO. At temperatures in the region of 1400°C it is possible to have a significant amount of Fe_3O_4, but at much higher temperatures there will be little undecomposed Fe_3O_4. For prolonged founding of the glass at somewhat lower temperature for periods up to 200 hr, Abou-El-Azm has shown that the microscopic particles of Fe_3O_4 coalesce into much larger particles. If one assumes that other impurities in the natural glasses do not seriously alter the general results obtained by Abou-El-Azm, his data can be used as the basis of a hypothesis to explain the magnetic properties of tektitic and volcanic glasses.

As is generally thought the tektites must have been subjected to very high

temperatures. Barnes (1958) has shown from a study of the lechatelierite in tektites that the melting temperature exceeded 1710°C. A temperature as high as this will not only explain the presence of lechatelierite, but in the light of Abou-El-Azm's results will also account for the high ferrous iron and lack of ferromagnetic impurities in tektites.

The obsidians on the other hand appear not to have reached temperatures much higher than 1400°C in most cases, and this temperature must have been well below the surface and near the lava source. Jaggar (1947, p. 150 and 411) in discussing the Hawaiian lavas suggests that the temperatures close to the source probably exceed 1350°C. However, once ejected over the surface the temperature is known to be much lower. If the lava remains plastic or molten even for several hours at a lower temperature it is very likely that some sub-microscopic size iron oxide particles will come out of solution and coalesce into the larger particles so often found in obsidian. Depending on the previous temperature and pressure conditions the amount of Fe_2O_3, Fe_3O_4 and FeO will vary. One can therefore see why the susceptibility of obsidians fall into a high and a low group, i.e. one rich, the other depleted in magnetite. The paramagnetic component of the susceptibility of the iron-bearing oxides in each group will thus be quite different. The paramagnetic susceptibility of magnetite, for instance is 425×10^{-6} e.m.u./g, whereas that for Fe_2O_3 is about 20×10^{-6} e.m.u./g. On heating, both compounds would dissolve, the ferromagnetism would disappear, and the resulting susceptibilities would be reduced where significant magnetite is present.

The data obtained on the Mayor Island obsidian and the basaltic glass from Hawaii show that these samples must have had higher source temperatures. This is indicated by the high ferrous iron content. The field independence observed for the magnetic susceptibilities of these samples suggests that they were also rapidly cooled, after ejection, thus precluding any significant crystallization of iron-bearing minerals.

Additional information is also presented which might be used in evaluating the current theories on the formation of tektites. If one assumes an extraterrestrial origin and that the tektite material were not glassy at the time it entered the earth's atmosphere, one would expect the value of σ to vary from inside to the outside of the tektite. On passing through the atmosphere the leading edge of the tektite would become hotter and tend to dissolve more of the iron. The low values of σ found throughout the tektites measured indicate the whole object was heated to a high temperature. It is, therefore, as if the glassy texture of the tektite predated its entry into the atmosphere.

The specimens of glass produced by two nuclear test shots have relatively low values of σ, i.e. most of the iron is in solution. This fact tends to lend credence to the comet theory of the formation of tektites, i.e. a flash of heat lasting but a few seconds appears to be almost sufficient to completely dissolve all of the impurities in the glass to the extent found in tektites. Thus, flash heating of a sedimentary rock caused by a comet impact could almost completely dissolve the iron even though there was not sustained heating. The glass formed at Imboden, Virginia could not be distinguished from a tektite on the basis of its magnetic properties, but this was heated over a period of several hours. From these data and absence

of ferromagnetism in all tektites, it would seem that when the tektite glass was first formed it probably was exposed to the intense heat for a minimum period of the order of a minute.

Although one cannot draw any definite conclusions on the origin of tektites from the magnetic data presented, some definitive information on the origin might be obtained by comparison of this data with new magnetic data observed on sedimentary rocks of similar composition, and which have been subjected to various conditions of temperature and pressure. Also a detailed study of a large number of specimens from a given locality would also be useful.

Acknowledgements—The writers wish to thank I. Friedman and R. L. Smith, U.S. Geological Survey for providing specimens and for many stimulating discussions and help in this work. We also wish to thank all others who generously provided specimens for our work, and to H. R. Branson of Howard University for his continued interest in this work.

This work is part of a programme being conducted by the U.S. Geological Survey on behalf of the Division of Research, U.S. Atomic Energy Commission.

Description of Samples

Samples described in Friedman (1958): 27-17, 40-15, 41-15, 42-1, 42-2, 43-3, 43-4, 43-5, 43-6, 43-7, 93-4, 96-2, 96-6, 96-7, 96-9, 96-10, 96-11, 97-1, 97-2, 97-9, 98-5.
Samples described in Friedman and Smith (1958): 39-2, 52-21, 53-9, 70-9, 70-11.
2-2. Obsidian cobbles, Peralta Canyon, Jemez Mountains, New Mexico. Collected by I. Friedman.
2-5. Obsidian from Big Glass Mountain, ½ mile north of crest of mountain. Collected by D. White.
15-2. Obsidian. Pupil from inlaid eye of coffin. Artifact found in Lisht, North Pyramid, Egypt. Metropolitan Museum of Art, New York City.
27-7i. Obsidian artifact from Naupe, Guayas Province, Ecuador. From I. Friedman.
39-1. Obsidian from Mono Craters, California, Collected by I. Friedman.
40-13. Welded Tuff, Ammon quadrangle, south-eastern Idaho. From I. Friedman.
40-13a. Same as 40-13 except heated to 1450°C.
47-13. Obsidian from Medicine Lake, California. From Big Glass Mountain flow. Collected by I. Friedman and R. L. Smith.
51-16. Obsidian from Little Glass Mountain, Medicine Lake Highlands, California. Collected by I. Friedman and R. L. Smith.
53-7. Obsidian from Mono Craters, Panum dome. Collected by I. Friedman and R. L. Smith.
65-3. Obsidian "marbles" from no. 3 dome, Truckee Meadows, 2·5 miles north-west of Steamboat Springs, Nevada. From I. Friedman.
65-8. Obsidian, float from Thomas Mountains, Utah. Collected by I. Friedman.
67-2a. Black "dike" glass, Bear Head, Jemez Mountains, New Mexico. From R. L. Smith and I. Friedman.
67-4. Obsidian from Xalpazquillo Pueblo, Mexico. Collected by C. Ross.
1396. Tektite from Empire, Georgia, from Dr. E. P. Henderson, U.S. National Museum.

3023-3. Obsidian from Prestahnukur, Iceland. Collected by I. Friedman and R. L. Smith.

3060-1. Tektite from Habri in south Bohemia. From I. Friedman.

S-1. Light brown glass formed by melting sandstone S-2 during power line failure. 4 September 1958 at Imboden, Wise County, Virginia, from J. S. Crosthwaite, Old Dominion Power Company, Big Stone Gap, Virginia,.

S-2. Brown sandstone, Imboden, Virginia, U.S.A., from J. S. Crosthwaite, Old Dominion Power Company, Big Stone Gap, Virginia.

S-3. Black sintered sandstone (S-2). Imboden, Virginia, from J. S. Crosthwaite, Old Dominion Power Company, Big Stone Gap, Virginia.

S-4. Black fused sandstone. Imboden, Virginia, from J. S. Crosthwaite, Old Dominion Power Company, Big Stone Gap, Virginia.

S-6. Glass resulting from underground nuclear blast (Rainier shot).

S-7. Tuff same as S-6 before blast.

H-1, H-2, H-3. Tektite from Australia. South Australia Museum. Adelaide, South Australia, from W. A. Cassidy.

RS-2, RS-3, RS-4, RS-5. Texas tektites from V. E. Barnes, University of Texas, Austin, Texas, through R. Stair, National Bureau of Standards.

RS-6, RS-7, RS-8, RS-9, RS-10. Java tektites from G. H. T. von Koenigswald, Mineralogisck Geologisck Instituut, Rijks Universiteit, Utrecht, Holland, through R. Stair, National Bureau of Standards. These specimens found in the Pithecanthropus deposits of middle Pleistocene age, Sangiran, Central Java.

References

Abou-El-Azm A. (1954) Spectrophotometric and magnetic studies of glasses containing iron in relation to their structure. *J. Soc. Glass Tech.* **38**, 101–196.

Barnes V. E. (1940) North American tektites. *Univ. Tex. Publ.* 3945, 477–656.

Barnes V. E. (1958) Properties of tektites pertinent to their origin. *Geochim. et Cosmochim. Acta* **14**, 267–278.

Cohen A. J. (1958) The absorption spectra of tektites and other natural glasses. *Geochim. et Cosmochim. Acta* **14**, 279–286.

Friedman I. (Special Editor) (1958a) Symposium on tektites. *Geochim. et Cosmochim. Acta* **14**, 257–379.

Friedman I. (1958b) The water, deuterium, gas and uranium content of tektites. *Geochim. et Cosmochim. Acta* **14**, 316–322.

Friedman I., Kohman T. P. and Cassidy W. A. (1958) Tektites. *Science* **127**, No. 3289, 91–94.

Friedman I. and Smith R. L. (1958) The deuterium content of water in some volcanic glasses. *Geochim. et Cosmochim. Acta* **15**, 218–228.

Honda K. (1910) Die thermomagnetischen Eigenschaften der Elemente. *Ann. Phys.* **32**, 1027–1063.

Jaggar T. A. (1947) Origin and development of craters. *Geol. Soc. Amer. Mem.* **21**, 508.

Linck G. (1926) Ein neuer kristallführender Tektit von Paucatambo in Peru. *Chem. d. Erde* **2**, 159.

Macdonald G. A. (1949) Petrography of the Island of Hawaii. *Prof. Pap. U.S. Geol. Surv.* 214-D, 51-96.

Marshall P. (1936) Geology of Mayor Island. *Trans. N.Z. Roy. Soc.* **66**, 337–345.

Owen M. (1912) Magnetochemische Untersuchungen—II. Die thermomagnetischen Eigenschaften der Elemente. *Ann. Phys.* **37**, 657–699.

Ross C. S. (1948) Optical properties of glass from Alamogordo, New Mexico. *Amer. Min.* **33**, 360–362.

Senftle F. E., Lee M. D., Monkewicz A., Mayo J. W. and Pankey T. (1958) Quartz helix magnetic susceptibility balance using the Curie–Cheneveau principle. *Rev. Sci. Instrum.* **29**, 429–432.

Sigamony A. (1944) The magnetic behavior of a tektite. *Proc. Indian Acad. Sci.* A 20, 15–17.

Smith W. C. and Hey M. H. (1952) Silica glass from the crater of Aouelloul (Adrar, western Sahara). *Bull. Inst. Franç. Afr. Noire* **14**, 765.

Stair R. (1955) The spectral-transmissive properties of some of the tektites. *Geochim. et Cosmochim. Acta* **7**, 43–50.

Geochimica et Cosmochimica Acta, 1959, Vol. 17. pp, 248 to 271. Pergamon Press Ltd. Printed in Northern Ireland

The relationship between the petrology and the thorium and uranium contents of some granitic rocks

J. M. Whitfield, J. J. W. Rogers and J. A. S. Adams
Department of Geology, The Rice Institute, Houston, Texas, U.S.A.

(*Received* 23 *February* 1959)

Abstract—Thorium and uranium contents of granitic rocks are intimately related to modal compositions and general petrologic features. Correlations are quite distinct between thorium content and common indices of general petrogenetic evolution, such as amount of dark minerals, percentage of anorthite in plagioclase, and ratio of potassium feldspar to plagioclase. Thorium content increases regularly toward the more acidic rocks, and the increase is most pronounced in the most highly alkalic samples. Uranium content generally shows little, if any, relationship to modal composition or other petrologic features, and the increase in abundance of uranium toward the more acidic rocks is irregular.

The greater petrogenetic control of thorium than of uranium content may be explained on the basis of oxidation and repeated loss of uranium from magmas during the later stages of their differentiation. Such an explanation assumes that magmas are originally derived from a relatively homogeneous source; remobilization, however, of different types of sedimentary or other rocks might provide granitic magmas of widely different initial thorium and uranium contents. The possibility that thorium is added hydrothermally to granites is partly supported by unusually high abundance of thorium in some red, porphyritic, allanite-bearing rocks, but the general petrologic control of thorium abundances argues against major secondary addition of material.

Introduction

The distribution of individual elements among igneous rocks has been a subject of considerable interest for some time. Studies of the major elements have, for example, shown the tendency for sodium and potassium to be concentrated in the more silicic rocks, whereas calcium and magnesium are generally found to be abundant only in the more basic rocks. Such studies have yielded a great deal of information concerning the process of evolution of igneous rocks by means of magmatic differentiation, selective mobilization of sediments, or other mechanisms. The purpose of the present study is to investigate the relationship between the abundance of thorium and uranium and the general petrology and mineralogy of granitic rocks.

The data presented in this paper consist of the thorium and uranium contents of forty-seven granitic rocks (and two related gabbros) from thirty-seven different plutons. Modal compositions are given for most of the samples. The major part of the work involves attempted correlation of the thorium and uranium values with modal compositions and with geologic relationships of the various plutons. Green and Polder vaart (1958) compared the relationships between the abundances of the major elements in igneous rocks; their study involved the average compositions of a large number of separate rock suites, whereas the present work concerns the analyses of individual samples.

The geochemistry of thorium and uranium in igneous rocks is reviewed in a recent summary by Adams *et al.* (1959) and need not be repeated here. In general, the abundances of thorium and uranium increase from basic to silicic rocks. Suites of related rocks almost invariably exhibit enrichment of the two elements in the later-forming members. Alkaline rocks are particularly enriched in thorium and

uranium, and a distinct correlation between both elements and potassium has been repeatedly found. The average abundances of thorium and uranium in granitic rocks may be estimated as 12 p.p.m. and 3·5 p.p.m., respectively. In this paper, the term "granitic rock" is taken to mean all quartz-bearing rocks from true granite to quartz diorite plus monzonite and syenite.

The work reported in this paper was done largely by the first writer (J. M. W.) as a Ph.D. thesis at The Rice Institute. Dr. Whitfield died shortly after receiving his degree, and the present paper has been prepared by the other writers (J. J. W. R. and J. A. S. A.). This study was supported by Grant C-009 from the Robert A. Welch Foundation.

Descriptions of all samples studied are given in the Appendix.

Procedure

The thorium and uranium contents reported in this paper were obtained by γ-ray spectrometry. The theory and practice of this method have been discussed adequately by Hurley (1956) and Adams *et al.* (1958). Consequently, only a brief summary of the methods and equipment used is given below. Modal analyses of the samples were obtained by standard point counting (1000 to 1500 points) of unoriented thin sections.

The precision of the γ-ray spectrometry analyses for thorium and uranium is generally well within ± 15 per cent. Comparison between different γ-ray spectrometers and with wet chemical methods indicate an accuracy of at least ± 15 per cent in most cases (see Adams and Weaver, 1958; Murray and Adams, 1958). The accuracy is somewhat less with rocks containing less than 1 p.p.m. of thorium or uranium or with rocks having a Th/U ratio of less than 0·5 or more than 10.

A total of forty-nine samples from thirty-seven different plutons in the United States and southern Canada was selected for examination from a suite of several hundred granitic rocks collected largely for the present study. Most samples weighed about 5 lb, and an effort was made to collect the freshest material from each locality. Depending on the grain size of the sample, from 700 to 1000 g were then broken by hydraulic crusher and hammer to $\frac{1}{4}$ in. size. This material was reduced to -60 mesh (most of it to -100 mesh) by passing through a rotary pulverizer. A few of the first samples studied were then thoroughly homogenized in a rotary blender, and 350 g of powder were sealed into an 8 oz can. Later samples were ground completely to -100 mesh with a mullite mortar and pestle. The powder was then homogenized, packed and sealed. All samples were allowed to attain radioactive equilibrium with respect to radon, which might have been lost in the pulverizing process, by keeping the powder in the cans for at least 1 week prior to counting. Greater than 99 per cent recovery of the original sample was obtained, the loss being mostly in the coarse breakage process. The pulverizing process was checked for contamination by grinding a sample of quartz sand of known activity and then analysing it; no increase in activity was detected.

The γ-ray spectrometer consists of three main components: the detector; the main electronic spectrometer, composed of several units; and the scaler.

The detector consists of a 3×3 in. cylindrical thallium-activated sodium iodide crystal encased in aluminium. The base consists of a fused silica window in silica-gel optical contact with a DuMont model 6363 multiplier photo-tube. The photo-tube has a μ-metal shield and has been operated at a 1270 V potential. The detector assembly is housed in a shield constructed of stacked, 1 in. steel plate with holes suitably cut to house the cylindrical liner, the detector probe and the 6 in. solid plug which covers it. A minimum of 6 in. of steel shields the crystal, and the whole assembly is situated in a 4 ft deep concrete pit with several feet of concrete on all sides.

The main spectrometer unit (Tracerlab advanced spectrometer model RLP-3 with some minor deletions) is composed of three main units: precision high voltage supply (RLI-7); pulse height analyser amplifier (RLX-12); and a pulse height analyser (special). The high voltage supply and amplifier are connected to line current through a Sola constant voltage transformer. The pulse height analyser amplifier is composed of two units, the linear amplifier subchassis (RLA-1) and the widener and gate generator (RLA-3). The pulses which pass through the "window" of the pulse height analyser are recorded on a Baird Atomic model 131 cold cathode glow tube scaler. In the scaler, the units digit counts on a 5 μsec decade strip, the next two digits on decatron glow tubes, and other digits on electromechanical counters.

The entire spectrometer and detector are situated in a temperature- and humidity-controlled room; ambient temperature varies from 72 to 76°C and relative humidity from 45 to 50 per cent.

Counts are made at three γ-energy levels (channels) in order to solve for the three unknown counting rates (uranium, thorium and potassium), and a fourth channel is counted as a check. The channels counted are 2·62 MeV (the Tl^{208} peak in the thorium series), 1·76 MeV (the Bi^{214} peak in the uranium series), 1·47 MeV (potassium), and 0·61 MeV (as a check).

The window is set at a width of 70 units (7 V). This width is a compromise between the desirability of keeping the window narrow to minimize the background contribution and the desirability of keeping the window wide in order to decrease the counting time and prevent drift from moving the peak out of the window. With the energy levels counted and the window width selected, counting times in the various channels are as follows:

Channel (MeV)	Time (hr)
2·62	3
1·76	10
1·47	0·5
0·61	0·5

For an average granitic rock, with approximately 12 p.p.m. thorium, 3·5 p.p.m. uranium and 4·5 per cent potassium, the percentage standard deviation calculated from the statistics of counting processes should be about 5 per cent with counting times of the above length.

Most of the samples were counted in a small, cylindrical, 8 oz can, 3·8 in. in diameter and 1·4 in. thick. Approximately 350 g of crushed rock were needed to fill these cans. The cans were placed on top of the crystal, which is not quite as satisfactory as using an annular cannister which covers all sides of the crystal. The difficulty with annular cannisters is that they are vastly more expensive than the simple cans used and require more sample (about 700 g). Samples counted in both 8 oz cans and annular cannisters give results within expected statistical counting error. Samples of low activity, having less than approximately 5 p.p.m. thorium and 2 p.p.m. uranium, should probably be counted in annular cannisters.

The γ-ray spectrometer was calibrated with standards of known uranium and thorium contents, prepared by the U.S. Atomic Energy Commission at New Brunswick. The thorium standard consists of monazite diluted with dunite, and the uranium standard consists of uraninite diluted with dunite. The potassium standard is composed of K_2CO_3.

Empirical reproducibility (precision) and instrument stability were checked by a system of quality control based on run numbers. Packed samples were numbered sequentially, and each tenth sample counted (whose run number was a multiple of 10) was succeeded in counting by a previously analysed sample whose run number was an odd multiple of 5. Cans were re-run in order of increasing number, and in this way six samples were counted twice. One sample was counted three times. The standard deviations of the samples observed from these re-runs are compared in Table 1 with the expected standard deviations calculated from counting statistics. In general, the observed deviations are similar to the calculated ones.

Table 1. Comparison of observed reproducibility and relative analytical error calculated by statistical methods

No. of repetitions	Sample	Can #	Observed % s.d.		% s.d. from counting statistics	
			Th	U	Th	U
2	Sc 12-60	20	0·93	8·10	3·90	3·75
2	JW 32	24	2·92	9·30	3·75	2·90
2	E 5-404	46	3·69	2·47	4·80	4·80
2	E 4-403	44	2·82	6·80	3·55	4·65
2	Sc 25-72	41	5·90	1·01	5·10	5·75
2	F 10-15	26	3·34	0·90	3·80	4·70
3	Sc 1-49	19	4·70	9·75	4·70	3·50
Average			3·47	5·48	4·23	4·29

Results

Thorium and uranium contents of the forty-seven granitic and two gabbroic rocks studied are listed in Table 2 in order of increasing Th/U ratio. Modal analyses of most of the rocks are listed in Table 3 in order of increasing ratio of potassium feldspar/plagioclase. The location and description of each of the rock bodies from which the samples were taken, and descriptions of the individual samples, are given in the appendix. The results are discussed in the following order: (a) the relationships between thorium, uranium, potassium and various petrographic parameters; (b) the thorium and uranium contents of various different types of granitic rocks; and (c) the variability of thorium and uranium within individual intrusions.

Correlation of thorium and uranium with other variables

Relationships between thorium, uranium and Th/U ratio are diagrammatically shown in Figs. 1 to 3. The general trend indicates a more marked increase of thorium than of uranium with increasing thorium or uranium in granitic rocks. This pronounced increase in thorium is indicated by the scatter of high thorium values to the right of the main linear trend in Fig. 1. Thorium forms more linear trends when plotted against Th/U ratio than does uranium, and in fact there appears to be no relationship between uranium and Th/U ratio.

Scatter diagrams of potassium content vs. thorium, uranium and Th/U ratio are shown in Figs. 4 to 6. Both uranium and Th/U ratio show little if any relationship to potassium; possibly both increase slightly with increasing potassium content, but the points are very diffuse. Thorium, however, exhibits a marked increase with increasing potassium content; this increase appears to be greatest at high values of potassium. If potassium is considered to be an index of evolution or of general progressive differentiation in granitic rocks, then thorium seems to increase at a more rapid rate and more regularly with differentiation than does uranium.

Table 2. Thorium, uranium and potassium contents of granitic rocks. Arranged in order of increasing Th/U ratio

Sample	Th/U	Th_γ (p.p.m.)	U_γ (p.p.m.)	K_γ (%)	U_f* (p.p.m.)	Th_{chem} (p.p.m.)
KA 80-408	0·2	0·07	0·3	0·8		
D 17-238	1·0	0·5	0·5	0·4		
W 13-194	1·4 ± 0·12	2·8 ± 0·22	2·0 ± 0·07	1·9 ± 0·07		
M 3-205	1·5 ± 0·13	2·5 ± 0·2	1·6 ± 0·06	2 ± 0·08		
JW-70	1·6 ± 0·15	3·1 ± 0·25	1·9 ± 0·08	1·8 ± 0·09		
S 14-166	1·8 ± 0·2	4·6 ± 0·32	2·6 ± 0·22	1·4 ± 0·05		
F 2-7	1·8 ± 0·14	9·2 ± 0·5	4·6 ± 0·1	4·3 ± 0·1	3·0	9·3
NH 47-349	2·0 ± 0·11	11 ± 0·6	5·5 ± 0·12	3·0 ± 0·12		
Y 24-119	2 ± 0·1	16 ± 0·6	8·3 ± 0·2	2·51 ± 0·12		
Y 1-96	2·2 ± 0·13	8·2 ± 0·4	3·8 ± 0·13	2·1 ± 0·09		
P 11-141	2·2 ± 0·18	3·4 ± 0·2	1·5 ± 0·08	1·5 ± 0·05	1·2	0·6
JW-32	2·3 ± 0·11	8·8 ± 0·33	3·8 ± 0·11	1·3 ± 0·1		
D 5-226	2·5 ± 0·15	8·7 ± 0·35	3·5 ± 0·15	2·0 ± 0·07		
KA 6-405	2·5 ± 0·13	12 ± 0·5	4·7 ± 0·14	3·5 ± 0·14		
M-4	2·6 ± 0·13	12 ± 0·5	4·6 ± 0·14	2·4 ± 0·08		
P 15-145	2·7 ± 0·2	4·5 ± 0·3	1·7 ± 0·1	1·5 ± 0·06		
D 9-230	3·1 ± 0·2	8·4 ± 0·5	2·8 ± 0·12	1·8 ± 0·21		
CB 3-45	3·1 ± 0·15	12 ± 0·5	4·0 ± 0·14	3·2 ± 0·1		
Sc 1-49	3·2 ± 0·2	10 ± 0·2	3·2 ± 0·1	3·3 ± 0·2		
Sc 15-63	3·2 ± 0·36	3·2 ± 0·25	1·0 ± 0·08	0·4 ± 0·04		
W 3-399	3·2 ± 0·16	12 ± 0·5	3·8 ± 0·11	3·4 ± 0·08		
A 13-268	3·3 ± 0·24	7·4 ± 0·44	2·3 ± 0·09	6·2 ± 0·15		
Sc 12-60	3·3 ± 0·18	11 ± 0·5	3·5 ± 0·13	2·3 ± 0·04		
P 13-143	3·3 ± 0·23	5·4 ± 0·25	1·7 ± 0·08	1·5 ± 0·06		
M 6-208	3·4 ± 0·34	3·5 ± 0·28	1·1 ± 0·06	1·6 ± 0·07		
A 4-259	3·4 ± 0·25	5·0 ± 0·28	1·5 ± 0·07	4·5 ± 0·17		
Sp 2-4	3·4 ± 0·18	17·0 ± 0·8	4·9 ± 0·1	2·9 ± 0·13	3·1	
Sc 25-72	3·5 ± 0·2	9·7 ± 0·5	2·8 ± 0·14	2·1 ± 0·1		
MW 3-76	3·5 ± 0·19	15 ± 0·6	4·5 ± 0·16	2·7 ± 0·07		
Y 7-102	3·6 ± 0·24	8·3 ± 0·4	2·3 ± 0·1	2·4 ± 0·1		
NH 43-345	3·6 ± 0·19	14 ± 0·35	3·8 ± 0·17	3·0 ± 0·08	1·73	14·1
Y 9-104	3·7 ± 0·22	13 ± 0·6	3·5 ± 0·13	1·2 ± 0·08		
Sc 8-56	3·9 ± 0·23	11 ± 0·5	3·0 ± 0·12	2·5 ± 0·1		
NH29-331	3·9 ± 0·17	22 ± 0·67	5·5 ± 0·18	3·5 ± 0·1		
F 16-21	4·3 ± 0·21	22 ± 0·45	5·0 ± 0·23	3·2 ± 0·1	3·4	
D 14-235	5·2 ± 0·35	13 ± 0·65	2·5 ± 0·11	2·7 ± 0·09		
P210G(407)	5·3	0·75	0·14	0·88		
E 4-403	5·5 ± 0·3	21 ± 0·6	3·9 ± 0·16	4·1 ± 0·14		
E 3-402	5·7 ± 0·6	22 ± 0·68	3·8 ± 0·04	4·2 ± 0·12		
E 5-404	6·0 ± 0·3	12 ± 0·5	2·0 ± 0·08	3·4 ± 0·1		
K 17-255	6·0 ± 0·13	15 ± 0·3	2·5 ± 0·07	4·3 ± 0·1		14·4
F 32-37	8·0 ± 0·5	37 ± 1·5	4·6 ± 0·23	4·5 ± 0·19		
12M	8·3 ± 0·1	5·2 ± 0·3	0·63 ± 0·06	2·8 ± 0·13		
KA 72-406	8·3	1·1	0·13	1·0		
KA 27-410	8·8 ± 0·7	18 ± 0·66	2·0 ± 0·14	2·5 ± 0·12		
Id 7-202	9·2 ± 0·92	7·7 ± 0·38	0·84 ± 0·07	3·1 ± 0·12		
V 1-409	9·6 ± 0·4	30 ± 0·5	3·1 ± 0·14	4·2 ± 0·16		
F 10-15	10 ± 0·5	39 ± 1·5	3·9 ± 0·16	4·5 ± 0·15	3·0	
F 19-24	25 ± 6·8	22 ± 0·8	0·89 ± 0·15	4·5 ± 0·2	0·85	
Average	4·42	11·35	2·96	2·69		

* Fluorimetric uranium determination.
All values are reported to two significant figures and are rounded off after calculation of Th/U ratio.

Specimen	R*	C.I.†	Quartz	Plagioclase‡	Potassium feldspar	Biotite	Hornblende	Opaques	Zircon	Apatite	Sphene	Epidote	Allanite	Muscovite	Chlorite
W 3-399		5·7	30		(64)	1·0	2·6	2·1	tr.	tr.	tr.				
KA80-(408)		3	18	79_{25}		3·0			tr.—§		tr.	tr.			
Y 9-104	0·01††	3·3	56	41_{30}	0·22	3·3			tr.	tr.	tr.+**	tr.+			tr.
P210G (407)	0·01	9·3	13	78_{15}	0·75	1·3	7·5	tr.	tr.		0·3	0·1	0·1		tr.
Sc 15-63	0·02	47	12	40_{50}	0·8		47	tr.							tr.+
W 13-194	0·03	24	19	55_{41}	1·5	21	2·9	tr.	tr.	tr.	tr.+	tr.	?		tr.
KA 72-406	0·03	8·2	32	58_{30}	1·9	2·0					4·0			2·2	tr.
S 14-166	0·06	14	20	62_{45}	3·9	6·2	7·2	0·5	tr.	tr.	tr.	tr.			tr.
P 15-145	0·06	12	30	55_{40}	3·3	9·2	2·8	tr.		tr.	tr.+				
P 11-141	0·07	20	24	53_{40}	4·0	14	6·0	0·1	tr.	tr.	tr.	tr.		tr.	
P 13-143	0·07	15	33	49_{40}	3·3	7·8	6·6	0·3	tr.	tr.	tr.+			0·2	
JW-70	0·12	14	37	43_{22}	5·3	10	4·2	0·2	tr.		tr.	0·1			
Y 1-96	0·14	14	23	56_{37}	7·8	7·1	6·3				0·2				tr.
M 6-208	0·17	20	12	59_{34}	10	5·0	12	1·7		tr.		tr.			tr.
M 4-A	0·19	9	27	54_{31}	10	8·2	0·3				0·3		0·1		
M 3-205	0·2	7·7	25	56_{37}	11	4·2	2·4	0·3		0·2	0·6				tr.
Y 7-102	0·21	8·0	28	52_{30}	11	7·2						0·6		0·1	0·1
Sc 8-56	0·32	9·6	36	41_{25}	13	8·1	1·3	0·2	tr.				tr.		
Id 7-202	0·32	7·5	30	48_{37}	15	6·9		0·3	tr.–		0·3	0·2			tr.
Sc 12-60	0·33	4·6	35	46_{20}	15	3·4	0·9	0·3	tr.	tr.	tr.				
Sc 25-72	0·35	3·9	44	39_{35}	13	3·0	tr.	tr.		tr.					
12 M	0·36	1·8	31	49_{15}	18	1·7		0·1	tr.	tr.					
E 5-404	0·58	11	29	38_{27}	22	11			tr.	tr.	tr.		?		
KA 27-410	0·58	2·4	31	42_{15}	24	2·4				tr.					tr.
NH 47-349	0·66	7·1	40	31_{15}	20	2·5			tr.	tr.				4·6	
E 4-403	0·68	10	44	26_{20}	18	10	0·1	0·1	tr.	tr.	tr.+		0·1		
Sc 1-49	0·73	2·9	40	33_{15}	24	2·9		tr.	tr.+						
F 16-21	0·78	14	28	33_{20}	25	11		1	2·1	0·1	tr.		tr.+		
E 3-402	0·8	11	26	35_{20}	28	9·5		0·6	0·2		0·66		0·3		
KA 6-405	0·8	14	18	38_{25}	30	9·6	4·6	tr.	tr.	tr.					
NH 29-331	0·82	2·2	37	33_{15}	27	2		0·2			tr.	tr.+			
NH 43-345	1	15	52	17_{27}	17	12			tr.	tr.				2·8	
F 10-15	1	3·4	31	32_{20}	33	2·8		0·3	tr.					0·3	tr.
V 1-409 (a)	1·07	2·4	24	35_{15}	38	1·5						tr.		0·9	tr.
V 1-409 (b)	1·25	3·7	27	30_{15}	38	3·6			tr.			tr.		0·1	tr.
F 32-37 (a)	1·43	4·5	32	26_{30}	38	2·8		0·1	tr.				tr.+	0·9	
F 32-37 (b)			38	30_{30}	27	2·9		0·2	tr.	tr.			tr.+	2·2	tr.
F 19-24 (a)	1·6	4·6	19	31_{31}	45	4·1		tr.	0·1	0·2			tr.+	tr.	
F 19-24 (b)			38	21_{31}	35	3·4		1·3						tr.	
A 4-259	1·6	17‡‡	28	22_{20}	35		14		tr.	tr.					
F 2-7	1·8	8·6	33	21_{10}	36			0·7						7·9	
K 17-255 (a)	1·7	3·8	26	26_{12}	45	3·2		0·6	tr.	tr.	tr.				
K 17-255 (b)	3·1	3·3	32	15_{12}	50	3·3		tr.							
A 13-268	4·8	7·4	20	12	60	5·3		2·1	tr.	tr.					tr.

* R is potassium feldspar/plagioclase ratio.
† C.I. is colour index; muscovite counted as a dark mineral.
‡ Subscript indicates per cent anorthite.
§ Tr– is a very scarce trace mineral.
** Tr+ is abundant trace mineral.
†† All values of percentages are reported to not more than two significant figures and are rounded off after calculation of R and C.I.
‡‡ A 4-259 contains 3 per cent garnet.

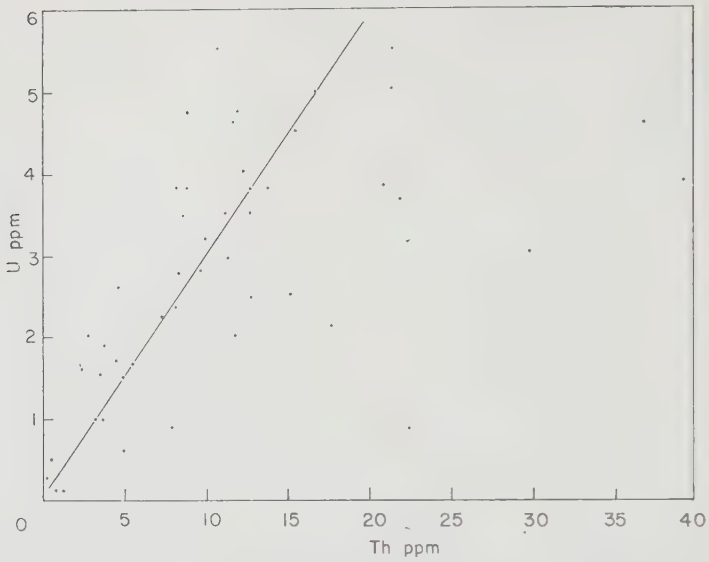

Fig. 1. Uranium content vs. thorium content of granitic rocks.

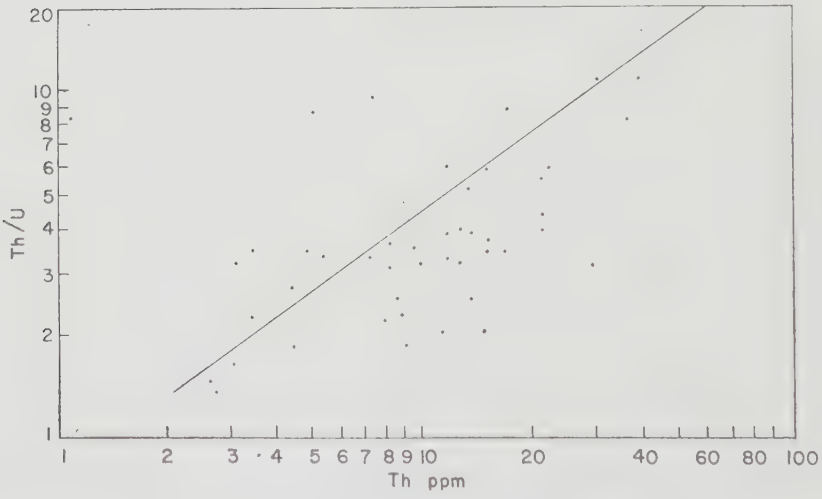

Fig. 2. Thorium content vs. Th/U ratio of granitic rocks.

Potassium feldspar/plagioclase ratio (denoted as R hereafter), quartz content, percentage of anorthite in plagioclase and colour index (defined by Shand, 1947) have all been considered indices of general petrogenetic evolution of granitic rocks. These petrographic parameters have been plotted against thorium and uranium contents and Th/U ratio in order to give further evidence concerning the behaviour of thorium and uranium during igneous petrogenesis. Several of the more important diagrams are shown in Figs. 7–11.

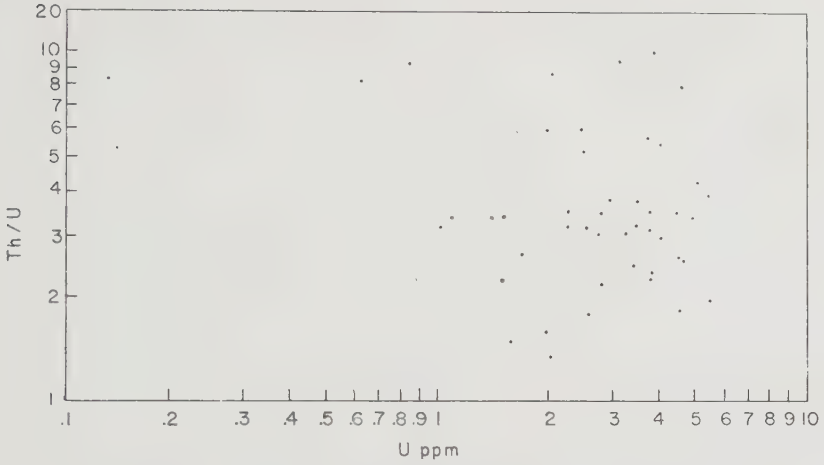

Fig. 3. Uranium content vs. Th/U ratio of granitic rocks.

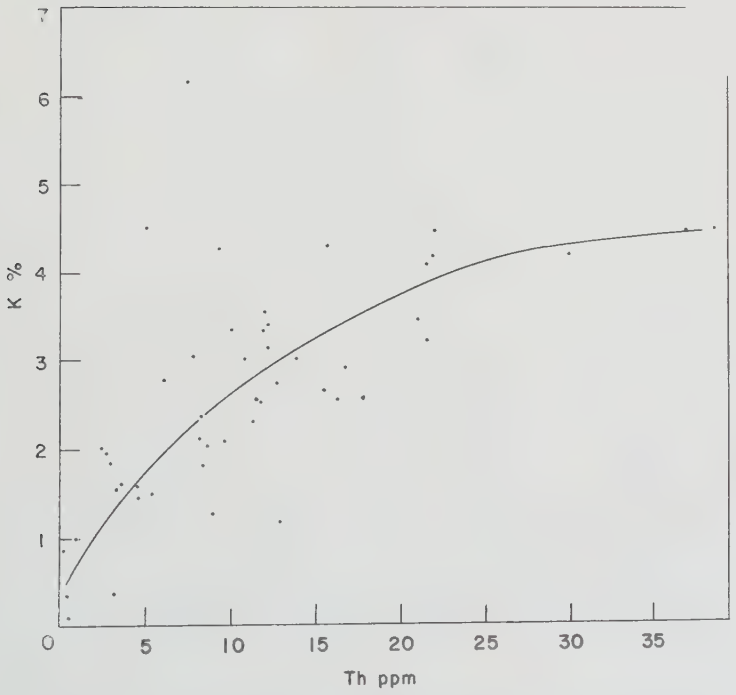

Fig. 4. Thorium content vs. potassium content of granitic rocks.

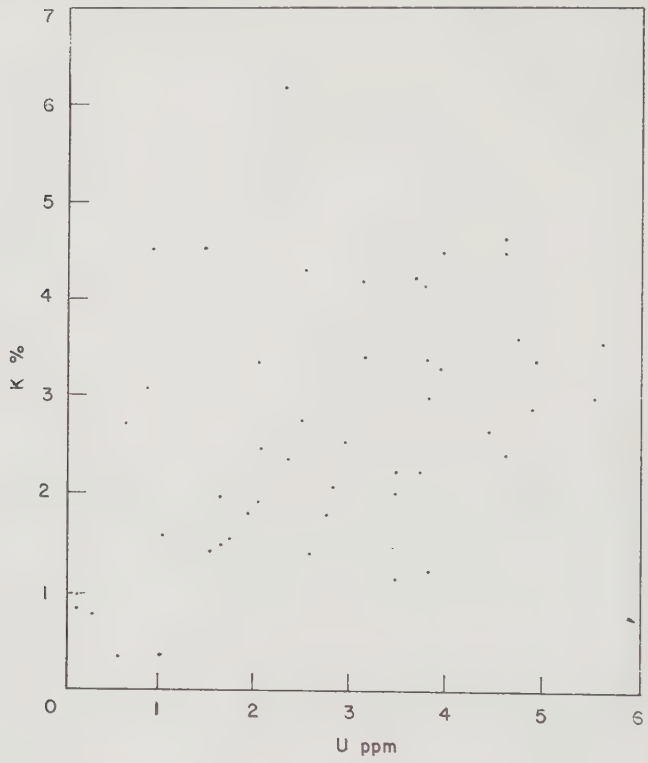

Fig. 5. Uranium content vs. potassium content of granitic rocks.

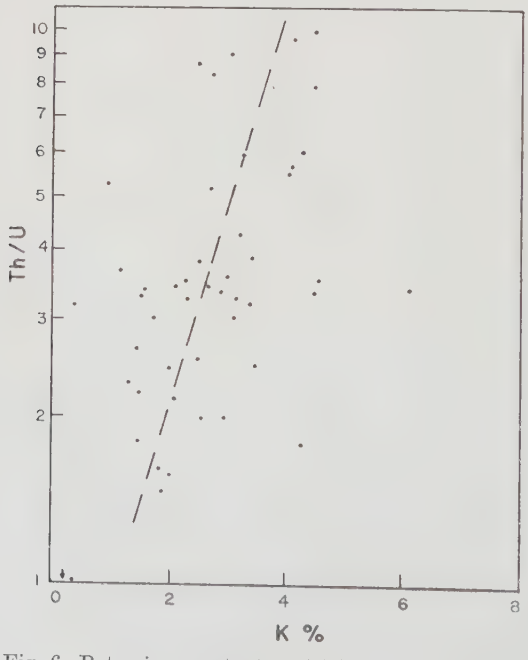

Fig. 6. Potassium content vs. Th/U ratio of granitic rocks.

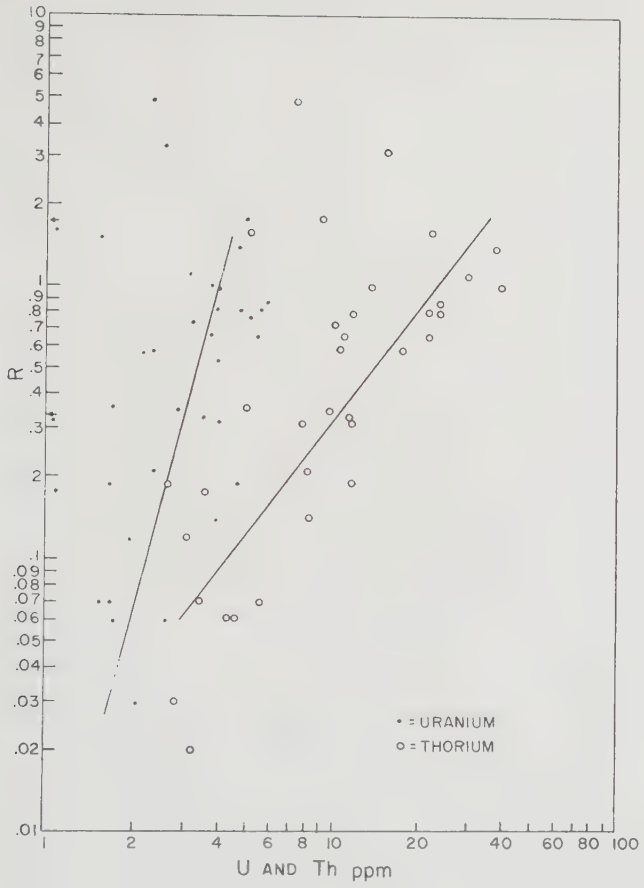

Fig. 7. Uranium and thorium contents vs. potassium feldspar/plagioclase ratio of granitic rocks.

Fig. 7 shows the relationships between thorium and uranium and R. The trend lines are generally straight. Apparently, in rocks with progressively higher R ratios, Th increases at an increasing rate relative to uranium but is proportional to R. Thus, thorium increases more rapidly with alkalinity (R) in these granitic rocks than does uranium. Fig. 7 is similar to Figs. 4 and 5. The Th/U ratio possibly increases slightly with increasing R, but relationships are quite obscure.

Relationships between thorium and uranium and colour index are shown in Figs. 8 and 9. Uranium content is apparently unrelated to colour index, though thorium quite markedly increases at increasing rate with decreasing colour index. Plotted data also indicate an increase in Th/U ratio with decreasing colour index. Plots of thorium, uranium and Th/U ratio vs. biotite content are, however, completely diffuse.

The relationship between thorium content and quartz content is shown in Fig. 10. If thorium values above 20 p.p.m. are ignored, the linear relationship of the remaining points is quite strong; possibly thorium contents greater than 20 p.p.m. are caused by secondary or hydrothermal addition of thorium to the

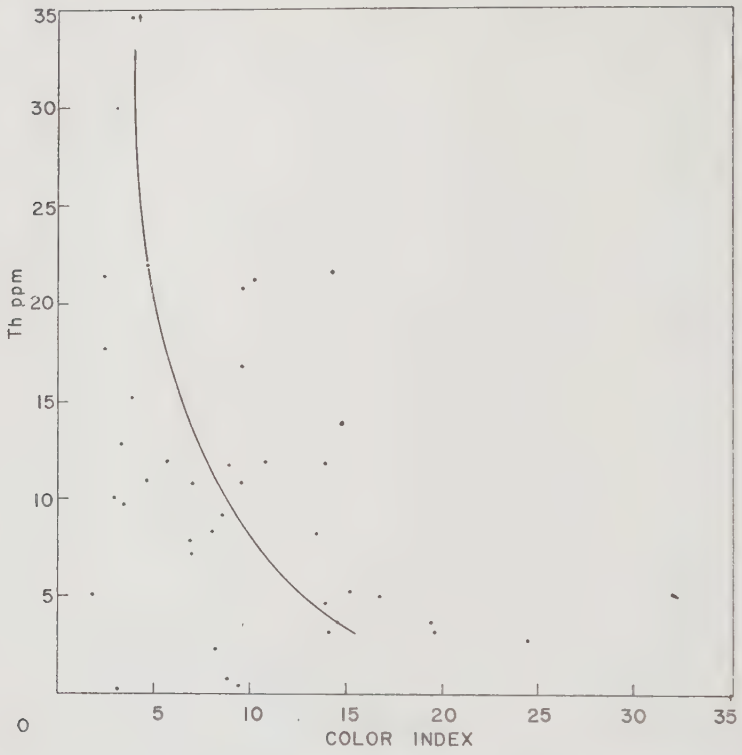

Fig. 8. Thorium content vs. colour index of granitic rocks.

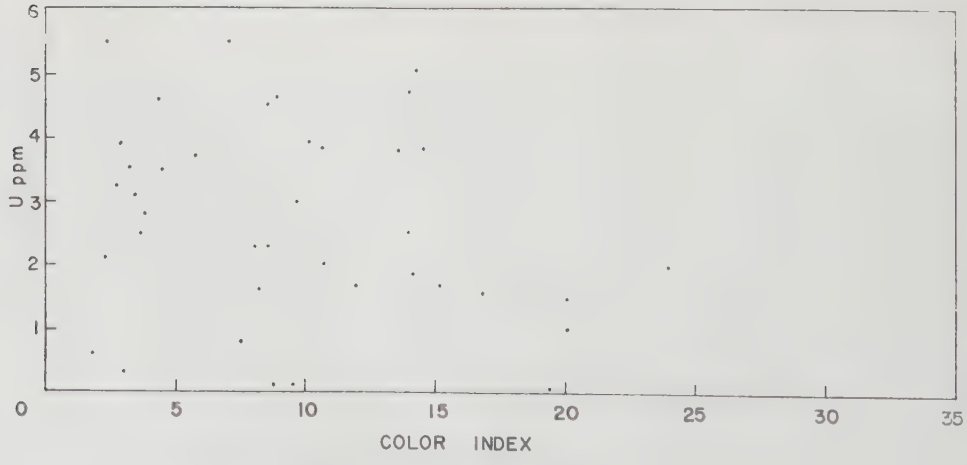

Fig. 9. Uranium content vs. colour index of granitic rocks.

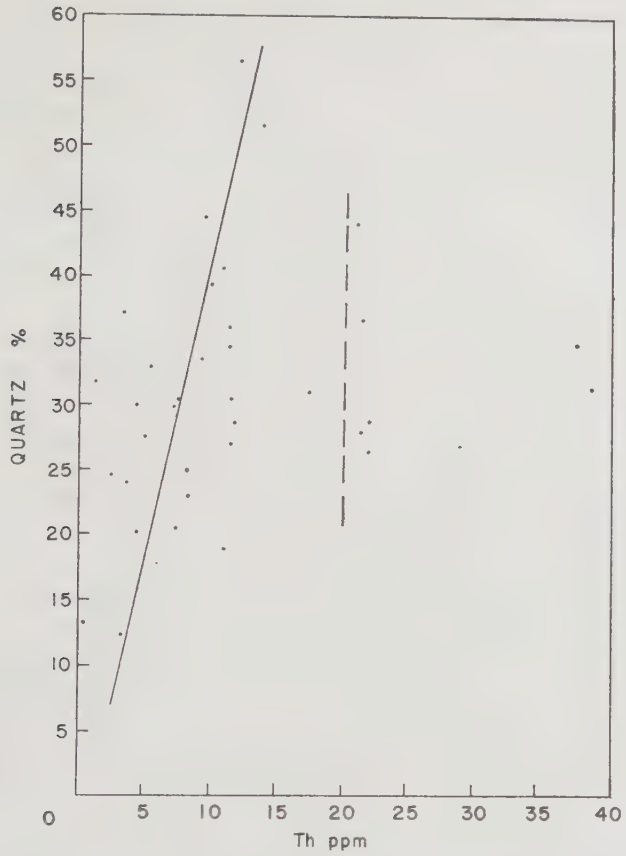

Fig. 10. Thorium content vs. quartz content of granitic rocks.

granites and should be considered apart from the main trend of igneous evolution. Plots of uranium vs. quartz content are quite diffuse, as are plots of Th/U vs. quartz.

Fig. 11 shows that thorium content increases at an increasing rate with decrease in anorthite content of plagioclase. Such a relationship is similar to those between thorium and the *R* ratio, colour index, and uranium content. Plots of uranium content and Th/U ratio vs. anorthite content are quite diffuse, and no trends can be distinguished.

In summary, uranium and thorium appear to vary systematically with potassium, *R*, and other petrographic parameters. Uranium trends are very diffuse but appear to be roughly linear. Thorium trends are much less diffuse and are commonly curved. Plots of Th/U ratio with the various parameters generally show little or no relationship.

The diffuseness of points in the diagrams is caused partly by within-pluton variation and partly by sampling variation. Much of the scatter may be caused by general imperfection of petrogenetic control of the uranium and thorium; thorium and uranium, however, are not significantly more variable than potassium or the various petrographic parameters. Granitic rocks representing different

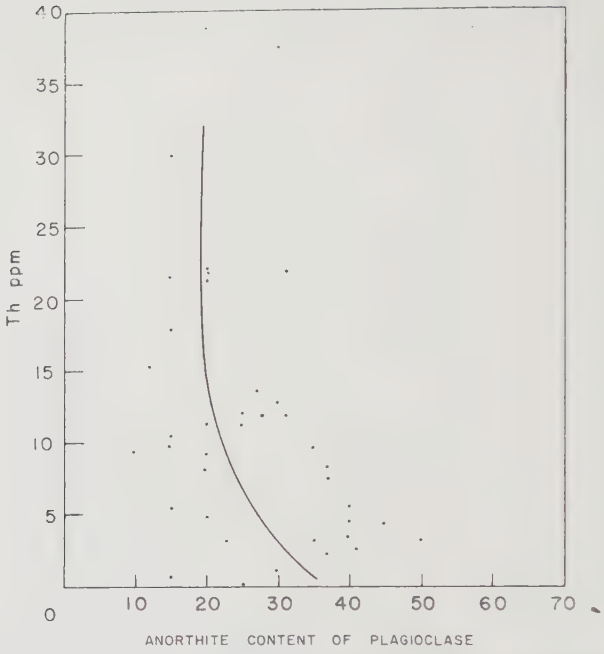

Fig. 11. Thorium content vs. anorthite content of plagioclase in granitic rocks.

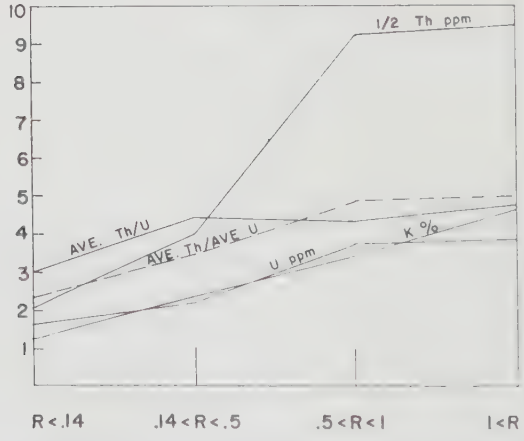

Fig. 12. Radiometric and petrographic parameters vs. potassium feldspar/plagioclase ratio (R) of granitic rocks. The plotted data consist of averages for groups subdivided on the basis of R ratio as indicated. The number of samples in each group is approximately equal.

environments and types of genesis may contain different amounts of thorium and uranium even though their major mineral components may be equal, and these differences may cause a significant amount of variation.

Thorium is more variable, as well as more systematically variable, in most cases, than uranium. Some of the thorium variability, however, is caused by a

few unusually thorium-rich granites, containing more than 20 p.p.m. Eight such granites have been analysed, and many of them are characterized by a red colour, porphyritic texture and abundance of allanite. The uranium in these rocks is not abnormally high, and in one case (F 19-24) it is extremely low (0·84 p.p.m.).

The wide scatter of points on the foregoing diagrams, in which individual analyses have been plotted, can be reduced by plotting averages of different rock types. This has been done in Fig. 12, in which both radiometric and petrographic parameters have been plotted against R (the ratio of potassium feldspar/plagioclase). This diagram substantiates the general conclusions discussed above, namely that thorium increases more pronouncedly during igneous evolution (increase in R) than does uranium. The Th/U ratio increases with R owing to the increase in absolute thorium content.

Thorium and uranium contents of selected groups of granitic rocks

Table 4 is a summary of averages of radiometric and petrographic data of samples grouped into several classes, on the basis of colour, geographic location or geologic age.

Table 4. Comparison of radiometric and petrographic average data of various groups of granitic rocks. Arranged in order of decreasing Th/U ratio

Classification	No. of samples	γ-ray data					Petrographic data				
		Th/U	Th (p.p.m.)	U (p.p.m.)	Av. Th / Av. U	K (%)	R	Q	An	C.I.	Bi
Rocky Mountains	11	6·9	15·7	2·9	5·4	3·3	0·8	28	27	8·1	4·7
Red	13	6·6	16·2	3·0	5·4	3·8	1·6	29	15	7·3	4·3
Canadian Shield*	7	5·9	11·0	1·8	6·1	2·5	0·7	24	20	6·2	3·4
Pre-Cambrian	24	5·6	14·0	2·6	5·4	3·2	1·1	27	20	9·8	4·8
Post-Cambrian	25	3·3	8·6	3·0	2·9	2·2	0·3	30	31	12	8·7
West Coast	16	2·9	8·5	3·1	2·7	1·8	0·18	31	34	14	7·2
Average	49	4·4	11	3	3·9	2·7	0·7	29	26	11	6·8

* Omitting rocks of the Duluth lopolith.

(1) Red granites contain an abnormally large amount of thorium with an average amount of uranium. As mentioned previously, many of these granites contain appreciable allanite.

(2) Table 4 shows averages of groups of granites from three different geographic areas from which a number of samples have been analysed. These areas include the southern Canadian Shield, the Rocky Mountains in the United States and the Pacific Coast (including the Southern California batholith and granites of the Sierra Nevada Mountains). The rocks of the Canadian Shield are anomalously high in av.Th/av.U ratio relative to R. This anomaly appears to be caused by low uranium content, inasmuch as thorium is present in average abundance. The low uranium content of the rocks from the Canadian Shield may be accounted

for by differential diffusion of uranium over thorium into upper layers of the crust during the intensive metamorphism which has affected the shield area. These upper layers have subsequently been eroded. Another possible explanation is that a series of exogenic cycles have occurred in the Canadian Shield, thus causing oxidation and loss of uranium before each succeeding period of magma generation.

(3) Pre-Cambrian granites have average lower Th/U ratios relative to R than do post-Cambrian rocks. Thus, relative to composition, the post-Cambrian rocks examined are enriched in thorium over uranium compared to pre-Cambrian rocks. If compositional differences (mostly alkalinity) be ignored, or if the differences in mineralogy noted for these samples be considered valid for all pre- and post-Cambrian granitic rocks, then there is an absolute and a relative (to uranium) decrease in thorium content with time (for further discussion see Marshall, 1957).

Variability of thorium and uranium within individual intrusions

The abundances of thorium and uranium are not constant throughout single intrusions. Though the present study is concerned primarily with the relationship between thorium and uranium contents and lithologic characteristics of individual samples, some information has been obtained concerning variation within intrusions.

Three samples (P 11-141, P 13-143 and P 15-145) were collected 2 miles apart, from the contact toward the central portion of the Bucks granodiorite in the northern part of the Sierra Nevada. Table 3 shows that the mineralogy of these samples is almost the same; the major differences are in the total amount of mafic material and in the biotite/hornblende ratio. In these samples the thorium content varies from 3·4 to 5·4, the uranium content varies from 1·5 to 1·7, and the Th/U ratio varies from 2·2 to 3·3. These variations are very small and not far from analytical error for samples of such low activity.

The Enchanted Rock batholith of Texas is represented by three samples collected in the central portion of the batholith within 200 ft of each other. Two of the samples (E 3-402 and E 4-403) are from the petrographically homogeneous porphyritic facies. The uranium and thorium contents of these two samples are almost exactly the same (see Table 2). The third sample (E 5-404) is from an aplite dike which cuts the porphyritic facies. It is mineralogically very similar to the coarse facies but entirely different texturally. The thorium and uranium contents of this aplite are both about one half that of the porphyritic rock, and therefore, the Th/U ratio is almost the same as that of the porphyritic facies.

Two samples of the Cathedral Peak granite were collected from the central portion of the Sierra Nevada. One sample (MW 3-76) is from the Mount Whitney area, and the other (Y 24-119) is from Yosemite National Park, 100 miles north of Mount Whitney. The rocks are very coarsely porphyritic and therefore no attempt was made to point count them. The samples, however, are very similar to each other both megascopically and microscopically. In both rocks thorium is high and of about equal abundance; uranium, however, is high in sample Y 24-119 (8·3 p.p.m.) but only slightly above average in sample MW 3-76 (4·5 p.p.m.). This difference in uranium content results in Th/U ratios of 2 and 3·5, respectively.

Three samples from the Idaho batholith have been examined. Sample 12M is from the light inner facies of the batholith. It has a low content of thorium (5 p.p.m.) and uranium (0·6 p.p.m.), and a Th/U ratio of 8·3. Samples M-4 and Id 7-202 were collected approximately 30 miles apart in the mafic outer facies of the batholith and are texturally and mineralogically distinct from 12M (see Table 3). These two samples are petrographically very similar to each other, but they differ widely in thorium and uranium contents. Sample 4M contains approximately average amounts of thorium and uranium and has a Th/U ratio of 2·6. Sample Id 7-202 is low in thorium (7·7 p.p.m.), extremely low in uranium (0·8 p.p.m.) and has a Th/U ratio of 9·2.

Two samples from the Pikes Peak batholith of the Colorado Front Range have been studied and analysed. Sample F 19-24 is from within 300 ft of the contact of the Pikes Peak granite with the Boulder Creek granite, which it intrudes. Sample F 10-15 is from another part of the batholith, one half mile from the contact. The two rocks are similar petrographically, but the plagioclase compositions, the potassium feldspar/plagioclase ratios and the colour indices differ slightly. In both rocks the thorium content is extremely high. In sample F 19-24 the uranium is very low, resulting in a Th/U ratio of 25, the highest found in the present study. Sample F 10-15 contains roughly an average amount of uranium but has a high Th/U ratio of 10 owing to the extremely high thorium content.

Two samples from the Marysville stock have been examined. Sample M 3-205 is from the centre of the stock, and sample M 6-208 is from the contact of the stock with the Helena dolomite. The petrography of the two samples is similar, but M 6-208 has five times as much hornblende and only half as much quartz as sample M 3-205. The desilication may be a result of contact reactions with the dolomite. The thorium content is higher and the uranium content lower in the border of the stock than in the centre.

Summarizing, in Bucks granodiorite and in the Enchanted Rock batholith, like petrographic types are of similar thorium and uranium contents. In the Idaho batholith, and probably in the Cathedral Peak and Pikes Peak granites, apparently similar petrographic types vary widely in uranium content and slightly in thorium content. In the Enchanted Rock batholith, the Marysville stock and, to a lesser extent, in the Pikes Peak granite, variations in thorium and uranium are accompanied by petrographic or textural variations; (this does not imply, however, a necessary genetic relationship between uranium or thorium and the petrographic variation). Where large variation in uranium occurs without concomitant gross petrographic change or thorium variation, it is highly possible that uranium may be out of secular radioactive equilibrium. Samples P 11-141, F 10-15, and F 19-24, from among the samples discussed in this section, however, have been checked by direct uranium chemical analysis and clearly shown to be in equilibrium.

It must be tentatively concluded that some variations of thorium and uranium contents within plutons cannot be entirely attributed to, or even related to, gross petrographic variations. Thus, in attempting to compare different types of plutons and general lithologic types, a certain amount of variation due to position within the pluton must be expected.

Conclusions

Any explanation proposed for the behaviour of uranium and thorium in granitic rocks must explain three major phenomena: (a) the increase of both uranium and thorium in the normal or generalized petrogenetic evolution of the granitic rocks; (b) the apparent increase of thorium relative to uranium during this evolution; (c) the greater and more systematic variation of thorium compared with the restricted (less than 6 p.p.m.) and irregular distribution of uranium.

The general increase of uranium and thorium may be adequately explained by their large size and high ionic charge, which effectively preclude their entry into the lattices of the common rock-forming minerals. The two elements are so

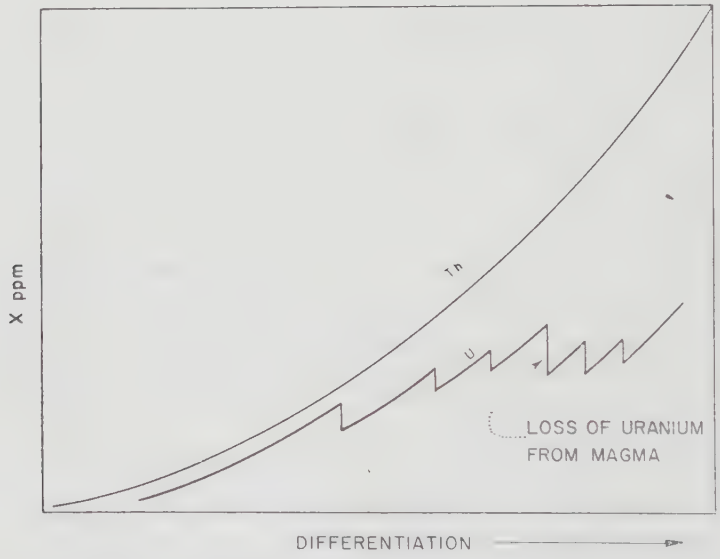

Fig. 13. Schematic representation of postulated loss of uranium relative to thorium during normal igneous differentiation.

similar, when in the tetravalent state, that the variation of Th/U ratios observed here probably cannot be explained by the slight differences in chemical character which do exist.

Uranium can be oxidized to the hexavalent state, but thorium cannot exist in this valence state. Hexavalent uranium is considerably more soluble than tetravalent thorium and, furthermore, forms many very soluble compounds. If uranium can be oxidized during magmatic activity, then it will tend to enter volatile phases and escape from the magma. Uranium may tend to follow thorium during differentiation but may be prevented from doing so by successive loss from the magma. This hypothesis is schematically presented in Fig. 13.

The postulated loss of uranium from the magma will explain the irregular distribution of uranium and its generally wider deviation than thorium from

petrogenetic control. Slight changes in the ambient magmatic oxidation conditions may profoundly affect the petrochemistry of uranium but not significantly affect the petrographic parameters that are being used as criteria of petrogenetic control. The factors that control the loss of fluids from a crystallizing magma are very complicated and variable; thus, magmas which crystallized in different environments may have lost different amounts of uranium to the surrounding rocks. Fig. 12 shows that in the late stages of differentiation there is an absolute decrease in uranium content in the rocks studied, which is most simply explained by loss of uranium from the magma.

The red colour, predominant in thorium-rich, relatively uranium-poor granites, may indicate oxidizing conditions during magmatic activity and consequent loss of uranium. This is a particularly appealing explanation for a rock such as F 19-24, which has an extremely high Th/U ratio, low uranium content and marginal position in the batholith. According to McKelvey *et al.* (1955) the oxidation potential of tetravalent uranium is roughly the same as that of ferrous iron, and consequently red, ferruginous rocks may have been sufficiently oxidized so that original tetravalent uranium was converted to the uranyl ion. Some authors, however, have observed selective retention of uranium in granitic magmas; see Senftle and Keevil (1947) for further discussion.

There is a possibility that the observed variation in Th/U ratio is not due to loss of uranium but due to addition of hydrothermal or deuteric thorium, primarily in the form of allanite. Secondary allanite has been described by Hutton (1951), and Tilton *et al.* (1955) have observed that the Essonville granite was an open system to thorium and its decay products. If thorium is secondary it should be variable in abundance and should have been irregularly controlled by major petrogenesis. This might be the case in some of the very thorium-rich granites; but, in general, thorium bears much more systematic relations to major petrographic parameters than does uranium. The source of late thorium would be as great a problem as the observed variation in Th/U ratios.

As stated above, the preceding discussion assumes that fractionation of thorium and uranium is unlikely unless the uranium is oxidized to the hexavalent uranyl ion. The tetravalent uranium ion is, however, slightly smaller than the thorium ion, and recent revisions of ionic radii place the tetravalent uranium very near, tetravalent zirconium well below and tetravalent thorium slightly above the critical size separating cations with sixfold and eightfold co-ordination with oxygen. Thus, there may be some tendency for fractionation without oxidation, and such differences in co-ordination number, particularly at lower temperatures, might explain the variability in thorium and uranium ratios found in accessory minerals such as zircon, sphene, monazite and apatite; abundances of thorium and uranium in a number of accessory minerals are given by Hurley and Fairbairn (1957).

In addition to the variations in thorium and uranium caused by plutonic processes, one must also consider the degree to which granites are derived from heterogeneous sources such as different types of sedimentary rocks. The granites may inherit and even magnify the wide differences in thorium and uranium concentrations found in sedimentary rocks.

Appendix

Samples studied in this investigation are arranged in order of sequential collection number, i.e. the number following the hyphen. Some odd samples with slightly different designations are included at the end of the appendix. Modal analyses of these rocks are included in Table 3. References cited provide information concerning the rocks but are not necessarily in agreement with the geologic and lithologic descriptions given here.

Sp 2-4. Spavinaw granite: The relations of this body of rock are not well known; it is thought to be pre-Cambrian. The sample was collected $\frac{1}{2}$ mile south-west of Spavinaw Dam along Route 22 in eastern Oklahoma; it is red, medium-grained granophyre or micrographic granite.

F 2-7 The Idaho Springs formation is a metasedimentary rock intruded by the Front Range pre-Cambrian granites. This sample was collected from Geneva Ridge in Section 8, T. 6 S, R. 75 W, Georgetown, Colorado. The hand specimen, taken from a massive quartzo-feldspathic segregation in strongly banded schists, is buff, fine- to medium-grained, allotriomorphic–granular to poikilo-blastic textured granite. Large grains of muscovite are present.

F 10-15 The Pikes Peak granite is second from the acidic end of the Front Range pre-Cambrian complex. It is discordant, massive, and uniform in composition and generally has sharp contacts. The hand specimen was taken $\frac{1}{2}$ mile from the contact of granite with schist and $\frac{1}{2}$ mile south-east of Shatters Crossing along Route 22. The specimen is pink, porphyritic quartz monzonite with pheno-crysts of microcline up to 1 cm in length in a medium-grained, hypidiomorphic groundmass which has incipient mortar texture.

F 16-21. The Boulder Creek granite (Lovering and Goddard, 1950), or Mount Evans quartz monzonite of Boos (1954), forms stocks and batholiths which are satellitic to, and intruded by, the Pikes Peak granite. The Boulder Creek granite is generally harmonious,* concordant, and gneissic. The specimen was taken from the summit of Mt. Evans and is grey, fine- to medium-grained quartz monzonite. The thin section shows considerable mortar texture and fracturing of all components except microcline.

F 19-24. Pikes Peak granite. The hand specimen was taken from the contact of the Pikes Peak granite with the Boulder Creek granite on Epaulet Mountain in Section 36, T.5 S, R. 75 W, Georgetown, Colorado. The specimen is pink, coarse-grained, porphyritic, quartz monzonite. Microcline is semi-poikilitic.

F 32-37. The Silver Plume granite (Mason Creek Pluton; Boos, 1954) is the youngest member of the Front Range pre-Cambrian complex. Plutons are concordant, harmonious and disconformable stocks and sheets located between the Pikes Peak granite and the Idaho Springs formation. The granite is presumably late- or post-kinematic. The hand specimen was collected along U.S. Route 285, 11 miles south-west of the intersection of Route 285 with the Parmalee Road in Colorado. It is light reddish-grey, hypidiomorphic–porphyritic, quartz monzonite with phenocrysts of microcline up to 1 cm in diameter.

CB 3-45. The Crested Butte porphyry was taken from a cliff on the south-west side of Crested Butte in Southwest Colorado. The intrusive is a member of the most acidic of a group of intrusives in the West Elk Mountains which may be related to the Laramide porphyries of the Front Range. This intrusive is either a stock or a laccolith and is disharmonious, disconformable and intrudes undeformed sediments. The hand specimen is from a cliff on the south-west side of Crested Butte and is a white seriate porphyry, with phenocrysts of sanidine, rounded (resorbed) quartz crystals, and some biotite and hornblende in a finely crystalline, felsophyric, mesostasis.

Sc 1-49. The Rubideaux granite is an acidic member of the lower Cretaceous (?) Southern California batholith (Larsen, 1948). All members of this series are disharmonious and discordant against other members of the series but locally concordant against the adjacent metamorphic wall rocks. Larsen feels that the series is a product of differentiation. The hand specimen was taken from Victoria Hill in the neighbourhood of Riverside, California; it is a greenish-grey, medium-grained, allotriomorphic–granular, seriate, quartz monzonite.

Sc 8-56. The Mt. Hole granodiorite is an intermediate member of the lower Cretaceous (?)

* In the sense of the term defined by Walton (1955).

Southern California batholith (LARSEN, 1948). The hand specimen is from the contact of Mt. Hole granodiorite with Mt. Woodson granodiorite in the vicinity of Swiss Dairy at Arlington Place, California; the specimen is grey, fine- to medium-grained, biotite–hornblende granodiorite.

Sc 12-60. The Woodson Mountain granodiorite is an intermediate member of the lower Cretaceous (?) Southern California batholith (LARSEN, 1948). The hand specimen was taken from the Arroyo del Torro, north of Elsinore, California, at the contact of the Woodson Mountain granodiorite with the Bedford Canyon formation; it is grey, medium-grained, hypidiomorphic–granular, seriate, biotite–hornblende–quartz tonalite. Inclusions with pleochroic haloes are abundant.

Sc 15-63. The San Marcos gabbro is the oldest and most mafic member of the lower Cretaceous (?) Southern California batholith (LARSEN, 1948). It is disconformable, discordant and disharmonious. The hand specimen was collected south-west of Elsinore along the Duluz Road and is dark grey, fine-grained, massive, hornblende gabbro.

Sc 25-72. The Roblar leucogranite is an acidic member of the lower Cretaceous (?) Southern California batholith. It is discordant, disharmonious and has been interpreted as being the product of differentiation (LARSEN, 1948). The hand specimen was taken 1 mile south-west of the Roblar Ranch sign on the Duluz–Fallbrook road; it is grey, massive, medium-grained, hypidiomorphic–granular, equigranular to seriate biotite granodiorite.

MW 3-76. The Cathedral Peak granite was collected from the Mt. Whitney area, California. This is part of a generally concordant (locally discordant) batholith of possible Upper Jurassic age which is continuous north of Mt. Whitney for more than 100 miles. The contacts are generally abrupt (MAYO, 1941) but locally become gradational (BRADLEY and LYONS, 1953). CLOOS (1933) discerns disconformable structure within the igneous rock and interprets it to indicate magmatic intrusion; BRADLEY and LYONS (1953) feel that the batholith is the product of granitization. The hand specimen was taken 2 miles from the eastern contact of the batholith in the vicinity of Consultation Lake on the Mt. Whitney trail; it is light grey, coarse-grained, porphyritic granite or quartz monzonite with idiomorphic phenocrysts or porphyroblasts of microcline (and some plagioclase) up to 2 in. in diameter.

Y 1-96. The Sentinel granodiorite is an intermediate member of the upper Jurassic (?) Yosemite igneous complex. It is generally discordant, disconformable, disharmonious and post-tectonic. The hand specimen was collected at the foot of Sentinel Dome on the north side of Yosemite Valley and is grey, medium-grained, hypidiomorphic-granular, ideally granitic textured, biotite–hornblende tonalite.

Y 7-102. The Bridalveil granite is a late, acidic member of the upper Jurassic (?) Yosemite igneous complex. It is discordant, disconformable and harmonious. The hand specimen was collected at the base of Bridalveil Falls in Yosemite National Park, California; it is grey, fine-grained hypidiomorphic–granular, typically granitic textured, biotite granodiorite.

Y 9-104. The El Capitan granite is an early member of the Upper Jurassic (?) Yosemite igneous complex. The pluton is disharmonious, disconformable and generally abruptly discordant. The sample was collected at the base of El Capitan in Yosemite Valley, California; it is grey, massive, medium- to coarse-grained, hypidiomorphic–granular tonalite characterized by abundant, very large, aggregates of quartz.

Y 24-119. The Cathedral Peak granite was collected from Yosemite Park (see MW 3-76 for complete description of the relations of this granite). The hand specimen was collected from a blasted outcrop 2 miles west of Tuolumne store on the Tioga Road. The specimen is light grey, coarse-grained, porphyritic granite or quartz monzonite with idiomorphic phenocrysts or porphyroblasts of microcline up to 2 in. in diameter.

P 11-141. The Bucks Granodiorite is an outlier of the upper Jurassic (?) Sierra Nevada complex. The pluton is mainly concordant and harmonious with profound local discordance and granitization or assimilation. This sample was taken from the Plumas–Merrimac area of California, on U.S. Route 24, 2 miles north of the Bridge across the North Fork of the Feather River. The sample is grey, massive, medium-grained, hypidiomorphic-granular, biotite–hornblende tonalite.

P 13-143. Same description as P 11-141; this sample was collected 2 miles further north along Route 24.

P 15-145. Same description as P 11-141; this sample was taken 4 miles further north along Route 24.

S 14-166. The Snoqualmie batholith is an upper Miocene or younger, discordant, disharmonious intrusion. This sample was collected north of Lake Keechelus, Washington, along Route 10, 3 miles south-west of Snoqualmie Pass. The hand specimen is from the contact of the granodiorite with the Guye formation. The hand specimen is grey, massive, medium-grained, hypidiomorphic–granular, typically granite textured, biotite–hornblende tonalite.

W 13-194. The Wallowa batholith is an upper Jurassic (?) complex pluton which is concordant on a large scale but discordant locally. The contacts are generally abrupt, with some notable exceptions. It is generally disconformable. This sample was collected S 50° E of Hummingbird Hill and immediately south-east of Looking Glass Lake in north-eastern Oregon. The sample is grey, massive, medium-grained, hypidiomorphic–granular, biotite–hornblende tonalite. This particular locality has been presented by Krauskopf (1943) as an example of granitization at the borders of the batholith.

Id 7-202. This is a sample of the dark outer facies of the Idaho batholith. The relations are very complicated, but the rock seems to be generally an autochthonous type of granite which is concordant, harmonious, conformable and shows much evidence of endomorphic replacement. This sample was collected along Route 15, where it crosses the Payette River at Banks, Idaho; it is a grey, massive, medium-grained, hypidiomorphic–granular, biotite granodiorite.

M 3-205. The Marysville granodiorite forms a small, 3 mile^2, stock which intrudes the Helena dolomite and the Empire formation, both of which are essentially undeformed except by the intrusion. The stock is concordant on a small scale but discordant on a large scale and is definitely disharmonious. The hand specimen was taken from the centre of the stock approximately 1 mile west of Marysville, Montana. The sample is a grey, fine-grained, hypidiomorphic–seriate granodiorite; it is almost a porphyry.

M 6-208. Marysville granodiorite, similar in all respects to M 3-205, but collected from the border of the stock at Drumlummon Mill in Marysville, Montana.

D 5-226. A sample from the intermediate red rock of the Duluth gabbro collected north-east of Enger Tower in Duluth, Minnesota from a transition between red rock and normal gabbro. The hand specimen is a red, fine-grained, hypidiomorphic to panidiomorphic rock composed of euhedral plagioclase, some anhedral quartz and oxidized mafic minerals.

D 9-230. Same collection locality as D 5-226; D 9-230 is intermediate between that sample and the gabbro. The hand specimen is a reddish, medium-grained, hypidiomorphic to panidiomorphic rock composed of euhedral plagioclase and pyroxene with intergranular quartz, chlorite and iron oxide (?) stain.

D 14-235. Duluth granophyre. Contacts with the main mass of gabbro are apparently abrupt. This sample was collected at the Kenwood Avenue quarry in Duluth, Minnesota; it is red, massive, fine-grained, panidiomorphic to hypidiomorphic granophyre. It is considerably altered to amorphous iron oxide.

D 17-238. Anorthositic gabbro from the Duluth lopolith. This sample was taken from the west branch of Enger Circle on Skyline Drive in Duluth, Minnesota. The hand specimen is dark grey to blue-black, coarse-grained, hornblende gabbro. The borders of crystals are commonly slightly fractured.

K 17-255. The Killarney granite is an irregular body of granitic rock in the Huronian sediments of central Canada. According to Quirke (1927, 1940) and Quirke and Collins (1930), the rock is a product of granitization. It is harmonious. The eastern contact of the granite with quartzite is completely transitional; the western contact is locally abrupt and locally transitional. The granite is massive to conformable. This sample was taken from the central part of the body at Le Hayes Point in Killarney, Ontario. The hand specimen is red, medium-grained, hypidiomorphic–granular, slightly seriate granite. The texture is rather strange; aggregates of very granular quartz are quite abundant.

A 4-259. The Adirondack "phacolithic" granite gneiss is a pre-Cambrian granite which intrudes Grenville gneisses. This body is a phacolith with completely gradational borders into gneiss on all sides. It is gneissic, harmonious, generally concordant and conformable and sillimanite- and garnet-bearing, particularly along the boundaries. This is believed to be a

product of metamorphism and metasomatism. The hand specimen was collected from Crane Pond, east of Paradox, New York, in the Adirondack Mountains. The hand specimen is red, slightly gneissic, medium-grained, allotriomorphic–granular, garnet-bearing, hornblende–quartz monzonite.

A 13-268. The Adirondack "red" granite generally forms concordant, conformable, harmonious bodies which commonly have gradational boundaries into adjacent gneiss and schist. This sample is the granitic end of a gneiss–granite transition along Route 9 just southeast of Cowne Point, New York. The specimen is pinkish-grey, massive, medium-grained, allotriomorphic–granular, biotite granite. The texture is not typically granitic; equigranular equant microcline and rounded quartz are characteristic.

NH 29-331. The Mascoma Group (Chapman, 1939) is a member of the upper Devonian (?) Oliverian magma series. Its plutons form the concordant, conformable, harmonious, gradationally bounded, gneiss-domes of New England. The hand specimen was collected from a quarried block 1 mile south of Goss School in the Mascoma quadrangle, New Hampshire; it is grey, gneissic, fine- to medium-grained, granoblastic, quartz monzonitic gneiss. The texture is metamorphic, not granitic.

NH 43-345. The Bethlehem gneiss is a mafic member of the upper Devonian (?) New Hampshire magma series. Bodies of this gneiss are generally concordant, conformable, harmonious and presumably synkinematic. This sample was taken along Route 10 approximately $1\frac{1}{2}$ miles north of North Grantham, New Hampshire; it is grey, strongly gneissic, medium-grained, allotriomorphic–granular or granoblastic, quartz monzonitic gneiss.

NH 47-349. The Concord granite is an acidic member of the upper Devonian (?) New Hampshire magma series. This granite occurs in dike-like intrusions and stocks (Chapman, 1952; Billings, 1954). The sample was taken along Route 11, $\frac{3}{4}$ mile south of Georges Mills, New Hampshire; it is grey, massive, fine-grained, allotriomorphic–granular, muscovite–quartz monzonite.

W 3-399. The Wichita Granophyre is a member of a pre-Cambrian stratiform complex in which granophyric material overlies gabbro and anorthosite (Hamilton, 1956). This hand specimen was collected at Elmer Thomas Dam in the Wichita Mountains of Oklahoma; it is red, massive, fine- to medium-grained, panidiomorphic to hypidiomorphic, semi-graphic granite.

E 3-402. The Enchanted Rock batholith is pre-Cambrian, slightly disharmonious, disconformable and discordant on a large scale (Hutchinson, 1956). The intrusion is apparently complex with peripheral zonation of petrographic types. This sample was taken from the porphyritic granite of the intermediate zone; it is red, massive, coarse-grained, hypidiomorphic–porphyritic, slightly seriate biotite quartz monzonite.

E 4-403. This Enchanted Rock batholith sample is from the same location and description as sample E 3-402. The present sample was collected 100 ft from E 3-402.

E 5-404. Enchanted Rock batholith; the present sample was collected from the same outcrop as was E 3-402 but from an aplitic dike cutting the porphyritic material. The hand specimen is grey, fine-grained, allotriomorphic–granular, aplitic, biotite–quartz monzonite.

KA 6-405. This sample of Cold Spring granite from the Cold Spring Granite Co. quarry in Rockville, Minnesota was donated by Dr. S. S. Goldich. The rock is grey, coarse grained, hypidiomorphic granular.

KA 72-406. The Northern Lights group is an autochthonous gneiss north-west of the Saganaga granite. Grout (1929a,b) feels that this is the root zone of some of the younger granites in northern Minnesota. The hand specimen is from the Canadian Rangers cabin on the north side of the north-west channel of Northern Lights Lake, east of the portage into Saganaga Lake. This sample is a fine-grained granoblastic gneiss, and was donated by Dr. S. S. Goldich.

P 210G (407). The Saganaga granite is a Laurentian (?) semi-concordant, harmonious granite or granite gneiss which Grout (1933) feels has been exposed to a depth of 25 km. This sample was collected by Dr. S. S. Goldich from the lower part, exposed in Saganaga Lake. The sample is grey, medium-grained, hypidiomorphic–granular, hornblende tonalite.

KA 80-408. The Burntside Gneiss is an early Algoman (?) gneissic granite which is conformable, generally concordant, and harmonious. This sample was collected from a small island

near the east end of Burntside Lake, Minnesota; it is a grey, massive to slightly gneissic, medium-grained, granitic gneiss.

V 1-409. The Vermillion granite is the largest batholith along the Canadian border in Minnesota. It is complex but generally harmonious. The sample was collected by Dr. S. S. Goldich near a road cut 200 ft east of the intersection of Echo trail and Sioux River, St. Louis County, Minnesota. The hand specimen is red, medium-grained allotriomorphic-granular, slightly seriate, quartz monzonite.

KA 27-410. This sample of the Montevideo granite gneiss is from the SE $\frac{1}{4}$, Section 20 on U.S. Route 212, Minnesota. The hand specimen is fine- to medium-grained, allotriomorphic seriate, granite gneiss.

M-4. Dark outer facies of the Idaho batholith (see sample Id 7-202 for a full description of the batholith). This specimen was taken on the north shore of Arrowrock Reservoir, 4 miles from the turnoff of the dam road from Route 20 east of Boise, Idaho. The sample is grey. medium-grained, hypidiomorphic–granular, biotite tonalite.

12 M. This sample is from the Inner facies of the Idaho batholith (Anderson, 1942, 1948). The hand specimen was collected on the north shore of Arrowrock Reservoir, 12 miles from the turnoff of the dam road from Route 20 east of Boise, Idaho; it is grey, medium-grained, allotriomorphic–granular, leucogranodiorite. There is considerable mortar texture.

JW 70. This is an aggregate of four samples of the Bonsal tonalite member of the lower Cretaceous (?) Southern California batholith. Its plutons are generally discordant, disharmonious, and disconformable. The plutons are characterized by elongate inclusions and schlieren. All samples are grey, medium-grained, hypidiomorphic–seriate, biotite-hornblende tonalite.

JW 32. This is an aggregate of several samples of the Mt. Morrison gneiss member of the Front Range igneous complex. There is considerable controversy over whether this is a paragneiss or an ortho-gneiss. It is harmonious and autochthonous. Texture is medium grained, and gneissic.

References

Adams J. A. S., Osmond J. K. and Rogers J. J. W. (1959) The geochemistry of thorium and uranium. *Physics and Chemistry of the Earth* Vol. 3. Pergamon Press, London.

Adams J. A. S., Richardson J. E. and Templeton C. C. (1958) Determinations of thorium and uranium in sedimentary rocks by two independent methods. *Geochim. et Cosmochim. Acta* **13,** 270–279.

Adams J. A. S. and Weaver C. E. (1958) Thorium-to-uranium ratios as indicators of sedimentary processes: example of concept of geochemical facies. *Bull. Amer. Ass. Petrol Geol.* **42,** 387–430.

Anderson A. L. (1942) Endomorphism of the Idaho batholith. *Bull. Geol. Soc. Amer.* **53,** 1099–1126.

Anderson A. L. (1948) Role of the Idaho batholith during the Laramide orogeny. *Econ. Geol.* **43,** 84–99.

Billings M. P. (1945) Mechanics of igneous intrusion in New Hampshire. *Amer. J. Sci.* **243a,** 40–68.

Boos M. F. (1954) Genesis of pre-Cambrian granitic pegmatites in the Denver Mountain Parks area, Colorado. *Bull. Geol. Soc. Amer.* **65,** 115–141.

Bradley C. and Lyons E. J. (1953) A mode of evolution of a granitic texture. *Geol. Soc. Amer. Mem.* **52,** 101–110.

Chapman C. A. (1939) Geology of the Mascoma quadrangle, New Hampshire. *Bull. Geol. Soc. Amer.* **50,** 127–180.

Chapman C. A. (1952) Structure and petrology of the Sunapee quadrangle, New Hampshire. *Bull. Geol. Soc. Amer.* **63,** 381–425.

Cloos E. (1933) Structure of the Sierra Nevada batholith. *Sixteenth Int. Geol. Congr. Guidebook* **16,** 40–45.

Green J. and Poldervaart A. (1958) Petrochemical fields and trends. *Geochim. et Cosmochim. Acta* **13,** 87–122.

Grout F. F. (1929a) The Saganaga granite, Minnesota–Ontario. *J. Geol.* **37,** 562–591.

Grout F. F. (1929b) Ages and differentiation of batholiths near the Minnesota–Ontario boundary. *Bull. Geol. Soc. Amer.* **40,** 791–809.

Grout F. F. (1933) Structural features of the Saganaga granite of Minnesota–Ontario. *Sixteenth Int. Geol. Congr. Rep.* **1,** 255–270.

Hamilton W. B. (1956) Pre-Cambrian rocks of Wichita and Arbuckle Mountains, Oklahoma. *Bull. Geol. Soc. Amer.* **67,** 1319–1330.

Hurley P. M. (1956) Direct radiometric measurement by gamma-ray scintillation spectrometer. *Bull. Geol. Soc. Amer.* **67,** 395–412.

Hurley P. M. and Fairbairn H. W. (1957) Abundance and distribution of uranium and thorium in zircon, sphene, apatite epidote and monazite in granitic rocks. *Trans. Amer. Geophys. Un.* **38,** 939–944.

Hutchinson R. M. (1956) Structure and petrology of Enchanted Rock batholith, Llano and Gillespie Counties, Texas. *Bull. Geol. Soc. Amer.* **67,** 763–806.

Hutton C. O. (1951) Allanite from Wilmot Pass, Fiordland, New Zealand. *Amer. J. Sci.* **249,** 208–214.

Krauskopf K. B. (1943) The Wallowa batholith. *Amer. J. Sci.* **241,** 607–628.

Larsen E. S. (1948) Batholith and associated rocks of Corona, Elsinore and San Luis Rey quadrangles, Southern California. *Geol. Soc. Amer. Mem.* **29,**

Lovering T. S. and Goddard E. N. (1950) Geology and ore deposits of the Front Range, Colorado. *U.S. Geol. Surv. Prof. Pap.* 223.

Marshall R. R. (1957) Isotopic composition of common leads and continuous differentiation of the crust of the earth from the mantle. *Geochim. et Cosmochim. Acta* **12,** 225–237.

Mayo E. B. (1941) Deformation in the interval Mt. Lyell–Mt. Whitney, California. *Bull. Geol. Soc. Amer.* **52,** 1001–1084.

McKelvey V. E., Everhart D. L. and Garrels R. M. (1955) Origin of uranium deposits. *Fiftieth Anniversary Volume of Econ. Geol.* 464–533.

Murray E. G. and Adams J. A. S. (1958) Thorium, uranium and potassium in some sandstones. *Geochim. et Cosmochim. Acta* **13,** 260–269.

Quirke T. T. (1927) Killarney gneisses and migmatites. *Bull. Geol. Soc. Amer.* **38,** 753–770.

Quirke T. T. (1940) Granitization near Killarney Ontario. *Bull. Geol. Soc. Amer.* **51,** 237–253.

Quirke T. T. and Collins W. H. (1930) Disappearance of the Huronian. *Geol. Soc. Canada, Memoir* 160.

Senftle F. E. and Keevil N. B. (1947) Thorium/uranium ratios in the theory of genesis of lead ores. *Trans. Amer. Geophys. Un.* **28,** 732–738.

Shand S. J. (1947) *Eruptive Rocks.* John Wiley, New York.

Tilton G. R., Patterson C., Brown H., Inghram M., Hayden R., Hess D. and Larsen E. S., Jr. (1955) Isotopic composition and distribution of lead, uranium and thorium in a pre-Cambrian granite. *Bull. Geol. Soc. Amer.* **66,** 1131–1148.

Walton M. (1955) The emplacement of "granite". *Amer. J. Sci.* **253,** 1–18.

Geochimica et Cosmochimica Acta, 1959, Vol. 17, pp. 272 to 285. Pergamon Press Ltd. Printed in Northern Ireland

Relationships among textural properties and modal compositions of some granitic rocks

J. M. Whitfield, J. J. W. Rogers and M. C. McEwen
Department of Geology, The Rice Institute, Houston, Texas

(*Received* 23 *February* 1959)

Abstract—Plots of modal percentages of mineral pairs in granitic rocks show negative correlation between the abundance of potassium feldspar and the abundances of plagioclase and biotite, and the percentage anorthite in plagioclase. A positive correlation is found between plagioclase and biotite, plagioclase and percentage anorthite in plagioclase, and biotite and percentage anorthite in plagioclase. The distribution of quartz is erratic as shown by the absence of correlation between quartz and other mineral abundances.

Study of modal compositions of groups of granitic rocks subdivided on the basis of various textural properties leads to characterization of granitic rocks in terms of two ideal "end members". One type of granite consists of subhedral zoned plagioclase laths with interstitial quartz and potassium feldspar; abundances of plagioclase, biotite and hornblende are comparatively high in this type, whereas potassium feldspar is scarce. The other end member granite contains roughly equal amounts of quartz, potassium feldspar and plagioclase, with minor biotite; all minerals are anhedral, and the plagioclase is twinned and unzoned. Complete gradation exists between these two types of granite.

The complete gradation between the two granitic textural and compositional types indicates that most granites have evolved by one general process. In view of the definite correlations, both positive and negative, among the abundances of potassium feldspar, plagioclase, biotite and percentage anorthite in plagioclase, it is proposed that this process is one of magmatic differentiation. The relationships can be explained by differentiation but would appear fortuitous if metasomatism were a major factor.

Introduction

In the course of studies of the thorium and uranium contents of a suite of granitic rocks, considerable information has been gathered concerning the petrography and modal compositions of the studied samples. The relationship between thorium and uranium contents and petrology of the granites is discussed in a companion paper (Whitfield *et al.*, 1959). The object of the present paper is to describe relationships among various petrographic parameters, including modal compositions and certain textural properties, of approximately one-hundred granitic rocks (ranging from quartz diorite to true granite). Most of the samples analysed for the companion paper are included, though a few have been omitted.

The samples studied in the present work were taken from an area encompassing much of the United States and parts of southern Canada. The areas or batholithic suites most abundantly represented in the collection are the Southern California batholith, the Sierra Nevadas, the Idaho batholith, the Front Range of Colorado, central and northern Minnesota and southern Ontario, the Adirondack Mountains and New England. Areas of single granitic bodies represented by a relatively small number of samples include some granitic rocks in Washington and Oregon, the Crested Butte porphyry in Colorado, the Spavinaw granite of Oklahoma, the Enchanted Rock batholith of central Texas and a few granites from the southern Appalachian Mountains.

The object of the sampling was to include as wide a range of granitic rock types as possible. Almost all samples taken were typical of rather large portions of the plutons which they represent. Aberrant samples showing the effects of

contamination by inclusions or nearby wall rocks were generally avoided, though three of the samples (two from the Southern California batholith) contain mafic inclusions, either autoliths or xenoliths, which contribute to the modal content of mafic material in the rocks. These three samples are included in the present study because they are typical of some types of plutons. Five of the rocks are migmatitic or highly gneissic; they are included in the study because, though of uncertain origin, they are typical of a large group of generally granitic rocks. All samples

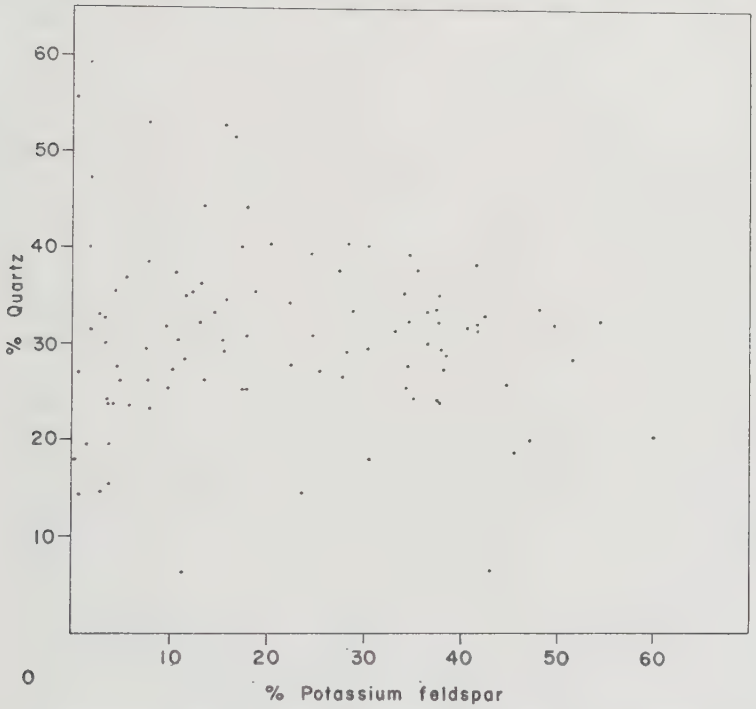

Fig. 1. Relationship between modal abundances of quartz and potassium feldspar in granitic rocks.

consisted solely of normal granitic minerals (quartz, feldspars, biotite, hornblende and standard accessories) except two samples of Adirondack red granite which contained small amounts of garnet. The ten rocks mentioned above plot as closely on the variation trends shown in Figs. 1–10 as do the other approximately ninety samples studied, and no unusual mineralogical ratios have been detected for any of the groups.

Modal analyses of the granites have been made by point counting of 1000 to 1500 points. In a very few samples of particularly coarse grain size the plotted compositions represent the average of analyses of two sections from the same hand specimen. Plagioclase compositions have been measured by the Michel–Levy method, and many have been checked by oil immersion measurements. Linear correlation coefficients have been calculated by standard methods on those cases in which relationships between plotted parameters were uncertain (Figs. 6–10).

Most of the data described in this study were collected by the first writer

(Whitfield) in connexion with a Ph.D. thesis at The Rice Institute. The present paper was written largely by the second writer (Rogers) after Dr. Whitfield's death. Studies in the geochemistry of thorium, of which the present work is a part, have been financed by Grant C-009 from the Robert A. Welch Foundation.

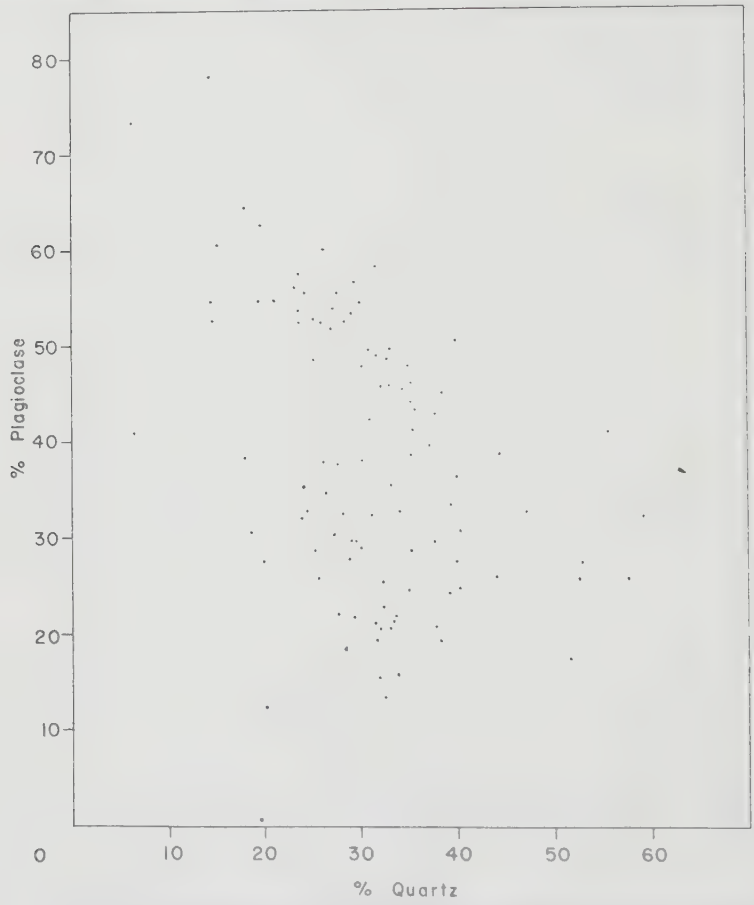

Fig. 2. Relationship between modal abundances of quartz and plagioclase in granitic rocks.

Results and Discussion

Comparison of modal abundances of mineral pairs

Plots of modal percentages of various minerals vs. each other and vs. the percentage of anorthite in plagioclase yield several interesting results. The different graphs, involving quartz, potassium feldspar, plagioclase, biotite, and percentage anorthite in plagioclase, are shown in Figs. 1–10. Other minerals, such as hornblende and accessory minerals, are not sufficiently abundant to provide accurate information.

The relationships between quartz and potassium feldspar, plagioclase, biotite and percentage anorthite in plagioclase are shown in Figs. 1–4, respectively. No general trend is apparent in any of these graphs, and it seems that the abundance

of quartz is not related to other compositional parameters. Though quartz is undoubtedly more abundant in silicic rocks than in basic ones, it appears to be rather erratically distributed within the range of granitic rock types (quartz diorite to true granite). Increase in quartz content with differentiation has been

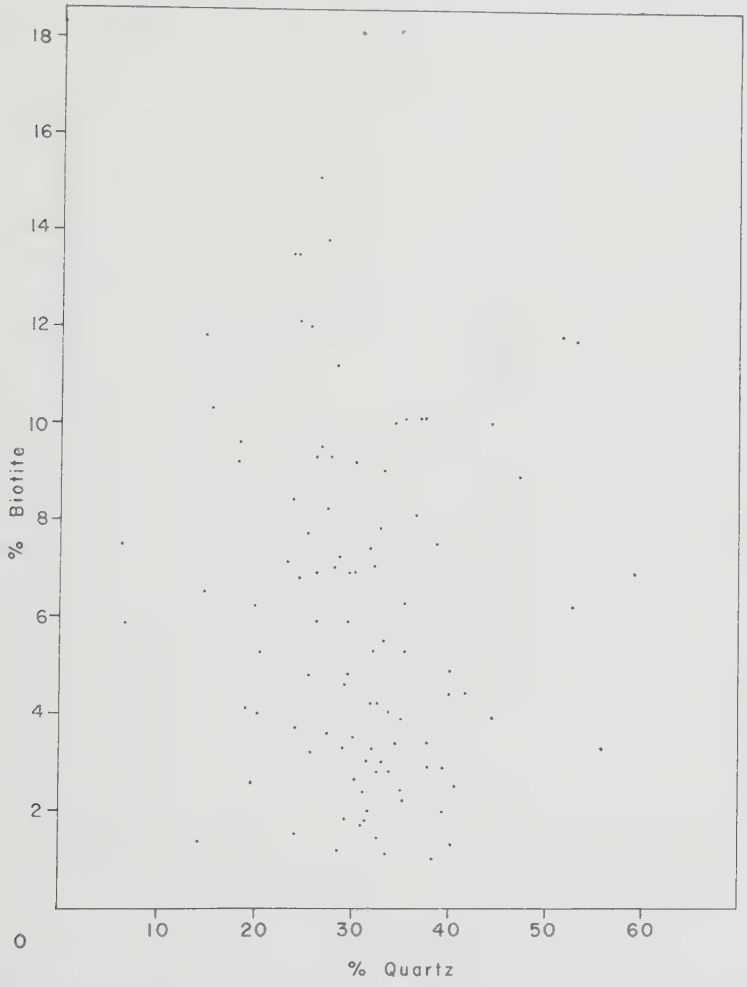

Fig. 3. Relationship between modal abundances of quartz and biotite in granitic rocks.

noted, however, in individual intrusions (Sargent, 1925) and batholithic suites (Larsen, 1948).

The most definite relationship found in the present study is that between potassium feldspar and plagioclase (Fig. 5). Increase in potassium feldspar content is definitely correlated with decrease in plagioclase. The nearly 1 : 1 relationship signifies that in most granitic rocks the total amount of feldspar is approximately constant (60 per cent). The ratio of potassium feldspar to plagioclase has been used as an index of general petrogenic differentiation in the companion paper (Whitfield *et al.*, 1959), though differentiation indices are generally based on

chemical, rather than modal compositions (see, for example, Simpson, 1954). A number of the points in Fig. 5 are somewhat off the main trend. Examination of the rocks represented by these aberrant points showed no particular textural or mineralogical similarities. The variation may be statistical sampling variation.

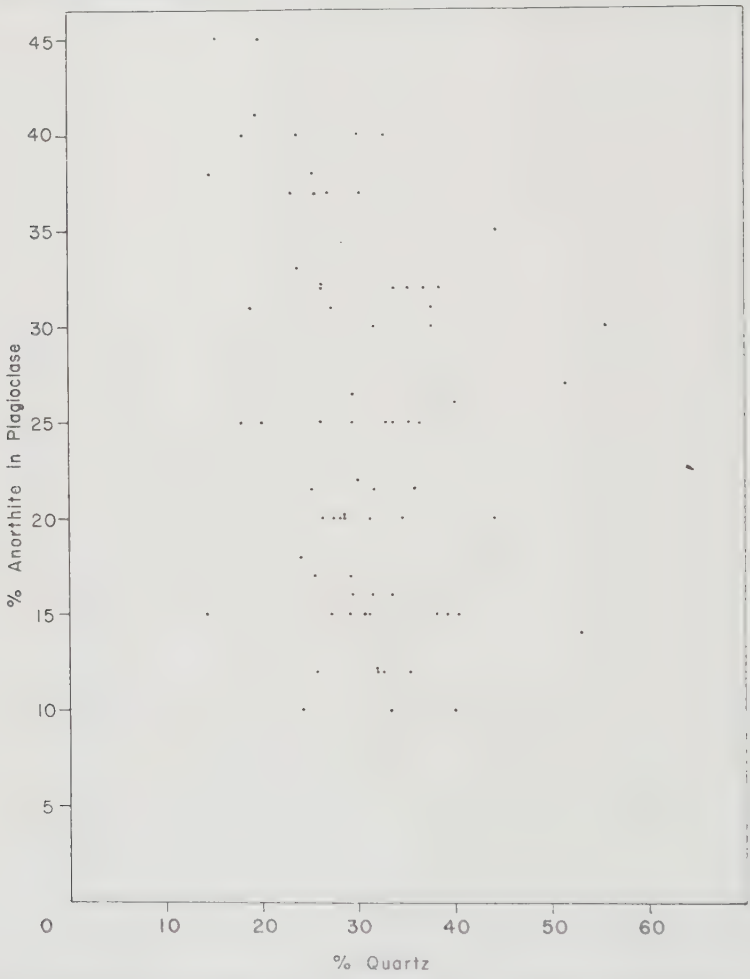

Fig. 4. Relationship between modal abundance of quartz and percentage anorthite in plagioclase in granitic rocks.

Though, as stated in the Conclusions, it is felt that the process of magmatic differentiation is generally responsible for the variations shown in Fig. 5 and succeeding diagrams, side effects such as assimilation might tend to cause some scatter of plotted points.

Plots were made of modal potassium feldspar vs. plagioclase for three individual series or areas of petrogenically related rocks (Southern California batholith; Front Range, of Colorado; and Yosemite, California). No differences were detected between trends of individual groups though the number of samples available from each sequence was too small for certainty.

The relationships of potassium feldspar to biotite and to percentage anorthite in plagioclase are shown in Figs. 6 and 7, respectively. Though the relationships are not as definite as in the case of potassium feldspar/plagioclase, correlation coefficients for both sets of data are quite high and test as significant at an extremely

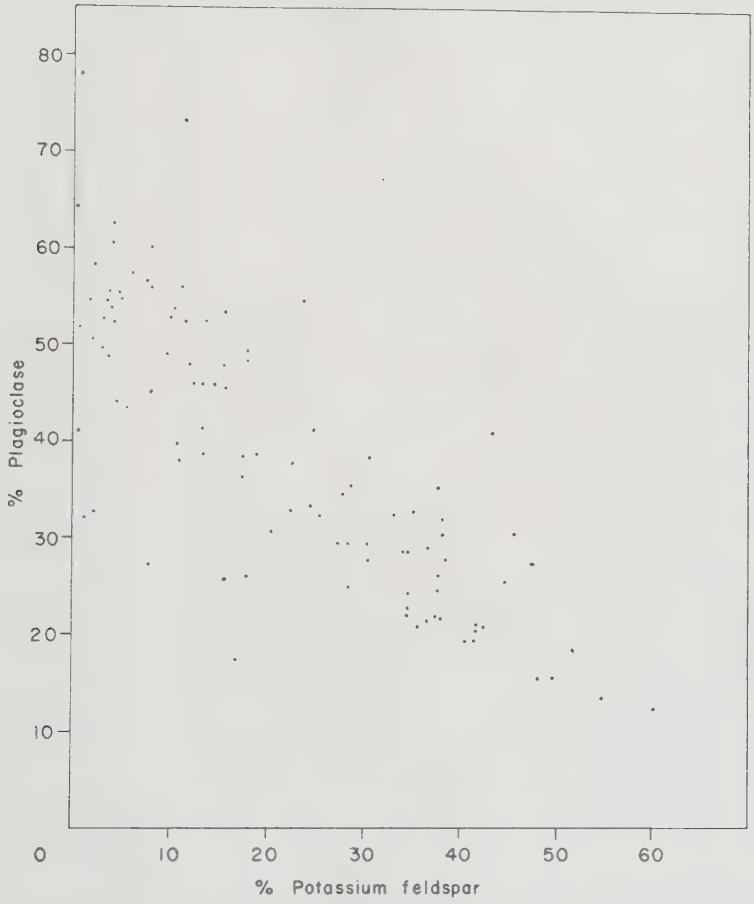

Fig. 5. Relationship between modal abundances of potassium feldspar and plagioclase in granitic rocks.

high confidence level (greater than 99·9 per cent). An increase in potassium feldspar content is generally accompanied by a decrease in mafic constituents, such as biotite and the percentage of anorthite. The general sequence from mafic rocks containing calcic plagioclase and biotite to acidic rocks containing potassium feldspar is well shown by Figs. 5–7.

The relationship between the percentage of plagioclase and its anorthite content is shown in Fig. 8. The correlation coefficient tests as significant at an extremely high confidence level. The relationship can be readily explained in terms of magmatic processes by stating that the early crystallization of calcic plagioclase simply impoverishes the residual melt in total plagioclase.

As shown by Fig. 9, biotite content and percentage anorthite in plagioclase are closely related. The correlation is expected in view of the fact that high biotite and high anorthite content are both indicative of comparatively mafic rocks. The relationship between the amounts of biotite and total plagioclase is

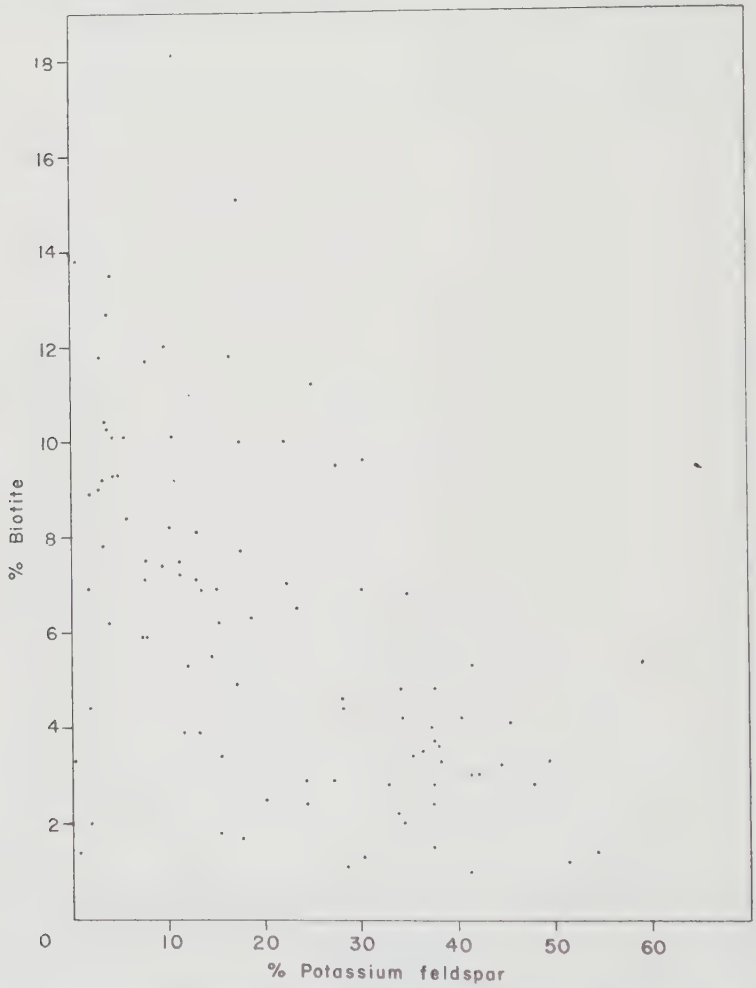

Fig. 6. Relationship between modal abundances of potassium feldspar and biotite in granitic rocks. Correlation coefficient is −0·560.

less certain (Fig. 10), though the correlation coefficient tests as significant at a high confidence level.

Relationship between modal composition and texture

Average modal compositions have been calculated for groups of granitic rocks characterized by different types of textures. In some cases, placing of individual rocks in some of the groups is quite difficult. For example, one of the comparisons made is between rocks characterized by zoned plagioclase and those characterized

by unzoned plagioclase. Many rocks, of course, contain both types of plagioclase, and such rocks were placed in one or the other groups on the basis of which type appeared must abundant. In some rocks (about 25), zoned and unzoned plagioclase appeared to be present in such equal amounts that no decision could

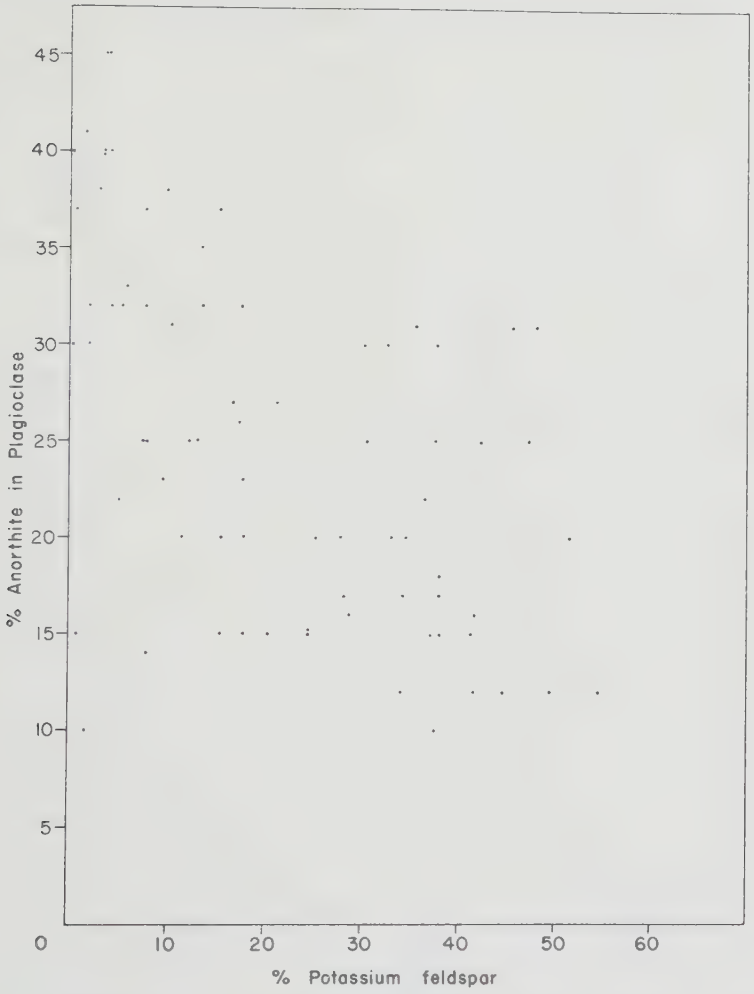

Fig. 7. Relationship between modal abundance of potassium feldspar and percentage anorthite in plagioclase in granitic rocks. Correlation coefficient is −0·636.

be made, and those rocks were omitted from the calculations. Similar considerations affect the other textural subdivisions attempted. Table 1 shows the average modal compositions of the different textural groups.

Rocks characterized by subhedral plagioclase generally contain less potassium feldspar, more plagioclase, and slightly more biotite and hornblende than rocks characterized by anhedral plagioclase. In keeping with the previously mentioned observations on the uniform amounts of quartz in granitic rocks containing different modal amounts of feldspars and other minerals, the abundance of quartz

is roughly the same in rocks containing subhedral plagioclase as in rocks containing anhedral plagioclase. The percentage of anorthite in plagioclase is relatively high in rocks characterized by subhedral plagioclase.

Rocks characterized by zoned or unzoned plagioclase show the same

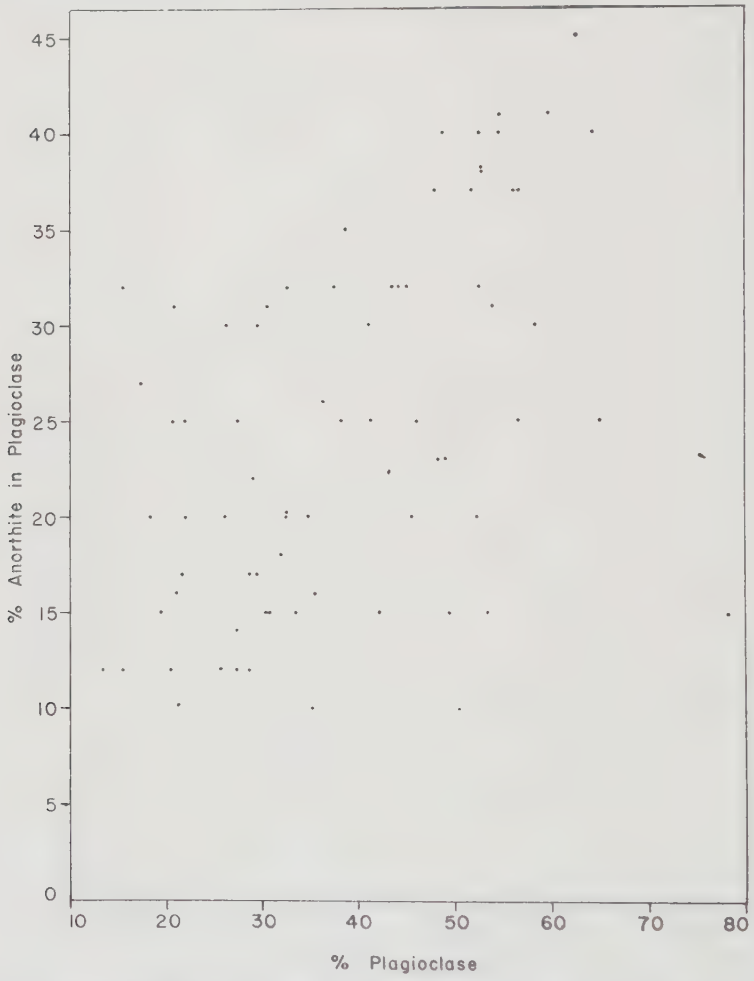

Fig. 8. Relationship between modal abundance of plagioclase and percentage anorthite in plagioclase in granitic rocks. Correlation coefficient is 0·555.

distinctions observed between rocks typified by subhedral or anhedral plagioclase. Compared to rocks with unzoned plagioclase, rocks with zoned plagioclase contain more plagioclase, a higher percentage anorthite in plagioclase, more biotite and hornblende and less potassium feldspar. In general, subhedral plagioclase grains are zoned and commonly untwinned, whereas anhedral grains are unzoned and well twinned. All of the relationships can be easily explained by considering zoned subhedral grains to be early crystallization products of a magma; they would, then, be logically most abundant in comparatively basic rocks containing

a high percentage plagioclase and biotite and a small amount of potassium feldspar. The comparatively high average anorthite content of zoned grains also indicates early crystallization.

In granitic rocks quartz occurs in two textural types: (1) in aggregates of

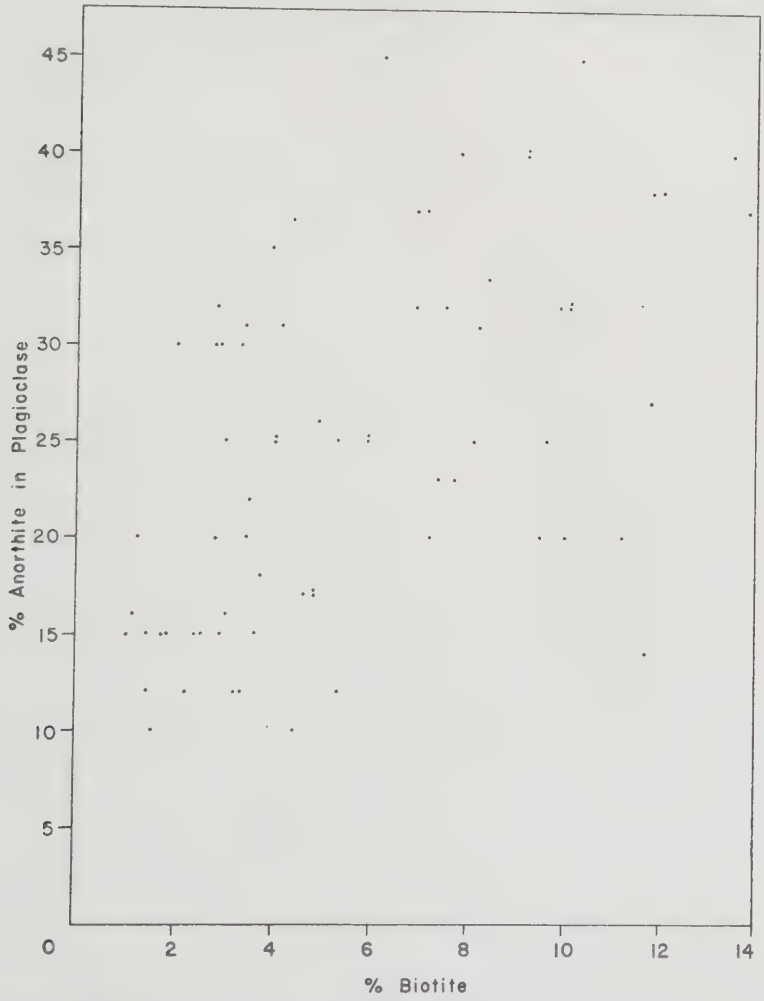

Fig. 9. Relationship between modal abundance of biotite and percentage anorthite in plagioclase in granitic rocks. Correlation coefficient is 0·671.

undulant, sutured, relatively large grains; and (2) as individual small grains, generally non-undulant, interstitial to plagioclase and, in some cases, to potassium feldspar. Rocks containing aggregate quartz have generally more potassium feldspar and less plagioclase than those containing individual quartz. The aggregates of quartz can be explained on the basis that quartz begins to crystallize relatively early during the solidification of a granitic magma. Calcic plagioclase finishes crystallization before quartz and is, consequently, subhedral against quartz. In relatively silicic magmas, however, comparatively early

crystallization of quartz results in aggregation of quartz grains prior to crystallization of potassium feldspar and sodic plagioclase. Early nucleation of quartz in such melts explains the presence of quartz phenocrysts in rhyolitic and dacitic lavas.

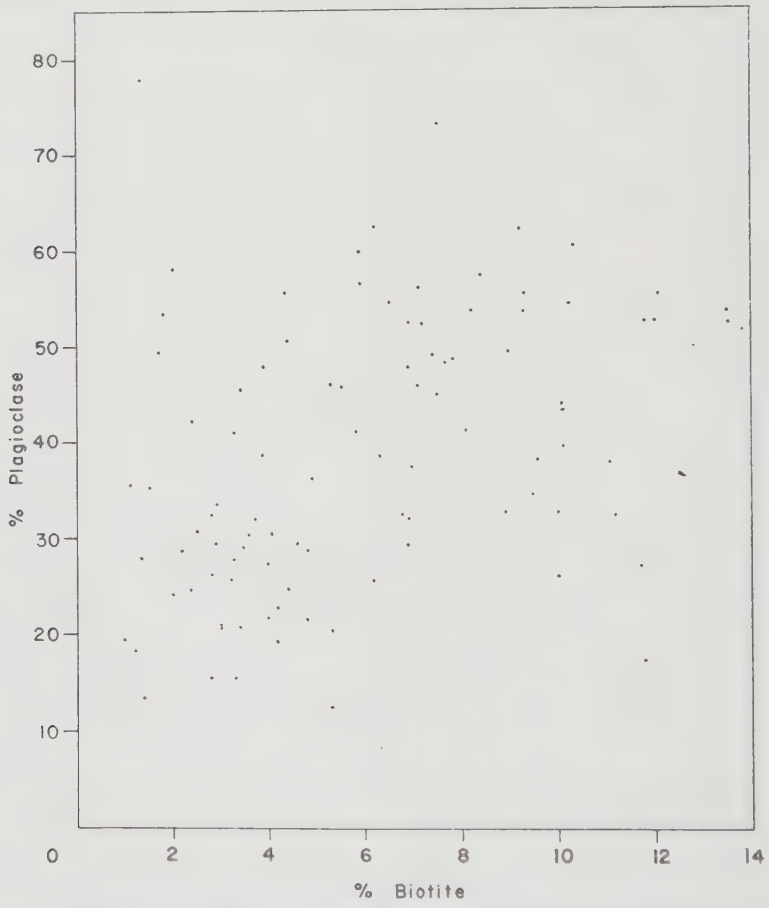

Fig. 10. Relationship between modal abundances of biotite and plagioclase in granitic rocks. Correlation coefficient is 0·364.

Some granites are characterized by euhedral crystals of potassium feldspar much larger than the other minerals in the rock. As shown by Table 1, these rocks contain a higher percentage of potassium feldspar, and consequently less plagioclase, than more equigranular granites.

Average grain sizes of granitic rocks have been sub-divided into coarse, medium and fine, the divisions being made at 1 and 5 mm. Porphyritic or markedly inequigranular rocks are omitted from the averages shown in Table 1. The major variation with grain size is the greater abundance of potassium feldspar in the coarser grained rocks. The reason for this relationship is simply that potassium feldspar grains tend to be larger than other minerals in granitic rocks; (this fact has previously been noted by Feniak, 1944). The large size of the grains

may be explained by the tendency of a growing potassium feldspar crystal to prevent nucleation of other feldspar grains in its neighbourhood (Rogers and Bogy, 1958).

Table 1. Average compositions (in volume percentage) of various textural groups of granitic rocks

Textural groups‡	Minerals*				
	Quartz	Potassium feldspar	Plagioclase†	Biotite	Hornblende
Subhedral plagioclase (45)	29·6	13·8	$45{\cdot}5_{30}$	7·5	2·9
Anhedral plagioclase (31)	33·8	28·5	$29{\cdot}9_{17}$	4·7	0·5
Zoned plagioclase (47)	29·4	12·5	$46{\cdot}8_{30}$	7·7	3·0
Unzoned plagioclase (28)	33·9	31·0	$28{\cdot}5_{19}$	4·1	0
Aggregate quartz (24)	33·6	30·4	$29{\cdot}1_{20}$	3·2	0·6
Individual quartz (32)	31·9	18·7	$39{\cdot}0_{25}$	6·7	1·8
Coarse, euhedral potassium feldspar (14)	29·9	33·9	$28{\cdot}4_{23}$	5·0	0·3
Anhedral potassium feldspar (61)	31·5	17·1	$41{\cdot}1_{26}$	6·7	2·3
Coarse grained (17)	28·6	34·7	$30{\cdot}3_{21}$	4·8	0·8
Medium grained (59)	30·3	18·5	$39{\cdot}9_{27}$	6·5	2·2
Fine grained (4)	36·9	8·8	$43{\cdot}4_{24}$	5·1	0·5

* Accessory minerals and alteration products are not listed.
† Percentage anorthite shown as subscript.
‡ Number of rocks in each group shown in parenthesis.

Idealized textures and compositions of granitic rocks

On the basis of the textural groups described in the previous section, granitic rocks can be subdivided into two idealized textural and compositional types:

(1) Rocks consisting of approximately 30 per cent quartz, 15 per cent potassium feldspar, 45 per cent plagioclase, (An_{30}), 5–10 per cent biotite, 2–3 per cent hornblende and minor amounts of accessory minerals. These rocks contain zoned, poorly twinned, subhedral plagioclase, fine grained anhedral potassium

feldspar and interstitial quartz. They show every evidence of early magmatic crystallization of plagioclase followed by quartz and potassium feldspar.

(2) Rocks consisting of approximately 30 per cent quartz, 30 per cent potassium feldspar, 30 per cent plagioclase (An_{20}), 5 per cent biotite and minor accessory minerals. These rocks contain unzoned, well twinned, anhedral plagioclase and aggregates of undulant, sutured quartz. The potassium feldspar ranges from fine grained and anhedral to coarse grained and subhedral.

Relatively few rocks would fall precisely in either category. Petrographically there seems to be a complete gradation between the two ideal "end members".

The first texture (no. 1, above) is closely approximated by some samples of the Southern California batholith (particularly from the more mafic members), and the second texture (no. 2, above) is characteristic of a number of plutons in the Front Range of Colorado. No consistent structural differences have been noticed between the two rock types.

Conclusions

The two different ideal granites described in the previous section might be attributed to two different processes of formation. The type of granite characterized by subhedral zoned plagioclase and interstitial quartz and potassium feldspar has the "typical granitic" texture which has been attributed to crystallization from a fluid magma. Conversely, equigranular rocks in which most of the minerals are anhedral and the plagioclase is well twinned might be considered as the product of replacement and recrystallization in the solid state. The difficulty in accepting two widely different modes of origin for the different types is the complete gradation found in nature between the "end members". For this reason, it seems more logical to propose that one general process is involved in the major petrogenic evolution of granitic rocks. In this connexion, it is important to note that the distinction between solid and fluid is very difficult to establish at great depths, where the high pressures make the fluids viscous, and the high pressures and temperatures make the solids plastic.

If it is assumed that the majority of igneous rocks have formed by one process, it is then necessary to hypothesize the nature of that process. For two principal reasons it is proposed that magmatic differentiation accounts for the evolution of most granitic rocks:

(1) The distinct negative correlation between potassium feldspar and plagioclase, biotite and percentage anorthite in plagioclase. These relationships can be readily explained by early magmatic crystallization of calcic plagioclase and ferromagnesian minerals and consequent enrichment of the magma in the potassium feldspar constituent. The negative correlation between potassium feldspar and plagioclase and biotite could also be explained by metasomatic replacement of the two minerals by potassium feldspar. Such a replacement however, would be expected to develop also a negative correlation, which is not found, between potassium feldspar and quartz, unless selective replacement of plagioclase and biotite were assumed. Furthermore, the relationships among plagioclase, biotite and percentage anorthite in plagioclase would seem highly fortuitous if the majority of granitic rocks had formed by replacement or

recrystallization of different types of pre-existing rocks. All of the mineral correlations are readily explained by fractional crystallization of a magma, and thus it seems logical to assume that the process is of primary significance.

(2) A second argument in favour of a magmatic origin for most granitic rocks is the distinct evidence of non-equilibrium and sequential crystallization in rocks containing zoned plagioclase and interstitial quartz and potassium feldspar. Zoning and abundance of myrmekite and albitic rims on plagioclase laths indicates that equilibrium was not established during the process of formation of the rocks. As shown by the mineralogy and texture of undoubted metamorphic rocks, solid-state replacement and recrystallization probably more closely approaches an equilibrium process than solidification of a fluid. On this basis, some of the equigranular granites containing unzoned, anhedral plagioclase may have formed by replacement and recrystallization, but the complete gradation from this type of granite into granites containing definite non-equilibrium mineral assemblages prevents any definite conclusions in favour of granitization.

Granitic rocks from a number of different areas and different rock units have been analysed to give the excellent mineralogical correlation shown in Fig. 5 and the fair correlations shown in Figs. 6–10. The fact that such unrelated samples yield such close correlations indicates that the differentiation process in different areas operates on relatively homogeneous original materials. For this reason, it may be proposed that the primary material for granitic magmas is comparatively uniform over areas as broad as the entire United States. Whether this primary material consists of remobilized sediments, subcrustal differentiates or other substances is not certain.

References

Feniak M. W. (1944) Grain sizes and shapes of various minerals in igneous rocks. *Amer. Min.* **29,** 415–421.

Larsen E. S. (1948) Batholith and associated rocks of Corona, Elsinore and San Luis Rey quadrangles, Southern California. *Mem. Geol. Soc. Amer.* **29**.

Rogers J. J. W. and Bogy D. B. (1958) A study of grain contacts in granitic rocks. *Science* **127,** 470–471.

Sargent H. C. (1925) Notes on the petrology of the Penmaemmawr Mountain—I; The acid segregations and veins—II. *Proc. Liverpool Geol. Soc.* **14,** 83–98, 123–142.

Simpson E. S. W. (1954) On the graphical representation of differentiation trends in igneous rocks. *Geol. Mag.* **91,** 238–244.

Whitfield J. M., Rogers J. J. W. and Adams J. A. S. (1959) The relationship between the petrology and the thorium and uranium contents of some granitic rocks. This volume p. 248.

Geochimica et Cosmochimica Acta, 1959, Vol. 17, pp. 286 to 304. Pergamon Press Ltd. Printed in Northern Ireland

Distribution of Ca, Sr and Ba in southern Norwegian pre-Cambrian alkali feldspars

K. S. Heier* and S. R. Taylor†

(*Received* 10 *April* 1959)

Abstract—Ca, Sr and Ba have been determined spectrochemically in alkali feldspars from gneisses, augengneisses, anatexe granites, diapire granites and small and large pegmatites from the pre-Cambrian basement rocks of southern Norway. Ca decreases in feldspars from large pegmatites, but not to the same extent as Sr and Ba. It is shown that Sr readily substitutes in K-feldspar. A close association of Ba and Sr was found. With increasing fractionation the Ba/Sr ratio decreases and is lowest in the large pegmatites, as are the absolute amounts of Sr and Ba. The behaviour of Ca, Sr and Ba is explained mainly by the relative bond strengths; Ba which forms the bond with most ionic character is preferentially accepted.

1. Introduction

This is the third of a series of papers on the trace element composition of alkali feldspars from augengneisses, gneisses, anatexe and post-orogenic granites, and small and large pegmatites from the pre-Cambrian basement complex of southern Norway. In previous papers (Taylor and Heier, 1958a; Heier and Taylor, 1959) data for Li, Na, K, Rb, Cs, Pb and Tl were given. In this paper we discuss the distribution and geochemistry of Ca, Sr and Ba. The geological and petrological conclusions will be given in a separate paper. The sample numbers and localities are the same as in our previous paper (Heier and Taylor, 1959, Table 7, Fig. 1.). In a few cases (samples 11, 15, 16) no more material was available for analysis.

2. Previous Work

An investigation of the geochemistry of strontium was carried out in Goldschmidt's laboratory at Göttingen by Noll (1934). Working in the same laboratory, von Engelhardt (1936) studied the geochemistry of barium. These two papers form the basis of modern geochemical thought concerning these two elements and are adequately summarized by Goldschmidt (1954) and Rankama and Sahama (1950). Hevesy and Würstlin (1934) published some strontium determinations in silicates, obtained using X-ray fluorescence methods of analysis. At an earlier date, Eskola (1922) synthesized artificial Sr and Ba feldspars.

Two useful papers by Bray (1942) and Shimer (1943) report determinations of Sr and Ba (and several other elements) in potash feldspars and other minerals and rocks, in particular from granites and associated feldspars. Turekian and Kulp (1956) studied the geochemistry of strontium with reference to its distribution in granites, basalts, shales and limestones. Rogers (1958) has determined Sr and Ba in potassium feldspar from a quartz monzonite and showed that the two elements were most abundant in the early fractions. Oftedal (1958a) has published semiquantitative determinations of Sr and Ba in the eruptive rocks of the Oslo region and also has used Sr and Ba data in a discussion

* Mineralogisk-Geologisk Museum, Oslo, Norway
† Department of Geology, University of Cape Town, South Africa.

of the origin of granite pegmatite in gneiss areas (Oftedal, 1958b). Gerasimovsky and Lebedov (1958) discuss the Sr/Ca ratio in rocks of the Lovosero massif.

3. Analytical Procedure

A d.c. arc spectrochemical technique was used. A preliminary procedure for the determination of Ca, Sr and Ba in alkali feldspars was given previously (Heier and Taylor, 1959). Since these three elements are much more involatile in a d.c. arc than the other elements determined previously (alkali elements, Pb and Tl) a separate analytical procedure is necessary. Commonly one of these elements serves as an internal standard for the other two. In our case the three alkaline earth elements were sought in one operation and palladium was selected as internal standard since it has proved suitable in general analytical schemes for the determination of these elements, and several others in igneous rocks (Ahrens, 1954). Selective distillation, which is such a useful feature in the determination of the volatile elements, must be suppressed and, in addition, a uniform arc temperature becomes critical since the only usable barium lines are ion lines. Since no suitable Pd ion lines are available, an atom–ion pair has been used to determine Ba. Although this runs contrary to theoretical principles and much practical spectrochemical experience, satisfactory precision was nevertheless attained. Bray (1942) also used Pd as an internal standard and employed the atom–ion pair Ba^{II} 4554/Pd^{I} 3481 to determine Ba in potash feldspars. The detailed working conditions are as follows:

Samples (—120 mesh bolting cloth) were mixed with 5 parts by weight of a carbon–palladium mix, which contained 10% $(NH_3)_4Pd(NO_3)_2$. Johnson–Matthey JM9 carbon powder was used. After stirring by hand, the mixture was ground for 15 min on a mechanical mortar.

Electrodes. The lower electrode (anode) was cut from National Carbon Co. Regular grade $\frac{3}{16}$ in. Inner diameter of cup 2·4 mm; depth 2·5 mm. Upper electrode was pointed Champion "Ship" carbon 5 mm diameter. Samples were burnt to completion at 6·8 A d.c. The arcing time varied from 60 to 80 sec.

Spectrograph. Hilger large quartz and glass; glass prism; wavelength range 3800–5300 Å; slit 10 μ; seven step sector (2 : 1 ratio). Wedge 11; Hilger F.958 quartz lens focused on diaphragm, Hilger F.1025 quartz lens focused on collimating lens of spectrograph. Ilford ordinary (N.30) plates, developed for 5 min in Kodak D.19.b developer at 18°C.

The following lines were read: Ca 4425·44; 4435·96; 4454·78. Sr 4607. Ba^{II} 4934. The internal standard line was Pd 4473. In basic rosks, such as W–I, Fe 4454·38 interferes with Ca 4454·78, but the line is usable in granite rocks or feldspars.

Standards. G–I and W–I were used as primary standards with the following values:

	Ca (%)	Ba (p.p.m.)	Sr (p.p.m.)
G–I	1·0	1300	240
W–I	7·9	220	180

The working curve for barium is shown in Fig. 1. Precision, expressed as relative deviation, is 8 per cent for Ba.

4. Analytical Data

The concentrations of Ca, Sr and Ba are given in Table 1. In Table 2, the data are recalculated as ideal feldspar formulae, with summations also given. Of the samples analysed 25 per cent fell within ± 1 per cent of 100 per cent, and 48 per cent fell within ± 2 per cent and 68 per cent within ± 3 per cent. Although

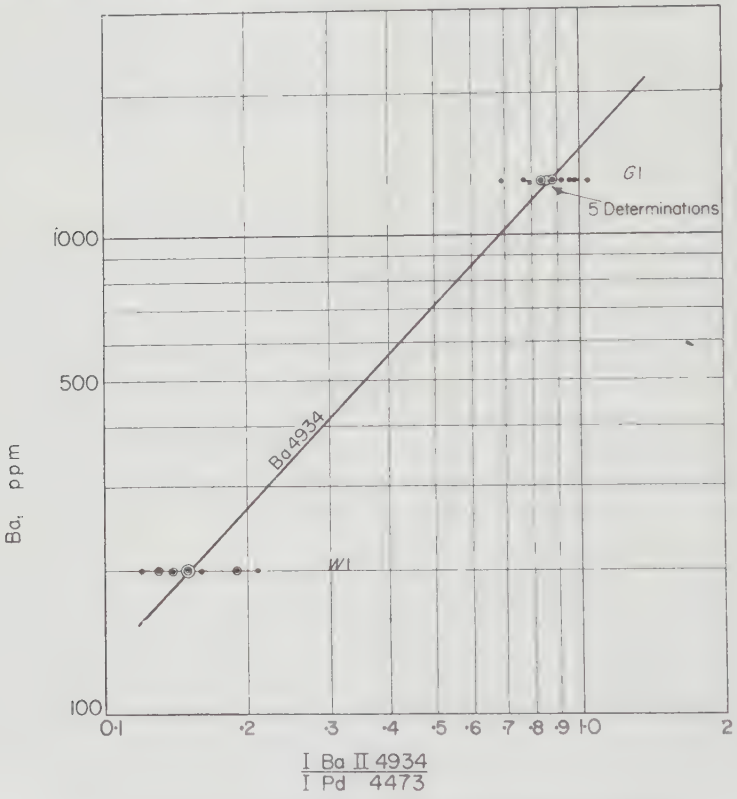

Fig. 1. Working curve for the determination of barium.

several different analytical techniques were employed (Na and K were determined by flame photometer, Li, Rb and Cs; Pb and Tl; and Ca, Sr and Ba by three different spectrochemical techniques) these summations are satisfactory. It should be recalled that an error of 0·1 per cent in the potassium determination makes an error of 0·7 per cent Or; an error of 0·1 per cent in determining Na makes an error of 1·1 per cent Ab and an error of 0·1 per cent in the Ca determination makes an error of 0·7 per cent An in the summation. Some of the samples whose summations total less than 100 per cent (1, 2, 4, 32, 43) are contaminated with quartz.

Although it has become customary to refer to the feldspars in terms of the three components Or, Ab and An we must consider the effect of the other

Table 1. Analytical results for Ca, Sr and Ba

Sample no.	*Rock type*	Ca (%)	Ba (p.p.m.)	Sr (p.p.m.)	Ba/Sr
	A. Bamble formation				
1	Sillimanite granite	0·22	1600	150	10·7
2	Arendalite	2·20	3000	337	8·9
3	Arendalite	1·10	1300	180	7·2
4	Arendalite	1·40	2500	150	16·7
5	Gneiss	0·65	3400	235	14·5
	B. Telemark formation				
6	Tinngranite	0·60	2500	170	14·7
7	Telemark granite	1·00	3500	445	7·9
8	Anatexe granite	0·30	4150	590	7·0
9	Oddersjå (Anatexe granite)	0·40	4750	420	11·3
10	Oddersjå (Anatexe granite)	0·80	5700	570	10·0
12	Oddersjå (Anatexe granite)	0·50	6300	650	9·7
13	Holum granite	0·40	9500	980	9·7
14	Holum granite	0·60	6900	725	9·5
17	Gneiss	0·35	6500	300	21·7
18	Augen gneiss	0·90	7000	770	9·1
19	Augen gneiss	1·10	~5000	820	6·1
20	Augen gneiss	0·90	3850	750	5·1
21	Augen gneiss	1·00	6800	1000	6·8
22	Augen gneiss	0·55	3000	270	11·1
23	Gneiss	0·40	1750	320	5·5
24	Gneiss	0·20	3700	285	13·0
25	Granitic gneiss	0·40	3750	260	14·4
	C. Herefoss (diapire) granite				
26	Granite	0·25	4100	345	11·9
27	Fine grained granite	1·05	3500	400	8·8
28	Coarse granite	0·35	1700	275	6·2
29	Coarse granite	0·35	7500	670	11·2
30	Coarse granite	0·25	6600	600	11·0
31	Coarse granite	0·40	7200	690	10·4
32	Coarse granite	0·40	2100	~210	10·0
33	Granite	0·75	3400	510	6·7
34	Fine grained granite	0·35	2000	270	7·4
35	Granite	0·25	1000	170	5·9
	D. Fevig (diapire) granite				
36	Granite	0·70	3200	620	5·2
37	Granite	0·85	3700	640	5·8
38	Granite	~0·60	3400	500	6·8
39	Granite	~0·85	3600	640	5·6
40	Granite	~0·35	2000	375	5·3
41	Granite	~0·65	3250	~600	5·4
42	Granite	~0·40	3300	570	5·8
43	Red granite vein in gneiss	~0·70	3700	345	10·7
	E. Farsundite				
44	Granite	~0·55	4000	370	10·8

Table 1 (*continued*)

Sample no.	Rock type	Ca (%)	Ba (p.p.m.)	Sr (p.p.m.)	Ba/Sr
	F. Small pegmatites				
45	Vein in gneiss	~0·30	3400	370	9·2
46	Vein in augengneiss	1·20	2000	275	7·3
47	Vein in augengneiss	~0·30	540	150	3·6
48	Vein in Oddersjå granite	~0·30	3000	350	8·6
49	Vein in gneiss	~0·45	1950	190	10·3
	G. Large pegmatites				
	Name				
50	Kalstad, Kragerö	~0·60	300	55	5·5
51	Kalstad, Kragerö	~0·40	180	35	5·1
52	Lindvikskollen, Kragerö	~0·50	810	100	8·1
53	Lindvikskollen, Kragerö	~0·30	640	80	8·0
54	Tangen, Kragerö	~0·25	85	35	2·4
55	Tangen, Kragerö	~0·40	50	20	2·5
56	Gloserhei, Arendal	~0·60	1700	120	14·2
57	Gloserhei, Arendal	~0·40	1425	75	19·0
58	Gloserhei, Arendal	~0·50	1475	115	12·8
59	Hinnebu, Aust–Agder	~0·40	655	140	4·7
60	Hinnebu, Aust–Agder	~0·40	500	90	5·6
61	Lauvrak, Aust–Agder	~0·40	420	100	4·2
62	Lauvrak, Aust–Agder	~0·35	350	100	3·5
63	Öygardstj., Aust–Agder	~0·45	500	220	2·3
64	Herefoss	~0·25	280	55	5·1
65	Herefoss	~0·18	110	32	3·4
66	Begervann	~0·30	750	150	5·0
67	Åmli	~0·40	1200	200	6·0
68	Stie	~0·20	73	55	1·3
69	Stie (Amazonite)	~0·20	50	45	1·1
70	Krossöl	~0·40	800	215	3·7
71	Valbeland	0·50	1650	310	5·3
72	Eretveit, Iveland	0·40	790	140	5·6
73	Eretveit, Iveland	0·30	450	155	2·9
74	Tuftan, Iveland	0·23	115	80	1·4
75	Tuftan, Iveland	0·35	170	140	1·2
76	Mannekleiv, Iveland	0·50	1600	260	6·2
77	Heia, Iveland	0·30	70	26	2·7
78	Knutten, Iveland	0·30	50	40	1·3
79	Uranium Mine, Evje	0·40	380	190	2·0
80	Uranium Mine, Evje	0·40	425	120	3·5
81	Flåt, Evje	0·40	160	40	4·0
82	Flåt, (Amazonite), Evje	0·20	210	180	1·2
83	Ås, Evje	~0·35	830	~350	2·4
84	Varoddbrua, Kristiansand	~0·35	120	45	2·7
85	Varoddbrua, Kristiansand	~0·30	400	65	6·2
86	Römteland 1	0·30	1000	135	7·4
87	Römteland 2	0·30	130	50	2·6
88	Römteland 3	0·35	190	70	2·7

Table 2. Total calculated feldspar compositions (weight per cent); analytical data for the alkali elements. Pb and Tl are given in HEIER and TAYLOR (in press)

Sample no.	K	Na	Ca	Ba	Sr	Rb	Cs	Pb	Tl	Sum
					A. Bamble formation					
1	87·36	4·45	1·53	0·44	0·06	0·11				93·95
2	38·23	33·63	15·27	0·82	0·13	0·03				88.11
3	41·08	48·79	7·63	0·35	0·07	0·04				97·96
4	41·94	37·28	9·71	0·68	0·06	0·02				89·69
5	53·47	40·12	4·51	0·93	0·09	0·07				99·19
					B. Telemark formation					
6	75·04	20·18	4·16	0·68	0·06	0·19				100·31
7	68·00	21·55	6·94	0·96	0·17	0·09				97·71
8	82·52	12·88	2·08	1·13	0·22	0·29	0·01			99·13
9	86·51	11·17	2·78	1·30	0·16	0·33				102·25
10	84·02	10·37	5·55	1·56	0·21	0·28				101·99
12	88·15	9·35	3·47	1·72	0·24	0·35				103·28
13	79·82	16·07	2·78	2·59	0·36	0·22				101·84
14	76·90	17·78	4·16	1·88	0·27	0·20				101·19
17	87·22	10·14	2·43	1·77	0·11	0·26				101·93
18	68·71	20·52	6·25	1·91	0·29	0·13				97·81
19	69·20	24·40	7·63	1·37	0·31	0·12		0·01		103·03
20	63·01	30·10	6·25	1·05	0·28	0·17				100·86
21	66·43	24·62	6·94	1·86	0·37	0·06				100·28
22	70·68	21·75	3·82	0·82	0·10	0·09				97·26
23	88·93	9·80	2·78	0·48	0·12	0·21				102·32
24	89·00	11·86	1·38	1·01	0·11	0·19				103·55
25	89·85	7·64	2·78	1·02	0·10	0·22				101·61
					C. Herefoss (diapire) granite					
26	87·00	10·60	1·74	1·12	0·13	0·15				100·74
27	74·69	19·27	7·29	0·96	0·15	0·13				102·49
28	83·23	14·48	2·43	0·46	0·10	0·17				100·87
29	79·25	16·76	2·43	2·05	0·25	0·12				100·86
30	79·46	17·90	1·74	1·80	0·22	0·11				101·23
31	77·50	19·73	2·78	1·97	0·26	0·11				102·35
32	69·99	20·18	2·78	0·57	0·08	0·17				93·77
33	67·43	27·36	5·20	0·93	0·19	0·15				101·26
34	91·01	9·94	2·43	0·55	0·10	0·13				104·16
35	90·85	10·37	1·74	0·27	0·06	0·16				103·45
					D. Fevig (diapire) granite					
36	58·74	33·29	4·85	0·87	0·23	0·08				98·06
37	56·39	35·91	5·89	1·01	0·24	0·07				99·51
38	62·09	32·15	4·16	0·93	0·19	0·07				99·59
39	62·30	30·21	5·89	0·98	0·24	0·13				99·75
40	64·72	29·64	2·43	0·55	0·14	0·14				97·62
41	62·51	29·98	4·51	0·89	0·22	0·11				98·22
42	60·88	31·81	2·78	0·90	0·21	0·08		0·01		96·66
43	53·83	35·68	4·85	1·01	0·13	0·11		<0·01		95·61
					E. Farsundite					
44	77·89	19·84	3·82	1·09	0·14	0·42				103·20

Table 2 (*continued*)

Sample no.	K	Na	Ca	Ba	Sr	Rb	Cs	Pb	Tl	Sum
					F. Small pegmatites					
45	80·24	15·62	2·08	0·93	0·14	0·11				99·12
46	74·76	13·79	8·33	0·55	0·10	0·13				97·66
47	78·04	18·47	2·08	0·15	0·06	0·16				98·96
48	77·54	21·66	2·08	0·82	0·13	0·24		<0·01		102·47
49	68·21	25·88	3·12	0·53	0·07	0·19				98·00
					G. Large pegmatites					
50	70·77	24·40	4·16	0·08	0·02	0·19				99·62
51	68·00	27·93	2·78	0·05	0·01	0·32				99·09
52	74·90	24·05	3·47	0·22	0·04	0·23				102·91
53	71·63	27·36	2·08	0·17	0·03	0·21				101·48
54	71·84	28·04	1·74	0·02	0·01	0·28				101·93
55	64·15	31·12	2·78	0·01	<0·01	0·04				98·11
56	73·34	23·48	4·16	0·46	0·04	0·04				101·52
57	75·33	21·77	2·78	0·39	0·03	0·24				100·54
58	75·83	24·05	3·47	0·40	0·04	0·30				104·09
59	78·60	17·21	2·78	0·18	0·05	0·53				99·35
60	79·67	19·15	2·77	0·14	0·03	0·53		0·01		102·30
61	81·45	15·85	2·77	0·11	0·04	0·61		0·01		100·84
62	82·95	14·71	2·43	0·10	0·04	0·76		0·01		101·00
63	79·46	20·18	3·12	0·14	0·08	0·21				103·19
64	81·10	17·10	1·74	0·08	0·02	0·26		0·01		100·30
65	77·18	24·51	1·25	0·03	0·01	0·29				101·90
66	93·06	6·87	2·08	0·20	0·06	0·27				101·16
67	80·38	17·21	2·77	0·33	0·07	0·26				101·02
68	78·82	22·12	1·39	0·02	0·02	0·31				102·68
69	77·39	24·40	1·39	0·01	0·02	0·51	0·01	0·01	0·01	101·35
70	82·73	21·77	2·77	0·22	0·08	0·21				102·45
71	73·41	27·93	3·47	0·45	0·12	0·18				103·21
72	76·90	19·61	2·78	0·21	0·05	0·30		0·01		99·86
73	76·75	21·66	2·08	0·12	0·06	0·24		0·01		100·92
74	74·19	25·30	1·60	0·03	0·03	0·47		0·02		101·64
75	75·90	23·60	2·43	0·05	0·05	0·44		0·02		102·49
76	82·16	13·00	3·47	0·44	0·10	0·29		0·01		99·47
77	70·92	29·30	2·08	0·02	0·01	0·36		0·01		102·70
78	71·20	27·13	2·08	0·01	0·01	0·39	0·01	0·02	0·03	100·88
79	70·13	27·47	2·78	0·10	0·07	0·22		0·02	0·01	100·80
80	71·84	27·02	2·78	0·12	0·04	0·19		0·03		102·02
81	74·48	20·29	2·78	0·04	0·01	0·25		0·02		97·87
82	83·45	14·36	1·39	0·06	0·07	0·66	0·20	0·01	0·03	100·23
83	72·13	22·46	2·43	0·23	0·13	0·11		0·01		97·50
84	77·39	20·29	2·43	0·03	0·02	0·46	0·03		0·01	100·66
85	75·33	20·75	2·08	0·10	0·02	0·31	0·01		<0·01	98·60
86	82·24	15·50	2·08	0·27	0·05	1·29	0·03	0·02	0·01	101·49
87	75·47	26·45	2·08	0·04	0·02	0·87	0·01	0·02	0·01	104·97
88	75·47	24·62	2·43	0·05	0·03	0·53		0·01		103·14

components as well. $BaAl_2Si_2O_8$ is usually more than 0·5 per cent except in the large pegmatites. $RbAlSi_3O_8$ reaches a maximum of 1·29 per cent (no. 86) but is usually much less as is $SrAl_2Si_2O_8$ although it reaches 0·36 per cent (no. 13). $CsAlSi_3O_8$ is usually insignificant as are $PbAl_2Si_2O_8$ and $TlAlSi_3O_8$. Thus the only additional phase which might be considered is Ba feldspar. Now K-feldspar

may accommodate up to 15 per cent Ba replacing K without appreciable structural alteration (Bragg, 1937) so that a separate structural phase need not be considered. The other elements Rb, Cs, Sr, Pb, Tl, are accommodated in the K-feldspar lattice (see later for discussion on Sr).

The Or, Ab and An contents are plotted in Fig. 2 which is a projection of the quaternary system Or–Ab–An–H_2O at 5000 bars water vapour pressure (Yoder *et al.*, 1957). With the exception of the samples from the arendalite (2, 3, 4)* all analyses fall within the field from which an Or–Ab rich feldspar will crystallize.

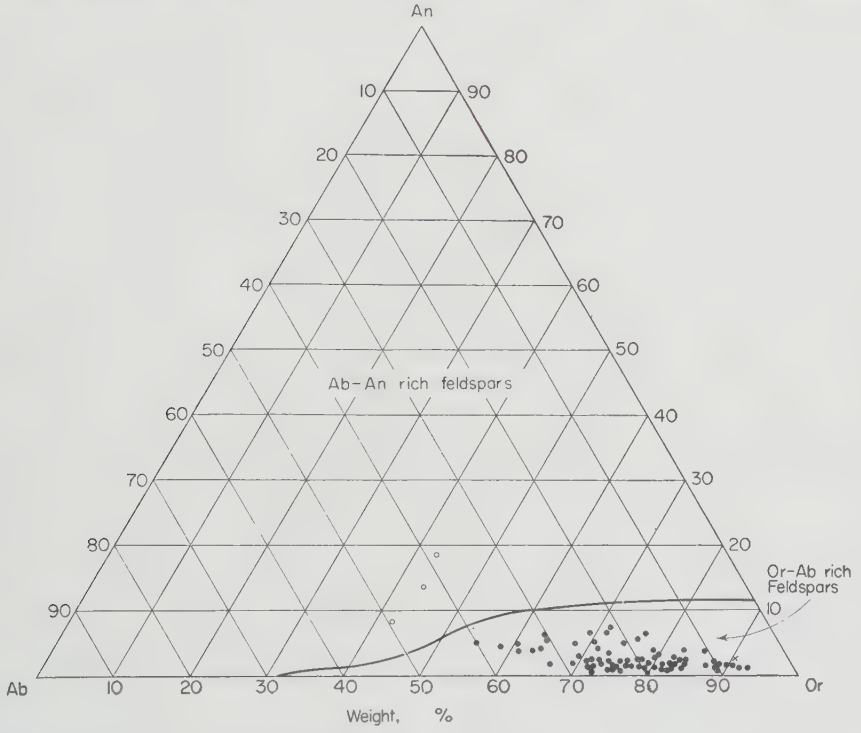

Fig. 2. Total feldspar compositions plotted on a projection of the system Or–Ab–An–H_2O at 5000 bars H_2O pressure (Yoder *et al*, 1957) Rb, Cs, Pb, Tl, Sr and Ba feldspars summed with Or.

5. Calcium Distribution

Most of the feldspars contain less than 0·6 per cent Ca, but it is possible to separate out feldspars from particular environments of formation which contain significantly greater amounts. The feldspars from the arendalite (2, 3, 4), augengneiss (18, 19, 20, 21), (but not no. 22) and an associated small pegmatite (46) contain more than 0·90 per cent Ca. The Fevig granite feldspars tend to be rather high (average 0·63 per cent Ca) and contain more calcium than those from the Herefoss granite (average 0·37 per cent Ca) (excluding one high value at the Kyllandsvn contact; 27).

* The significance of the composition of the arendalite feldspars has been discussed previously (Taylor and Heier, 1958b).

In so far as a trend can be distinguished, it seems that those feldspars formed at higher metamorphic temperatures are able to accomodate more calcium as might be expected.

6. The Distribution of Strontium and Barium

The augengneiss feldspars possess the greatest amounts of Ba and Sr, with the exception of one from the breccia junction at Herefoss (22). The others range from 3850 to 7000 p.p.m. Ba and from 770 to 1000 p.p.m. Sr, and form a distinct group in Fig. 3. The anatexe granite feldspars also form a group in the same vicinity in the

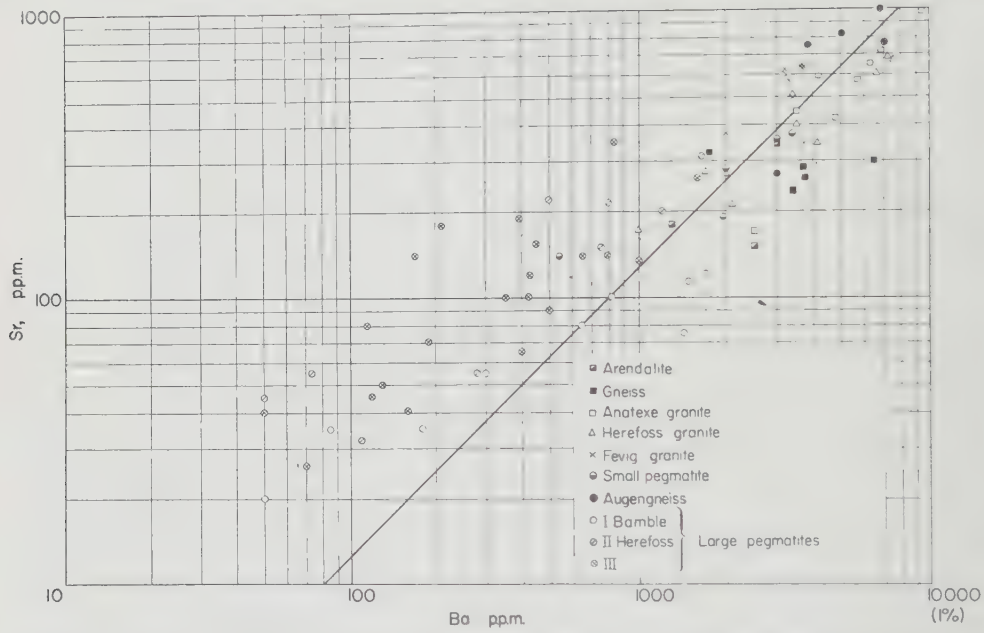

Fig. 3. Barium–strontium relationship for all samples. The close association of Sr and Ba is clear.

figure and are also high in both Ba and Sr ranging from 3500 to 9500 p.p.m. Ba and from 420 to 980 p.p.m. Sr. Six of the feldspars from the Herefoss granite fall in this range and are rather distinct from the remainder. The Fevig granite feldspars form a more uniform group, containing less Ba (2000–3700 p.p.m.) than the Herefoss feldspars, but similar amounts of strontium (345–640 p.p.m.). Somewhat lower average levels are recorded in the gneisses, in which Ba ranges from 1750 to 6500 p.p.m. and Sr from 235 to 320 p.p.m. Similar amounts are found in the feldspars from the small pegmatite veins and lenses which have from 1950 to 3400 p.p.m. Ba and from 190 to 370 p.p.m. Sr except for one associated with the augengneiss (47).

Values for the Herefoss feldspars are spread widely and reflect the heterogeneous nature of the granite. The ranges are from 1000 to 7500 p.p.m. Ba and from 170 to 690 p.p.m. Sr but, as mentioned before, two groups emerge. Samples 28, 32, 34 and 35 have distinctly less Ba and Sr than the others. Of these samples, 34 and 35

come from the appendix to the granite (Heier and Taylor, 1959, Fig 10) and also show high Cs, Tl and Pb, and may be thought of as the most differentiated parts of the granite. Samples 28 and 32 also contain more Rb than the average Herefoss feldspars and would seem to represent more highly differentiated portions.

In the Fevig granite the sample in the centre (40) which contains most Rb and the lowest K/Rb ratio (Heier and Taylor, 1959) also has the lowest amounts of Ba and Sr. Similarly, the feldspar from the red granite vein in the gneiss adjacent to the granite, and which is considered to be a late off-shoot from the granite, contains similar quantities of Sr (and Rb) as the central region.

The arendalites tend to have low Ba and Sr contents (1300–3000 p.p.m. Ba; 150–370 p.p.m. Sr) in spite of being the most calcium-rich feldspars (see later).

The feldspars from large pegmatites form a distinct group in that they contain less Ba and Sr than the feldspars from the other rock types. There is, nevertheless a considerable overall spread from 50 to 1800 p.p.m. Ba and from 20 to 350 p.p.m. Sr. Furthermore, smaller groupings based mainly on locality appear within the broader picture, so that no simple explanation covers all cases. In our last paper (Heier and Taylor, 1959) we separated the large pegmatite feldspars into three groups mainly on the basis of K/Rb ratios. Those in group I (nos. 50–58) (the Kragerø and Arendal pegmatites in the Bamble formation) have high Ba/Sr ratios, containing less Sr than the other large pegmatite feldspars (except two from Tangen, 54, 55). They also are markedly deficient in lead and have normal K/Rb ratios. Perhaps here should also be included the feldspars from the pegmatite at Varoddbrua (84, 85) near Kristiansand, which is also in the Bamble formation. These feldspars have similar high Ba/Sr ratios and low amounts of lead although enriched in Rb,Cs and Tl.

Those pegmatites associated in the field with the Herefoss granite (nos. 63–71) form group II. They fall, in common with the granite, into two divisions. Five of the pegmatite feldspars (63, 66, 67, 70 and 71) have Ba and Sr contents approaching that of the more differentiated Herefoss feldspars (28, 32, 34, 35) and contain more Ba and Sr than the other large pegmatite feldspars. Their association with, and derivation from the granite seems clear. The remaining samples (64,65, 68 and 69) contain very much less Ba and Sr (and much more Cs and Pb) and are closer in composition to the feldspars from the majority of the large pegmatites in the Telemark formation (group III). They nevertheless may be derived from the Herefoss granite since our data shows that increased fractionation decreases the Ba and Sr concentrations.

The large pegmatite feldspars which formed group III of Heier and Taylor (1959) have lower Ba/Sr ratios than those of group I (arithmetic mean, a.m. = 3·5; geometric mean, g.m. = 3·1) as shown by Fig. 4. They occur largely in the Telemark formation (except for those at Hinnebu and Lauvrak, 59–62). The amazonite feldspar samples (69, 82) have the lowest Ba/Sr ratios and the tendency toward low Ba/Sr ratios seems typical of extreme processes.

7. Substitution of Sr in K-Feldspar

The theoretical dividing line between six- and eightfold co-ordination for cations surrounded by O^{2-} lies at a radius ratio (R^{+}/RO^{2-}) of 0·73. The radius

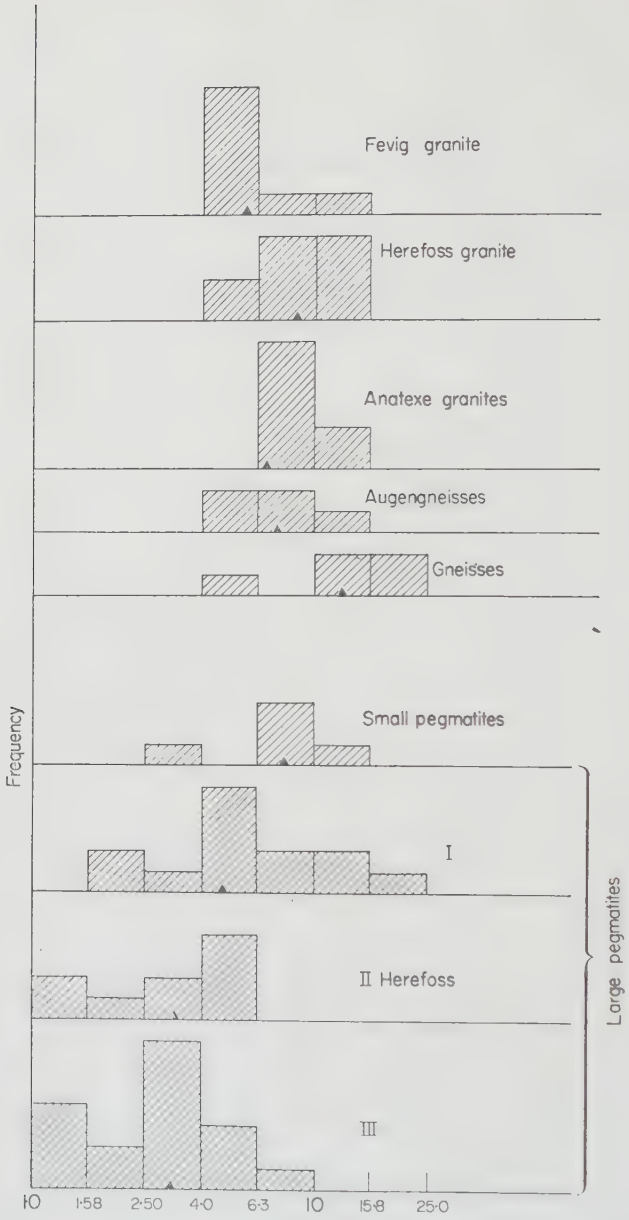

Fig. 4. Frequency plots for Ba/Sr ratios of feldspars from the different rock types. (Position of calculated geometric mean is indicated by ▲).

ratio for Ca^{2+} is 0·71. Consequently it exhibits the well-known ability to appear in either six- or eightfold co-ordination. Sr^{2+} with a radius ratio of 0·84, occurs in eightfold or greater co-ordination in ionic structures (except for SrO: see Section 10). Radius ratios of K^+ and Ba^{2+} are 0·95 and 0·96. Pb^{2+} which is commonly found in K-feldspars in amounts from 20 to 100 p.p.m. (Wedepohl, 1956; Heier and Taylor, 1959) has a radius of 1·20 Å and a radius ratio of 0·86 and is

thus very close in size to Sr^{2+}. On purely geometrical considerations, leaving aside types and strengths of bonds, lead and strontium can be accommodated in the K-feldspar lattice quite readily. Comparing the structures of the three feldspars, Or, Ab and An—in orthoclase K has six oxygens at 2·85 Å and four more at 3·1 Å (Bragg, 1937), in albite Na has seven oxygens at less than 3·1 Å (Bragg, 1937) and in anorthite Ca has eight oxygens at less than 3·1 Å (Sörum 1953) although in both minerals six of the oxygens are much closer.

Frondel (1958) has discovered that minerals of the alunite structure type are geochemical hosts for strontium, which is found in the 12 co-ordinated positions in the lattice. These minerals are formed under near surface conditions ("zone of weathering, the deeper ground water circulation and hypogene hydrothermal environments", Frondel, 1958), where other factors such as hydration of ions may be important. He also shows that Sr is incorporated in alunite type minerals in preference to coexisting calcite, apatite and anhydrite. Thus there is ample evidence that Sr can substitute in the K positions in K-feldspar.

Barium (Ba^{2+}, 1·34 Å) is almost identical in size to potassium (K^{+}, 1·33 Å) and has long been known to replace potassium in K-feldspar.

8. Calcium–Strontium Relationship

Strontium (Sr^{2+}, 1·18 Å) is often regarded as a close associate of calcium (Ca^{2+}, 1·02 Å). In the potash feldspars analysed here however, it shows a close association with barium (Ba^{2+}, 1·34 Å) (Fig. 3.) and a much weaker relation to calcium (Fig. 5.). Where a trace element can substitute for two major elements and is intermediate in size between them, a simple relationship is not to be expected. Gerasimovsky and Lebedov (1958) found that in the Lovosero massif rocks "a direct dependence between the Sr and Ca content . . . has not been established: this is accounted for by the fact that Sr isomorphously replaces not only Ca but also K" (see previous section).

Turekian and Kulp (1956, p. 209) write that "in the case of the granitic rocks Sr was found to be a function of the Ca content". This relationship is also apparent from Fig. 10, p. 277 of their paper. We have analysed the potash feldspars, one of the major mineral phases of granitic-type rocks, and find no apparent relation between the calcium and strontium contents. However, in most of the rock types from which we separated the K-feldspars, plagioclase in the oligoclase–andesine range is a major component, occurring in amounts comparable to the potash feldspar. This is probably also the case for those rocks containing more than 1% Ca in Fig. 10 of Turekian and Kulp (1956).

Goldschmidt (1954, p. 246) gives data indicating that the Ca/Sr ratio in oligoclase and orthoclase differs by a factor of about 10. He gives a Ca/Sr ratio of 140 for oligoclase and 12·5 for orthoclase (Sr/Ca ratios of 0·007 and 0·08, respectively, in the original reference). The Ca and Sr plots for the host rocks in our case could therefore be expected to lie to the right of the feldspar plots in Fig. 5.

There is thus not necessarily any disagreement between our data and that of Turekian and Kulp (1956). Heier (unpublished data) has determined Ca and Sr in coexisting K-feldspar and plagioclase from granulite and amphibolite facies gneisses from Langøy, North Norway. These data are plotted in Fig. 6 together

with results for some of their host rocks. It can be seen readily from this figure that the Ca/Sr ratio in K-feldspar is much less than the same ratio in coexisting plagioclase, confirming the data of Goldschmidt (1954). The plots for the four host rocks in Fig. 6. show the same sort of trend as Fig. 10 of Turekian and Kulp (1956) and lie within the limits of their Ca–Sr plots. (Note that we have plotted Ca as abscissa).

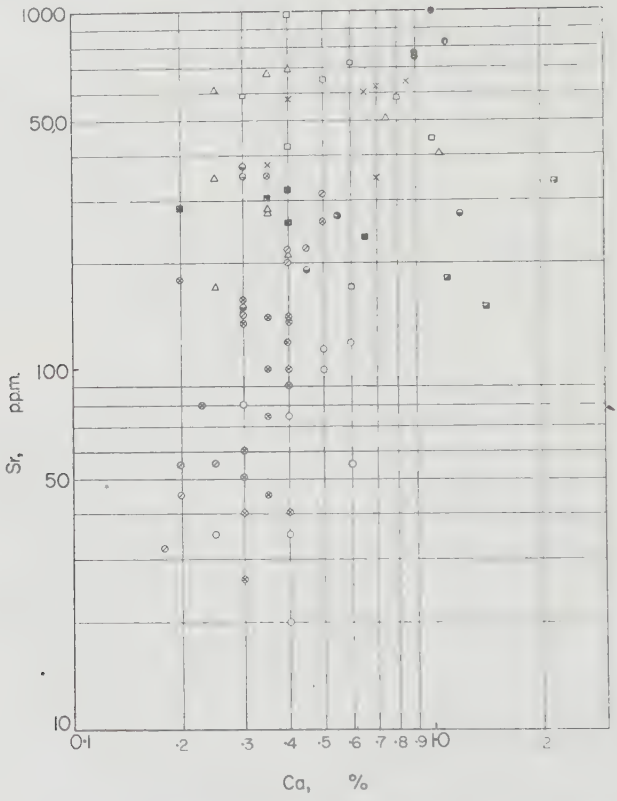

Fig. 5. Calcium–strontium relationship for all samples.

It can be seen from Fig. 10 of Turekian and Kulp (1956) that the Ca/Sr ratio increases with decreasing amounts of Ca and Sr. This is the direction of increasing fractionation in granitic rocks. Our data given in Table 1 and plotted in Fig. 5 show that there is a marked increase in the Ca/Sr ratios in the feldspars from large pegmatites.

The calcium rich "mesoperthitic" arendalite feldspars (nos. 2, 3, 4, Table 1) plot well to the right of the K-feldspars in Fig. 5. They have a Ca/Sr ratio comparable with that of normal plagioclase (see also Fig. 6 where two mesoperthites (1 and 2) from Langøy, N. Norway are plotted). Taylor and Heier (1958b), discuss at some length the origin of these mesoperthites based on the fact that they are depleted in Rb (relative to potassium). They plot in the plagioclase field of Fig. 2, and are probably crystallographically closer to the plagioclases than to the potash feldspars.

9. Relative Abundance of Barium and Strontium (Ba/Sr Ratios)

While the absolute amounts of Ba and Sr vary by large amounts, a glance at Fig. 3 shows that the Ba/Sr ratios lie within a small range, and that there is a close association between the two elements in alkali feldspars. Values for Ba/Sr are given in Table 1 and both arithmetic and geometric means for the ratios in the feldspars from the various rock types are given in Table 3. Frequency plots of

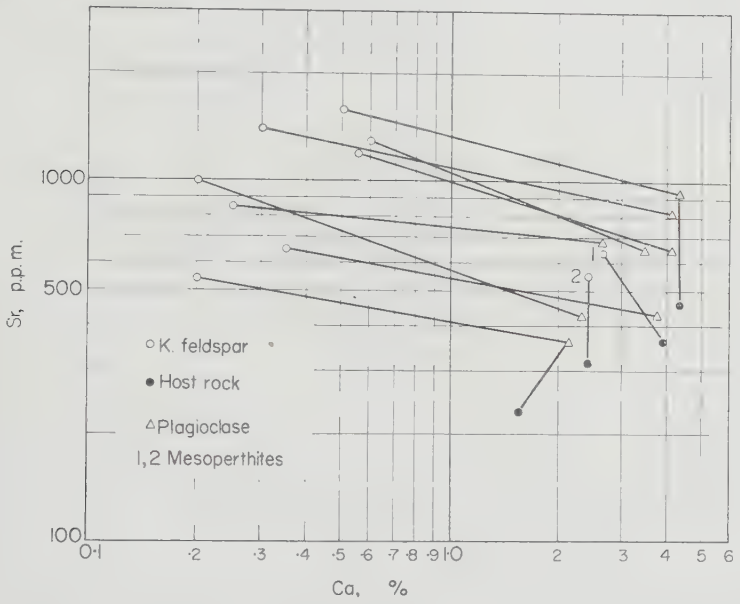

Fig. 6. Ca and Sr in some coexisting K-feldspars and plagioclases (and some host rocks) from granulite and amphibolite facies gneisses from Langøy, North Norway (Heier, unpublished data).

this data are given in Fig. 4, using a logarithmic scale. A power factor of 1·58 is used to give the interval. The arithmetic mean (a.m.) is greater than the geometric mean (g.m.) in all cases, so that positive skewness results if a linear scale is used. The distribution pattern thus evidently approaches lognormality. From Table 3 and Figs. 3 and 4, it can be seen that the Ba/Sr ratios are not constant and that the ratio decreases as the absolute concentration of the two elements falls. Bray (1942) and Shimer (1943) found that the Ba/Sr ratios were in general smaller in feldspars from pegmatites than in feldspars from the parent granites.

The ratios for the feldspars from augengneiss (g.m. 7·3), anatexe granites (g.m. 6·6) and small pegmatites (g.m. 7·8) are very similar. Higher ratios are found in the gneisses (g.m. 12·7). The Herefoss granite feldspars (g.m. 8·7) fall into two groups with (g.m. 9·8 and 7·2). The Fevig feldspars (from a much more uniform granite) have distinctly lower ratios (g.m. 5·7).

The feldspars from the large pegmatites show much variation. Those from Kragerø have comparatively high ratios (g.m. 4·7). The feldspars from Gloserhei, Arendal have very high ratios. In general, the large pegmatite feldspars from the Bamble formation have high Ba/Sr ratios (including 84 and 85, Varoddbrua) and

fall to the right of the remainder in Fig. 3. The large pegmatites associated with the Herefoss granite (group II) fall into two distinct groups, one rather close in composition to the granite feldspars and with a g.m. of 4·2. The samples (64, 65, 68, 69) have a g.m. of 2·2 much more comparable to the group III g.m. of 3·1.

10. Relative Geochemical Behaviour of Ca, Sr and Ba in K-Feldspars

We have noted that as the absolute amounts of Ca, Sr and Ba decrease, so do the ratios between these elements alter. The relative decrease in the three elements is in the order Ca < Sr < Ba so that both the Ca/Sr ratio increases and the Ba/Sr ratio decreases with increasing fractionation of the K-feldspars.

Table 3. Arithmetic and geometric means of Ba/Sr ratios

	Arenda-lite	Gneiss	Augen-gneiss	Anatexe granite	Herefoss granite	Fevig granite	Small pegma-tites	Large pegmatites		
								Group I 50–58	Group II 63–71	Group III 59–62 72–88
Arithmetic mean	10·9	14·0	7·6	9·3	9·0 10·0* 7·4†	5·7	8·3	8·6 5·3‡	3·7 4·4§ 2·4**	3·5
Geometric mean	10·2	12·7	7·3	6·6	8·7 9·8* 7·2†	5·7	7·8	6·9 4·7‡	3·2 4·2§ 2·2**	3·1

* Nos. 26, 27, 29, 30, 31, 33 Herefoss (Compare Anatexe granite).
† Nos. 28, 32, 34, 35 More differentiated Herefoss granite.
‡ Nos. 50–55.
§ Nos. 63, 66, 67, 70, 71 Closely comparable to Herefoss granite.
** Nos. 64, 65, 68, 69 Related to group III.

Bray (1942, p. 805) found that Sr increased relative to Ba in potash feldspars from pegmatites compared with those from the parent granites. He explains this as follows: "Parent-rock potash feldspars formed at higher temperatures than those in pegmatites, and therefore in the former the structures were disordered and more tolerant to substitutional ions. This accounts for decreases in both BaO and SrO in the pegmatite mineral. At higher temperatures the feldspar structure is tolerant to both Sr and Ba as substitutes for K (ionic radii : Ba 1·43 Å; K 1·33 Å; Sr 1·27 Å) but at the lower pegmatite temperatures the tolerance for the smaller Sr ion must be greater than for the larger Ba ion, a fact that explains the lower ratios for the parent-rock potash feldspars." The above explanation is based on the use of the Goldschmidt ionic radii, but is invalid if the Ahrens ionic radii are used, since in this set of radii, Ba^{2+} is almost identical in size to K^{+} and the much smaller Sr^{2+} should be preferentially excluded, leading to the reverse of what is observed. In terms of Bray's explanation it would be difficult, for example to account for the well-known enrichment of Rb^{+} in pegmatite feldspars, since this large ion (radius 1·47 Å) should not be readily accommodated at lower temperatures, and should thus be concentrated in earlier fractions. While we do not deny that temperature of formation is of great importance in controlling the admittance of ions to crystal lattices, we do not believe it to be the cause of the lower Ba/Sr

ratios in pegmatite feldspars and we prefer an explanation based on relative bond-strengths, which is discussed in detail below.

Some properties of Ca, Sr and Ba are set forth in Table 4. It can be seen by comparing either the electronegativity or ionization potential values that barium will form the most ionic bond. On the basis of the ionization potentials Ca forms the bond with most covalent character. AHRENS (1953) and RINGWOOD (1955) have commented on the weakening effect of partial covalent character, so that

Table 4. Some properties of Ca, Sr and Ba.

Valency–electrons	Ionization potential 1st	2nd	Electronegativity	Radius
Ca $4s^2$	6·11	11·87	1·0	1·01
Sr $5s^2$	5·69	10·98	1·0	1·18
Ba $6s^2$	5·21	9·95	0·9	1·34

Data from MOELLER (1952). Radii from AHRENS (1953). Strontium radius from AHRENS (unpublished data).

bond-strength should increase in the order Ca, Sr, Ba. These considerations, however, hold strictly only for ions of about the same size in compounds of the same structure type. Evidence from melting points and other physical constants of simple compounds is often used to establish relative bond strengths. The data from the oxides and fluorides given in Table 5 show a far from simple picture. The chlorides have different structures and are thus not directly comparable.

The bond strength in the oxides as derived from the physical constants in Table 5. decreases from Ca to Ba. A possible explanation for this behaviour, which runs contrary to prediction, is that the large sizes of Sr and Ba favour a high co-ordination number and that in the NaCl structure with all ions in sixfold co-ordination, the smaller cations form the most stable structures. The calculated co-ordination numbers for Ca, Sr and Ba with O^{2-} are 6, 8 and 12. Thus, structures in which Sr and Ba are surrounded by six oxygens are rather loosely packed. This is shown by the "packing index" figures* in Table 5. The more ionic character of the Ba—O bond is thus offset by the less closely packed structure. Perhaps some distortion of the oxygens occurs, since BaO has a very high refractive index compared with SrO and CaO. AHRENS (1958) should be consulted for an explanation of the use of refractive indices to indicate polarization of anions.

In the fluorides, the cations are in eightfold co-ordination, which is a more stable geometrical arrangement for the larger cations. The type of bonding in this case should exert more influence on the stability of the structure. The data given in Table 5 are somewhat conflicting, but in any event, the Sr—F bond appears weaker than the Ba—F bond, in accord with predictions based on

* The "packing index" was proposed by FAIRBAIRN (1943) to denote closeness of packing in ionic structures. It is defined as

$$\frac{\text{vol. ions in unit cell}}{\text{vol. unit cell}} \times 10.$$

We have multiplied this expression by 10 to get a figure giving percentage of unit cell occupied by ions.

ionization potential and electronegativity. The refractive indices are much closer than for oxides.

When Ca, Sr and Ba substitute in the potassium positions in K-feldspar, the co-ordination number is larger and nearer the calculated values for Sr and Ba.

Table 5. Comparative data for oxides and fluorides of Ca, Sr and Ba

Compound	Structure type	Melting point (°C)	Heat of formation (kcal)	Lattice energy (kcal)	Packing index (× 10)	Refractive indices	Co-ordination no. of cation
CaO	NaCl	2580	151·71	842	57·7	1·838	6
SrO	NaCl	2430	140·7	791	55·4	1·870	6
BaO	NaCl	1923	133·1	747	51·8	1·98	6
CaF_2	CaF_2	1360	286·26	–	63·0	1·434	8
SrF_2	CaF_2	1190*	288·89	–	55·5	1·442	8
BaF_2	CaF_2	1280	287·70	–	52·8	1·475	8

Melting point, heats of formation and refractive indices from Hodgman (1958).
Lattice energy data from Moeller (1952).
* Moeller (1952) gives 1450°C as melting point of SrF_2.

Under these conditions, bond type should exert a major influence on bond-strength, and the Ba—O bond, with most ionic character, should be strongest, and the Ca—O bond weakest.

This is indicated by the calculated values for heats of formation and melting points of $CaAl_2Si_2O_8$, $SrAl_2Si_2O_8$ and $BaAl_2Si_2O_8$ given in Table 6. It is seen from these figures that the stability increases with the atomic weight of the alkaline

Table 6. Heats of formation and melting points of $CaAl_2Si_2O_8$, $SrAl_2Si_2O_8$ and $BaAl_2Si_2O_8$

	ΔH (kcal/mol.)	M.P. (°C)
$CaAl_2Si_2O_8$	−59	1553
$SrAl_2Si_2O_8$	−78	1660
$BaAl_2Si_2O_8$	−93	1720

Values for heats of formation from Ramberg (1953) p. 345, Table 8. Melting point data from Goldsmith (1950) p. 534. The source of this data is not clear from the text of Goldsmith's paper.

earth metals. The values refer to theoretical pure feldspars (of differing structures) and cannot be directly used in our case, where the three elements substitute for potassium in the K-feldspar structure. Nevertheless, an increase of bond-strength in accordance with theory is shown. Barium, very close in size to potassium, will cause least distortion of the structure by substituting in the potassium positions. This is the reverse of the case with the oxides. Thus, in comparing ions of differing sizes, several conflicting effects operate.

In summary, as is clearly illustrated in Figs. 3 and 5, the concentration of the

three elements in potash feldspar decreases with increasing fractionation. This is in accord with the classical capture principle of GOLDSCHMIDT, the divalent alkaline earth ions entering the lattice at the expense of the univalent potassium. In a crystallization series, the sequence of entry is in the order Ba, Sr, Ca, so that Ba decreases more rapidly than Sr (so that the Ba/Sr ratio decreases with increasing fractionation) and Sr in turn enters the lattice more readily than Ca, so that the Sr/Ca ratio decreases (or, as used here, the Ca/Sr ratio increases). This is not in accord with the principle that the smaller ion is preferentially incorporated (an explanation which would hold for the oxides). It seems clear that in the K-feldspar structure, the more ionic character of the Ba—O bond leads to the preferential entry of Ba compared with Sr.

Acknowledgements—The writers wish to express their thanks to Mrs. N. GARTON for performing the spectrographic analyses and to Professors L. H. AHRENS and T. F. W. BARTH for critical reading of the manuscript and constructive suggestions.

REFERENCES

AHRENS L. H.(1953)The use of ionization potentials—I. Ionic radii of the elements. *Geochim. et Cosmochim. Acta* **2**, 155–169.

AHRENS L. H. (1954) *Spectrochemical Analysis of Silicates*. Pergamon Press, London.

AHRENS L. H. (1958) Variation of refractive index with ionization potential in some isostructural crystals. *Mineral. Mag.* **31**, 929 -936.

BRAGG W. L. (1937) *Atomic Structure of Minerals*. Cornell University Press.

BRAY J. M. (1942) Spectroscopic distribution of minor elements in igneous rocks from Jamestown, Colorado. *Bull. Geol. Soc. Amer.* **53**, 765–814.

ENGELHARDT W. VON (1936) Die Geochemie des Bariums. *Chem. d. Erde* **10**, 187.

ESKOLA P. (1922) The silicates of strontium and barium. *Amer. J. Sci.* **203**, 332–375.

FAIRBAIRN H. W. (1943) Packing in ionic minerals. *Bull. Geol. Soc. Amer.* **54**, 1305–1374.

FRONDEL C. (1958) Geochemical enrichment of strontium in minerals of the alunite structure type. *Bull. Geol. Soc. Amer.* **69**, 1567.

GERASIMOVSKY V. I. and LEBEDOV V. I. (1958) On the strontium/calcium ratio in rocks of the Lovosero massif. *Geochemistry* No. 6, 557.

GOLDSCHMIDT V. M. (1954) *Geochemistry* (Edited by MUIR A.) Oxford University Press.

GOLDSMITH J. R. (1950) Gallium and germanium substitutions in synthetic feldspars. *J. Geol.* **58**, 518–536.

HEIER K. S. and TAYLOR S. R. (1959) Distribution of Li, Na, K, Rb, Cs, Pb and Tl in southern Norwegian pre-Cambrian alkali feldspars. *Geochim. et Cosmochim. Acta.* **15**, 284–304

HEVESY, G. V. and WÜRSTLIN, K. (1934) Über die häufigkeit des Strontiums. *Z. anorg. Chem.* **216**, 312.

HODGMAN C. D. (Editor) (1958) *Handbook of Chemistry and Physics*. (40th Ed.) Chemical Rubber Publishing Company.

MOELLER T. (1952) *Inorganic Chemistry*. John Wiley, New York.

NOLL W. (1934) Geochemie des Strontiums. Mit Bemerkungen zur Geochemie des Bariums. *Chem. d. Erde* **8**, 507.

OFTEDAL I. (1958a) On the distribution of strontium and barium in the eruptive rocks of the Oslo region. *Norsk geol. Tidsskr.* **38**, 221–229.

OFTEDAL I. (1958b) On the development of granite pegmatite in gneiss areas. *Norsk geol. tidsskr.* **38**, 231–244.

RAMBERG H. (1953) Relationships between heats of reactions among solids and properties of the constituent ions and some geochemical implications. *J. Geol.* **61**, 318–352.

RANKAMA K. and SAHAMA T. G. (1950) *Geochemistry*. Chicago University Press.

RINGWOOD A. E. (1955) The principles governing trace element distribution during magmatic crystallization—I. The influence of electronegativity. *Geochim. et Cosmochim. Acta* **7**, 189–202.

Rogers J. J. W. (1958) Textural and spectrochemical studies of the White Tank quartz monzonite, California. *Bull. Geol. Soc. Amer.* **69**, 449–464.

Shimer J. A. (1943). Spectrographic analysis of New England granites and pegmatites. *Bull. Geol. Soc. Amer.* **54**, 1049–1066.

Sörum H. (1953). The structures of the plagioclase feldspars. II. *Acta Cryst.* **6**, 413–417.

Taylor S. R. and Heier K. S. (1958a) Alkali elements in potash feldspar from the pre-Cambrian of southern Norway. *Geochim. et Cosmochim. Acta* **13**, 293–302.

Taylor S. R. and Heier K. S. (1958b) Rubidium depletion in feldspars. *Nature, Lond.* **182**, 202–203.

Turekian K. K. and Kulp J. L. (1956). The geochemistry of strontium. *Geochim. et Cosmochim. Acta* **10**, 245–296.

Wedepohl K. H. (1956) Untersuchungen zur Geochemie des Bleis. *Geochim. et Cosmochim. Acta* **10**, 69–148.

Yoder H. S., Stewart D. B. and Smith J. R. (1957). Ternary feldspars. *Carnegie Inst. Wash. Year Book* **56**, 207–214.

Geochimica et Cosmochimica Acta, 1959, Vol. 17, pp. 305 to 314. Pergamon Press Ltd. Printed in Northern Ireland

Teneurs en cuivre et en zinc des eaux thermales au Japon

M. Ichikuni
Laboratoire de chimie, Faculté des Sciences, Université Métropolitaine de Tokio
Sétagaya, Tokio, Japan

(*Received* 4 *April* 1959)

Résumé—On a constaté la lognormalité de la répartition du cuivre et du zinc dans les eaux thermales. Le pH joue un rôle important dans la répartition du zinc: les eaux au pH supérieur à 5 contiennent en général moins de zinc que celles au pH inférieur à 5. Au contraire, la teneur en cuivre ne subit pas d'influence du pH. Il semble que le potentiel d'oxydo-réduction règne sur la répartition du cuivre.

Abstract—Lognormality of the distribution of copper and zinc in thermal waters is shown. The pH plays an important role in the distribution of zinc: the concentration of zinc is higher in waters of pH below 5 than in those of pH above 5. The copper content, however, is not influenced by the pH. The distribution of copper is controlled probably by the oxidation–reduction potential.

Introduction

De nombreuses études géochimiques récentes ont recours à la méthode statistique. Dans les études des éléments mineurs dans les roches volcaniques, Ahrens (1954a, b) a souligné la signification géochimique de la lognormalité de leur répartition de fréquence. D'autre part, dans les études des eaux douces, Hanya et Sawada (1956) ont montré que la même loi est également valable pour quelques composants majeurs dans les eaux souterraines ou celles de rivière. Les études statistiques des eaux thermales ont été inaugurées par Iwasaki, et reprises récemment par Nishimura (1955). Ces auteurs n'ayant traité que les composants majeurs, les recherches des composants mineurs restent encore peu satisfaisantes au point de vue statistique. Il va sans dire que, sans les compléter, on n'arrivera pas à résoudre les problèmes de l'état de traces d'éléments en solution et du mécanisme de dissolution de ceux-ci.

Lorsqu'on traite un certain nombre d'échantillons par la méthode statistique, la connaissance du type de la répartition de fréquence est indispensable. La description statistique s'effectue ensuite. C'est avec les résultats ainsi obtenus qu'on peut examiner de divers facteurs déterminant les milieux géochimiques des eaux, tels que la température, le pH et le potentiel d'oxydo-réduction. Dans ce rapport, on étudiera d'abord le type de la répartition de fréquence du cuivre et du zinc, donnant la base à l'étude de l'influence du pH sur leur répartition. On discutera ensuite la teneur moyenne en ces métaux des eaux thermales.

Kuroda (1940) est resté le seul qui a déterminé la teneur moyenne en zinc des eaux thermales au Japon. Seulement les sources thermales choisies par Kuroda n'étant pas semées d'une façon uniforme dans tout le Japon, son résultat serait loin d'une moyenne véritable de teneur en zinc. En ce qui concerne la répartition du cuivre, on n'a aucun article à citer jusqu'ici. C'est le présent rapport qui envisage le premier ce problème par voie statistique. Il facilitera donc la comparaison de la répartition du cuivre ou du zinc avec celle d'autres éléments.

Données d'analyse

On a rassemblé des données d'analyse des eaux thermales publiées après l'article de Kuroda. On les partage en deux groupes selon le pH des eaux: l'un comprend les eaux au pH inférieur à 5, l'autre, celles au pH supérieur à 5. Ce pH a été choisi comme seuil des deux groupes, car on y trouve le minimum de la fréquence des sources (Nishimura, 1955) et les caractères des eaux sont entièrement différents d'un groupe à l'autre.

Les données sont toutes réunies dans le Tableau 1 avec toutes les indications nécessaires.

Tableau 1. Données d'analyse des eaux thermales

No.	Situation	Température (°C)	pH	Cu (γ/l.)	Zn (γ/l.)	Dosage effectué par
	Sources au pH inferieur à 5					
1	Beppu	49,0	2,40	5	18	Kawakami *et al.* (1956a)
2	Beppu	64,8	2,30	15	390	
3	Beppu	61,5	2,20	7	32	
4	Beppu	68,0	2,32	14	210	
5	Beppu	84,0	2,00	4	2300	
6	Beppu	83,0	2,90	16	2200	
7	Beppu	97,5	2,67	52	290	
8	Beppu	94,0	2,88	5	130	
9	Beppu	98,0	2,35	37	1950	
10	Beppu	60,0	2,07	5	2900	
11	Beppu	63,0	2,48	16	840	
12	Hakoné	78,0	2,3	—	132	Kuroda (1940)
13	Hakoné	—	—	—	120	
14	Hakoné	53,5	2,5	—	34	
15	Hakoné	42,0	2,6	—	25	
16	Hakoné	—	—	—	20	
17	Iriyamabé	—	—	—	<10	Kuroda (1940)
18	Nasu	69,9	1,5	28	138	Ikeda (1954)
19	Noboribétsu	99,5	3,2	72	77	Uzumasa et Akaiwa (1958a)
20	Tamagawa	97,0	1,2	6	2990	Ichikuni
21	Tamagawa	97,0	1,2	8	3310	
22	Tamagawa	86,5	1,8	—	12	
23	Tamagawa	67	2,1	—	16	
24	Tamagawa	50	2,0	—	21	
25	Unzen	95,5	1,35	20,5	360	Kawakami *et al.* (1956b)
26	Unzen	55,5	2,08	5,1	205	
27	Unzen	58,8	1,88	1,6	345	
28	Unzen	61,0	2,90	0,	102	
29	Zaô	43,5	1,5	—	508	Misumi (1953)

Tableau 1 (*continued*)

No.	Situation	Température (°C)	pH	Cu (γ/1.)	Zn (γ/1.)	Dosage effectué par
	Sources au pH superieur à 5					
30	Ajiro	—	—	—	46	Kuroda (1940)
31	Arima	—	—	—	2010	Kuroda (1940)
32	Arima	—	—	—	164	
33	Arima	—	—	—	140	
34	Arima	—	—	—	96	
35	Arima	96	5,8	134	192	Ikeda (1955)
36	Beppu	54,0	7,14	7	17	Kawakami *et al.* (1956a)
37	Beppu	42,5	7,21	5,3	48	
38	Beppu	57,8	7,04	10,4	44	
39	Beppu	58,0	7,04	8,7	75	
40	Beppu	56,0	7,16	22	—	
41	Beppu	54,0	7,60	8,1	35	
42	Beppu	52,0	6,60	6,0	0,6	
43	Beppu	49,5	6,98	—	2	
44	Beppu	58,5	6,15	7,4	10	
45	Beppu	57,0	7,10	5,5	3,6	
46	Beppu	53,0	7,30	2,0	17	
47	Beppu	43,5	6,98	1	8	
48	Beppu	45,5	7,10	16	62	
49	Beppu	51,0	7,75	7	7	
50	Beppu	64,5	7,44	8,6	17	
51	Beppu	50,0	6,85	4,4	8,0	
52	Beppu	59,5	7,16	14	3,9	
53	Beppu	60,5	6,86	5,9	1,0	
54	Beppu	61,0	6,92	8,2	1,0	
55	Beppu	60,0	7,05	9,4	9.2	
56	Beppu	59,5	6,62	7,0	6,0	
57	Beppu	53,5	6,50	7,8	13	
58	Beppu	55,0	6,58	3,0	142	
59	Beppu	45,0	6,50	6,0	16	
60	Beppu	59,0	6,60	3,0	1,4	
61	Beppu	52,0	6,90	3,0	1,2	
62	Beppu	46,0	6,42	6,0	12	
63	Beppu	51,5	7,08	11	9,0	
64	Beppu	48,0	7,12	9,0	14	
65	Beppu	54,2	7,30	10,7	6,0	
66	Beppu	45,5	6,38	9,0	90	
67	Beppu	62,0	6,80	2,0	1,0	
68	Beppu	58,5	6,92	9,0	14	
69	Beppu	54,0	6,68	5,0	9,0	
70	Beppu	55,0	6,95	8,0	16	
71	Région Est du dépt. de Hiroshima	9,6	7,2	1	7	Sugihara (1951)

Tableau 1 (*continued*)

No.	Situation	Température (°C)	pH	Cu (γ/1.)	Zn (γ/1.)	Dosage effectué par
72	Région Est du dépt. de Hiroshima	11,5	7,6	2	20	
73	Région Est du dépt. de Hiroshima	25,0	6,6	45	130	
74	Région Est du dépt. de Hiroshima	20,0	6,6	21	7	
75	Région Est du dépt. de Hiroshima	13,0	6,3	14	297	
76	Région Est du dépt. de Hiroshima	12,5	6,2	0,4	1	
77	Région Est du dépt. de Hiroshima	20,0	6,3	8	40	
78	Ikaho	—	—	—	156	Kuroda (1940)
79	Jôzankéi	—	—	62	61	Uzumasa et Akaiwa (1958b)
80	Jôzankéi	—	—	234	96	
81	Masutomi	—	—	—	284	Kuroda (1940)
82	Masutomi	—	—	—	224	
83	Masutomi	—	—	—	215	
84	Masutomi	—	—	—	164	
85	Masutomi	—	—	—	126	
86	Masutomi	—	—	—	113	
87	Masutomi	—	—	—	102	
88	Masutomi	—	—	—	102	
89	Masutomi	—	—	—	88	
90	Masutomi	—	—	—	80	
91	Masutomi	—	—	—	80	
92	Masutomi	—	—	—	80	
93	Masutomi	—	—	—	78	
94	Masutomi	—	—	—	64	
95	Masutomi	—	—	—	64	
96	Masutomi	—	—	—	60	
97	Masutomi	—	—	—	39	
98	Masutomi	—	—	—	35	
99	Masutomi	—	—	—	26	
100	Masutomi	—	—	—	26	
101	Masutomi	—	—	—	<10	
102	Matsunoyama	—	—	—	<10	Kuroda (1940)
103	Matsunoyama	—	—	—	<10	
104	Misasa	—	—	—	235	Kuroda (1940)
105	Misasa	—	—	—	140	
106	Misasa	—	—	—	136	
107	Misasa	—	—	—	81	

Tableau 1 (*continued*)

No.	Situation	Température (°C)	pH	Cu (γ/l.)	Zn (γ/l.)	Dosage effectué par
108	Misasa	—	—	—	66	
109	Monkawa	—	—	—	113	Kuroda (1940)
110	Nanashiguré	—	—	—	73	Kuroda (1940)
111	Noboribétsu	90,5	7,2	215	92	Uzumasa et Akaiwa (1958a)
112	Shimo-kuro-béra	—	—	—	<10	Kuroda (1940)
113	Shiobara	—	—	—	36	Ikeda (1954)
114	Shiobara	—	—	—	75	
115	Suwa	57,0	8,2	—	8	Ichikuni
116	Suwa	54,0	7,3	—	43	
117	Suwa	94,1	8,0	—	6	
118	Suwa	79,9	7,8	—	67	
119	Suwa	51,1	8,1	—	3	
120	Suwa	66,7	8,1	—	2	
121	Suwa	71,6	—	—	62	
122	Suwa	44,6	8,0	—	12	
123	Suwa	80,6	8,2	—	21	
124	Suwa	66,5	8,1	—	1	
125	Suwa	75,4	8,0	—	10	
126	Suwa	63,5	7,5	—	4	
127	Suwa	81,5	8,1	—	6	
128	Suwa	53,4	7,4	—	1	
129	Suwa	50,0	8,0	—	1	
130	Suwa	60,8	7,5	—	9	
131	Suwa	52,5	8,0	—	46	
132	Suwa	77,0	8,1	—	1	
133	Suwa	61,4	8,1	—	3	
134	Suwa	78,4	8,1	—	8	
135	Suwa	42,1	7,6	—	17	
136	Suwa	47,8	7,8	—	2	
137	Suwa	50,0	8,1	—	3	
138	Suwa	76,0	7,9	—	7	
139	Suwa	73,1	8,1	—	16	
140	Suwa	44,2	—	—	4	
141	Suwa	42,8	—	—	12	
142	Suwa	43,2	—	—	2	
143	Suwa	37,5	—	—	6	
144	Suwa	45,7	—	—	10	

Discussion

(1) Répartition du cuivre: le Tableau 1 contient 64 sources dont la teneur en cuivre est indiquée: 19 sources au pH inférieur à 5, et 45 sources au pH supérieur à 5. Le nombre de la fréquence a été compté pour chaque groupe sur les intervals logarithmiques de concentration: de 0,21 à 0,46, de 0,46 à 1.0, de 1,0 à 2,1 γ/l., . . . Les histogrammes de la Fig. 1 en montrent le résultat. On peut constater que sa

répartition de fréquence, indépendante du pH des sources, est approximativement lognormale.

Le maximum de la fréquence apparaît dans les deux groupes à l'interval de 4,6 à 10 γ/l.

Etant donné de la lognormalité de la répartition, la moyenne géométrique conviendrait d'exprimer statistiquement la présence du cuivre dans les eaux

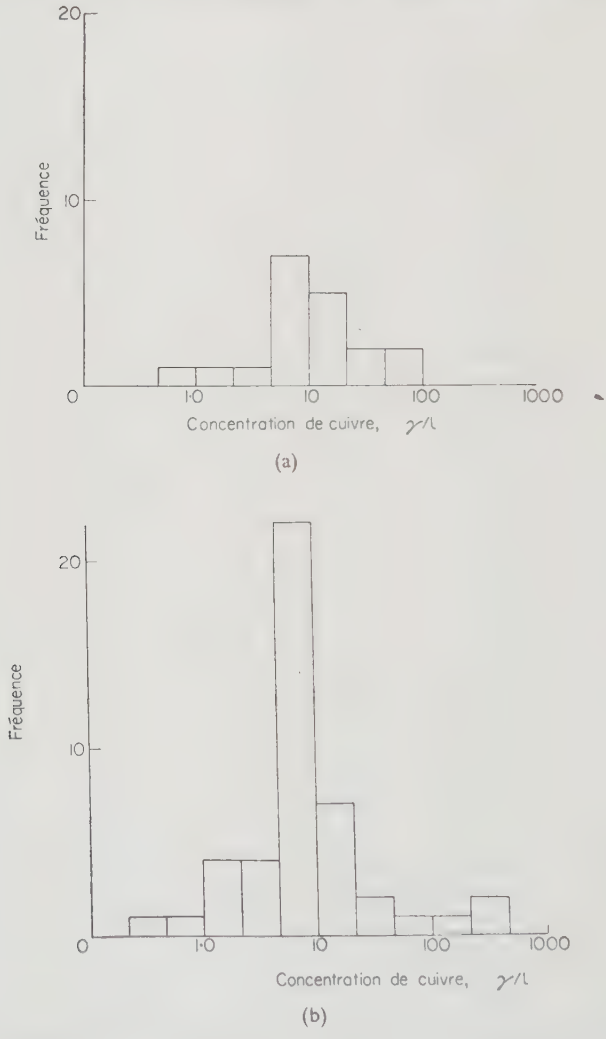

Fig. 1. (a) Histogramme montrant la répartition du cuivre dans les eaux thermales au pH inférieur à 5. (b) Histogramme montrant la répartition du cuivre dans les eaux thermales au pH supérieur à 5.

thermales. On a pourtant montré dans le Tableau 2 les moyennes géométrique et arithmétique, pour en donner l'idée de comparaison.

D'après le Tableau 2 on jugera qu'il n'y a pas de différence de teneur en cuivre entre les sources au pH supérieur à 5 et les autres sources. On donnera donc une valeur de 10 γ/l. à la teneur moyenne de toutes les sources. Ce résultat veut

dire que le pH n'exerce pas une influence définitive sur la répartition du cuivre, mais cela suggère plutôt la présence d'autres facteurs qui jouent un rôle plus important que le pH. Lors de la dissolution des minerais sulfurés en milieu acide, la présence de l'hydrogène sulfuré, ou plus généralement dit, un potentiel bas

Tableau 2. Teneur moyenne en cuivre des eaux thermales

Type de source	g.m. (γ/l.)	a.m. (γ/l.)
Sources au pH inférieur à 5	10	17
Sources au pH supérieur à 5	9	22
Toutes les sources	10	19

g.m., moyenne géométrique; a.m., moyenne arithmétique.

d'oxydo-réduction, empêche la dissolution du cuivre dans une grande mesure (Ichikuni et Kamiya, 1959). Il est bien probable que la présence de l'hydrogène sulfuré dans les eaux thermales donne également une grande influence sur la teneur en cuivre.

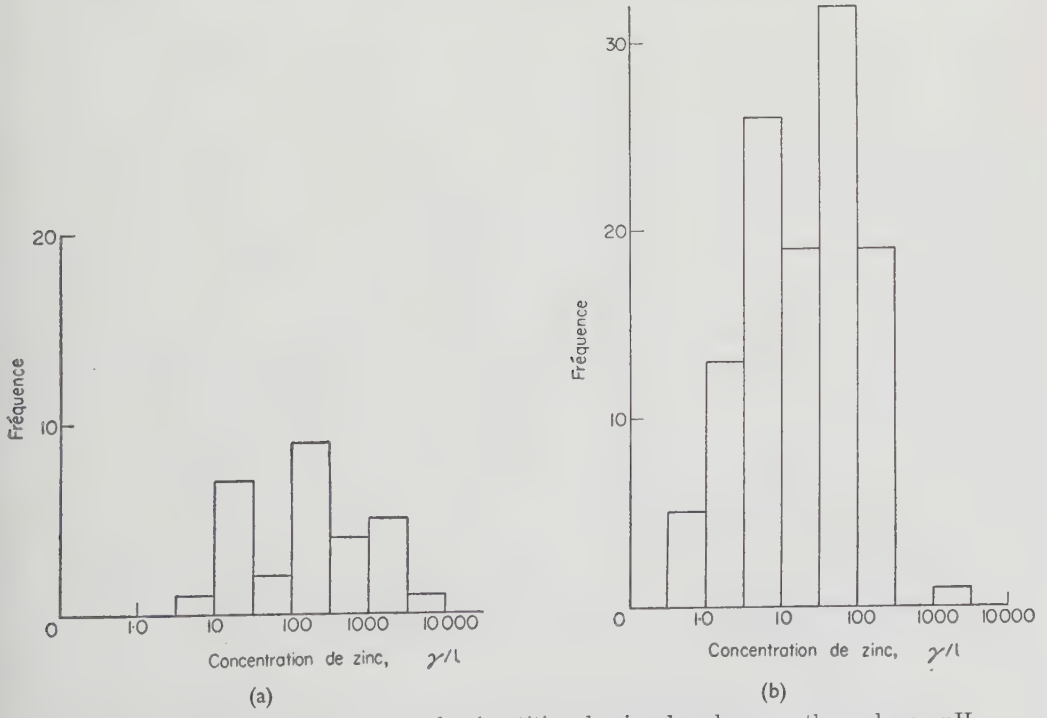

Fig. 2. (a) Histogramme montrant la répartition du zinc dans les eaux thermales au pH inférieur à 5. (b) Histogramme montrant la répartition du zinc dans les eaux thermales au pH supérieur à 5.

La lognormalité trouvée pour la répartition de fréquence de quelques composants majeurs dans les eaux douces (Hanya et Sawada, 1956) semble valable pour les composants mineurs dans les eaux thermales.

(2) Répartition du zinc: on a ici 29 sources au pH inférieur à 5, et 115 sources au pH supérieur à 5. Ayant trouvé la ressemblance à la lognormalité dans la répartition du cuivre, on a compté la fréquence sur une échelle logarithmique de concentration: de 0,32 à 1,0, de 1,0 à 3,2 γ/l., . . . Les histogrammes de Fig. 2 en montrent le résultat. La répartition du zinc semble obéir à la loi de lognormalité comme celle du cuivre.

La différence de la teneur en zinc existant entre les sources au pH supérieur à 5 et les autres sources est bien visible. Les premières ont le maximum de la fréquence à une teneur de 32 à 100 γ/l, tandis que les dernières l'ont à une teneur de 100 à 320 γ/l. D'où on comprend que le pH des eaux exerce une influence importante sur la concentration de zinc. Il va sans dire qu'il y a d'autres facteurs agissant sur le zinc. On se contente donc de dire pour le moment que la concentration de zinc est généralement grande dans les eaux à une petite valeur de pH.

Le Tableau 3 montre les moyennes géométrique et arithmétique de teneur en zinc des deux groupes de sources.

Tableau 3. Teneur moyenne en zinc des eaux thermales

Type de source	g.m. (γ/l.)	a.m. (γ/l.)
Sources au pH inférieur à 5	190	750
Sources au pH supérieur à 5	17	67
Toutes les sources	23	192

g.m., moyenne géométrique; a.m., moyenne arithmétique.

Les eaux des sources au pH inférieur à 5 contiennent à peu près dix fois plus grand de zinc que celles des autres sources.

(3) Relation entre le cuivre et le zinc: plus la valeur de Cu/Zn est petite, plus la teneur en zinc est grande. Fig. 3 représente cette relation. Pour les sources au pH supérieur à 5, la teneur en cuivre a la tendance d'augmenter avec celle en zinc; il n'y a pas un grand écart entre la teneur en cuivre et celle en zinc, tandis que pour les sources au pH inférieur à 5, la teneur en cuivre n'augmente pas avec l'acidité des eaux qui favorise une grande teneur en zinc de celles-ci. Cette tendance aboutit à une petite valeur de Cu/Zn dans les eaux thermales acides.

(4) Répartition du cuivre et du zinc dans l'hydrosphère: la comparaison des teneurs en cuivre et en zinc des eaux thermales avec celles des eaux douces et de l'eau de mer nous intéresse particulièrement. Le Tableau 4 indique les résultats obtenus par Morita (1950a,b) sur de divers types d'eau et ceux du présent rapport.

La teneur en cuivre des eaux douces ou de l'eau de mer est approximativement égale à celle des eaux thermales. En ce qui concerne la teneur en cuivre, on ne remarque pas de différence considérable entre les eaux douces et les eaux thermales. À propos des sources au pH supérieur à 5, elles ne diffèrent pas des eaux douces par la teneur en zinc, mais les sources au pH inférieur à 5, au contraire, contiennent

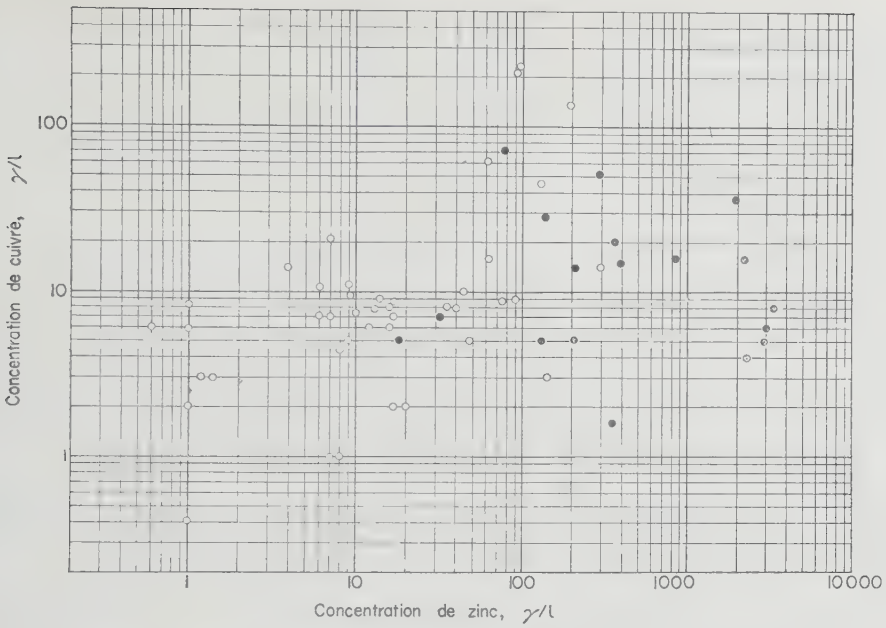

Fig. 3. Relation entre le cuivre et le zinc: ○: sources au pH supérieur à 5; ●: sources au pH inférieur à 5.

plus de zinc que les autres types d'eau. Si l'étude de la répartition du zinc s'effectue entièrement sur les rivières acides qui sont propres au Japon, on pourra saisir d'une manière concrète la signification géochimique du pH sur la répartition du zinc dans l'hydrosphère. Les effets des substances co-existantes sur la teneur en cet élément restent comme problème à résoudre.

Le rapport Cu/Zn reste à peu près le même pour les eaux douces, l'eau de mer et les eaux thermales au pH supérieur à 5. Le zinc peut être fourni dans l'hydrosphère par la dissolution de minerais sulfurés, les activités thermales et les activités

Tableau 4. Teneurs en cuivre et en zinc de divers types d'eau

Type d'eau	Cu (γ/l.)	Zn (γ/l.)	Cu/Zn
Sources thermales au pH inférieur à 5	10	190	0,05
Sources thermales au pH supérieur à 5	9	17	0,53
Sources non-thermales	0,6	2,4	0,25
Rivières	1,5	4,5	0,33
Lacs	1,2	4,4	0,27
Etangs	2,2	11,8	0,19
Pluie	0,7	3,6	0,19
Neige	1,3	6,5	0,20
Mer	2,4	5,6	0,43

humaines. Lors de l'examen détaillé du rapport Cu/Zn, on doit prendre en considération le fait que le zinc reste en état dissous assez longuement dans les eaux courantes par rapport au cuivre.

Une petite valeur de Cu/Zn des sources acides peut s'expliquer qualitativement par la présence de l'hydrogène sulfuré dans les eaux, ou un potentiel bas d'oxydoréduction des eaux. Une étude plus approfondie sera exigée pour l'explication complète de ce phénomène.

Remerciements—L'auteur exprime ses remerciements sincères à Monsieur le professeur Noguchi qui a bien voulu lire cet essai, et à Monsieur le professeur Hanya auquel il doit l'idée de cette étude et qui a conseillé au cours de son exécution.

Bibliographie

Ahrens L. H. (1954a) The lognormal distribution of the elements. *Geochim. et Cosmochim. Acta* **5,** 49–73.

Ahrens L. H. (1954b) The lognormal distribution of the elements—II. *Geochim. et Cosmochim. Acta* **6,** 121–131.

Hanya T. et Sawada F. (1956) Etude statistique sur les caractères géochimiques des eaux douces au Japon. *Geochim. et Cosmochim. Acta* **9,** 249–255.

Ichikuni M. et Kamiya H. (1959) Dissolution des minerais sulfurés en divers milieux. Travaux en cours.

Ikeda N. (1954) Etudes chimiques des eaux thermales de Nasu—III. *J. Chem. Soc. Japan, Pure Chem. Sect.* **75,** 368–371.

Ikeda N. (1955) Etudes chimiques des eaux thermales d'Arima—VI. *J. Chem. Soc. Japan, Pure Chem. Sect.* **76,** 842–844.

Kawakami H. *et al.* (1956a) Etudes chimiques des eaux thermales de Beppu. *J. Chem. Soc. Japan, Pure Chem. Sect.* **77,** 1327–1332.

Kawakami H. *et al.* (1956b) Etudes chimiques des eaux thermales d'Unzen—III. *J. Chem. Soc. Japan, Pure Chem. Sect.* **77,** 1779–1780.

Kuroda K. (1940) Zinc content of the hot springs of Japan. *Bull. Chem. Soc. Japan* **15,** 88–92.

Misumi S. (1953) Etude sur une source thermale à Zaô. *Mem. Univ. Yamagata* **2,** 207–213.

Morita Y. (1950a) Etudes sur la répartition du cuivre et du zinc—III. Répartition du cuivre et du zinc dans les eaux douces. *J. Chem. Soc. Japan, Pure Chem. Sect.* **71,** 209–212.

Morita Y. (1950b) Etudes sur la répartition du cuivre et du zinc—IV. Teneurs en cuivre et en zinc de l'eau de mer. *J. Chem. Soc. Japan, Pure Chem. Sect.* **71,** 246–248.

Nishimura M. (1955) Etudes chimiques des eaux thermales—XXVIII. Considérations statistiques sur les composants majeurs dans les eaux thermales. *J. Chem. Soc. Japan, Pure Chem. Sect.* **76,** 349–353.

Sugihara K. (1951) Etudes chimiques des sources minérales dans la région de Sanyô. *J. Chem. Soc. Japan, Pure Chem. Sect.* **72,** 1019–1022.

Uzumasa Y. et Akaiwa H. (1958a) Etudes chimiques des eaux thermales—XXXIX. Variation de teneur en composants mineurs (1). *J. Chem. Soc. Japan, Pure Chem. Sect.* **79,** 654–658.

Uzumasa Y. et Akaiwa H. (1958b) Etudes chimiques des eaux thermales—XXXX. Variation de teneur en composants mineurs (2). *J. Chem. Soc. Japan, Pure Chem. Sect.* **79,** 1021–1024.

Geochimica et Cosmochimica Acta, 1959, Vol. 17, pp. 315 to 319. Pergamon Press Ltd. Printed in Northern Ireland

Der Meteorit von Breitscheid—I

Einleitung

F. A. Paneth
Max-Planck-Institut für Chemie, Mainz

Abstract—On 11 August 1956 a stone meteorite fell at Breitscheid in the Dillkreis (50° 51′ N, 8° 12′ E) the weight of which was supposed to be about 1·5 kg. But before recognition of its meteoritic character the stone was broken to pieces so that the total weight of the fragments amounted only to 970 g. The petrographic examination showed in thin sections a multiplicity of most characteristic chondrules; the Breitscheid meteorite is a bronzite–olivine–chondrite. It is remarkable that troilite was found in primary as well as in secondary formation and that ilmenite could be proved to be a meteoritic mineral. The total chemical analysis corresponds very well with the petrographic results.

Helium, neon, argon, tritium, potassium and uranium were measured by special methods which partly had to be developed only during the course of work. Furthermore, it was found that the isotopic composition of helium and neon greatly differs from that of the corresponding terrestrial gases. A geological age of 3300 million years results from the argon/potassium ratio. The content of helium and neon differs widely in various parts of the meteorite; a phenomena which has to be explained in detail. An irradiation age of about 20 million years for the Breitscheid meteorite would result from the ratio helium-3 to tritium in one part of the meteorite.

Zusammenfassung—Am 11 August 1956 fiel ein Steinmeteorit im Dorf Breitscheid im Dillkreis (50° 51′ n.B., 8° 12′ ö.L.); sein Gewicht betrug wahrscheinlich rund 1,5 kg, doch wurde der Stein vor dem Erkennen seiner Meteoritnatur zerschlagen und das Gesamtgewicht der bekannten Bruchstücke erreicht nur 970 g. Die petrographische Untersuchung liess in Dünnschliffen eine Vielfalt sehr charakteristischer Chondren erkennen; der Breitscheid-Meteorit ist ein Bronzit–Olivin–Chondrit. Bemerkenswert ist, dass darin Troilit sowohl in primärer wie in sekundärer Bildung vorliegt und dass Ilmenit mit Sicherheit als meteoritisches Mineral nachgewiesen werden konnte. Die chemische Gesamtanalyse stimmt sehr gut mit dem petrographischen Befund überein.

Durch spezielle Verfahren, die zum Teil erst im Laufe dieser Arbeit entwickelt wurden, wurde der Gehalt an Helium, Neon, Argon, Tritium, Kalium und Uran bestimmt. Im Helium und Neon wurde das Isotopenverhältnis gemessen, das sich sehr wesentlich von dem des terrestrischen Helium und Neon unterscheidet. Aus dem Argon–Kalium Verhältnis ergibt sich ein geologisches Alter von 3300 Millionen Jahren. Der Helium- und Neongehalt variiert von Stelle zu Stelle in überraschend starkem Masse, eine Erscheinung, die näherer Aufklärung bedarf; aus dem Verhältnis des Heliums-3 zu Tritium an einer Stelle würde ein Bestrahlungsalter des Breitscheid-Meteoriten von *ca.* 20 Millionen Jahren folgen.

1. Beobachtung des Falles

Am 11 August 1956 fiel zwischen 15,30h und 15,45h ein Meteorstein auf eine mit vereinzelten Obstbäumen bestandene Wiese im Dorfe Breitscheid im Dillkreis (50 Grad, 51 Minuten nördlicher Breite; 8 Grad, 12 Minuten östlicher Länge). Das Herabfallen des Meteoriten wurde von mehreren Personen gesehen und gehört. Frau Josefine Reich war vor ihrem Haus mit dem Aufhängen von Wäsche beschäftigt; sie hörte ein anschwellendes Geräusch, wie das Zischen einer dampfablassenden Lokomitive. Als sie in die Richtung des Schalles blickte, sah si ein der Luft einen von Westen in einer Spiralbahn heranfliegenden dunklen Körper, der in etwa 40 m Entfernung mit einem dumpfen Ton im Erdboden verschwand; auch nahm sie das Krachen eines abbrechenden Astes wahr. Herr Josef Klier, der wenige Meter von Frau Reich entfernt Holz hackte, hörte dasselbe wie sie, sah aber den Fäll des Meteoriten nicht, da er mit dem Rücken zur Einschlagstelle stand. Zwei weitere Dorfbewohner, Herr Rudolf Zenzinger und Fräulein Vorck standen nebeneinander in etwa 600 m Entfernung von der Einschlagstelle und

etwas tiefer, so dass sie das Landen des Meteoriten auf dem Erdboden nicht sehen konnten; sie nahmen aber, von ihrem Standpunkt, am südwestlichen Himmel einen rotglühenden Körper wahr, der auf einer von rechts nach links verlaufenden Bahn mit einer Neigung von etwa 40 Grad zum Erdboden herabstürzte.

Etwa 2 Minuten vorher hatte ein Düsenflugzeug die Ortschaft überflogen. Der fallende Gegenstand und die Schallerscheinungen erinnerten Frau Reich an Fliegerbomben; sie vermutete daher, dass das Flugzeug eine solche verloren hätte und vermied es, sich der Fallstelle zu nähern. Ihr Mann aber, Herr Karl Reich, der im Haus gearbeitet und das Geräusch auch gehört hatte, ging gleich hin und fand neben einem Apfelbaum einige frisch abgebrochene Äste und ein Loch in der Erde, in dem ein schwarzer Stein steckte, der sich deutlich warm, aber nicht heiss, anfühlte. Da er ihn mit der Hand nicht herausheben konnte, holte er eine Spitzhacke und grub ihn aus. Dabei bemerkte er, dass der Stein in vier ungleiche Teile zerbrochen war und dass unter ihm ein Basaltblock lag, auf den er offenbar aufgeprallt und dabei zersprungen war. Herr Reich konnte die Stücke in seinem Garten leicht wieder zusammensetzen. Das Aussehen des Steines mit seinem grauen Innern und der schwarzen Rinde fiel ihm und den hinzugekommenen Nachbarn auf, doch waren sie alle der Meinung, dass er vom Flugzeug herabgefallen, wahrscheinlich ein Brocken Zement, und jedenfalls ohne Wert sei. Die vier Stücke wurden in weitere zerschlagen, und wer Lust hatte, nahm etwas davon mit. Ein Bruchstück wurde in einen Ofen der benachbarten Westerwalder Tonindustrie gelegt, um zu erproben, ob es schmelzen würde.

Erst einige Tage später sah ein Chemiker, Herr Günther Thielmann, der im Laboratorium der Eisenwerke Burg beschäftigt ist, einen der Steine und vermutete sofort, dass er meteoritischer Natur sei. Nachdem er eine orientierende Analyse ausgeführt hatte, sandte er eine kleine Abhandlung über diesen und andere Meteoritfälle an die lokale Zeitung *Dill-Post*, wo sie am 1. September erschien.

Einen Bericht aus anderer Feder, der aber nichts Wesentliches zu dem des Herrn Thielmann hinzufügte, brachte am 20. September die *Dill-Zeitung*. (Das Falldatum ist hier irrtümlich als 4. August angegeben.) Da aber beide Blätter nur eine sehr beschränkte Verbreitung haben und vielleicht auch weil beide Aufsätze sich in allgemeinen Betrachtungen über Meteore und Meteorite ergingen, statt vor allem die Aufmerksamkeit auf den aktuellen Fall von Breitscheid zu lenken, drang die Nachricht nicht in weitere Kreise und das seltene Ereignis wäre vielleicht bald vergessen worden, wenn nicht die *Frankfurter Rundschau* in ihre Ausgabe vom 25. September zehn Zeilen darüber aufgenommen hätte; diese kurze Notiz wurde von der im Max-Planck Institut für Chemie tätigen Chemotechnikerin, Fräulein Ilsemarie Schüler, gesehen und in das Institut gebracht. Am nächsten Morgen fuhr einer der wissenschaftlichen Assistenten, Dr. Klaus Ebert, nach Breitscheid und kam mit zwei Stücken des Steines zurück, deren Betrachtung jeden Zweifel an der Echtheit des Meteoriten ausschloss.

Unsere erste Aufgabe musste es sein, so viel von dem wissenschaftlich wertvollen Material zu retten, als noch möglich war. Da Dr. Ebert erfahren hatte, dass die Stücke bereits unter sehr verschiedene Besitzer verteilt waren, liessen wir eine Anzeige in den Dill-Blättern und im Wiesbadener Kurier und Tagblatt erscheinen, durch die Besitzer von Stücken des Breitscheider Meteoriten gebeten

wurden, sich mit dem Max-Planck-Institut in Verbindung zu setzen. Diese Aufforderung hatte keinen direkten Erfolg, veranlasste aber einen Studenten der Universität Marburg, Herrn Horst F. Hauschild aus Herborn, uns seine Dienste für Nachforschungen nach dem Verbleib der Stücke anzubieten. Herr Hauschild hat das 8 km von Herborn in westlicher Richtung gelegene Dorf Breitscheid mehrmals besucht und ist sorgfältig jeder Spur nachgegangen. Er hat sich auch selbständig nach den Umständen des Falles erkundigt; die oben gemachten Angaben stützen sich auf die von ihm und von Dr. Ebert gesammelten Zeugenaussagen und sind unabhängig von den Berichten der Zeitungen. Beide Herren haben auch das durch den Meteoriten geschlagene Loch untersucht; aus seiner Neigung und den abgeschlagenen Zweigen des Baumes konnten sie bestätigen, dass der Meteorit im Einklang mit den Wahrnehmungen der Beobachter von Westen und in einem Winkel von 35–40 Grad zur Horizontalen angekommen ist. Eine Berechnung der Bahn oder der Geschwindigkeit ist bei der Spärlichkeit der Angaben der Augenzeugen natürlich nicht möglich; die Licht- und Schallerscheinungen waren auch, verglichen mit denen anderer Meteoritfälle, so wenig eindrucksvoll, dass keine Nachrichten über Beobachtungen aus grösserer Entfernung zu erhoffen waren.

Abschliessend möchten wir die Tatsache unterstreichen, dass ein Meteorit, der am Tage und in einer bewohnten Gegend Deutschlands niederging, dessen Fall mehrere Personen wahrnahmen, und der ohne jede Schwierigkeit gefunden wurde, trotzdem für die moderne Meteoritforschung, die an solchem Material hohes Interesse hat, fast verlorengegangen wäre. Wir möchten darum die Bitte aussprechen, dass jeder, der künftig von einem Meteoritfall in Deutschland Kenntnis erhält, sich nicht mit einer Mitteilung an ein lokales Blatt begnügen, sondern sich direkt mit dem Max-Planck-Institut für Chemie in Mainz in Verbindung setzen möge, wo Mittel zur Erwerbung von Meteoriten aus den Händen der glücklichen Finder zur Verfügung stehen.

2. Die Stücke des Meteoriten

Durch beharrliche Bemühungen ist es uns gelungen, acht Stücke des zerschlagenen Meteoriten von Breitscheid für das Max-Planck-Institut zu erwerben. Sechs von diesen fanden sich noch bei Einwohnern von Breitscheid; obwohl bei manchen dieser Besitzer die anfängliche Unterschätzung des Wertes in das Gegenteil umgeschlagen war, konnten wir alle diese Stücke kaufen. Ein siebentes Stück, das den Weg zu einem Sammler gefunden hatte, wurde uns liebenswürdigerweise von diesem wieder zur Verfügung gestellt im Austausch gegen einen früher gefallenen Meteoriten, der nicht für unsere Forschungen, wohl aber vom Standpunkt eines Sammlers als gleichwertig betrachtet werden konnte. Das achte Stück schenkte uns ein junges Mädchen, das zur Zeit des Falles in Breitscheid auf Ferien gewesen war und dieses ansehnliche Stück mit nach Hause genommen hatte, nach freundlicher Aussprache aber einen als Anhänger gefassten und als Amulett tragbaren Splitter des Steines vorzog. Als für unsere Zwecke nutzlos geworden mussten wir dass Stück ansehen, das in dem oben erwähnten industriellen Ofen 12 Stunden auf 1300° erhitzt worden war; es befindet sich jetzt im Heimatmuseum in Herborn.

Die acht in das Max-Planck-Institut gekommenen Stücke des Breitscheid-Meteoriten besassen zusammen ein Gewicht von 796 g. Herr Karl Reich gab das Gewicht der vier von ihm ausgegrabenen Stücke mit drei bis dreieinhalb Pfund an. Es scheint der Mühe wert, diese Schätzung zu vergleichen mit Berechnungen des Maximalgewichtes, die sich auf die Dimensionen des vom Meteoriten geschlagenen Loches stützen. Als dieses Loch von Herrn Hauschild und Dr. Ebert untersucht wurde, war es bereits durch das Herausgraben des Steines erweitert; nach unten aber war es durch den Basalt begrenzt, und da der Meteorit nicht aus dem Loch herausragte, kann seine Dimension in dieser Richtung nicht mehr als 15 cm betragen haben. Nach der Beschreibung der ersten Beobachter und nach den in unserem Besitz befindlichen Randstücken, scheint er ungefähr die Form eines Ziegelsteines gehabt zu haben, dessen längste Kante die eben erwähnte Länge hatte. Die beiden darauf senkrechten Dimensionen dürften nach den vermuteten Abmessungen des ursprünglichen Loches nicht wesentlich über 8 resp. 5 cm betragen haben. Daraus ergibt sich, unter Zugrundelegung eines Raumgewichtes von 3,3 (siehe S. 335), ein Maximalgewicht des ganzen Steines von etwa 2 kg, das als Stütze des von Herrn Reich geschätzten Wertes von mindestens 1,5 kg angesehen werden kann.

Die Differenz zwischen dem Gewicht der von uns erworbenen acht Stücke und dem Anfangsgewicht erklärt sich durch das Fehlen des nun im Herborner Museum befindlichen Stückes (82 g), den Verbrauch von Material für die analytischen Arbeiten von Herrn Thielmann (schätzungseise 10 g) und das Gewicht einer Anzahl von kleinen und kleinsten Stücken, die in Breitscheid und einigen anderen Orten in verschiedenen Händen geblieben sind, deren Gesamtgewicht aber nach den Erkundigungen des Herrn Hauschild höchstens 80 g betragen dürfte. Ausserdem ist aber sicherlich beim Zerschlagen der Steine eine nicht unbeträchtliche Menge Material in kleine Stücke zerbrochen oder zerstäubt und dadurch verlorengegangen; dass die Zertrümmerung in recht roher Weise erfolgt ist, geht daraus hervor, dass von unseren acht Stücken nur drei zu einem Block mit einem Gewicht von 365 g zusammengepasst werden konnten (siehe Petrographische Untersuchungen, Abb. 3); die anderen waren durch Abreiben und Verlust dazwischen liegenden Materials zu stark verändert, als dass eine sichere Rekonstruktion der ursprünglichen Form des Meteoriten durch Zusammensetzen der Bruchstücke möglich gewesen wäre.

Während demnach das Gewicht aller Stücke, von deren Verbleib oder Verwendung wir Kenntnis haben, nur rund 790 g beträgt, möchten wir annehmen, dass das ursprüngliche Gewicht nahe bei 1500 g gelegen war.

3. Die Ausführung der wissenschaftlichen Untersuchung

Bekanntlich sind alle Meteorite ein wissenschaftlich sehr wertvolles Material. Ihre chemische Analyse liefert Grundlagen für die Beurteilung der kosmischen Häufigkeit der Elemente, ihre petrographische Untersuchung lässt Schlüsse auf ihre Entstehungsweise zu, die Anwendung von Methoden der radioaktiven Altersbestimmung erlaubt die Bestimmung ihrer Erstarrungszeit und das Studium ihrer Isotopenzusammensetzung eröffnet Einblicke in die Wirkung der kosmischen Strahlung auf Materie. Da diese Wirkung u.a. in der Erzeugung kurzlebiger

Nuklide besteht, die in Meteoriten, deren Falldatum weit zurückliegt, bereits abgeklungen sind, haben frisch gefallene Meteorite, wie der von Breitscheid, für die Erforschung der kosmischen Strahlung ein ganz besonderes Interesse. Es war unser Bestreben, diesen Stein möglichst vielseitig sowohl nach den klassischen Methoden der Meteoritforschung wie nach den modernen radiochemischen Verfahren zu untersuchen.

Die Einrichtungen des Max-Planck-Instituts für Chemie und die Schulung seiner wissenschaftlichen Mitarbeiter erlaubten es uns, einen grossen Teil der geplanten Forschungen in diesem Institut auszuführen; dazu gehört die chemische Gesamtanalyse des Meteoriten, die auf die Helium-Uran- und die Argon-Kalium-Methode gestützten Altersbestimmungen und die Feststellung verschiedener durch die kosmische Strahlung erzeugter Nuklide. Da wir noch nicht über eine Apparatur zum Nachweis des durch die Einwirkung der Höhenstrahlung erzeugten Tritiums verfügten, waren wir den Herren K. Goebel und P. Schmidlin im "CERN"-Institut von Prof. Gentner in Genf sehr dankbar, dass sie diese Untersuchung durchführten, die naturgemäss nicht unbegrenzt aufgeschoben werden darf; wir hoffen, die Tritium-Messungen in naher Zukunft im Max-Planck-Institut fortführen zu können. Für die Feststellung der Isotopenzusammensetzung der aus den Meteoriten isolierten Edelgase Helium und Neon konnten wir, wie in früheren Jahren, die Hilfe von Herrn Dr. K. I. Mayne in Oxford in Anspruch nehmen. Ganz ausserhalb der Arbeitsrichtung unseres Instituts lag das petrographische Studium des Meteoriten; dieses hat Prof. Dr. Hans Hentschel vom Institut für Mineralogie und Petrographie der Universität Mainz übernommen.

Da die Resultate dieser getrennten Forschungen naturgemäss in mannigfacher Weise zueinander in Beziehung stehen, haben wir es für zweckmässig gehalten, in den hier folgenden Abschnitten sämtliche bisher am Breitscheid Meteoriten ausgeführte Untersuchungen zusammenzustellen.

Geochimica et Cosmochimica Acta, 1959, Vol. 17, pp. 320 to 322. Pergamon Press Ltd. Printed in Northern Ireland

Der Meteorit von Breitscheid—II

Chemische Analyse

Else Vilcsek
Max-Planck-Institut für Chemie, Mainz

Ungefähr 90 g des Meteoriten wurden für verschiedene chemische Untersuchungen verwendet. Sie wurden in einem Stahlmörser grob zerkleinert und dann in einer Achatschale pulverisiert. Von dem so hergestellten fein gepulverten und gut durchmischten Material wurden die für die chemische Analyse benötigten Proben entnommen. Die Analyse wurde im makroanalytischen Masstab durchgeführt, die Einwaagen lagen daher zwischen 0.5 g und 1 g; die Substanz wurde in lufttrockenem Zustand eingewogen.

Zur Bestimmung der im Meteoriten enthaltenen Kieselsäure wurde in einem Platintiegel mit wasserfreiem Natriumcarbonat aufgeschlossen, die Schmelze in Salzsäure gelöst und die Kieselsäure daraufhin auf dem üblichen Weg abgeschieden. Sie wurde geglüht, gewogen und mit Flussäure abgeraucht. Das Gewicht des dabei verbliebenen geringen Rückstandes wurde vom Gewicht der ersten Wägung abgezogen, der Rückstand nochmals mit Natriumcarbonat aufgeschlosen und die salzsaure Lösung dieser Schmelze mit dem Filtrat aus der ersten Kieselsäureabscheidung vereinigt. Aus der so erhaltenen Lösung wurde nunmehr die Phosphorsäure nach Woy mit Ammonium molybdat gefällt und bestimmt. Aus der jetzt phosphorsäurefreien, jedoch molybdänhaltigen Lösung, wurde nach Entfernung der Salpetersäure, das Molybdän in salzsaurer Lösung mit Schwefelwasserstoff abgeschieden.

Die Metalle der Gruppe III wurden mit Ammoniumsulfid gefällt, der Niederschlag in Königswasser gelöst und die mehrwertigen von den zweiwertigen Metallen nach der Acetatmethode getrennt. Die dabei als Niederschlag erhaltenen basischen Acetate wurden in Salzsäure gelöst und die Trennung wiederholt. Die salzsaure Lösung des zweiten Niederschlages wurde mit Natronlauge und Bromwasser versetzt, gekocht und von dem dabei entstandenen Niederschlag abfiltriert. Nach dem Ansäuern des Filtrates wurde daraus das Aluminium mit Ammoniak abgeschieden und zum Oxyd verglüht. Um den Ballast der Alkalisalze zu entfernen, wurden Kobalt, Nickel und Mangan aus den vereinigten Filtraten der Acetattrennung mit Ammoniumsulfid gefällt, der Sulfidniederschlag in Königswasser gelöst und nachdem ein pH Wert von 4.3 eingestellt worden war, Kobalt und Nickel mit Oxin gefällt und abgeschieden. Das Filtrat wurde dann mit Ammoniak schwach alkalisch gemacht und durch erneuten Zusatz von Oxin das Manganoxinat ausgefällt. Der Niederschlag wurde abfiltriert, in Salzsäure gelöst und das Oxinat bromometrisch bestimmt (Berg, 1935).

Der aus Nickel- und Kobaltoxinat bestehende Niederschlag wurde in Salzsäure gelöst und das Nickel aus dieser Lösung mit Diacetyldioxim abgeschieden und

bestimmt; das Kobalt wurde aus dem Filtrat der Diacetyldioximfällung als Anthranilat gefällt (Funk und Ditt, 1933).

Das nach der Abtrennung der Gruppe III verbliebene Filtrat enthielt noch Calcium und Magnesium. Das Calcium wurde mit Ammoniumoxalat gefällt, der Niederschlag in Salzsäure gelöst und nochmals gefällt und das Calcium daraufhin als Oxyd bestimmt. Aus den nach der Fällung des Calciums erhaltenen Filtraten wurde das Magnesium nach Zerstörung des Ammoniumoxalates als Magnesiumammoniumphosphat abgeschieden, zu Magnesiumpyrophosphat verglüht und ausgewogen.

Um den Gesamteisengehalt des Meteoriten zu bestimmen, wurde eine Probe mit Flussäure und Schwefelsäure zur Entfernung der Kieselsäure abgeraucht, der Rückstand mit Wasser aufgenommen und der geringe unlösliche Anteil abfiltriert. Dieser wurde mit Kaliumpyrosulfat aufgeschlossen und die Lösung der Schmelze mit der Hauptlösung vereinigt. Platinspuren, die aus den verwendeten Platingefässen herrühren konnten, wurden mit Schwefelwasserstoff abgetrennt. Im Filtrat wurde das Eisen mit Wasserstoffperoxyd oxydiert und die Hydroxyde mit Ammoniak gefällt. Der Niederschlag wurde gelöst, das dreiwertige Eisen nach Zimmermann-Reinhardt mit Zinn(II)-chlorid reduziert und anschliessend durch Titration mit Kaliumpermanganat bestimmt. Die Bestimmung des Anteils des metallischen Eisens wurde nach der Methode von Wilner-Merck durchgeführt. Sie beruht darauf, dass beim Kochen der Probe mit einer neutralen Quecksilber(II)-chloridlösung in einer Kohlendioxyd-Atmosphäre nur metallisches Eisen als Eisen(II)-ion in Lösung geht. Dieses wurde, nach Abfiltrieren des Rückstandes, mit Kaliumpermanganat titriert.

Zur Chrombestimmung wurde die Probe mit einem Natriumcarbonat–Natriumnitrat-Gemisch aufgeschlossen, die Schmelze mit Wasser ausgelaugt, mit wenigen Tropfen Alkohol bis zum Sieden erhitzt um das Manganat zu reduzieren, der Rückstand abfiltriert und gut mit heissem Wasser gewaschen. Das Filtrat enthielt das Chrom als Chromat. Die Extinktion dieser Lösung wurde in einem Elektrophotometer bestimmt. Der Chromgehalt ergab sich aus einer Eichkurve, die mit Hilfe natriumcarbonathaltiger Standardchromatlösungen aufgenommen worden war.

Auch der Titangehalt wurde colorimetrisch ermittelt. Dazu wurde die Probe mit Natriumcarbonat aufgeschlossen und, nach Entfernung der Kieselsäure, das Eisen mit schwefliger Säure reduziert. Mittels Kupferron wurde das Titan nebst wenig Eisen gefällt (Cunningham, 1933), der Niederschlag abfiltriert, verascht und mit Kaliumpyrosulfat aufgeschlossen. Die Schmelze wurde in Schwefelsäure gelöst und das Titan mit Wasserstoffperoxyd colorimetrisch bestimmt.

Zur Bestimmung der Alkalimetalle wurde die Probe mit Flussäure und Schwefelsäure zersetzt und nach Abrauchen der Schwefelsäure längere Zeit bei 900° geglüht (Cornes, 1944). Dabei wird der Grossteil der Sulfate thermisch zerlegt und man erhält die wasserunlöslichen Oxyde. In den wässerigen Auszug gehen nur die Alkalisulfate, kleine Mengen Calciumsulfat und unzersetzt gebliebenes Magnesiumsulfat. Der Rückstand wurde nun mit heissem Wasser ausgelaugt und die Oxyde abfiltriert. Im Filtrat wurde das Magnesium mit Barytwasser gefällt und das Calcium und überschüssiges Barium mittels Ammoniumcarbonat

abgeschieden. Durch Eindampfen mit Schwefelsäure wurden die Alkalien in die Sulfate übergeführt und die Summe Natriumsulfat + Kaliumsulfat ausgewogen. Nun wurde mit Essigsäure aufgenommen und aus der Lösung das Kalium mit Natriumtetraphenyloborat gefällt (Flaschka, 1952). Der so erhaltene Wert wurde auf Kaliumsulfat umgerechnet und durch Differenzbildung der Natriumgehalt errechnet.

Zur Ermittlung des Schwefelgehaltes wurde eine Probe mit einem Natriumcarbonat–Natriumnitrat-Gemisch aufgeschlossen, die Schmelze mit kaltem Wasser ausgelaugt und vom Rückstand abfiltriert. In dem mit Salzsäure angesäuerten Filtrat wurde mit Bariumchlorid das Bariumsulfat gefällt.

Der Wassergehalt des Meteoriten wurde durch Trocknung einer Probe bis zur Gewichtskonstanz bei 110° bestimmt.

Die Ergebnisse der chemischen Analyse sind in der folgenden Tabelle zusammengestellt:

	(%)		(%)
Fe	16,30	MgO	24,02
Ni	1,33	CaO	1,48
Co	0,08	Na_2O	1,03
FeS	5,59	K_2O	0,14
SiO_2	37,30	P_2O_5	0,09
TiO_2	0,12	H_2O^-	0,16
Al_2O_3	4,48	Cr_2O_3	0,39
MnO	0,30	C	0,34
FeO	7,46	Summe	100,61

Fe_{total}: 25,65%

Der Borgehalt des Meteoriten wurde von H. Harder (Sedimentpetrographisches Institut der Universität Göttingen) spektralanalytisch bestimmt. Es ergab sich ein Wert von

$$1{,}6 \cdot 10^{-5}\ \text{g}\ B_2O_3/\text{g}$$

Die Einzelheiten dieses Verfahrens erscheinen in einer gesonderen Arbeit.

Für ihre Hilfe bei der Ausführung der Analysen möchte ich Fräulein U. Scheerer herzlich danken.

Literatur

Berg R. (1935) *Das Oxychinolin "Oxin"*. Stuttgart.
Cornes J. J. S. (1944) *Analyst* **69**, 237.
Cunningham Th R. (1933) *Industr. Engng. Chem. (Anal.)* **5**, 305.
Flaschka H. (1952) *Z. analyt. Chem.* **136**, 99.
Funk H. und Ditt M. (1933) *Z. analyt. Chem.* **93**, 291.

Geochimica et Cosmochimica Acta, 1959, Vol. 17, pp. 323 to 338. Pergamon Press Ltd. Printed in Northern Ireland

Der Meteorit von Breitscheid—III

Petrographische Untersuchung

H. Hentschel
Universität Mainz, Mineral.-petrogr. Institut, sowie
Hessisches Landesamt f. Bodenforschung in Wiesbaden

Abstract—The meteorite of Breitscheid is a grey-veined bronzite–olivine–chondrite containing nickel–iron and troilite.

It has a remarkably high volume of pores of about 10 per cent. The density of the solid is 3·7, of the stone as a whole 3·3.

The chondrules take about 20 per cent of the volume of the stone.

The ore minerals are: nickel–iron (kamacite and taenite), troilite, chromite, ilmenite and besides, in the melting crust, magnetite. Especially ilmenite—until recently doubtful as a constituent of meteorites—could be proved in a convincing manner.

The silicate constituents are: olivine, bronzite, clinopyroxene, plagioclase (?), glass and a few minerals which could not be identified.

The mineral composition and the fabric are described. In addition the mineral composition, calculated by chemical analysis, is given.

It is remarkable that troilite appears in two varieties one of which evidently is secondary, because it is always embedded in nickel–iron in a metasomatic manner.

Zusammenfassung—Der Meteorit von Breitscheid ist ein grauer geaderter Nickeleisen- und Troilit-führender Bronzit–Olivin–Chondrit.

Eigentümlich ist ihm ein hohes Porenvolumen von ca. 10%. Die Dichte des Steins ist 3,7, sein Raumgewicht 3,3.

Die Chondren machen etwa 20 Vol % des Steins aus.

Erzminerale sind: Nickeleisen, (Kamazit und Taenit) Troilit, Chromit, Ilmenit, in der Schmelzrinde ausserdem noch Magnetit. Insbesondere liess sich Ilmenit, —als Meteoritenmineral bis vor kurzem noch für unsicher geltend—, in gut bestimmbarer Form einwandfrei nachweisen. Die silikatischen Komponenten umfassen: Olivin, Bronzit, Klinopyroxen, Plagioklas (?), Glas und einige weitere unbestimmbar gebliebene Minerale. Mineralische Zusammensetzung und Gefüge werden beschrieben und durch den aus der Analyse berechneten Mineralbestand ergänzt. Beachtlich erscheint, dass Troilit in zweierlei Form auftritt, von denen die eine für sekundär gehalten wird, weil ihre Erscheinungsweise auf eine metasomatische Entstehung aus festem Nickeleisen hindeutet.

I. Äussere Merkmale des Meteoriten

Form und Aussehen einiger Bruchstücke des Meteoriten vermitteln die Abb. 1–3. Die feine Rauhigkeit der Kruste, sowie die teils glattflächige teils grubig ausgetiefte äussere Umgrenzung des Steins treten dabei ebenfalls in Erscheinung. Die flache rechtkantige Form des Meteoriten lässt sich aus dem Eckstück der Abb. 1 und 2 (linkes Objekt), sowie aus der aus drei Bruchstücken zusammengefügten Partie der Abb. 3 ebenfalls erkennen. Auch der bedeutende Farbkontrast zwischen Kruste und Steininnerem wird durch die Abbildungen annähernd naturgetreu wiedergegeben.

1. *Die Kruste*

Die Schmelzrinde des Meteoriten ist von nichtglänzend matter dunkelschwarzgrauer Farbe. Ihre Rauhigkeit beruht auf sehr schmalen Schmelzstriemen, die gratartig Bruchteile eines Millimeters aufragen und eng in Millimeterabständen nebeneinanderliegen. Ausserdem verzweigen und vereinigen sich diese Schmelzstriemen und bilden dadurch eine Art Netzwerk, das der Rinde bei Betrachtung mit einer Lupe ein fast schuppiges Aussehen verleiht.

Die Dicke der Rinde beträgt etwa 0,2 mm. Sie ist ausschliesslich Aussenhaut

des Steins. Nirgends wurde ein Vordringen in das Steininnere beobachtet. Über ihr mikroskopisches Gefüge wird weiter unten berichtet.

2. *Das Steininnere*

Zur Kruste steht die hellgraue Innensubstanz des Meteoriten in auffälligen Farbkontrast. Die verschiedenen Mineralkomponenten insbesondere die Opakminerale Nickeleisen und Troilit sowie die Chondren bewirken eine Sprenkelung im Farbton. Kleine vereinzelte Rostflecken tragen auch dazu bei, obwohl Rost auf den Bruchflächen der abgebildeten Stücke kaum in Erscheinung tritt. Deutlich heben sich aber vor allem auf frischen Bruchflächen des Meteoriten die reichlich vorhandenen Chondren mit ihrer etwas dunkler grauen Farbe aus der übrigen Masse heraus.

Neben dieser Sprenkelung und Chondreneinstreuung zeigt die Meteoritensubstanz eine Aufgliederung in zwei etwas verschiedenfarbig getönte Anteile, einen hellgrauen Anteil und einen etwas dunkler grauen, die sich gegenseitig durchdringen. Diese Durchdringung lässt keine Regelmässigkeit irgendwelcher Art erkennen. Gewisse Teile des Steins bestehen ganz und gar aus der helleren Substanz; in anderen Partien herrscht diese zwar noch vor, wird aber vereinzelt von der dunkelgrauen Substanz adernartig durchsetzt (Abb. 4). Die dunkelgraue Substanz kann aber auch weitaus dominieren. Dann nimmt der hellgraue Anteil nur noch kleine inselartige Bezirke ein, die teils scharf begrenzt und eckig erscheinen, teils auch mit unscharfen verwaschenen Konturen in der dunkelgrauen Substanz "schwimmen" (Abb. 5).

Die Meteoritensubstanz erscheint damit als inhomogen. Aber diese Inhomogenität beruht nur, um einen mikroskopischen Befund vorwegzunehmen, auf einer geringen dunkleren Einfärbung der Grundmassebasis in der dunkelgrauen Substanz, ohne dass sonst Unterschiede in der Zusammensetzung oder im Gefüge zwischen der hellgrauen und der dunkler grauen Gesteinsmasse festgestellt werden konnten: im Dünnschliff lassen sich die beiden Substanzen praktisch nicht mehr unterscheiden, auch ihre gegenseitigen Abgrenzungen sind nicht mehr erkennbar.

Worauf diese verschiedene Einfärbung beruht, wann und wie sie erfolgte, das sind Fragen, die von mir nicht beantwortet werden können. Die Beobachtung aber, dass an Haarrissen im Stein die dunkelgraue Substanz scharf absetzt, gibt einen gewissen Hinweis dafür, dass die hellgraue Substanz wohl die ursprünglich zunächst allein vorhandene war, und dass Teile von ihr durch irgend eine Einfärbung, Infiltration, Durchgasung oder durch einen ähnlichen Prozess einer minimalen Stoffzufuhr stellenweise in die dunkelgraue Substanz überführt wurde, nachdem der Stein längst im wesentlichen seinen jetzigen Gefüge- und Mineralbestand erlangt hatte.

Die fleckenartige Verteilung von hell- und dunkelgrauer Substanz nach der herkömmlichen Auffassung als Brekziengefüge anzusehen, und die hellen Partien, wie sie etwa Abb. 5 zeigt, als Fragmente in einer dunkelgrauen Matrix anzusprechen, wie sich solche Deutung auf den ersten—oberflächlichen—Blick hin anbietet, halte ich für unrichtig. Sie widerspricht bei genauerer Beobachtung dem Sachverhalt: es sind keine Grenzen von "Fragmenten" eines Brekziengefüges feststellbar.

Abb. 1.

Abb. 2

Abb. 1 und 2. Zwei Bruchstücke des Meteoriten. Stück *A*, rechts: 206.1 g und Stück *B*, links: 46 g Vorder- und Rückseitenansicht (natürl. Grösse).

Abb. 3. Drei Bruchstücke des Meteoriten, von rechts nach links: Stück *A* 206,1 g, *C* 140,7 g und *E* 18,5 g; aneinanderpassend zusammengefügt (natürl. Grösse).

Abb. 4. Eine Bruchfläche des Meteoriten, vorwiegend aus hellgrauer Substanz bestehend, mit dunkelgrauer "Aderung". Die schwarzgraue Sprenkelung wird von Nickeleisenkörnern (mit etwas Rost) und Troilit, sowie von Chondren verursacht. Stück *D* 33 g (natürl. Grösse). (Aus diesem Stück wurden die Dünn- und Anschliffe gefertigt.)

Abb. 5. Eine Bruchfläche des Meteoriten, vorwiegend dunkelgraue Substanz zeigend, mit Inseln von hellgrauer Substanz. Pseudo-Brekzienstruktur! Stück *C* 140,7 g (natürl. Grösse).

Die Steinmasse hat einen festen inneren Zusammenhalt, sie ist nicht krümelig, auch die Chondren lösen sich nicht leicht aus ihrem Verband. So geht ein beim Zerschlagen des Steins entstehender Bruch teils mitten durch Chondren hindurch, teils umläuft er diese.

II. Das Gefüge

Das Gefüge wird im wesentlichen ausser durch die Anwesenheit von Chondren durch den innigen Verband von metallischen bzw. metallsulfidischen mit silikatischen Mineralkörnern bestimmt.

Grösste und auffälligste Gefügekomponente sind die Chondren, über deren Interngefüge und mineralische Zusammensetzung weiter unten berichtet wird. Sie machen nach überschlägiger Messung etwa 20 Vol % der Gesamtmasse der Meteoritensubstanz aus. Die Grösse dieser annähernd kugeligen oder ellipsoidischen Gebilde, die gelegentlich auch nur als Teilstücke vorliegen, schwankt vorwiegend zwischen 0,5–1,5 mm Durchmesser. Einzelne wenige Chondren erreichen aber bis 4 mm Durchmesser. Bei den kleineren Chondren und den Bruchstücken ist die Begrenzung gegen die umhüllende Substanz im mikroskopischen Bild nicht immer gut zu erkennen, und es lässt sich manchmal nicht sicher entscheiden, ob ein vollständiges Chondrum oder nur ein Teil eines solchen vorliegt.

Die silikatische Substanz ausserhalb der Chondren besteht aus einem unregelmässigen Haufwerk recht ungleichgrosser Kristallkörner, unter denen grössere teils idiomorphe, teils nichtidiomorphe Kristalle einsprenglingsartig hervortreten. Ihre Grösse übersteigt aber nicht 1 mm maximalen Korndurchmesser. Die Grundmasse umfasst kleinere teils rundliche, teils eckig bruchstückartige Kristallkörner bis hinab zu Korndurchmessern von einigen μ, die in eine Matrix eingebettet sind, die teils aus feinstem Mineralgrus, teils bzw. stellenweise aber auch aus einem bräunlich durchsichtigen meist aber aus getrübtem oder fast undurchsichtigem Glas besteht.

Dieses bei terrestrischen Erstarrungsgesteinen nicht auftretende Gefüge wird seit langem bei Steinmeteoriten als tuff-, mörtel- oder mikrobrekzienähnlich beschrieben, obwohl trotz der Ähnlichkeit mit den Gefügen klastischer Gesteine wie Tuffen oder Brekzien die Übereinstimmung nicht weit geht.

Das starke Überwiegen des silikatischen Anteils über den nichtsilikatischen Anteil der Erzminerale (vgl. S. 322) begünstigt, dass die beiden Haupterzkomponenten (Nickeleisen und Troilit) nicht als zusammenhängendes Gewebe sondern als isolierte Einzelkörner auftreten, die in das silikatische Korngemenge schmitzenartig eingestreut sind. Die unregelmässig buchtige z.T. auch stark zergliederte Form dieser Erzmineralkörner stimmt etwa mit dem Bild von Zwickelräumen überein, die im Erstarrungsgefüge eines magmatischen Gesteins von den letztausgeschiedenen Mineralphasen eingenommen werden.

Besser als jede Beschreibung vermitteln die Bilder eines An- und Dünnschliffes eine anschauliche Vorstellung des Korngefüges (Abb. 6 u. 7).

Eine Besonderheit des Gefüges wird aus diesen Mikrofotographien allerdings nicht sichtbar und ist auch auf Bruchflächen weder mit freiem Auge noch mit der Lupe erkennbar: der Stein hat ein nicht unbeträchtliches *Porenvolumen*, das 10% übersteigt. Diese Porigkeit wäre wohl der direkten Beobachtung überhaupt

entgangen, wenn sie nicht bei der Dichtebestimmung festgestellt worden wäre (siehe S. 335). Dadurch aufmerksam geworden, liess sich der Porenraum zwar nicht im Dünnschliff, dafür aber im Anschliff mikroskopisch gut erkennen. Es sind jene Partien, die mit dem zur Schliffimprägnation verwendeten Harz (Canadabalsam oder Kunstharz) gefüllt sind und sich durch das auch noch gegenüber den Silikaten geringe Reflexionsvermögen des Harzes bemerkbar machen. Sie durchschwärmen netzartig und nesterartig die silikatischen Bereiche des Meteoriten. Genau erfassbar sind sie aber deswegen nicht, da sie sich nicht von jenen beim Schleifprozess unvermeidbaren Ausbrüchen kleiner Mineralfragmente unterscheiden lassen, die bei der Imprägnation mit Harz zugekittet wurden.

Es muss wohl als problematisch angesehen werden, ob die Poren insgesamt seit der Bildung der Silikatminerale bestanden haben, oder ob sie gänzlich oder zum Teil später durch Auswanderung von Mineralsubstanz entstanden sind.

Da anscheinend der *quantitativen* Erfassung von Hohlräumen in Steinmeteoriten bislang wenig Beachtung geschenkt worden ist, obwohl vielfache Hinweise auf poröse, bröckelige und lockere Beschaffenheit von Meteorsteinen in der älteren Literatur anzeigen, dass die Existenz von offenen Zwischenräumen im Steingefüge durchaus bekannt war, wurde vergleichsweise am Steinmeteorit von Carcote eine Bestimmung des Porenvolumens vorgenommen. Es ergab sich dabei (unter den gleichen Versuchsbedingungen) ein Hohlraum von nur 0,4%.

Inzwischen sind von russischer Seite offenbar systematische Untersuchungen über die Porosität von Meteoriten in Gang gekommen, wie man jüngst aus dem Referat von Krinow (1957) über die 7. russische Meteoritenkonferenz 1956 in Moskau erfahren konnte. Darnach haben Burkser und Alekseewa für die Porosität in Steinmeteoriten Werte ermittelt, die zwischen 6–18% liegen.

III. Der modale Mineralbestand

Die Erzminerale

Beobachtet wurden Nickeleisen, Troilit, Chromit, Ilmenit und Magnetit; letzteres Mineral ausschliesslich in der dünnen Schmelzrinde des Meteoriten. Die vier erstgenannten Minerale sind im Anschliff durch ihr verschiedenes Reflexionsvermögen und weitere spezifische Merkmale gut zu unterscheiden (Abb. 7, 13, 14 und 15).

Nickeleisen. Dieses Mineral hat das beste Reflexionsvermögen im Anschliff des Meteoriten, es erscheint reinweiss. Die Korngrösse übersteigt nicht 1 mm maximalen Durchmesser. Anzeichen von Innenstrukturen sind ohne Anschliff-Ätzung nicht wahrnehmbar. Die grösseren Körner sind stets xenomorph und von buchtig oder fingerig zergliederter Form. Sie liegen inmitten silikatischer Substanz, aber stets ausserhalb der Chondren, und vertreten dabei gewissermassen Teile der Grundmasse. Häufig treten dabei nesterartige Häufungen auf (vgl. Abb. 6 und 7). Kornverwachsungen mit Troilit sind selten, dafür aber sind filigrane Durchwachsungen von Nickeleisen und Troilit recht häufig. Ich halte sie für Verdrängungen von Nickeleisen durch Troilit (vgl. S. 328). Ausser den grösseren Nickeleisenkörnern enthält die Grundmasse, nun auch innerhalb der Chondren, zahlreiche, kleinere rundliche bis angedeutet eckige Einzelkörner meist von 10–20 μ oft aber auch nur von 1–5 μ Grösse. Diese finden sich auch in der glasigen Matrix, die

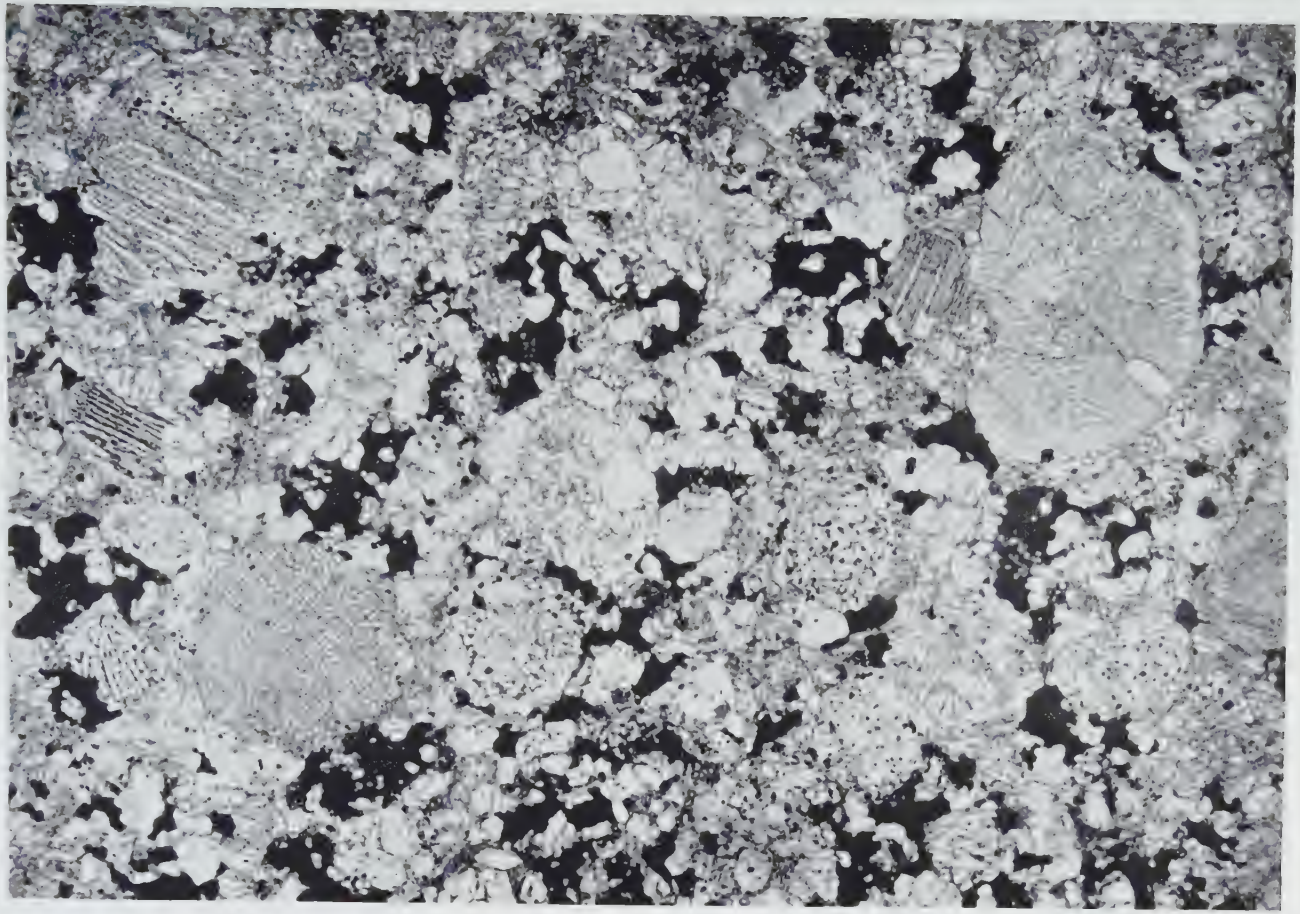

Abb. 6. Dünnschliff im durchfallenden nichtpolarisierten Licht. Schwarz: Nickeleisen, Troilit, Ilmenit und Chromit. Weiss: Kristalle der Silikate (vorwiegend Olivin und Bronzit). Rundliche Gebilde: mono- und polysomatische Olivin- und Bronzit- Chondren. Grau: Grundmasse. Schliff Nr. 3704 (25-fach).

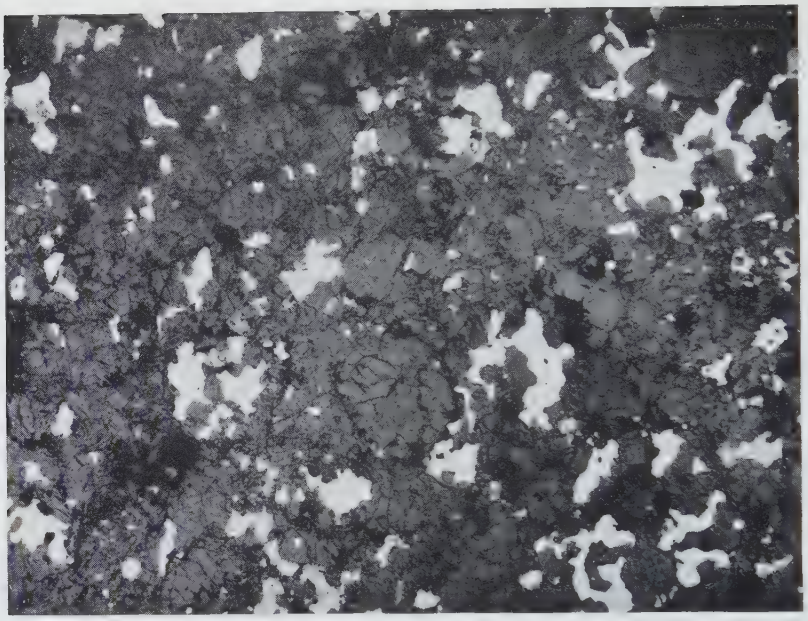

Abb. 7. Anschliff im auffallenden nichtpolarisierten Licht. Reinweiss: Nickeleisen; grauweiss meliert: Troilit; grau (mit glatter Oberfläche): Chromit (nur drei Kristallkörner); schwarzgrau: silikatische Substanz einschl. der Chondren; tiefschwarz: Ausbrüche und Porenraum. Anschliff Nr. 25 (25-fach) (Die gleiche Vergrösserung wie Abb. 6!).

Abb. 8. Nickeleisenkorn, Kamazit geätzt, mit drei Systemen NEUMANN'scher Linien; Anschliff im auffallenden Licht (100-fach).

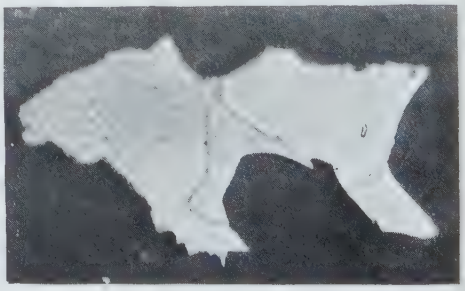

Abb. 9. Taenit-Korn in Kamazit. Durch unscharfe Mikroskop-Einstellung in den Konturen verstärkt. – Anschliff im auffallenden Licht (230-fach).

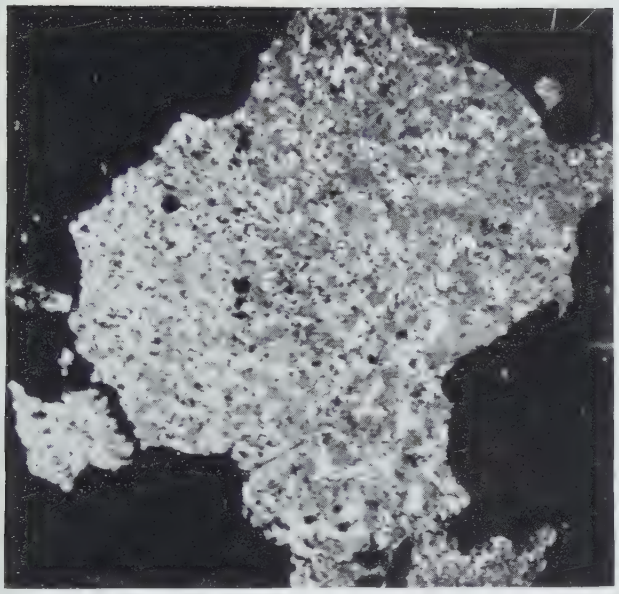

Abb. 10. Troilit-Korn, aus einem Pflasteraggregat kleiner Einzelkristalle bestehend, inmitten von Silikatsubstanz (schwarz). Anschliff im polarisierten Licht zwischen gekreuzten Nicols (330-fach).

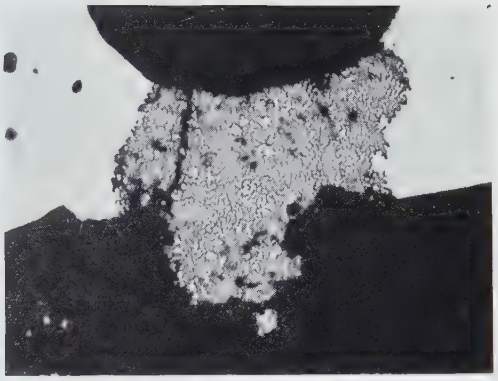

Abb. 11. Nickeleisen (weiss), verdrängt durch sekundären Troilit (dunkelgrau, löcherig) mit Inselchen von Nickeleisen. (Der Troilit durch Anlaufen stark gedunkelt). Schwarzer Anteil: Silikatsubstanz. Anschliff im auffallenden (nicht-polarisierten) Licht (300-fach).

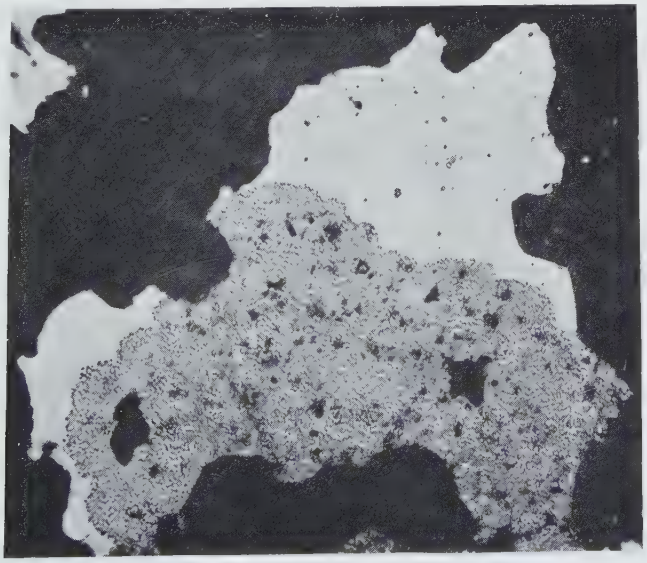

Abb. 12. Sekundärer Troilit (wie Abb. 17) in kamazitischem und taenitischem Nickeleisen. Die Grenze zwischen Taenit und Kamazit ist durch unscharfe Einstellung des Mikroskops sichtbar gemacht. Anschliff im auffallenden Licht (175-fach).

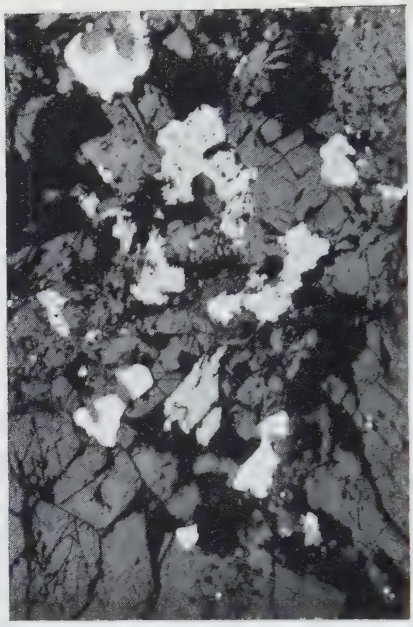

Abb. 13. Paragenese: Nickeleisen (weiss), Troilit (grauweiss meliert), Chromit (grau; zwei grössere nichtidiomorphe Kristallkörner) und silikatische Substanz (schwarzgrau). Ausbrüche sind schwarz. Anschliff im auffallenden Licht (75-fach).

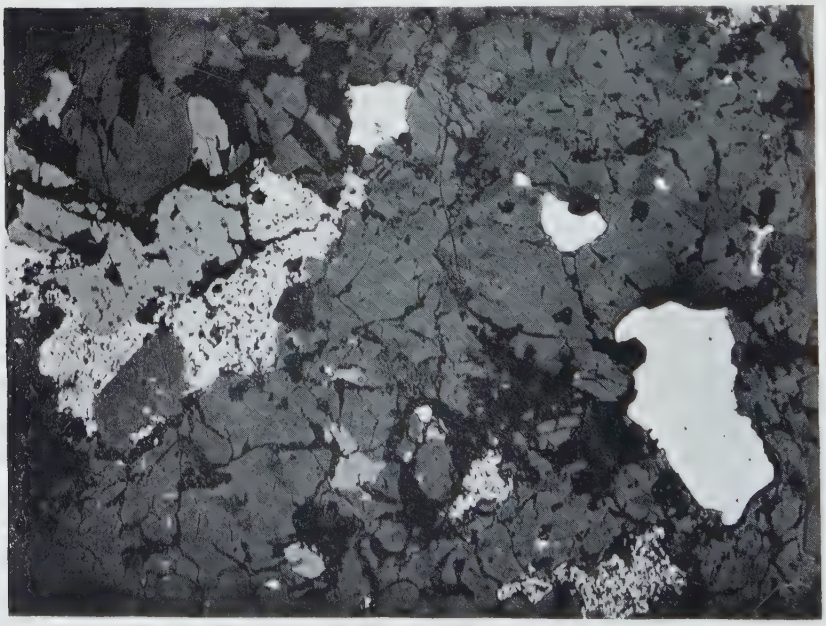

Abb. 14. Paragenese: Nickeleisen (weiss), Troilit (grauweiss meliert), *Ilmenit* (grau: ein grosses Korn mit Spaltrissen), Chromit (grau wie Ilmenit: einige kleine Körner), silikatische Kristalle (dunkelgrau, sehr viel). Silikatisches Glas (dunklergrau, in kleinen Flekken und Schmitzen). Schliffausbrüche und Porenraum: schwarz. Anschliff (No. 25) im auffallenden Licht (175-fach).

feine Fugen in skelettigen Olivinkristallen oder in strahlig gewachsenen Pyroxen-Aggregaten erfüllt. Planimetrierungen von Anschliffen ergaben bei Vernachlässigung der Kleinkörner einen Gehalt von 6–7 Vol % Nickeleisen (vgl. S. 325).

Nach Ätzung mit alkoholischer Pikrinsäure erscheinen bei vielen grösseren Körnern Neumann'sche Linien; selbst Kleinkörner von nicht mehr als 0,2 mm Durchmesser weisen sie auf. Widmannstättensche Figuren wurden dagegen nicht beobachtet. Das Nickeleisen dürfte sonach im wesentlichen aus Kamazit bestehen. Die Ätzung lässt auch erkennen, dass die xenomorphen Nickeleisenkörner meistens *Einkristalle* sind (Abb. 8).

Für *Taenit* werden kleine unregelmässig geformte, saum- zacken- oder schmitzenartige Partien gehalten, die sehr selten randlich in kleineren Kamazitkörnern liegen und sich nach Farbe und Reflexionsvermögen kaum von diesem unterscheiden. Bei relieffreien Anschliffen sind sie kaum zu beobachten, aber bei ein wenig Reliefpolitur sind sie durch ihre über Kamazit liegende Härte deutlich wahrnehmbar (Abb. 9). Die Korngrösse liegt bei 0,1 mm Ø, meist sogar niedriger, selten höher. Zunächst hielt ich dieses Mineral allerdings für Cohenit. Eine spezifische Cohenit-Ätzung (Perry, 1944) verlief aber negativ. Ausserdem liess sich in einem Fall beobachten, dass sekundärer Troilit (siehe weiter unten) gleichmässig auf Kamazit wie auch auf einem benachbarten vermeintlichen Cohenitkorn entwickelt war, ohne offenbar von der Korngrenze und der Verschiedenheit der beiden Minerale Notiz zu nehmen (Abb. 12). Solches Verhalten dürfte sich für Taenit wohl erwarten lassen, kaum aber für Cohenit.

Die Körner von Nickeleisen sind, wie sich am hier untersuchten Material feststellen liess, Ausgangspunkt für die Bildung von *Rost*, einer sehr lästigen, leider aber häufigen Begleitkomponente der Steinmeteorite. Soweit Stücke vor Berührung mit Wasser verschont geblieben sind, weist frisches Material des Breitscheid-Meteoriten allerdings kaum Rost auf, aber es bedarf bei Benetzung mit Wasser zu seiner Entstehung kaum Stunden, wie bei nasser Schliffherstellung festgestellt werden konnte. Das entstehende Eisenhydroxyd bildet unregelmässige Höfe um die Nickeleisenkörner. Nicht unwesentlich begünstigt dürfte die Rostbildung im Breitscheidmeteoriten dadurch sein, dass der beträchtliche Porenraum sowohl das Wasser begierig kapillar aufsaugt und damit für eine intensive intergranulare Benetzung sorgt als auch Platz für Lösung und Wiederabsatz des Eisens reichlich verfügbar hält. Weitere Begünstigung mag die Rostbildung durch eventuell anwesende Spuren flüchtiger Komponenten (Cl, F) erfahren, die im Porenraum frei vorhanden oder an den Wandungen adsorptiv gebunden sein mögen.

Nur ein schmaler Streifen von ca. 1 mm Breite unter der Schmelzrinde wird von der Verrostung gemieden. Das hängt vermutlich irgendwie mit der Erhitzung dieses Bereichs bei der Entstehung der Schmelzrinde während des Fluges durch die Atmosphäre zusammen. Möglicherweise wurden dabei auch Spuren rostfördernder flüchtiger Komponenten aus diesem rindennahen Teil des Steinmeteoriten vertrieben.

Die Rostverfärbung erschwert die Dünnschliffmikroskopie von Steinmeteoriten, während sie im Anschliff praktisch überhaupt nicht in Erscheinung tritt. Eine Behandlung der Dünnschliffe vor dem Eindecken mit einer wässerigen Lösung

von Natriumdithionit als Bleichungsmittel hat sich dabei sehr bewährt, sogar noch bei starken und sehr alten Verrostungen, wie sich z.B. erfolgreich bei Material des Carcote-Meteoriten erproben liess.

Der Troilit. Verhält sich nach Korngrösse und Kornform etwa wie Nickeleisen. Sein Mengenanteil ist aber wesentlich kleiner: 4.5 Vol % wurden planimetrisch ermittelt. Durch seinen cremestichigen Farbton hebt sich dieses Mineral im Anschliff, vor allem wenn dieser etwas angelaufen ist, sehr deutlich von Nickeleisen ab (vgl. Abb. 7 und 13). Dazu kommt eine stets vorhandene Löcherigkeit der Troilitkörner, die dem Nickeleisen ganz fremd ist. Vor allem aber ist Troilit durch seine im reflektierten polarisierten Licht (X Nicols) gut hervortretende Doppelbrechnung gekennzeichnet. Letztere macht auch deutlich, dass die Troilitkörner nicht wie die des Nickeleisens aus Einkristallen bestehen, sondern dass sie sich ausnahmslos aus einem Vielkristallaggregat zusammensetzen, einem Pflastermosaik von Kleinkristallen mit etwa 10 μ Korndurchmesser (Abb. 10). Die erwähnten feinen Löcher inmitten des Troilits sind dabei an die Korngrenzen der kleinen Einkristalle gebunden.

Das Vielkristallaggregat der Troilitkörner ist für ein aus einer Schmelze stammendes primäres Erstarrungsprodukt ungewöhnlich. Es liegt nahe, an einen Kornzerfall im festen Zustand zu denken, wie ihn etwa ein Modifikationswechsel beim Übergang von einer Hoch- zu einer Tieftemperaturform verursachen könnte. Polymorphie von FeS ist seit langem bekannt: die bei 970 liegende Umwandlung könnte dafür vielleicht in Frage kommen.

Der Aufbau der Troilitfelder aus Kleinkristallen ist schon bekannt. Er wird u.a. von Hugi (1930) vom Meteoriten von Ulmitz beschrieben und mit einer allerdings nicht sehr deutlichen Abbildung belegt.

Während die hier ins Auge gefassten Troilitkörner normalerweise isoliert inmitten der Silikatsubstanz liegen und nur selten an Nickeleisenkörner grenzen, ist ein beträchtlicher Mengenanteil des Troilits ganz an Nickeleisen gebunden, und zwar sitzt dieser Anteil wie ein löcheriger Schwamm inmitten von Nickeleisen (Abb. 11 und 12) Dieser *sekundäre Troilit*, wie ich ihn nennen möchte, stellt meines Erachtens eine Verdrängung von Nickeleisen durch Troilit dar. Meist vom Rand eines Nickeleisenkorns ausgehend, hat sich Troilit dabei deltaartig in Nickeleisen vorgeschoben und ausgebreitet, hat zugleich aber winzige rundliche oder zungenartige Inseln von Nickeleisen von einigen μ Grösse bestehen lassen.

Diese Restinseln mögen das bei der Sulfurierung des Nickeleisens nicht mit aufgenommene Nickel in einem besonders Ni-reichen Eisen enthalten (sie mögen vielleicht sogar aus Taenit bestehen) und damit ihre Existenz auf eine ähnliche Weise begründen wie die Quarz-"Würmchen" im Myrmekit bei der metasomatischen Verdrängung von Kalifeldspat durch Plagioklas in metamorphen Gesteinen.

Alle Stadien dieses Vordringens bis zur gänzlichen Erfüllung eines Nickeleisenkorns lassen sich zahlreich in einem einzigen Anschliff beobachten. Dennoch sind so entstandene sekundäre Troilitkörner infolge der zahlreichen darin enthaltenen kleinen Rückstandsinseln von Nickeleisen nicht mit primärem Troilit zu verwechseln, da dieser gänzlich frei von Nickeleisen-Einschlüssen ist.

Gefügebilder ganz analog dieser Verwachsung "sekundären" Troilits sind bei terrestrischen Gesteinen (insbesondere aus der Gruppe der metamorphen Gesteine)

sowie bei Erzmineralgemengen eine sehr bekannte Erscheinung, und ihre Deutung als eine Verdrängungserscheinung (gelegentlich auch als eine Entmischung aus fester Phase) ist weitgehend anerkannt (vgl. S. 336).

Sekundärer Troilit zeigt aber wie primärer das gleiche innere Pflastermosaik eines Vielkristallaggregates sehr kleiner Einkristalle, d.h., der Kornzerfall hat den sekundären wie primären Troilit in gleicher Weise betroffen. Sollte dieser Kornzerfall, wie vermutet wurde, tatsächlich auf einen Modifikationswechsel zurückgehen, so stünde fest, dass die metasomatische Verdrängung des Nickeleisens durch sekundären Troilit in der Hochtemperaturmodifikation von FeS erfolgt ist.

Aus einer Anschliffintegration, die sich nur auf den Anteil primären und sekundären Troilits bezog, ergab sich:

76,5% primärer und 23,5% sekundärer Troilit.

Bei dieser Messung wurden allerdings die kleinen Restinseln von Nickeleisen in den Feldern von sekundärem Troilit mit übermessen. Deren Anteil schwankt beträchtlich; er liesse sich aber infolge der geringen Grösse dieser Inselchen nur mit einem unverhältnismässig hohen Zeitaufwand einigermassen zuverlässig ermitteln. Man kann sich mit einer rohen Schätzung begnügen, da der mögliche Fehler bei der Gesamtintegration des Troilits wahrscheinlich wesentlich grösser ist und wenig Garantie besteht, ob bei der Vermessung eines Anschliffs schon der Mittelwert für den Meteoriten erreicht wurde. Rechnet man mit 10–20% restlichem Nickeleisen innerhalb des sekundären Troilits, so reduziert sich dessen Anteil auf *ca* 20% des Gesamtgehalts an Troilit. Die Grenzen etwas weit genommen, ergibt sich damit, dass 1/4–1/5 der Troilitmenge *sekundärer* Entstehung ist.

Neben dem primären und sekundären Troilit der Grosskörner (Korndurchmesser 1 mm–0,1 mm) finden sich, wie bei Nickeleisen, in den Mineralgrus und in die glasige Matrix der Grundmasse zahlreiche ausserordentliche kleine mehr eckig-idiomorphe als rundliche Troilit-Kristallkörner von 10–1 μ Korndurchmesser eingestreut, über deren primäre oder sekundäre Natur wegen ihrer geringen Grösse nicht mehr sicher entschieden werden kann.

Chromit. Bildet teils idiomorphe, teils unregelmässig gerundete Kristallkörner von 0,2–0,05 mm Korndurchmesser (Abb. 13 und 14). Im Anschliff ist dieses Mineral von Nickeleisen und Troilit durch Kornform, geringes Reflexionsvermögen, Isotropie und gute Politur leicht zu unterscheiden. Die für Chromit typischen braunroten Innenreflexe lassen sich allerdings nur äusserst selten beobachten. Auch im durchfallenden Licht wurden selbst bei besonders dünnen Dünnschliffen die Chromitkörner nicht braun durchscheinend, wie es Chromite aus terrestrischen Gesteinen sehr häufig zeigen.

Ausser diesen schon bei schwachen Mikroskopvergrösserungen erkennbaren häufigen, wenn auch nicht gerade sehr zahlreichen grösseren Körnern beherbergt die feinkristalline und die glasige Matrix der Grundmasse zahlreiche winzige idiomorphe Chromitkriställchen von 1–5 μ Ø. Dabei fällt auf, dass diese Einstreuung nicht gleichmässig ist, und dass kleine begrenzte Grundmasseteile z.B. auch der Bezirk eines Chondrums, besonders reich mit diesen winzigen Chromiten durchsetzt sind. Die Diagnose solch kleiner Körner ist allerdings etwas unsicher, wenn auch das geringe Reflexionsvermögen zumindest eine Verwechslung mit Nickeleisen oder Troilit völlig ausschliesst und die Übereinstimmung der Körner

unter sich nach Farbe und Reflexionsvermögen Gewissheit gibt, dass nur eine einzige Mineralphase die Kornhaufen bildet. Ähnlich reflektierende Erzminerale wie Magnetit und Ilmenit können bei diesen extrem kleinen Korngrössen von Chromit nicht zuverlässig unterschieden werden. Der kontinuierliche Übergang von diesen Kleinstkörnern zu den grösseren Chromitkörnern macht aber einen Irrtum unwahrscheinlich.

Eine Planimetrierung wurde nicht vorgenommen. Als dritthäufigstes Erzmineral rangiert Chromit seiner Menge nach deutlich mit Abstand nach Nickeleisen und Troilit. Diese Beobachtung steht in Einklang mit dem aus der Analyse berechneten Mengenverhältnis dieser Minerale (vgl. Tab. 1, S. 335).

Ilmenit. Einzelne wenige Erzkörner von teils idiomorpher, teils rundlicher Form mit einer zwischen 0,2 0,05 mm Ø liegenden Korngrösse wurden zuerst auch für Chromit gehalten, bis ihre Doppelbrechung, sowie ihre lamellare Verzwillingung und schliesslich auch ihr ein wenig besseres Reflexionsvermögen mit einem zart gelbrosafarbenen Ton erkannt wurden. Es handelt sich um Ilmenit. Reflexionsvermögen, Art der lamellaren Verzwillingung nach mehreren Flächenlagen, sowie Andeutung einer Spaltbarkeit oder Absonderung parallel zu der Verwachsungsebene der Lamellenzwillinge stimmen aufs beste mit Ilmeniten aus terrestrischen Gesteinen und Erzen überein, wenn auch die bei diesen häufig auftretenden Entmischungen in Form von Lamellen oder Disken von Hämatit und Spinellen hier gänzlich fehlen. Bei dem niedrigen Oxydationsgrad der Meteoritensubstanz wären diese auch gar nicht zu erwarten (Abb. 14 und 15).

Die etwas auffällig geringen Unterschiede im Reflexionsvermögen und in der Reflexionsfarbe (im auffallenden Licht) zwischen Ilmenit und Chromit mögen ihre Ursache darin haben, dass durch teilweisen Ersatz von Fe″ durch Mg im Ilmenit dieser etwas nach dem mit Ilmenit isomorphen Mineral Geikielith, $MgTiO_3$ (mit dessen geringerem Reflexionsvermögen) zu tendiert.

Noch vor kurzem galt Ilmenit als ein in Meteoriten nicht mit Sicherheit erkanntes Mineral. Judin (1958) hat wohl als erster diesen Zweifel endgültig beseitigt und in einer Reihe von Steinmeteoriten Ilmenit nachgewiesen.

Magnetit. Aus Magnetit bestehen die zahlreichen – idiomorphen Erzkörnchen (1–5 μ Ø), die in der dünnen schwärzlichen Schmelzrinde und nur auf diese beschränkt auftreten. Abb. 16 zeigt im Anschliff die buchtige, wohl infolge mehrfach erfolgten Abreissens ungleich dicke Schmelzrinde, unter der grössere Blasen ein weiteres Abreissen von Schmelzrindenteilen vorbereitet haben. Die mit Magnetitkriställchen besetzte äussere Zone dieser Schmelzrinde ist maximal 0,1 mm breit. Ausserhalb dieser Zone findet man nach dem Steininneren zu keine weiteren Körner dieses Minerals. (Wegen der Unterscheidung von sehr kleinen Chromitkriställchen vergleiche das bei Chromit gesagte.)

Die Silikatkomponenten

Olivin. Unter der silikatischen Substanz des Meteoriten dominiert dieses Mineral weitaus. Mit gut idiomorphen aber auch gerundeten Kristallen stellt es innerhalb und ausserhalb der Chondren den Hauptanteil auch der Einsprenglinge. Ausser völlig intakten Kristallen mit Korngrössen nicht über 1 mm Ø gibt es nicht wenig skelettig ausgebildete. Im extremen Falle kann ein skelettiger

Abb. 15. *Ilmenit*-Kristallkorn aus Abb. 14 stärker vergrössert und zwischen gekreuzten Nicols mit zwei Systemen von Zwillingslamellen. Unter dem linken Teil des Ilmenitkorns ein isotropes Chromitkorn (schwarzgrau). Umgebung des Ilmenitkorns: Troilit (grauweiss meliert) und Silikate (wolkig weiss-grau und schwärzlich). Anschliff im auffallenden Licht (300-fach).

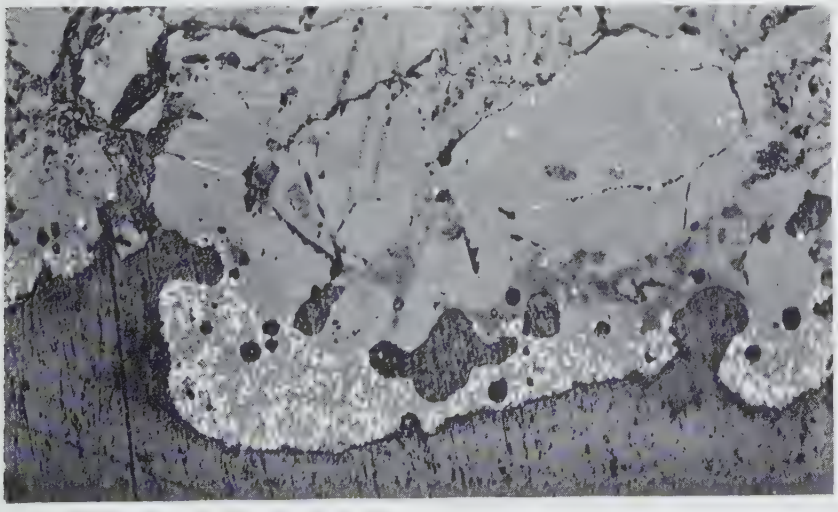

Abb. 16. Schmelzrinde quergeschnitten: buchtig und blasig, mit zahlreichen Magnetitkriställchen (weiss). Grau: silikatische Substanz mit feinen von Troilit ausgefüllten Haarrissen (grauweiss) in der Nähe der Schmelzrinde und mit feinen offenen Rissen (schwarz). Schwarzgraue Flecken innerhalb der silikatischen Substanz: primäres Glas. Schwarzgrau mit schwarzgrauen (Schleif)-Striemen: Kunstharzeinbettungsmittel: ausserhalb der Schmelzrinde und in Buchten und Blasen der Schmelzrinde. Dünn- Anschliff (Nr. 3705). im auffallenden Licht (170-fach)

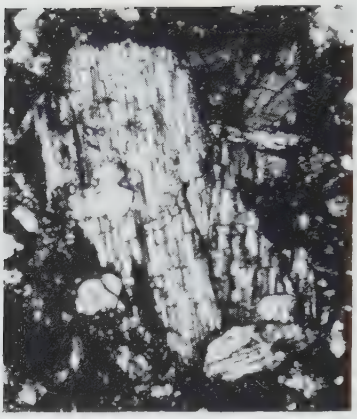

Abb. 17. Orthopyroxene, lamellar verzwillingt. Ein grösserer Kristall und links darunter, mit dem grösseren verwachsen, 2 kleinere Kristallkörner. (Umgebung der Orthopyroxene: Grundmasse mit kleinen Olivin- und Bronzitkörnern in feinkristalliner und glasiger Basis.) Dünnschliff (Nr. 3705) im durchfallenden Licht zwischen gekreuzten Nicols (60-fach).

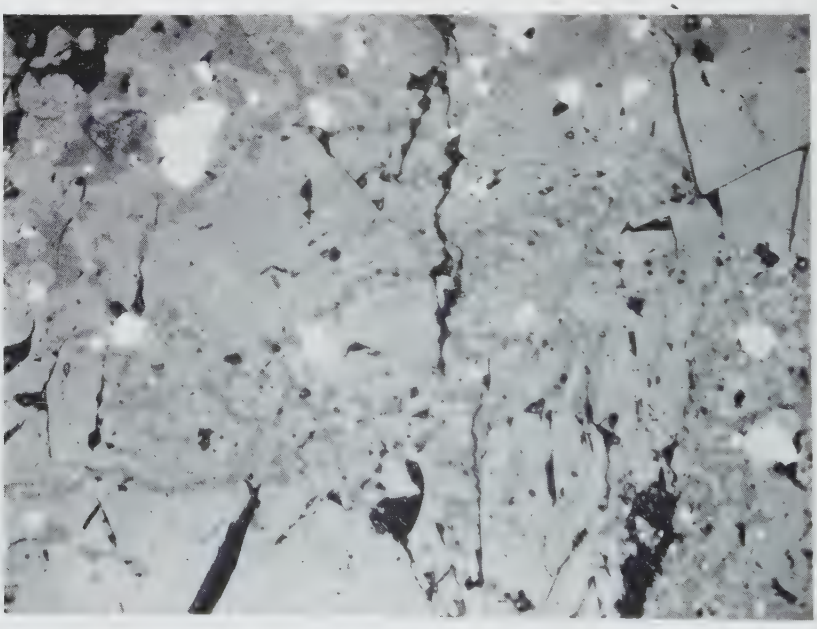

Abb. 18. Glas (dunkelgrau) in kleinen Flecken und in netz- und adernartigen Schmitzen inmitten des silikatischen Kristallkorngemenges (hellgrau). Einzelne Körner von Nickeleisen (weiss). Porenräume und Schliffausbrüche: schwarz. Anschliff imauffallenden Licht (200-fach).

Olivinkristall aus einer Vielzahl dünner paralleler gleichorientierter Platten bestehen (bis zu 35 wurden gezählt bei einer Lamellierung nach (010)), deren Zwischenraum (einige μ breit) von Glas oder einem feinkristallinen Gemenge ausgefüllt ist. Solche Olivine haben äusserlich gern ovale Form und bilden damit monosomatische Chondren.

Abgesehen von der Zwischenmasse bei Skelettkristallen ist der Olivin selbst völlig frei von Einschlüssen, seine frühe Bildung als Erstausscheidung damit anzeigend. Die Kristalle erscheinen im Dünnschliff bei durchfallendem Licht farblos und zeigen im polarisierten Licht keine Zonarstruktur. Vermessungen des Achsenwinkels liessen sich gut mit dem U-Tisch durchführen. Folgende Werte wurden gemessen:

$$2V_\gamma = 85°,\ 86°,\ 88°,\ 88°,\ 92°,\ 92°,\ 92°,\ 92°$$

Legt man einen Wert von $2V_\gamma = 90 \pm 2°$ zugrunde, so entspricht dies einem Mg-reichen Olivin der Zusammensetzung: Forsterit 90 ± 5 Fayalit 10 ± 5.

Orthopyroxen (*Bronzit*). Ist die zweithäufigste silikatische Mineralkomponente. Die Kristalle sind farblos, meist etwas langgestreckt bei idiomorpher oder auch xenomorpher Form mit einer Korngrösse, die auch bei einsprenglingsartigen Kristallen 1 mm maximalen Durchmesser nicht überschreitet. Die Einsprenglinge liegen entweder einzeln in der Grundmasse, z.T. haben sie dabei auch poikilitisch einzelne kleinere Olivinkörner eingeschlossen, oder sie sitzen, ein porphyrisches Gefüge bildend, zu mehreren in polysomatischen Chondren. Neben diesen kompakten Kristallen gibt es vor allem verschiedene Typen skelettiger Kristalle, die, einzeln oder aggregiert, stets aber dabei Chondren bilden. Darunter sind auch solche mit dem wohlbekannten excentrisch-strahligen Gefüge. Die Fugenfüllung skelettiger Kristalle besteht wie bei den Olivinen aus glasiger oder feinkristalliner Grundmasse, der reichlich winzige Körnchen (1–5 μ Ø) der Erzminerale Chromit, Troilit und Nickeleisen beigemengt sind.

Die Diagnose des Orthopyroxens bereitet gewisse Schwierigkeiten. Am wenigsten noch die Chondren-bildenden Skelettkristalle, die sich durch ihre durchweg niedrige Doppelbrechung gut von skelettigen Olivinen unterscheiden lassen. Bei nichtskelettigen Kristallen fehlen aber oftmals die Spaltrisse nach (110), so dass die Einmessung der optischen Orientierung (mittels U-Tisch) erschwert ist. Ausserdem tritt bei einsprenglingsartigen Kristallen ziemlich häufig eine merkwürdige Verzwillingung auf, die lamellierten Plagioklasen recht ähnlich sieht, die aber nicht über eine gut einmessbare konstante Verwachsungsebene verfügt. Vor einer Verwechslung mit Plagioklas schützt sicher der über $n = 1{,}65$ liegende mittlere Brechungsquotient. Dieser Wert wurde im Pulverpräparat durch Immersion ermittelt. Die Verzwillingung scheint nach (100) zu erfolgen. (100) ist auch Achsenebene. Bei Einstellung auf n_z im U-Tisch werden die Lamellen unsichtbar. Damit zeigen sich dieselben Befunde, die Scholtz (1937) von Hypersthenen aus südafrikanischen basischen Gesteinen beschreibt. Die von ihm gebrachte Abbildung ist nicht deutlich genug, um diese Verzwillingung für identisch mit der hier erörterten zu halten. Scholtz betitelt die Abbildung (Fig. 9, Tafel 23 seiner Arbeit) mit „obscure twinning in hypersthene." Ich könnte dasselbe zu der hier gezeigten Orthopyroxen-Verzwillingung sagen (Abb. 17).

Lacroix (1933) erwähnt auch Verzwillingungen von Bronzit-Hypersthen aus einem Meteoriten. Leider macht er darüber aber keine näheren Angaben.

Das verzwillingte Mineral hat durchweg niedrige Doppelbrechung mit grauweissen Polarisationsfarben. Damit schliesst sich aus, an eine Verwachsung von Orthopyroxen mit Klinopyroxen oder mit Diopsid, etwa auf Grund einer Entmischung, zu denken. Eine klinopyroxenische Entmischung oder Verwachsung gäbe sich sofort durch die stärkere Doppelbrechung des monoklinen Pyroxens zu erkennen.

U-Tisch-Vermessungen brachten für 2 V der nicht verzwillingten Orthopyroxene etwas streuende Werte, die z.T. auf Messschwierigkeiten zurückzuführen sind. Es wurde gemessen:

$$2V\alpha = 68 - 72°,\ 70°,\ 72°,\ 76°,\ 86°,\ 88°$$

Dem entspricht ein *Bronzit* mit einem Gehalt von 13–25 Mol % Ferrosilit. Die Menge des Bronzits ist beträchtlich, eine planimetrische Erfassung musste aber unterbleiben, da Verwechslungen mit Olivin (in Lagen mit niedriger Doppelbrechung) ohne U-Tisch nicht zu vermeiden gewesen wären. So kann nur gesagt werden, dass die aus der chemischen Analyse berechnete Menge im Einklang mit den Schliffbeobachtungen steht.

Klinopyroxen. Dieses Mineral begleitet in sehr geringer Menge den Orthopyroxen. Es bildet gelegentlich einen sehr schmalen Saum um grössere Orthopyroxenkristalle und ist an seiner stärkeren Doppelbrechung gut zu erkennen. Die Erscheinungsweise dieser Verwachsung ist dieselbe, die Jérémine und Lelubre (1952) beschreiben und abbilden (*Ibid.* Abb. 4, S. 220). Auch in strahligen Bronzitaggregaten (von Chondren) ist ein Klinopyroxen beteiligt, ohne dass sich seine Kornform deutlich erkennen liesse. Geschlossene einheitliche porphyrische Kristalle fehlen aber gänzlich, so dass sich optische Konstanten des Klinopyroxens nicht gewinnen liessen.

Plagioklas und andere Silikate. Ausser Olivin und Bronzit sind am Aufbau des Meteoriten noch weitere gering absorbierende durchsichtige Minerale beteiligt, aber es gelang nicht, eins davon mit Sicherheit zu identifizieren.

Zwillingslamellierter Plagioklas hat sich in Dünnschliffen nur mit einem einzigen xenomorphen Korn nachweisen lassen, und auch diese Bestimmung ist nicht ganz sicher.

Kleine zwickelfüllende xenomorphe Körner von niedriger Licht- und Doppelbrechung sind gar nicht so selten. Teils führen sie Spaltrisse, teils fehlen solche auch. Aber welches Mineral oder welche Minerale das sind, liess sich nicht ermitteln. Auch Pulverpräparate gaben keine Aufklärung. Es liess sich damit aber wenigstens feststellen, dass ein Mineral mit $1{,}538 < n < 1{,}56$ beteiligt ist, das schwache Doppelbrechung und 2-Achsigkeit mit grossem Achsenwinkel aufweist. Das könnte Plagioklas sein. Maskelynit wurde nicht mit Sicherheit beobachtet.

Ein weiteres unbekanntes Mineral bildet ferner in sehr geringer Menge kleine lichtbräunliche Tropfen (Mikrochondren), die excentrisch radialstrahlige Aggregierung aus feinsten gerade auslöschenden Nadeln mit positiver Längsrichtung zeigen.

Glas. Gehört mit zu den wesentlichen Komponenten des silitkaischen Anteils.

Es bildet die Basis der Grundmasse und sitzt überall innerhalb und ausserhalb der Chondren in den Zwickeln zwischen den grösseren und kleineren Kristallen von Olivin, Bronzit und der anderen nicht ermittelten Minerale, ferner inmitten des Mineralgruses der Grundmasse sowie in den Fugen skelettiger Olivine sowie skelettiger oder radialstrahliger Bronzite und Bronzitaggregate. Wegen des grossen Unterschiedes im Brechungsquotienten gegenüber Olivin und Orthopyroxen lässt sich die Glaskomponente im Dünnschliff nur schlecht, im Anschliff dagegen ausgezeichnet beobachten, nachdem erkannt worden war, dass Glas gegenüber vermutlich allen kristallisierten Silikaten deutlich niedrigeres Reflexionsvermögen im auffallenden Licht besitzt (Abb. 18). Wenn es gelegentlich reichlicher in Fugen grobskelettiger Olivine auftritt, kann es im durchfallenden Licht mit bräunlichem Farbton klar durchsichtig sein.

Aus Pulverpräparaten der silikatischen Meteoritensubstanz liess sich ermitteln, dass isotrope Substanz von etwa lichtbräunlicher Farbe mit $n < 1{,}585$, aber auch isotrope Substanz mit $n \sim 1{,}63$ vorhanden ist. Dieser relative hohe Brechungsquotient spricht nicht dafür, dass vorwiegend allein der normative Feldspatanteil durch die Glaskomponente vertreten ist. Ein Teil des Metasilikates, angereichert an $FeSiO_3$, wie es sich aus der Verschiebung der Schmelzzusammensetzung bei der Pyroxen-Kristallisation ergibt, ist möglicherweise mit in die Glaskomponente eingetreten und hat damit den hohen Brechungsquotienten bewirkt.

Es muss aber dahingestellt bleiben, ob die Glaskomponente überhaupt homogen ist. In den Chondren und ausserhalb von ihnen mögen die glasigen Anteile recht verschiedene Zusammensetzung haben.

Die Chondren. Form, Gefüge und Zusammensetzung der Chondren variieren beträchtlich. Wenn auch kugelige Form vorherrscht, so sind doch ellipsoidische Körper mit starker Excentrizität nicht selten, wie auch Chondren-Bruchstücke sowie Verwachsungen von Chondren mit nahezu planer Verwachsungsfläche. Über Grösse der Chondren und Mengenanteil wurde schon berichtet. Nach ihrer Zusammensetzung gibt es einfache, mono-mineralische Chondren, nur aus Olivin oder aus Bronzit bestehend, die teils monosomatisch, aus einem meist skelettigen einzigen Kristall, oder polysomatisch aus mehreren bis zahlreichen Kristallen derselben Art zusammengesetzt sind. Ferner sind komplexe Chondren vorhanden, die sich mit porphyrischem Gefüge aus einer kristallin-glasigen Grundmasse mit Einsprenglingen von Olivin und Bronzit aufbauen. Excentrisch-strahlige Chondren weisen die grössten Dimensionen auf. Sie bestehen stets aus Pyroxen. Auch skelettige Bronzitchondren, aus einem oder einigen wenigen Kristallen aufgebaut, gehören zu den grösseren Chondren. Skelettige Olivine dagegen bilden vorwiegend kleinere Chondren. Ein Dünnschliffbild lässt erkennen, dass viele Typen von Chondren ohne jede erkenngare Auswahl oder besondere Anordnung nebeneinander vorkommer (vgl. Abb. 6). Da neue Chondrentypen nicht beobachtet wurden, kann auf eine Wiederholung der zahlreichen Beschreibungen von Chondren hier verzichtet werden. Einschlägige Literaturhinweise enthält z.B. die schon zitierte Arbeit von Jérémine und Lelübre (1952).

Die Schmelzrinde. Die 0,1–0,2 mm dicke Schmelzkruste liess sich in Dünn-Anschliffen gut untersuchen. Über den Magnetitgehalt der äusseren Zone wurde unter diesem Mineral schon berichtet (vgl. Abb. 16).

Die Einbettungssubstanz der Magnetitkriställchen ist silikatisches Glas, das etwas weiter (nur vielleicht 0,1 mm) in das Innere des Steins vordringt als diese. Dieses Schmelzrindenglas, sekundär gegenüber dem Glas der Grundmassebasis des Steins, im Flug des Meteoriten durch die Atmosphäre aus den Silikaten des Meteoriten entstanden, weist im Anschliff bei auffallendem Licht etwa dasselbe Reflexionsvermögen wie die kristallisierten Silikate auf, während das primäre Glas deutlich ein geringeres Reflexionsvermögen zeigt. Im 0,2 mm Bereich der Schmelzrinde ist Troilit offenbar flüssig geworden. Er hat sich dabei entweder aus diesem Bereich ganz entfernt, oder sich in kleinen runden Kügelchen (Tropfen) wie auch als Auskleidung sehr feiner Haarrisse in der inneren Schmelzrindenzone, wieder ausgeschieden.

VI. Normativer Mineralbestand und chemische Betrachtungen

Die von Vilczek angefertigte Analyse wurde in der üblichen Weise auf normative Minerale umgerechnet.

Nur bei der Berechnung der Mengenanteile von Olivin und Orthopyroxen ist nicht, wie es sonst Brauch ist, dasjenige molekulare Verhältnis von MgO : FeO in Ansatz gekommen, wie es in der Bauschanalyse vorliegt, nachdem FeO um (die geringen) Beträge vermindert wurde, die den Mengen von TiO_2 und Cr_2O_3 molekularaequivalent sind. Es wurde vielmehr ein Olivin berechnet, wie er im Meteorit von Breitscheid tatsächlich auftritt, d.h., ein Forsterit-Fayalit-Mischkristall $Fo_{90}\,Fa_{10}$, (d.h. MgO : FeO = 9 : 1).

Die verbleibenden Restbeträge von FeO und MgO, zu Orthopyroxen verrechnet, ergeben, wie aus der Tabelle zu entnehmen ist, ein Molekularverhältnis von MgO : FeO = 76 : 24, während nach den kristalloptischen Daten bei den im Breitscheid-Meteorit auftretenden Orthopyroxenen ein Molekularverhältnis von Enstatit : Ferrosilit = ca. 80 : 20 realisiert ist. (vgl. S. 332). Die Übereinstimmung ist überraschend gut.

Beobachteter und berechneter Mineralbestand im Ganzen fügen sich gut zueinander, wenn man berücksichtigt, dass der errechnete Fledspatgehalt grösstenteils als Glaskomponente vorliegt. Lediglich für Phosphorsäure und Kohlenstoff wurden keine mineralischen Repräsentanten gefunden. Diese können mit ihrer geringen Menge in der Grundmasse aber der Beobachtung dadurch leicht entgehen, dass diese einerseits oft fast opak getrübt ist und dass andererseits das starke Relief der vorherrschenden hochlichtbrechenden Minerale Olivin und Pyroxen die unmittelbar an die Körner dieser Minerale angrenzenden Bereiche der Grundmasse optisch überdeckt.

Die Analyse des Breitscheid-Meteoriten fügt sich aufs beste in den Rahmen der "zuverlässigen" Analysen chondritischer Steinmeteorite ein, wie sie nach kritischer Überprüfung von Urey und Craig (1953) tabellarisch zusammengestellt worden sind. Bedient man sich dieser Tabelle, so finden sich 4 Meteorite, die dem von Breitscheid chemisch sehr verwandt sind, wie Tabelle 2 zeigt. Diese 4 Meteorite gehören übrigens, wie auch der hier beschriebene, zur "Hoch"-Gruppe von Urey und Craig. Als einzige Besonderheit erweist sich der hohe Al_2O_3 Gehalt des Breitscheid-Meteoriten. Es ist der höchste Wert in der Urey–Craig'schen

Tabelle 1. Chemische Analyse und daraus berechneter Mineralbestand (anal. Vilcsek, 1957)

	(%)		(%)
SiO_2	37,30	Or $(K_2O \cdot Al_2O_3 \cdot 6SiO_2)$	0,83
TiO_2	0,12	Ab $(Na_2O \cdot Al_2O_3 \cdot 6SiO_2)$	8,38
Al_2O_3	4,48	An $(CaO \cdot Al_2O_3 \cdot 2SiO_2)$	6,84
Cr_2O_3	0,39	Feldspat: $Or_5\ Ab_{53}\ An_{42}$	——16,05
FeO	7,46	En $(MgO \cdot SiO_2)$	18,08
MnO	0,30	Fs $(FeO \cdot SiO_2)$*	7,36
MgO	24,02	Orthopyroxen $En_{76}\ Fs_{24}$	——25,44
CaO	1,48		
Na_2O	1,03	Fo $(2MgO \cdot SiO_2)$	29,24
K_2O	0,14	Fa $(2FeO \cdot SiO_2)$*	4,71
P_2O_5	0,09	Olivin $Fo_{90}\ Fa_{10}$	——33,95
H_2O^-	0,16		
Fe	16,30	Merrillit $(3CaO \cdot Na_2O \cdot P_2O_5)$	0,22
Ni	1,33	Ilmenit $(FeO \cdot TiO_2)$	0,23
Co	0,08	Chromit $(FeO \cdot Cr_2O_3)$†	0,91
FeS	5,59	Accessorien	—— 1,36
C	0,34	Silikatischer Anteil (+ Acc.)	——76,80
	——100,61	Nickeleisen $(Fe_{92,5}, Ni_7, Co_{0,5})$	17,71
		Troilit	5,59
		Kohlenstoff	0,34
			——100,44

Spez. Gewicht α = 3,7
Raumgewicht γ = 3,31‡
Porenvolumen v = 10,5%‡

* MnO ist bei FeO mit verrechnet.
† Inclusive 0,19 Al_2O_3, das bei der Silikatberechnung übrig geblieben ist.
‡ Raumgewicht und Porenvolumen ergaben sich bei Ermittlung des spez. Gewichtes nach der Schwebemethode. Als Flüssigkeit wurde Aethanol verwendet, und es wurde die Menge von Aethanol extra bestimmt, die nach mehrere Stunden langem Eintauchen eines grösseren Bruchstücks unmittelbar nach Herausnahme aus der Flüssigkeit im äusserlich trockenen Stein enthalten war. Fehlerquellen lassen sich nach dieser Bestimmung nicht ganz ausschliessen. Da sie aber z.T. entgegengesetztes Vorzeichen haben, dürften sie das Endresultat zusammengenommen nicht sehr beeinflussen. Der wahre Wert für das Porenvolumen mag wohl am ehesten noch etwas höher liegen.

Tabelle der "Superior"–Analysen von Chondriten, wenn auch der Meteorit von Suwahib nahezu den gleichen Al_2O_3–Gehalt besitzt.

Nach der Prior'schen Gliederung der Meteoriten gehört der Breitscheid-Meteorit zur:

Chondritengruppe 2, dem Cronstad-Typ

Die von Prior (1919) dafür als massgeblich gehaltenen Zahlenwerte sind für den Breitscheid-Meteoriten:

Gew. % Nickeleisen		17,7
Verhältnis Fe : Ni im Nickeleisen	ca.	12
Verhältnis MgO : FeO i.d.Mg.-Silikaten	ca.	6

Diese Werte passen sehr gut in die von Prior für diese Gruppe gegebene Datensammlung (Prior, 1919, S. 29).

Tabelle 2. Analysen chondritischer Steinmeteorite, die dem Breitscheid-Meteoriten chemisch sehr ähnlich sind

	(1) Breitscheid	(2) Cronstad	(3) Collescipoli	(4) Merua	(5) Stelldalen
SiO_2	37,30	37,24	36,31	36,88	35,71
TiO_2	0,12	0,30	0,18	0,13	—
Al_2O_3	4,48	2,41	3,67	2,53	2,11
Cr_2O_3	0,39	0,37	0,60	0,37	0,40
FeO	7,46	8,06	5,94	7,45	8,10
MnO	0,30	0,04	0,31	0,18	0,25
MgO	24,02	23,61	23,42	23,61	23,16
CaO	1,48	1,45	1,18	1,82	1,61
Na_2O	1,03	0,67	1,31	0,59	0,62
K_2O	0,14	0,07	0,24	0,07	0,15
P_2O_5	0,09	0,25	sp	0,29	0,30
Summe					72,41
Silik.+Acc.	76,81	74,47	73,16	73,92	
Fe	16,30	17,57	18,30	18,17	18,85
Ni	1,33	1,63	1,56	1,82	1,77
Co	0,08	0,23	0,10	0,11	0,17
Nickeleis.	17,71	19,43	19,96	20,10	20,79
Troilit	5,59	5,17	6,23	5,68	6,22

Zu Analyse (1): gehören noch $H_2O^- = 0{,}16$, $C = 0{,}34$; zu Analyse (2): $H_2O = 0{,}34$; zu Analyse (3): $H_2O^+ = 0{,}07$, $H_2O^- = 0{,}06$; zu Analyse (4): $H_2O = 0{,}35$; zu Analyse (5): $Cl = 0{,}04$ und $P = 0{,}01$.
Die Analysen (2), (4) und (5) sind ausserdem in der von Urey und Craig (1953) korrigierten Fassung wiedergegeben. Die Korrekturen beruhen auf ganz geringfügigen Umrechnungen im nichtsilikatischen Anteil.

Zur Frage des sekundären Troilits

Es war vermutet worden (S. 329) dass 20–25% des Troilits sekundärer Entstehung sind. Um einen Überblick zu gewinnen, um welche Beträge von primärem und sekundärem Troilit in Bezug auf die chemische Analyse es sich dabei handelt, und um welche Mengen von Fe und S, wurden die entsprechenden einfachen Berechnungen durchgeführt, deren Ergebnisse die nachstehende Tabelle 3 enthält. Sucht man nach einer physikalisch-chemischen Begründung für die sekundäre

Tabelle 3. Prozentanteile von Fe, S und FeS auf Grund der Bauschanalyse des Meteoriten, aufgeteilt nach primärem und sekundärem Troilit

Troilit	(1) %-Verhältnis prim : sekund.	(2) Gew. % am Gesamtgehalt von 5.59 Troilit.	(3) Fe-Gehalt (von Spalte 2)	(4) S-gehalt (von Spalte 2)	(5) Mol.-verhältnis Fe : S ohne sulfuriertes Fe
Primär	75–80	4,20–4,50	2,66–2,85	1,54–1,56	$Fe_1S_{1,35}$–$Fe_1S_{1,25}$
Sekundär	25–20	1,40–1,10	0,89–0,70	0,51–0,40	

Troilitbildung d.h. für die nach Vorliegen der festen Nickeleisen-Phase an diesem Mineral erfolgte Sulfurierung, so scheinen mir 2 Möglichkeiten die einfachste und nächstliegende Erklärung für dieses Phänomen zu bieten:

(1) Geht man von der Voraussetzung aus, dass die Troilit-Teilschmelze Lieferant des gesamten Schwefels war, dass aber die Erstarrung dieser Schmelze nur primären Troilit der oben angegebenen %-Menge geliefert hat, so müsste die Sulfidschmelze einen Schwefelgehalt gehabt haben, der das Verhältnis Fe : S = 1 : 1 übersteigt mit Werten, wie sie in Spalte 5 der Tabelle 3 enthalten sind. Dann müsste sich bei der Erstarrung dieser Sulfidschmelze entweder ein festes Sulfid zunächst mit dem entsprechenden Schwefelüberschuss gebildet haben. Dieser wäre dem natürlichen Magnetkies mit seinem Zuviel an Schwefel, bekanntlich bis $FeS_{1,2}$ ansteigend, überraschend ähnlich. Eine spätere Reaktion im festen Zustand müsste dann zusätzlich angenommen werden, bei welcher der über das Molverhältnis 1 : 1 hinausgehende Schwefel aus dem primären Sulfid abwanderte und mit Nickeleisen unter Bildung des sekundären Troilits reagierte.

(2) Das primär sich ausscheidende Sulfid ist, wie es jetzt vorliegt, ohne Schwefelüberschuss gebildet worden. Dann müsste der überschüssige Schwefel der flüssigen Phase mit oder ohne Zwischenschaltung einer Dampfphase in statu nascendi mit dem schon ausgeschiedenen Nickeleisen unter Bildung sekundären Troilits reagiert haben.

Aus Tabelle 3, Spalte 3 ist ersichtlich, dass die in Reaktion getretene Menge von Nickeleisen nicht ganz 1% der Gesamtmasse des Meteoriten ausmacht; das ist zwar nicht viel, aber doch schon erheblich in Bezug auf den Gehalt an metallischem Fe, von dem etwa 6% betroffen sind.

Das interessante Phänomen des "sekundären" Troilits hat in der Meteoritenliteratur bislang anscheinend nur 2-mal eine Behandlung erfahren. In der umfassenden Untersuchung von Perry (1944) wird nicht darüber berichtet, so dass man geneigt ist, an eine an sich seltene Erscheinung zu denken.

Dasselbe feine Implikationsgefüge von Troilit und Nickeleisen, das hier als sekundärer Troilit bezeichnet wird, hat nach Beschreibung und Abbildung (Tabelle II, Fig. 2 ihrer Arbeit) beim Meteoreisen von Buen Huerto F. Heide *et al.* (1932) vorgelegen. Diese Autoren haben es als Eutekt-gefüge gedeutet. Die Erscheinungsweise im Breitscheid-Meteoriten spricht nicht für diese Erklärung, zumindest nicht bei diesem Meteoriten.

Hugi (1930) hat aber am Meteorit von Ulmitz Troilit mit kleinen Nickeleiseneinschlüssen beobachtet und abgebildet. Nach Beschreibung und Bild scheint es sich bei diesem Meteorit um dieselbe Erscheinung zu handeln, die im Meteorit von Breitscheid von mir als sekundärer Troilit bezeichnet wurde. Hugi gibt aber eine ganz andere Erklärung dafür. Er denkt an eine Emulsion von Nickeleisentröpfchen in Sulfidschmelze und deren Fixierung bei der Erstarrung. Diese Auffassung dürfte kaum haltbar sein, denn der zu beobachtende Sachverhalt schliesst meines Erachtens eine postsekundärtroilitische Erstarrung des Nickeleisens ganz eindeutig aus.

Anerkennung—Der Verfasser möchte nicht unterlassen, für freundlichst gewährte Ratschläge und Hinweise den Herren Ramdohr-Heidelberg und Heide-Jena auch an dieser Stelle nochmals

aufs herzlichste zu danken. Letzterer hatte insbesondere die Liebenswürdigkeit, das Manuskript dieser Arbeit vor Drucklegung durchzusehen.

Das restliche Material des Meteoriten wird aufbewahrt im Max-Planck-Institut für Chemie in Mainze, die Schliffe (Dünnschliff Nr. 3702–3708, und Anschliffe Nr. 25-28) befinden sich im Gewahrsam des Hessischen Landesamtes für Bodenforshung in Wiesbaden.

Literatur

Heide F., Herschkowitsch E. und Preuss E. (1932) Ein neuer Hexaedrit von Cerros del Buen Huerto, Chile. *Chem. d. Erde* **7,** 483–502.

Hugi E. (1930) Der Meteorit von Ulmitz (Kt. Freiburg). *Mitt. Naturforsch. Ges. Bern.* 34–121.

Jérémine E. und Lelubre M. (1952) Sur la météorite d'Oubari. *Geochim. Cosmochim. Acta* **2,** 217–228.

Judin I. A. (1958) Undurchsichtige Minerale der Steinmeteorite. *Meteoritika* **16,** 78–104.

Krinow E. L. (1957) 7. Meteoritenkonferenz in der UdSSR. *Chem. d. Erde* **19,** 86–110.

Lacroix A. (1933) Sur une chute de météorite survenu au Cambodge, le 9 janvier 1932. *C. R. Acad. Sci., Paris* **197,** 565–567.

Perry St. H. (1944) The metallography of meteoric iron. *U.S. Nat. Mus. Bull.* **184.**

Prior G. T. (1919) On the genetic relationship and classification of meteorites. *Min. Mag.* **18.** 26–44.

Scholtz D. L. (1937) The magmatic nickelferous ore deposits of East Griqualand and Pondoland. *Trans. Geol. Soc. S. Africa* **39,** 81–208.

Urey H. C. and Craig H. (1953) The composition of the stone meteorites and the origin of the meteorites. *Geochim. Cosmochim. Acta* **4,** 36–82.

Geochimica et Cosmochimica Acta, 1959, Vol. 17, pp. 339 to 351. Pergamon Press Ltd. Printed in Northern Ireland

Der Meteorit von Breitscheid—IV

Radiochemische Untersuchungen

A. HELIUM UND NEON

H. König,* H. Wänke* und K. I. Mayne†

Einleitung

Der Edelgasgehalt eines Meteoriten ist nicht nur für Altersbestimmungen, sondern auch wegen des Studiums der Einwirkung der Höhenstrahlung von besonderem Interesse. Argon-40 und teilweise auch Helium-4 werden in Steinmeteoriten wohl hauptsächlich durch den radioaktiven Zerfall von Kalium einerseits und von Uran und Thorium andererseits gebildet. Trifft ein Teilchen der Höhenstrahlung, im wesentlichen schnelle Protonen mit Energien von etwa 1GeV und mehr, auf einen Atomkern, so kommt es zu Kernprozessen, die sich als eine Absplitterung leichter Kernbausteine beschreiben lassen, wobei ein Restkern zurückbleibt, der gegenüber dem getroffenen Kern eine verminderte Massen- und Ordnungszahl hat. Ein Teil des Helium-4 und die Gesamtmengen des Helium-3, Neon-20, -21 und -22 und Argon-36 und -38, sowie ein allerdings sehr kleiner Teil des Argon-40 werden auf diese Weise durch die Einwirkung der Höhenstrahlung erzeugt. Die zu erwartende Isotopenzusammensetzung dieser Edelgase weicht deshalb auch stark von derjenigen der in der Atmosphäre enthaltenen Edelgase ab. Während im atmosphärischen Helium das Isotop der Masse 3 ganz ausserordentlich selten ist ($1{,}3 \cdot 10^{-4}$ %) hat man in Meteoriten bereits Konzentrationen bis zu 25% gefunden (Mayne *et al.*, 1952). Ebenso ist Neon-21 im atmosphärischen Neon sehr selten (0,26%) und die Konzentration von Neon-20 übertrifft die von Neon-22 etwa um einen Faktor 10. In dem durch die Höhenstrahlung gebildeten Neon hingegen sind alle drei Neonisotope mit etwa der gleichen Häufigkeit zu erwarten.

Im Gegensatz zu den Eisenmeteoriten (Reed und Turkevich, 1955; Reed *et al.*, 1958) sind in den Steinmeteoriten wegen ihres wesentlich höheren Gehalts an Uran und Thorium (Patterson *et al.*, 1953; Hamaguchi *et al.*, 1957; Hernegger und Wänke, 1957; Ebert *et al.*, 1957; Bate *et al.*, 1957) beträchtliche Mengen Helium-4 radiogenen Ursprungs. Leider ist es bis jetzt nicht möglich, den genauen Anteil des "radiogenen" bezw. "kosmogenen" Heliums am Gesamtgehalt von Helium-4 anzugeben. Alle Altersbestimmungen an Steinmeteoriten nach der Heliummethode sind daher mit einem mehr oder weniger grossen Unsicherheitsfaktor behaftet. Allerdings kann die Menge des "kosmogenen" Helium-4 aus den Mengen Helium-3 und Neon abgeschätzt werden. Es ist daher von grosser Wichtigkeit, stets wenigstens eines der beiden reinen Höhenstrahlungsprodukte zu messen.

Durchführung der Experimente

Die zerkleinerten, jedoch nicht fein pulverisierten (Sieb: 100 Maschen/cm²) Meteoritproben wurden in einem Platintiegel in ein einseitig geschlossenes Quarzrohr gebracht, welches am offenen Ende mit Hilfe eines Normalschliffes an

* Max-Planck-Institut für Chemie, Mainz.
† Clarendon Laboratory, Oxford.

eine Hochvakuumapparatur angeschlossen wurde. Die Proben wurden zunächst bei 120–150°C etwa 6 Stunden unter ständigem Pumpen erhitzt. Anschliessend blieben die Proben über Nacht im Vakuum stehen, wobei das Quarzrohr bereits von einem Wasserkühlmantel umgeben war. Kurz vor der eigentlichen Erhitzung wurde nochmals kurze Zeit abgepumpt, und schliesslich wurden die Proben mit Hilfe einer Hochfrequenzanlage induktiv auf ca. 1350°C erhitzt. Nach 3 Stunden waren, wie durch Nacherhitzungen (auf gleiche Temperatur und ebenfalls 3 Stunden) festgestellt werden konnte, ca. 99,7% des Heliums und ca. 98% des Neons ausgetrieben. Während des Erhitzens wurde der Gasdruck des Systems durch Adsorption des grössten Teils der auftretenden Gase an mit siedendem Stickstoff gekühlter Aktivkohle, unter 10^{-2} Torr gehalten, um Gasentladungen und eventuell damit verbundene Verluste an Helium und Neon zu vermeiden. Die in Freiheit gesetzten Gase wurden mit etwa 20 cm^3 NTP reinstem, elektrolytisch im Vakuum hergestelltem Sauerstoff in eine Apparatur zur Mikroanalyse von Edelgasen übergespült, die der von Chackett *et al.* (1953) beschriebenen sehr ähnlich war. Zunächst erfolgte an einem auf 400 °C gehaltenen Palladiumkontakt die Verbrennung des gesamten Wasserstoffs zu Wasser, worauf in einer 15-stufigen Trennkolonne die eigentliche Abtrennung von Helium und Neon durch fraktionierte Adsorption und Desorption an Aktivkohle bei der Temperatur des siedenden Stickstoffs durchgeführt wurde.

Die voneinander getrennten reinen Edelgase Helium und Neon wurden mit Hilfe eines Wärmeleitfähigkeitsmanometers nach Pirani gemessen und schliesslich zur weiteren massenspektrometrischen Analyse abgefüllt. Die Messgenauigkeit der Anlage selbst ist bei 10^{-6} cm^3 NTP Helium oder Neon besser als 1%.

Die Isotopenanalyse des Helium und Neon wurde mit einem der üblichen 60° Massenspektrometer nach Nier mittels einer dynamischen Methode ausgeführt; die Messung des Ionenstrahls erfolgte mittels eines zehnstufigen Be–Cu–Elektronenverstärkers, gefolgt von einem Gleichstromverstärker. Die Eichung des Systems geschah mit eigens hergestellten Helium-Isotopen-Mischungen aus ^3He und ^4He und mit atmosphärischem Neon. Bei der Heliumanalyse war das Auflösungsvermögen des Instruments genügend, um die ^3He-Linie vom HD-Hintergrund zu trennen, der etwa 1% der Höhe der He-Linie betrug; die Genauigkeit der Messungen ist nicht grösser als 2%.

Die Neonanalyse ist weniger genau, wahrscheinlich nicht mehr als 5%, und zwar wegen der Gegenwart von Hintergrundlinien bei den Massen 20 und 22, die auch nach wiederholtem Ausheizen der Spektrometerröhre nicht verschwanden. Eine weitere Schwierigkeit bestand in der Entfernung des an den Wänden adsorbierten Neon, nachdem eine Eichung mit atmosphärischem Neon erfolgt war.

Diskussion der Ergebnisse

Während Parallelbestimmungen zerkleinerter und homogenisierter Proben innerhalb geringer Fehler übereinstimmende Ergebnisse lieferten, kam es bei von verschiedenen Stellen des Meteoriten entnommenen Proben zu stark schwankenden Werten sowohl für den Helium- als auch für den Neongehalt. Die Ursachen dieser Schwankungen konnten noch nicht geklärt werden, und es bedarf weiterer eingehender Untersuchungen hierzu.

In Tabelle 1 ist nur der Edelgasgehalt jener Probe angegeben, für die auch bereits eine massenspektroskopische Untersuchung durchgeführt wurde.

Eine Berechnung des Heliumalters ist dadurch erschwert, dass weder der "kosmogene" Anteil des Helium-4 bekannt ist noch Thoriumbestimmungen am Meteoriten Breitscheid durchgeführt worden sind. Wir haben diesen Anteil gleich dem dreifachen Betrag der gefundenen Helium 3-Menge gesetzt; ein solches Verhältnis wurde von MAYNE *et al.* (1952) in Eisenmeteoriten aufgefunden. Der Thoriumgehalt ist nach einer Arbeit von BATE *et al.* (1957) für alle Steinmeteoriten

Tabelle 1

$^3He + ^4He$ (10^{-6} cm^3 NTP)	Ne (10^{-8} cm^3 NTP)	He 3/4	Ne 20/21/22	$^3He/Ne$
10,2	25,9	0,048	28,5/30,5/41,0	1,8

etwa gleich der vierfachen Uranmenge anzusetzen. Mit diesen Annahmen und einem Urangehalt von $1{,}3 \cdot 10^{-8}$ g/g ergibt sich für den Meteoriten Breitscheid ein Heliumalter von $2{,}5 \cdot 10^9$ Jahren.

Während Eisenmeteorite ein Helium-3/Neon-Verhältnis von ca. 35 aufweisen (EBERT und WÄNKE, 1957), ergab sich für Breitscheid ein solches von 1,8. Dies ist durchaus zu verstehen, da bei Steinmeteoriten für die Neonerzeugung hauptsächlich die Atomkerne von Silizium, Aluminium und Magnesium verantwortlich sind. Aus diesen nur wenige Massenzahlen entfernten Kernen erfolgt die Neonerzeugung mit wesentlich grösseren Wirkungsquerschnitten als aus den Eisenkernen im Falle der Eisenmeteorite (FRIEDLANDER *et al.*, 1954). Ausserdem sind vermutlich Wirkungsquerschnitte für die Helium-3-Produktion für Protonen mit Energien, wie sie der Höhenstrahlung entsprechen, für die leichten Atomkerne kleiner als für Eisen (CURRIE *et al.*, 1956). Die gefundenen Werte stimmen gut mit den bisher bekanntgewordenen Arbeiten von REASBECK und MAYNE (1955), GERLING (1956), GERLING und LEVSKI (1956) und REYNOLDS und LIPSON (1957) über das Edelgasverhältnis von Steinmeteoriten überein.

Anerkennung—Herrn B. SPETTEL sei für seine Mithilfe an dieser Arbeit herzlichst gedankt. Der Deutschen Forschungsgemeinschaft danken wir für die leihweise Überlassung eines HF-Generators.

LITERATUR

BATE G. L., HUIZENGA J. R. und POTRATZ H. A. (1957) *Science* **126,** 612.
CHACKETT K. F., REASBECK P. und WILSON E. J. (1953) *Geochim. Cosmochim. Acta* **3,** 261.
CURRIE L. A., LIBBY W. F. und WOLFGANG R. L. (1956) *Phys. Rev.* **101,** 1557.
EBERT K. H., KÖNIG H. und WÄNKE H. (1957) *Z. Naturforsch.* **12a**, 763.
EBERT K. H. und WÄNKE H. (1957) *Z. Naturforsch.* **12a**, 766.
FRIEDLANDER G., HUDIS J. und WOLFGANG R. L. (1955) *Phys. Rev.* **99,** 263.
FRIEDLANDER G., MILLER J. M., WOLFGANG R., HUDIS J. und BAKER E. (1954) *Phys. Rev.* **94,** 727.
GERLING E. K. (1956) *Dokl. Akad. Nauk SSSR* **107,** 555.
GERLING E. K. und LEVSKI L. K. (1956) *Dokl. Akad. Nauk SSSR* **110,** 750.

Hamaguchi J., Reed G. W. und Turkevich A. (1957) *Geochim. Cosmochim. Acta* **12,** 337.
Hernegger F. und Wänke H. (1957) *Z. Naturforsch.* **12a,** 759.
Mayne K. I., Paneth F. A. und Reasbeck P. (1952) *Geochim. Cosmochim. Acta* **2,** 300.
Patterson C., Brown H., Tilton G. und Inghram M. (1953) *Phys. Rev.* **92,** 1234.
Reasbeck P. und Mayne K. I. (1955) *Nature, Lond.* **176,** 186.
Reed G. W., Hamaguchi J. und Turkevich A. (1958) *Geochim. Cosmochim. Acta* **13,** 248.
Reed G. W. und Turkevich A. (1955) *Nature, Lond.* **176,** 794.
Reynolds J. H. und Lipson J. I. (1957) *Geochim. Cosmochim. Acta* **12,** 330.

B. TRITIUM

K. Goebel* und P. Schmidlin*

Es ist von Interesse, bei einem frisch gefallenen Meteoriten auch die radioaktiven Isotope zu bestimmen. Für solche Messungen eignet sich insbesondere das Tritium, da es eine günstige Halbwertszeit von 12,26 Jahren hat und der Erzeugungsquerschnitt von Tritium in Kernprozessen, die durch die kosmische Strahlung induziert werden, von derselben Grössenordnung wie der von Helium-3 und Helium-4 ist. Ferner lässt sich das Tritium als gasförmige Substanz ähnlich wie die Edelgase leicht quantitativ abtrennen. Soweit die Wirkungsquerschnitte für die Meteoritensubstanz in dem entsprechenden Energieintervall durch Laboratoriumsversuche bekannt sind, kann aus der Tritiumerzeugung pro Gramm Meteorit auf die Intensität der kosmischen Strahlung zur Zeit des Falles geschlossen werden.

Eine neue Aussage gewinnt man, wenn man berücksichtigt, dass das Helium-3 zum Teil durch radioaktiven Zerfall des Tritiums gebildet wurde. Die Zahl der so entstandenen Helium-3 Atome, dividiert durch die Zahl der Tritiumzerfälle pro Zeiteinheit, ergibt das sogenannte Bestrahlungsalter des Meteoriten, das heisst die Zeit, während der der Meteorit der Höhenstrahlung ausgesetzt war. Dabei ist vorausgesetzt, dass die Intensität der Höhenstrahlung während dieser Zeit konstant war und keine Verluste an Helium-3 durch Diffusion stattfanden. Messungen des Tritiumgehaltes wurden bisher von Fireman *et al.* (1957) an 2 Eisenmeteoriten und von Begemann *et al.* (1957) an einem Steinmeteorit ausgeführt. Im Vergleich zu diesen Messungen ist eine Tritiummessung am Breitscheid von besonderem Interesse, da der Meteorit wesentlich kleiner ist als der früher untersuchte Norton County und sein Falldatum nicht so weit zurückliegt wie das der von Fireman untersuchten Eisenmeteorite.

Aufschlussmethode

Das bei den Tritiummessungen am Meteoriten Breitscheid verwendete Aufschlussverfahren entspricht im wesentlichen der auch für Edelgase benützten Methode der Austreibung der Gase durch starke Erwärmung der Probe im Induktionsofen. Die zur Abtrennung des Tritiums verwendete Apparatur ist der von Fireman *et al.* (1957) und von Currie *et al.* (1956) benutzten Anordnung ähnlich. Im wassergekühlten Quarzkolben wird die Probe im Metalltiegel erhitzt. Zu Anfang des Versuches wird Wasserstoff (etwa 5 cm³ n.t.p., das sind 8 Torr im

* CERN—European Organisation for Nuclear Research, Genf, Division Synchro-Cyclotron.

Aufschlussvolumen) als Träger zugesetzt. Nachdem bei abgeschlossenem Kolben dieser Trägerwasserstoff mit der heissen Probe und dem entweichenden Gas gut vermischt ist, beginnt man nach etwa einer Stunde Heizzeit die langsame Evakuierung des Kolbens mit einer Töplerpumpe. Danach lässt man den Wasserstoff des in einem Vorratsgefäss gesammelten Gasgemisches durch ein Palladiumröhrchen bei 550° diffundieren. Mit Hilfe einer heissen Tantalwendel (1500 bis 2000°) können die Kohlenwasserstoffe, die beim Aufschluss entstehen, zerlegt werden.

Zur Reduktion des Wassers dient ein Magnesiumofen (500°C), der ebenfalls mit dem Vorratsgefäss verbunden ist. Die durch Cracken und Reduktion freigesetzten Wasserstoffmengen diffundieren dabei gleichzeitig durch das Palladium. Die Diffusion des Wasserstoffes wird wesentlich begünstigt durch stetiges Abpumpen mit einer Quecksilberdiffusionspumpe, die auf der einen Seite des Palladiums ein Vacuum von weniger als 10^{-5} Torr erzeugt. Mit einer zweistufigen Töplerpumpe, deren zweite Stufe zur Bewältigung hoher Gasdrucke eingerichtet ist, kann der Wasserstoff in ein auf der Apparatur aufgeschmolzenes Zählrohr gedrückt werden.

Die Abtrennung des Tritiums aus dem Gasgemisch war in Testversuchen kontrolliert worden, wobei der Wirkungsgrad der Abtrennung besser war als 99%. Diese Testversuche wurden bei Tritiumaktivitäten, die 10^2 bis 10^3 mal grösser waren als die Aktivitäten bei den Breitscheidmessungen, durchgeführt, wobei ein Wasserstoff–Tritiumgemisch aus bestrahlten Eisentargets verwendet wurde. Bei allen Versuchen war nach 3 Stunden Wasserstoffdiffusion die nicht diffundierte Restaktivität kleiner als 10%. Nach Spülen mit nochmals der gleichen Menge Trägerwasserstoff lag die Restaktivität bei weniger als 1%. Die zweite Trägerzugabe erfolgte auch bei den Tritiummessungen am Breitscheid, wobei dieselbe Menge Wasserstoff verwendet wurde.

Die Reduktion von Wasserdampf an Magnesium bei gleichzeitiger Diffusion des freiwerdenden Wasserstoffes durch Palladium ist quantitativ. Zum Beispiel zersetzten sich 3 cm^3 n.t.p. Wasserdampf bei einer Temperztur von 500°C in einer Stunde. Der Restdruck entsprach ca. 1% der Ausgangsmenge. Um eine mögliche Adsorption von Wasserstoff am Magnesium zu vermeiden, wurde der Ofen vor Beginn des Versuches in heissem Zustand mit Wasserstoff abgesättigt.

Das Cracken von Kohlenwasserstoff wurde durch Testversuche mit Methan kontrolliert. Während der Zerlegung wurde der freiwerdende Wasserstoff ständig durch das Palladiumventil abgepumpt; hierbei war in allen Fällen der Restdruck der unzersetzten Gase nach 3 Stunden kleiner als 5% des Anfangsdruckes. Tantal erwies sich beim Cracken als schneller wirksam als Wolfram.

Vor Beginn der Versuche wurde der Tiegel bei 1700° ausgeheizt, und die Meteoritenprobe bei Zimmertemperatur ein bis zwei Tage entgast. Erst danach wurde die Probe in den Tiegel eingefüllt, wobei der Aufschlussteil nicht mehr geöffnet wurde.

Die Abtrennung des Tritiums aus den Breitscheidproben

Die Versuchsbedinungen beim Aufschluss der beiden Breitscheidproben waren die folgenden:

Probe 1. 7,78 g des Meteoriten wurden im Platintiegel induktiv erwärmt, nachdem 8 Torr Wasserstoff im Aufschlusskolben als Trägergas zugegeben worden

waren. Mit dem Erhitzen der Probe auf 1000°C während einer Stunde stieg der Gasdruck langsam im Kolben an. Nach einer Stunde wurde auf 1300°C erhöht und diese Temperatur für die Dauer einer weiteren Stunde belassen. Nachdem die Probe auf 1400°C gebracht worden war, begann der Meteorit zu schmelzen. Die Temperatur wurde dann stetig langsam heraufgesetzt, um am Ende der 5. Stunde 1700°C zu erreichen, diese Temperatur wurde eine halbe Stunde gehalten.

Am Ende der ersten Heizperiode von 5½ Stunden wurde mit der Extraktion des Wasserstoffs durch das Palladium begonnen. Nach einer Wartezeit von 10 Stunden erfolgte eine zweite Carrierzugabe (8 Torr), und in einer weiteren Heizperiode von 2 Stunden erhitzte man den Tiegel nochmals auf 1550°C. Wegen des starken sich bei 1700° bildenden Platinspiegels schien es angebracht, die Temperatur in der zweiten Heizperiode etwas zu erniedrigen. Der Quarzkolben und der sich auf ihm gebildete Beschlag wurden am Ende des Versuches durch Hochheizen des Kolbens ohne Wasserkühlung ausgeheizt, um eventuell adsorbierten Wasserstoff zurückzugewinnen. Wie bei der ersten Extraktion liess man den Wasserstoff der zweiten Heizperiode 8 Stunden lang durch das Palladium diffundieren.

Probe 2. In einem Molybdäntiegel wurden 10,38 g des Meteoriten geschmolzen. Sofort nach dem Einschalten der vollen Leistung des Generators schmolz der Meteorit unter starker Gasentwicklung und Bildung eines dicken Belages auf der Quarzwand. Nach *ca.* 15 Minuten schmolz der Molybdäntiegel infolge ungleichmässiger Erwärmung auf einem beträchtlichen Teil seiner Länge durch. Wegen der schlechteren Koppelung konnte im Tiegel nur noch eine Temperatur von 1300°C erzeugt werden. Die Heizdauer wurde deshalb im Vergleich zum ersten Versuch erhöht. Nach einer Heizzeit von 4,5 Stunden und einer weiteren Wartezeit von 8 Stunden erfolgte die zweite Zugabe von Trägerwasserstoff. Auch die zweite Heizperiode dauerte nochmals 4,5 Stunden (bei 1300°C). Danach erfolgte die Abtrennung des Wasserstoffes aus dem freigesetzten Gasgemisch (wie bei Versuch 1 nach 8-stündiger Diffusion). Das Restgas wurde zur weiteren Analyse ebenfalls abgetrennt. Um Tritiumverluste zu vermeiden, schloss man hieran noch einen Nachversuch an, indem man die zweite Probe für weitere 5 Stunden auf 1300°C erhitzte. In der oben beschriebenen Weise wurde bei diesem Nachversuch ebenfalls der Kolben und der Niederschlag entgast. Die beim Nachversuch frei werdenden Gase wurden zum abgetrennten Wasserstoff des Hauptversuches hinzugegeben.

Die Zählapparatur

Zur Bestimmung der Tritiumaktivität wurde eine Anordnung, wie sie von Libby (1957) beschrieben wird, verwendet. In einer Eisenabschirmung von 20 cm Dicke befand sich eine Antikoinzidenzanordnung, bestehend aus dem inneren Zählrohr, das die Probe enthält, und einem Doppelring aus zwanzig Antikoinzidenzzählrohren. Das aktive Zählvolumen der äusseren Zählrohre war 40 cm lang bei einem Durchmesser von 14 mm. Dagegen war die aktive Länge des Tritiumzählrohres 25 cm bei einem Durchmesser von 30 mm. Letzteres bestand aus einem Plexiglasrohr von 2 mm Wandstärke, innen mit Kupfer bedampft und mit Plexiglasscheiben und Apiezonwachs verschlossen. Als Anode diente ein 0,1 mm starker Stahldraht. Mit einer Füllung von 60 Torr Argon und 50 Torr Aethylen hatte das Zählrohr eine Einsatzspannung (Geiger Müller-Bereich) von 1700 V.

Das Plateau war über 200 V lang, in der oben beschriebenen Abschirmung registrierte man einen Nulleffekt von ca. 60 cpm, davon zwei bis drei Antikoinzidenzen. Plateau und Nulleffekt des Zählrohres konnten vor dem Aufsetzen auf die Wasserstoffapparatur gemessen werden. Das Zählrohr wurde erst an der Apparatur zur Wasserstoffaufnahme wieder geöffnet. Nachdem der Wasserstoff in das Zählrohr gefüllt war, wurde dieses abgezogen, wobei das Verlustvolumen genau bestimmt werden konnte.

Mit Hilfe einer Löschstufe liess sich eine Totzeit der Schaltung zwischen 1 und 10 msec einstellen. Damit konnte man den Einfluss der Totzeit auf die Zählrate (infolge unterdrückter Nachimpulse) kontrollieren.

Ergebnisse der Messungen

Die Zusammenstellung der Messergebnisse zeigt die Tabelle 2. Das Tritium der ersten Probe wurde in das Zählrohr P 1003 gefüllt. Dieses hatte einen Nulleffekt

Tabelle 2

Probe (g)	Zählrohr	Nulleffekt	Effekt (T) (c.p.m.)	Bemerkungen
1 (7,78)	P 1003	2,43	3,78 ± 0,06	Gesamteffekt
	P 1002	2,01	3,69 ± 0,06	Tritium aus P 1003 umgefüllt
	P 1003	2,49	—	Alte Füllung ohne T
2 (10,38)	P 1001	2,71	4,27 ± 0,08	Hauptversuch
			0,4 ± 0,04	Nachversuch

von 2,43 cpm. Es zählte mit Tritium 6,21 cpm was einem Effekt von 3,78 cpm für das Tritium entspricht. Die Zählrate war über einem Plateau von 100 V konstant und fiel nicht ab bei einer Verlängerung der Totzeit der Löschstufe auf 4 msec. Zur Kontrolle liess man nach Beendigung dieser Messung die Zählrohrfüllung nochmals in die Apparatur, extrahierte den Wasserstoff und füllte diesen in das Zählrohr P 1002. Die alte Füllung wurde in das Zählrohr P 1003 zurückgepumpt. Es ergab sich dort eine Zählrate von 2,49 cpm d.h. der alte Nulleffekt. Das neue Zählrohr P 1002 zählte nach einem Nulleffekt von 2,01 cpm für das Tritium allein 3,69 cpm was mit dem Wert im ersten Zählrohr gut übereinstimmt.

Unter Einberechnung kalibrierter Verluste beim Abziehen des Zählrohres P 1003 ergibt sich somit für die erste Probe ein Effekt von 3,8 cpm Tritium. Sämtliche Zählraten haben einen statistischen Fehler von weniger als 1%. Der Gesamtfehler der Tritiummessung ist exakt schwer angebbar; nach dem Ergebnis der Kontrollversuche liegt er unterhalb 10%. Zurückgerechnet auf das Falldatum ergibt sich mit einer Halbwertszeit von 12,26 Jahren ein Tritiumgehalt von 4,2 dpm das sind 0,54 ± 0,05 dpm/g Tritium.

Die zweite Probe wurde im Zählrohr P 1001 gemessen, dessen Nulleffekt 2,71 com betrug. Mit Tritium zählte P 1001 6,98 cpm also ein Effekt fur das

Tritium von 4,27 cpm. Der beschriebene Nachversuch erbrachte noch einen Effekt von 0,4 cpm. Dabi muss berücksichtigt werden, dass hierin auch das Tritium aus der Desorption des Belages und des Quarzkolbens enthalten war. Der Gesamteffekt beträgt also für die zweite Probe 4,7 cpm das sind bei einem Gewicht der Probe von 10,38 g 0,46 cpm/g Meteorit. Für den frisch gefallenen Meteoriten ergibt sich hieraus durch Rückwärtsrechnung ein Wert von $0{,}51 \pm 0{,}05$ dpm. Die Übereinstimmung der Tritiumwerte für die beiden Meteoritenproben liegt innerhalb der Fehlergrenze.

3. Diskussion der Ergebnisse

Der Wert für die Zahl der Tritiumzerfälle 0,54 cpm zur Zeit des Falles gibt zusammen mit jeweils einer weiteren Annahme Aufschluss über die Intensität der Höhenstrahlung zur Zeit des Falles und über das Strahlungsalter des Meteoriten.

(*a*) *Das Bestrahlungsalter des Meteoriten Breitscheid*

Man versteht darunter die Zeit, während der der Meteorit der kosmischen Strahlung im Weltraum ausgesetzt war, und nimmt allgemein an, dass er am Beginn dieser Periode aus einem grösseren Objekt herausgebrochen ist. Diese Zeit lässt sich bestimmen, wenn man die pro Zeiteinheit zerfallenden Tritiumatome zum radioaktiven Zerfallsprodukt des Tritiums, dem Helium-3, in Beziehung setzt. Man muss jedoch dabei eine Annahme über die zeitliche Veränderung der Höhenstrahlungsintensität machen, da diese allein für die Produktionsrate des Tritiums verantwortlich ist. Es zerfallen im Gleichgewicht stets ebenso viele Tritonen wie durch kosmische Strahlung gebildet werden. Nehmen wir an, dass die kosmische Strahlung stets im Mittel die gleiche Intensität hatte wie heute, dann lässt sich aus 0,54 cpm/g und $1{,}26 \cdot 10^{13}$ Atome He^3/g (siehe vorhergehende Arbeit) berechnen, dass der Meteorit 49,6 Ma einer Höhenstrahlung der gegenwärtigen Intensität ausgesetzt war. Für diesen Wert ist jedoch eine Korrektur anzubringen, durch die die Direktproduktion von Helium-3 durch die kosmische Strahlung berücksichtigt wird. Zur Zeit liegen zwei Messungen über die Direktproduktion von Helium-3 und Tritium in Eisentargets vor. Die erste von Martin *et al.* (1954) wurde mit 350 MeV Protonen an einem dicken Eisentarget durchgeführt. An zwei verschiedenen Stellen des Eisentargets erhielt man die folgenden Werte: $He^3/T = 0{,}73$ bzw. 0,64 (Faktor C). Neuerdings haben Schaeffer und Zähringer (1958) diese Werte bei zwei verschiedenen Energien gemessen und erhielten die folgenden Werte für C:

$$He^3/T(450\ \text{MeV}) = 1{,}4$$
$$He^3/T(\ \ 3\ \text{GeV}) = 2{,}4$$

d.h. in beiden Fällen mehr Helium-3 als Tritium. Die Unsicherheit, die durch die Verschiedenheit dieser Ergebnisse bedingt, ist muss bei der Berechnung des Strahlungsalters berücksichtigt werden. Nehmen wir einen Quotienten von 2,0 an, so erhalten wir

$$\frac{1{,}26 \cdot 10^{13}}{0{,}54 \cdot 3 \cdot 5{,}26 \cdot 10^5} = 14{,}7\ \text{Ma}$$

mit dem alten Wert von 0,7 dagegen

$$\frac{1{,}26 \cdot 10^{13}}{0{,}54 \cdot 1{,}7 \cdot 5{,}26 \cdot 10^{5}} = 26{,}0 \text{ Ma}$$

Während die Isotopenanalyse des Heliums (siehe vorhergehende Arbeit) an einer anderen Meteoritenprobe durchgeführt wurde als die oben beschriebenen Tritiummessungen, wurde an der zweiten auf Tritium untersuchten Probe (10,38 g) eine weitere Helium-3 Bestimmung durchgeführt. Die massenspektrometrische Untersuchung durch Fechtig und Kistner am Physikalischen Institut der Universität Freiburg ergab einen Helium-3 Wert von $0{,}92 \cdot 10^{13}$ Atome pro Gramm Meteorit. Zusammen mit dem Tritiumwert dieser Probe ergibt sich ein Bestrahlungsalter von

$$11{,}5 \text{ Ma}(C = 2{,}0) \text{ bzw. } 20{,}2 \text{ Ma}(C = 0{,}7)$$

Wodurch die Abweichung der Werte an verschiedenen Stellen des Meteoriten, die ausserhalb der experimentellen Fehlergrenzen liegt, bedingt ist, wird noch in weiteren Versuchen zu klären sein. Es muss betont werden, dass die angegebenen Werte von C für Eisen gefunden wurden und dass bei den leichteren Elementen—wie sie in den Steinmeteoriten vorkommen—das Verhältnis C von den obigen Werten abweichen kann.

Der bisher publizierte Wert über das He^3/T-Strahlungsalter für den Norton County Meteorit (Begemann *et al.*, 1957) liegt bei 260 Ma (mit $C = 0{,}7$). Er ist also um den Faktor 10 grösser als der Wert für den Breitscheid. Geiss (1957) weist jedoch darauf hin, dass sowohl aus den unterschiedlichen Heliumwerten (Paneth *et al.*, 1953) an Sideriten als auch aus dem A^{38}-Gehalt der Chondrite und Achondrite auf echte Unterschiede der Strahlungsalter geschlossen werden kann. Dieser Meinung möchten wir uns mit dem Vorbehalt anschliessen, dass zu einer eingehenden Diskussion der Strahlungsalter noch mehr direkte Messungen nach der He^3/T-Methode vorliegen und im Fall des Meteoriten Breitscheid die in neueren Experimenten gefundenen Schwankungen der Heliummengen aufgeklärt werden sollten.

(b) *Die Intensität der kosmischen Strahlung*

Der Meteorit Breitscheid ist ein nur etwa 1,5 kg schwerer kleiner Chondrit, dessen präatmosphärische Masse klein war im Vergleich mit der Absorptionslänge der kosmischen Strahlung (mittlere Energie ~ 3 GeV). Deshalb kann er direkt als "cosmic ray target" angesprochen werden. Unter der Annahme, dass die Tritiumerzeugungsquerschnitte für die leichten Elemente, wie sie von Currie *et al.* (1956) gemessen wurden, auf den Steinmeteoriten angewandt werden können, lässt sich aus der Zahl 0,54 cpm/g, der Zahl der Tritonen, die pro Minute erzeugt werden, auf die mittlere Intensität der Höhenstrahlung schliessen. Gehen wir aus von den Tritiumerzeugungsquerschnitten für leichte Elemente, welche bisher aus direkten Experimenten zur Verfügung stehen, nämlich (2,05 GeV) N: 25 mb, O: 30 mb, Mg: 30 mb und Al: 37 mb, so ist nach der Zusammensetzung des Meteoriten Breitscheid mit einem Erzeugungsquerschnitt von 30 mb zu rechnen. Mit diesem Wert ergäbe sich dann eine Intensität von 0,44 Primärteilchen/sec cm^2

sterad. gegenüber 0,24/sec-cm²-sterad. in der Polgegend im Jahre 1954 (Neher, 1956; Neher und Anderson, 1958) und 0,27 mit Raketenaufstiegen in 87°C Breite (Meredith *et al.*, 1955) gemessen. Beim Vergleich der beiden Ergebnisse, muss berücksichtigt werden, dass die Wirkungsquerschnitte noch nicht mit ausreichender Genauigkeit bestimmt worden sind. Neuerdings wurden neben anderen die Wirkungsquerschnitte für die Tritiumerzeugung in Aluminium und Magnesium (Kuznetsov und Mekhedow, 1958) zwischen Protonenenergien von 120 und 660 MeV gemessen. Für Aluminium erhält man 16 mb (120 MeV) und 46 mb (660 MeV), für Magnesium 19 mb (300 MeV) und 43 mb (660 MeV). Der Wert für Aluminium (Fehler ca. 30%) stimmt gut mit dem Wirkungsquerschnitt von Currie *et al.* (1956) bei 450 MeV überein. Es ist, wie die Werte von Fireman und Zähringer gegenüber denen von Currie *et al.* für Eisen zeigen, auch mit höheren Erzeugungsquerschnitten für die leichteren Elemente zu rechnen. Damit würde sich der oben berechnete Wert für die Primärintensität verringern.

Eine andere Deutungsmöglichkeit liegt in der Annahme –wenn die Wirkungsquerschnitte als richtig angesehen werden –dass die kosmische Strahlung unter Einbeziehung des energiearmen Teils des Spektrums tatsächlich die obige Intensität ausserhalb der Erde erreicht.* Bei der Kleinheit des Meteoriten Breitscheid können energiearme Protonen bis zu etwa 100 MeV bei der Tritiumproduktion beteiligt sein (Goebel, 1958).

Die energiearme Komponente der kosmischen Strahlung ändert sich, wie Neher (1956) zeigen konnte, in einem zeitlichen Zyklus, wodurch die Totalintensität der kosmischen Strahlung starken Schwandungen unterworfen ist. Falls die energiearme Komponente bei der Tritiumerzeugung tatsächlich eine wesentliche Rolle spielen sollte, wäre der Tritiumgehalt der Meteorite vom Falldatum abhängig. Die gemäss dem Falldatum so zu erwartenden Unterschiede der Tritiumwerte sind jedoch wesentlich kleiner als die entsprechenden Intensitätsschwankungen der kosmischen Strahlung, da die Halbwertszeit des Tritiums etwa ebensogross ist wie die vermutliche Periode der zeitlichen Schwankungen der Höhenstrahlung. Ausserdem ist die Frage noch offen, ob die Helium-3 und Tritiumverluste infolge von Diffusion nicht eine Rolle bei den verschiedenen Tritiumkonzentrationen spielen. Auch hier sind die bisherigen Messergebnisse nicht ausreichend, um weitere Schlüsse und Vergleiche zu ziehen; jedoch sei hervorgehoben, dass das Falldatum des Norton County Meteoriten acht Jahre vor dem des Meteoriten Breitscheid liegt.

Unter Berücksichtigung der diskutierten Unsicherheiten kann für den Meteoriten Breitscheid ein Bestrahlungsalter von ca. 20 Ma errechnet werden. Die Primärintensität ausserhalb der Erde ergibt sich zu 0,44 Teilchen/sec-cm²-sterad.

Die Autoren danken Herrn Professor Dr. W. Gentner für seine Unterstützung und sein Interesse an der vorliegenden Untersuchung. Besonderer Dank gilt den Herren Dipeomphysikern H. Fechtig und G. Kistner für die Durchführung der massenspektrometrischen Untersuchung.

* Dieser Fluss von ca. 10 Nukleonen/cm² sec entspricht dem von Fireman und Schwarzer (1957) angegebenen Wert für eine Meteoritenprobe des "Norfolk". Auch ist unser Wert von 0,54 cpm doppelt so hoch wie für den Norfolk (=0,293 cpm), was mit dem erwarteten Verhältnis der Tritiumerzeugung in Stein- und Eisenmeteoriten übereinstimmt.

Literatur

Begemann F., Geiss J. und Hess D. C. (1957) *Phys. Rev.* **107,** 540.
Currie L. A., Libby W. F. und Wolfgang R. L. (1956) *Phys. Rev.* **101,** 1557.
Fireman E. L. und Schwarzer D. (1957) *Geochim. Cosmochim. Acta* **11,** 252.
Fireman E. L. und Zähringer J. (1957) *Phys. Rev.* **107,** 1695.
Geiss J. (1957) *Chimia* **2,** 249.
Goebel K. (1958) CERN Report 1958, 2 SC-Division.
Kuznetsov V. V. und Mekhedow V. N. (1958) Tritium production by 120–660 MeV protons in metals. Report. Dubna, 1958.
Libby W. F. (1957) *Radiocarbon Dating* pp. 66 *et seq.* University of Chicago Press.
Martin G. R., Mayne K. I., Thomson S. J. und Wardle G. (1954) *Phil. Mag.* **45,** 410.
Meredith L. M., van Allen J. A. und Gottlieb M. G. (1955) *Phys. Rev.* **99,** 198.
Neher H. V. (1956) *Phys. Rev.* **103,** 228.
Neher H. V. und Anderson H. (1958) *Phys. Rev.* **109,** 608.
Paneth F. A., Chackett K. F., Reasbeck P. und Wilson E. I. (1953) *Geochim. Cosmochim. Acta* **3,** 257.
Schaeffer O. A. und Zähringer J. (1958) *Phys. Rev.* **113,** 674.

C. URAN

K. H. Ebert,* F. Hernegger,† H. König‡ und H. Wänke‡

Wegen der ausserordentlichen Kleinheit der in Meteoriten zu erwartenden Uranmengen bedarf es der Anwendung sehr spezieller Bestimmungsmethoden. Der Urangehalt des Meteoriten Breitscheid wurde nach zwei verschiedenen Methoden bestimmt. In beiden Fällen handelte es sich um Neutronenaktivierungsanalysen, und zwar unter Ausnutzung der Spaltung des Urans-235 durch langsame Neutronen. Die gefundenen Werte gelten daher nur unter der Voraussetzung, dass das Isotopenverhältnis des in Meteoriten enthaltenen Urans identisch ist mit dem des irdischen Urans. Diese Annahme erscheint auf Grund einer neueren Arbeit von Hamaguchi *et al.* (1957) jedoch gut gesichert.

Da beide Bestimmungen bereits an anderer Stelle ausführlich beschrieben wurden (Hernegger und Wänke, 1957; Ebert *et al.*, 1957), seien hier nur die wesentlichsten Merkmale angeführt. Die eine der beiden von uns verwendeten Methoden zur Uranbestimmung entspricht der von Smales (1952) angegebenen: sie benützt das aktive Spaltstück Barium-140 mit einer Halbwertszeit von 12,8 Stunden. Eine gewisse Schwierigkeit ergibt sich aus der Tatsache, dass das im natürlichen Barium zu 0,1 % enthaltene Barium-130-Isotop unter Neutroneneinfang in Barium-131 übergeht, welches durch K-Einfang mit einer Halbwertszeit von 11,6 Stunden in Cäsium-131 zerfällt; letzteres ist wiederum instabil und geht unter K-Einfang in Xenon-131 über. Eine Unterscheidung der Strahlungen der beiden Bariumisotope war jedoch mit Hilfe von Absorbern möglich. Nach dieser Methode ergab sich für den Meteoriten Breitscheid ein Urangehalt von $1{,}5 \cdot 10^{-8}$ g Uran/g Met. Nebenbei erhielten wir einen Wert für den Bariumgehalt von $2{,}5 \cdot 10^{-6}$ g/g.

Im zweiten Fall verwendeten wir eine neue, speziell für die geringen in den Meteoriten enthaltenen Uranmengen entwickelte Methode (Ebert *et al.*, 1957).

* Institut für chemische Technologie der Technischen Hochschule, München.
† Institut für Radiumforschung und Kernphysik, Wien.
‡ Max-Planck-Institut für Chemie, Mainz.

Hierbei wird die Aktivität des ebenfalls bei der Uranspaltung entstehenden Xenon-133 benutzt. Nach dieser Methode ergab sich ein Wert von $1{,}23 \cdot 10^{-8}$ g Uran/g. In Anbetracht der Schwierigkeit, so kleine Konzentrationen exakt zu messen, kann die Übereinstimmung der nach den beiden Methoden erhaltenen Werte als befriedigend bezeichnet werden.

Anerkennung—Fräulein I. Schüler und Herrn B. Spettel sei für ihre Mithilfe an dieser Arbeit herzlichst gedankt. Der Deutschen Forschungsgemeinschaft danken wir für die leihweise Überlassung eines Zählgerätes.

Literatur

Ebert K. H., König H. und Wänke H. (1957) *Z. Naturforsch.* **12a,** 763.
Hamaguchi H., Reed G. W. und Turkevich A. (1957) *Geochim. Cosmochim. Acta* **12,** 337.
Hernegger F. und Wänke H. (1957) *Z. Naturforsch.* **12a,** 759.
Smales A. A. (1952) *Analyst* **77,** 778.

D. KALIUM–ARGON

H. König* und H. Wänke*

Zur Erfassung des Zeitpunktes des letzten Erstarrens eines Minerals oder eines Meteoriten eignet sich die Kalium-Argonmethode besonders gut. Verluste an Argon durch Diffusion, die beim Helium sehr gross sein können, sind hier in den meisten Fällen vernachlässigbar. Trotzdem ergeben sich bei Altersbestimmungen von Meteoriten nach der Kalium-Argonmethode Schwierigkeiten wegen des im Vergleich gegenüber den meisten irdischen Mineralien sehr kleinen Kaliumgehaltes. Wir haben nun hierfür eine neue Methode entwickelt, die gegenüber den bisherigen manche Vorteile bietet. Die genaue Beschreibung dieser Methode erfolgt demnächst an anderer Stelle, deshalb sei hier nur auf die wesentlichsten Merkmale eingegangen.

Die zu untersuchende Probe wird als ganzes, unzerkleinertes Stück in eine kleine Quarzphiole gegeben, gut evakuiert, abgeschmolzen und 1 Woche im Reaktor mit etwa 10^{12} n/cm^2-sec bestrahlt. Nach der Bestrahlung wird die Quarzphiole aufgeschlagen, die Probe pulverisiert und mit Natriumhydroxyd unter Vakuum aufgeschlossen. Vorher wird eine kleine Menge Luftargon als Träger zugegeben. Nach dem Aufschluss wird dieses Argon zusammen mit den im Meteoriten durch die Bestrahlung entstandenen radioaktiven Argonisotopen von allen anderen Gasen abgetrennt, in kleine Stahlküvetten mit dünnem Kunststoffenster eingefüllt und unter einem Glockenzählrohr gezählt. Bei der Bestrahlung im Reaktor entstehen drei radioaktive Isotope des Argons, nämlich die Kerne Argon-37, Argon-39 und Argon-41. Die Reaktionen, die zu diesen Kernen führen, sind die folgenden:

$$^{40}\mathrm{Ca}(n, \alpha)^{37}\mathrm{A} \xrightarrow[\mathrm{K}]{35\ \mathrm{d}} {}^{37}\mathrm{Cl}$$

$$^{39}\mathrm{K}(n, p)^{39}\mathrm{A} \xrightarrow[\beta]{260\ \mathrm{a}} {}^{39}\mathrm{K}$$

$$^{40}\mathrm{A}(n, \gamma)^{41}\mathrm{A} \xrightarrow[\beta]{1{,}82\ \mathrm{h}} {}^{41}\mathrm{K}$$

* Max-Planck-Institut für Chemie, Mainz.

Alle diese drei radioaktiven Argonisotope können auf Grund ihrer sehr verschiedenen Halbwertszeit bzw. Energie leicht voneinander unterschieden werden. Durch Vergleich mit Standardpräparaten ergibt sich somit aus der Aktivität von Argon-39 der Kaliumgehalt, bzw. aus der Aktivität von Argon-41 der Argongehalt der Probe. Nebenbei erhält man über Argon-37 noch ein Mass für den Calciumgehalt. Argon-41 entsteht allerdings auch noch durch die Reaktion $^{41}K(n, p)^{41}A$, doch beträgt dieser Anteil in unserem Falle nur etwa 20% und kann leicht korrigiert werden.

Bei dieser Methode werden Verfälschungen durch Verunreinigung mit Luftargon während des Austreibens bzw. Abtrennens des Argons von vornherein ausgeschieden. Bei Proben irdischer Mineralien lassen sich solche Verunreinigungen durch eine massenspektroskopische Analyse des Argons auf Grund der beiden im atmosphärischen Argon enthaltenen Argonisotope-36 und -38 leicht korrigieren. Anders bei den Meteoriten, da diese selbst Argon-36 und -38 enthalten, welches durch die Höhenstrahlung entsteht.

Ein weiterer Vorteil der angeführten Methode besteht darin, dass Kalium- und Argonbestimmungen an ein und demselben Stück ausgeführt werden, wodurch Fehler durch Inhomogenität der Proben ausgeschlossen sind. Da es für die eigentliche Altersbestimmung nur auf das Verhältnis der Aktivitäten von Argon-39 zu Argon-41 ankommt, so scheiden Fehler durch nicht vollständigen Aufschluss bzw. durch Verluste bei der Abtrennung des Argons ebenfalls aus.

Nach dieser Methode erhielten wir für das Kalium-Argonalter des Meteoriten Breitscheid einen Wert von $3{,}33 \pm 0{,}12 \cdot 10^{-9}$ Jahren. Hierbei benützten wir für das Verzweigungsverhältnis des Kaliumzerfalls den von McNair *et al.* (1955) angegebenen Wert $\lambda_k/\lambda_\beta = 0{,}124$ und eine Halbwertszeit des Kalium-40 von $1{,}27 \cdot 10^9$ Jahren. Als Absolutwerte erhielten wir $32 \cdot 10^{-6}$ cm³ Argon NTP/g und $0{,}82 \cdot 10^{-3}$ g Kalium/g. Die Genauigkeit der Altersbestimmung beträgt ca. 5%.

Der Kaliumgehalt wurde ausserdem noch auf eine andere Weise bestimmt. Unter Verwendung der Reaktion

$$^{41}K(n, \gamma)^{42}K \xrightarrow[\beta]{12{,}5\,h} {}^{42}Ca$$

wurde eine Neutronenaktivierungsanalyse durchgeführt. Die genaue Beschreibung dieses Verfahrens erfolgt demnächst in einer eigenen Arbeit. Für den Kaliumgehalt des Meteoriten ergab sich der Wert von $0{,}90 \pm 0{,}02$ g/g.

Anerkennung—Die chemische Laborarbeit der Kaliumaktivierungsanalyse wurde von Fräulein Ch. Emig und von Frau H. Szigeti in zum Teil sehr selbständiger Weise durchgeführt; für ihre hierbei bewiesene ausserordentliche Einsatzfreudigkeit sei ihnen herzlichst gedankt. Ebenso danken wir Herrn B. Spettel für seine Mithilfe bei den gasanalytischen Arbeiten. Die in dieser Arbeit beschriebenen Untersuchungen am Meteorit von Breitscheid wurden unterstützt durch Sachbeihilfen des Bundesministeriums für Atomkernenergie und Wasserwirtschaft, sowie durch eine Leihgabe der Deutschen Forschungsgemeinschaft.

The research reported in this paper has been sponsored in part by the Geophysics Research Directorate, Air Force Cambridge Research Center of the Air Research and Development Command, United States Air Force, through its European Office.

Literatur

McNair A., Glover R. N. und Wilson H. W. (1955) *Phys. Rev.* **99**, 771.

Geochimica et Cosmochimica Acta, 1959. Vol. 17. p. 352. Pergamon Press Ltd. Printed in Northern Ireland.

PAPERS TO BE PUBLISHED IN FUTURE ISSUES

W. COMPSTON: The carbon isotopic compositions of certain marine invertebrates and coals from the Australian Permian.

N. YAMAGATA, Y. MURAKAMI and T. TORII: Biogeochemical investigation in a serpentine–chromite ore district.

U. SCHINDEWOLF and M. WAHLGREN: The rhodium, silver and indium content of some chondritic meteorites.

C. E. ADAMS, N. H. FARLOW and W. R. SCHELL: The compositions, structures and origins of radioactive fallout particles.

E-AN ZEN: Carbonate equilibria in the open ocean and their bearing on the interpretation of ancient carbonate rocks.

H. FECHTIG, W. GENTNER and G. KISTNER: Räumliche Verteilung der Edelgasisotope im Eisenmeteoriten Treysa.

A. P. TUDGE: A method of analysis of oxygen isotopes in orthophosphate—its use in the measurement of paleotemperatures.

M. S. CROWLEY and R. ROY: The effect of formation pressures on sheet structures, a possible case of Al–Si ordering.

G. L. BATE, H. A. POTRATZ and J. R. HUIZENGA: Scandium, chromium and europium in stone meteorites by simultaneous neutron activation analysis.

J. R. MERRILL, E. F. X. LYDEN, M. HONDA and J. R. ARNOLD: The sedimentary geochemistry of the beryllium isotopes.

H. G. F. WINKLER and H. VON PLATEN: Experimentelle Gesteinsmetamorphose III—Ultrametamorphase Kalkhaltiger Tone.

D. M. KEMP and A. A. SMALES: Neutron activation results for vanadium and scandium in G-1 and W-1.

R. E. MARINGER and G. K. MANNING: Aerodynamic heating of the Grant meteorite.

L. A. AHRENS, R. R. BROOK and S.R. TAYLOR: The determination of trace elements in silicate rocks by a combined spectrochemical-anion exchange technique.

E. A. VINCENT and J. H. CROCKET: Studies in geochemistry of gold—I. The distribution of gold in rocks and minerals of the Skaergaard intrusion.

E. A. VINCENT and J. H. CROCKET: Studies in the geochemistry of gold—II. The gold content of some basic and ultrabasic rocks and stony meteorites.

F. A. PANETH: The discovery and the earliest reproductions of the Nidmanstätten figures.

E. J. CATANZARO and P. W. GAST: Isotopic composition of lead in pegmatitic feldspars.

E. L. FIREMAN and J. DEFELICE: Argon-39 and tritium in meteorites.

P. E. BROWN and B. J. RUSHTON: Some chemical data on the Mourne Mountain granite G2.

K. H. WEDEPOHL: Spurenanalytische Untersuchungen an Tiefseetonen aus dem Atlantik.

H. HAMAGUSHI, R. KURODA and H. ISHIKAWA: The distribution of minor elements in the rocks of Sakura-jima volcano.

P. M. HURLEY, H. W. FAIRBURN, W. H. PINSON and G. FAURE: K–A and Rb–Sr minimum ages for the Pennsylvanian section in the Narragansett basin.

K. KREJCI-GRAF und F. E. WICKMAN: Ein geochemisches Profil durch den Lias alpha.

A. T. WILSON and G. T. FERGUSSON: Origin of terrestrial tritium.

W. G. ERNST: The stability relations of magnesioriebeckite.

INFORMATION FOR CONTRIBUTORS

I. GENERAL

1. Papers on *geochemistry* should be submitted to the appropriate Executive Editor—Prof. L. R. WAGER for papers from the United Kingdom and British Commonwealth, and for papers in English from Europe; Prof. C. W. CORRENS for papers in German or French; Prof. E. INGERSON for papers from the American continents. Papers on *cosmochemistry* should be sent to Prof. W. A. WAHL. Papers submitted for publication will naturally be judged from the standpoint of scientific originality and novelty. Technical details of apparatus used in scientific investigation can, however, be presented in brief notes. Critical comments or preliminary results requiring early publication should be submitted as letters to the editors. Where possible, letters should be confined to 500 words. The preparation of progress reports and review articles will be invited by the editors from time to time. The journal appears as independent and complete numbers, which are combined into volumes of about 300 pages.

2. Only papers which have not been previously published can be accepted. Authors must agree not to publish elsewhere a paper submitted to and accepted by *Geochimica et Cosmochimica Acta*.

3. Fifty reprints of each paper are provided free. Additional copies can be purchased if ordered at the time the first proofs are returned. A reprint order form will accompany first proofs.

II. SCRIPT REQUIREMENTS

1. Scripts must be written in one of the three official languages—English, French or German.

2. The script should be typed (not a carbon copy). The text must be ready for printing and should be carefully checked for errors. Authors will receive proofs for correction.

3. Illustrations should accompany the script, mounted on separate sheets. Line diagrams that require to be redrawn should include all relevant details. Half-tone illustrations should be restricted to the minimum necessary. Photographs should be enlarged sufficiently to permit their clear reproduction, and if words or numbers appear on them, two copies should be sent, one clearly printed and the other without inscription. All illustrations should be provided with descriptive legends, which should be given on a separate sheet. Any lettering on diagrams—other than Greek letters, symbols, etc.—should be stencilled and should be sufficiently large and bold to permit reproduction when the diagram has been reduced to a size suitable for inclusion in the journal.

4. References in the text should be given by quoting the author's name and year of publication, i.e. AHRENS (1952). *Full references should be listed at the end of each paper, in alphabetical order, in the following manner:*

AHRENS, L. H. (1952) The use of ionization potentials—I. Ionic radii of the elements. *Geochim. et Cosmochim. Acta* **2**, 155–169.

and should include the full title of the article, standard abbreviated title of the journal, year, volume, number and inclusive page numbers.

5. The text of articles submitted should be concise and in a readily understandable style. The technical description of the methods used should only be given in detail when such methods are new. The essential contents of each paper should be briefly recapitulated in an abstract in English. Such an abstract, may, however, be submitted by the author in the language of the original typescript for translation into English by the editorial staff.

6. To conserve space, authors are requested to mark less important portions of the paper (such as description of methods, record of experimental results, etc,) for printing in smaller type.

7. Indices of refraction should be denoted by the symbols α, β, γ, ω, ε, n, and vibration directions by X, Y, Z, O and E.

Pergamon Press are also publishers of the following Journals:

JOURNAL OF NUCLEAR ENERGY (*including* THE SOVIET JOURNAL OF ATOMIC ENERGY*). PART A: REACTOR SCIENCE; PART B: REACTOR TECHNOLOGY; PART C: PLASMA PHYSICS—ACCELERATORS—THERMONUCLEAR RESEARCH
HEALTH PHYSICS (*The Official Journal of the Health Physics Society*)
JOURNAL OF INORGANIC AND NUCLEAR CHEMISTRY
TETRAHEDRON (*The International Journal of Organic Chemistry*)
TALANTA (*An International Journal of Analytical Chemistry*)
INTERNATIONAL JOURNAL OF APPLIED RADIATION AND ISOTOPES
BIOCHEMICAL PHARMACOLOGY
ARCHIVES OF ORAL BIOLOGY
* BIOPHYSICS
* JOURNAL OF MICROBIOLOGY, EPIDEMOLOGY AND IMMUNOBILOGY
* PROBLEMS OF HEMATOLOGY AND BLOOD TRANSFUSION
* PROBLEMS OF VIROLOGY
* PROBLEMS OF ONCOLOGY
* SECHENOV PHYSIOLOGICAL JOURNAL OF THE U.S.S.R.
* PAVLOV JOURNAL OF HIGHER NERVOUS ACTIVITY
* ELECTRIC TECHNOLOGY, U.S.S.R.
* RADIO ENGINEERING
* RADIO ENGINEERING AND ELECTRONICS
* TELECOMMUNICATIONS
* PHYSICS OF METALS AND METALLOGRAPHY
* THE ABSTRACTS JOURNAL OF METALLURGY
* APPLIED MATHEMATICS AND MECHANICS
CHEMICAL ENGINEERING SCIENCE
JOURNAL OF ATMOSPHERIC AND TERRESTRIAL PHYSICS
PLANETARY AND SPACE SCIENCE
BULLETIN GÉODÉSIQUE
ANNALS OF THE INTERNATIONAL GEOPHYSICAL YEAR
SPECTROCHIMICA ACTA
JOURNAL OF THE MECHANICS AND PHYSICS OF SOLIDS
ACTA METALLURGICA (*for the Board of Governors of Acta Metallurgica*)
INTERNATIONAL JOURNAL OF THE PHYSICS AND CHEMISTRY OF SOLIDS
DEEP-SEA RESEARCH
JOURNAL OF NEUROCHEMISTRY
JOURNAL OF PSYCHOSOMATIC RESEARCH
JOURNAL OF INSECT PHYSIOLOGY
INTERNATIONAL JOURNAL OF AIR POLLUTION
INTERNATIONAL ABSTRACTS OF BIOLOGICAL SCIENCES (*for Biological and Medical Abstracts Ltd.*)
RHEOLOGY ABSTRACTS
VACUUM
OPERATIONAL RESEARCH QUARTERLY
ANNALS OF OCCUPATIONAL HYGIENE
ELECTROCHIMICA ACTA

* *Translations of Russian journals published on behalf of the Pergamon Institute, a non-profit-making foundation*

Leaflets giving further details and subscription rates of each of these journals are available on request

18Jan.
FILED IN STACKS
6 Jan 64
20 Apr 64

THE GEOCHEMICAL SOCIETY

OFFICERS

J. Frank Schairer, President
Tom F. W. Barth, Vice-President
Konrad B. Krausfopf, Secretary
George T. Faust, Treasurer

COUNCILLORS

John A. S. Adams, 1957–1959
Alfred O. Nier, 1957–1959
E. F. Osborn, 1958–1960
H. G. Thode, 1958–1960
Albert E. J. Engel, 1959–1961
Friedrich G. Hontermans, 1959–1961

REGIONAL VICE-PRESIDENTS

Louis H. Ahrens
Rui Ribeiro Franco
Ing. Georges Ordoñez
C. W. Correns
William S. Fyfe
Ken Sugawara

COMMITTEES

Auditing Committee:

Joseph J. Tregoning, Chairman
William L. Hill
C. R. Nasser

Constitution and By-Laws Committee:

Michael Fleischer, Chairman
Julian R. Goldsmith
Denis M. Shaw

Education Committee:

H. D. Holland, Chairman
J. A. S. Adams
D. M. Henderson
Kurt E. Lowe
G. D. Nicholls
Hans P. Eugster

Membership Committee:

R. M. Garrels, Chairman
Harvey C. Diebl
Chester B. Slawson
James E. Slosson
Irving Breger

Nominating Committee:

Wm. T. Pecora, Chairman
T. G. Sahama
C. E. Tilley
G. Tunell

Programme Committee:

H. T. Evans, Chairman
Gordon J. F. MacDonald
H. E. Lowenstam

Publications Committee:

E. W. Heinrich, Chairman
Julian R. Goldsmith
John C. Maxwell
N. W. Rakestraw
S. C. Robinson
L. R. Wager
Earl Ingerson

Research Committee:

C. G. Dodd, Chairman
W. F. Bradley
R. A. Rowland
T. G. Thompson

Russian Translations Committee:

Earl Ingerson

Standards Committee:

Alvin Van Valkenberg, Chairman
Michael Fleischer
Loren Stieff
George Switzer
George Tilton

Tellers Committee:

Charles Meyer, Chairman
Henry R. Cornwall
Colin O. Hutton